

*Exploring the human Hsp70-Hop-Hsp90 system  
for Tau recognition*

DISSERTATION

FOR THE AWARD OF THE DEGREE  
"DOCTOR RERUM NATURALIUM"  
OF THE GEORG-AUGUST-UNIVERSITÄT GÖTTINGEN

WITHIN THE DOCTORAL PROGRAM  
PHYSICS OF BIOLOGICAL AND COMPLEX SYSTEMS (IMPRS-PBCS)  
OF THE GEORG-AUGUST UNIVERSITY SCHOOL OF SCIENCE (GAUSS)

SUBMITTED BY

ANTONIA-FRANZISKA MOLL  
(NÉE LOTT)

FROM SCHRAMBERG, GERMANY

GÖTTINGEN (2021)

## **Thesis advisory committee (TAC)**

Prof. Dr. Markus Zweckstetter

Max-Planck Institute for Biophysical Chemistry (MPIBPC), *Research group for Protein Structure Determination using NMR*, Göttingen, Germany

German Center for Neurodegenerative Diseases (DZNE), *Research group for Translational Structural Biology in Dementia*, Göttingen, Germany

Prof. Dr. Holger Stark

MPIBPC, *Department of Structural Dynamics*, Göttingen, Germany

Prof. Dr. Kai Tittmann

Georg-August-Universität Göttingen, *Department of Molecular Enzymology*, Göttingen, Germany

## **Members of the examination board**

First Reviewer: Prof. Dr. Markus Zweckstetter; MPIBPC / DZNE, Göttingen, Germany

Second Reviewer: Prof. Dr. Holger Stark; MPIBPC, Göttingen, Germany

## **Further members of the examination board**

Prof. Dr. Michael Meinecke

University Medical Center Göttingen (UMG), *Department of Cellular Biochemistry*, Göttingen, Germany

Prof. Dr. Henning Urlaub

MPIBPC, *Department of Bioanalytical Mass Spectrometry*, Göttingen, Germany

Dr. Alexander Stein

MPIBPC, *Research group of Membrane protein biochemistry*, Göttingen, Germany

Date of thesis submission: February 19, 2021

Date of thesis defense: March 30, 2021

# Promovierendenerklärung

**Name** Lott, Antonia-Franziska

(Name, Vorname)

**Anschrift** Zur Hohen Warte 19, 37077 Göttingen

(Straße, PLZ Wohnort)

Ich beabsichtige, eine Dissertation zum Thema *‘Exploring the human Hsp70-Hsp-Hsp90 system for Tau recognition’* an der Georg-August-Universität Göttingen anzufertigen. Dabei werde ich von Herrn Prof. Dr. Markus Zweckstetter betreut.

Ich gebe folgende Erklärung ab:

1. Die Gelegenheit zum vorliegenden Promotionsvorhaben ist mir nicht kommerziell vermittelt worden. Insbesondere habe ich keine Organisation eingeschaltet, die gegen Entgelt Betreuerinnen und Betreuer für die Anfertigung von Dissertationen sucht oder die mir obliegenden Pflichten hinsichtlich der Prüfungsleistungen für mich ganz oder teilweise erledigt.
2. Hilfe Dritter wurde bis jetzt und wird auch künftig nur in wissenschaftlich vertretbarem und prüfungsrechtlich zulässigem Ausmaß in Anspruch genommen. Insbesondere werden alle Teile der Dissertation selbst angefertigt; unzulässige fremde Hilfe habe ich dazu weder unentgeltlich noch entgeltlich entgegengenommen und werde dies auch zukünftig so halten.
3. Die Ordnung zur Sicherung der guten wissenschaftlichen Praxis an der Universität Göttingen wird von mir beachtet.
4. Eine entsprechende Promotion wurde an keiner anderen Hochschule im In- oder Ausland beantragt; die eingereichte Dissertation oder Teile von ihr wurden/werden nicht für ein anderes Promotionsvorhaben verwendet.

Mir ist bekannt, dass unrichtige Angaben die Zulassung zur Promotion ausschließen bzw. später zum Verfahrensabbruch oder zur Rücknahme des erlangten Grades führen können.

Göttingen, den 19. Februar 2021

---

(Unterschrift)

## Acknowledgments

To all of you, who have helped and supported me during these three years of my graduate work, who have constantly questioned my work critically and thus pushed and motivated me further. To everyone who has taken the time specifically for this - thank you so much!

- First of all, a big thanks to Prof. Dr. Markus Zweckstetter, my first supervisor and thus contact person number one. I don't even remember how many times I asked, "can we discuss this briefly?" - and brief was a relative matter of opinion here - and you took your time at all times. It was the perfect balance between the freedom you gave me in terms of research direction and also student supervision, and the support I could always count on to pursue my interests and achieve my scientific goals. If I wanted to go to a conference - was approved, I came out of the lab with a broken hand - I got a personal assistant, I meant to do some more training in graphic design alongside the PhD - "well then apply that to your work". In the last three years you gave me the opportunity to learn so much, to teach, to write and to review. Thank you for your trust, your commitment and your critical eye, which always motivates me to take an even closer look.
- Many thanks to the members of my Thesis Advisory Committee, Prof. Dr. Markus Zweckstetter, Prof. Dr. Holger Stark and Prof. Dr. Kai Tittmann, for accompanying and supporting me during my doctoral studies. Every meeting with you was wonderfully straightforward, relaxed and productive at the same time. Everyone brought their own perspectives on my results, which raised new questions and helped me to drill down on my scientific goal in more detail. Thank you for your time, feedback, and enthusiasm for science, which I hope many others besides me can benefit from.
- Parts of this work were done in co-operation with the lab of Prof. Dr. Henning Urlaub. I deeply thank you for this great collaboration, which was essential and invaluable for the progress of this project. All mass spectrometry data in this work were done in his group, which performed the corresponding sample preparation, sample measurement as well as data analysis. Dear Henning, thank you very much for the opportunities you opened up for me and your relaxed and patient way of combining fun with diligence. Many thanks to the whole team, who I was allowed to contact so often and who helped me at any time.

In particular, I thank Dr. Momchil Ninov and Dr. Kuan-Ting Pan for their expertise and help and time they put into this project.

- I owe an equally great collaboration to Prof. Dr. Holger Stark. His input with new ideas and his own methods has contributed significantly to the progress of this work. I am very grateful that I was and still am allowed to profit from his immense knowledge. Thank you for sharing your laboratory space and equipment that made the multitude of experiments possible in the first place, and for two fantastic collaborators that you provided me with.



- Thanks to Dr. Erik Schliep and Cole Townsend for the irreplaceable help you have given me and for the many scientific discourses that have always provided new impulses. To you, Erik, thank you for the introduction to the lab, your patience in showing me new methods, and the help with data analysis. When Erik left the project due to a new job, Cole took over the collaboration. Dear Cole, thank you for all the energy and time you have dedicated to the project since then. You are such a calm person and scientist, with whom everything can be talked through and rethought once more, to bring out the very best in the end. I am very grateful for this and hope that our collaboration will continue for a long time.
- A huge thanks goes out to my former and existing colleagues in the Zweckstetter group. Thank you to Dr. Gwladys Riviere Dr. Tina Ukmar-Godec Dr. Taekyung Yu, Dr. Lisa Ramirez, Dr. Timo Strohäker, Dr. Alain Ibanez de Opakua, Matthew Percival, Christian Pantoja Rivillas, Dr. Adriana Savastano, Maria Babu, Zheng Shen, Dr. David Flores, Pijush Chakraborty, Dr. Filippo Favretto, Dr. Marija Rankovic, Irina Lushpinskaia, Dr. Milan Zachrdla, and Dr. Anton Abyzov for the warm and friendly working atmosphere that leaves plenty of room for discussions of personal ups and downs in addition to the day-to-day scientific discussions.
- Thanks to Dr. Gwladys Riviere and Dr. Tina Ukmar-Godec with whom I was privileged to share the office and who both gave me many life lessons in their own unique way.
- A special thanks to Dr. David Flores and Sol Cima-Omori. They both were my right hand during the four weeks it was broken and not usable. It is unbelievable to me to this day how kindly and carefully you helped me. This thanks also goes to you, Markus, who made this possible at all. Thank you very much!
- Thanks to Conny Mascher and Sol Cima-Omori, who literally keep the lab running. Thank you for always being available, for always helping where you can and for supporting all of us with your work. You guys are doing a great job.
- Also a great thanks to the rotation student Gianina Butnariu and the master student Arjun Bhatta, who I was allowed to work with, for helping me improving my teaching skills and grow as a teacher.
- Thank you to the entire NMR II department at the MPIBPC for helping me in front of and next to the spectrometers, for the deep interest in my work, and for numerous precious conversations.
- I thank the fantastic team of the IMPRS-PBCS, for their continued encouragement, great organization and advice. I was very lucky to benefit from numerous courses and travel fellowships offered by this program. Thank you Antje and Frauke for your support.
- Many thanks to the administrative team of the DZNE Göttingen, Ulrike Kramer and Daniel Riester, for their extensive bureaucratic help and assistance.

- Thanks also to the great PhD / Postdoc community of the MPIBPC for the weekly get-togethers and the one or the other bigger party.

Insbesondere danke ich meinem Verlobten, meinen beiden Schwestern, meinem Bruder, meinen Eltern, meinen Großeltern, meine Schwiegereltern *in spe* und allen Freunden, die mich durch meine Doktorandenzeit begleitet haben. Ich bin so stolz, wenn ihr nach meiner Forschung fragt und mich damit immer weiter antreibt, komplizierte Dinge ganz einfach zu beschreiben. Das hilft mir selbst noch besser zu verstehen, neu zu hinterfragen und bringt mich dazu, meine Forschung mit ganz anderen Augen zu sehen. Ein riesengroßes Dankeschön an Denis, Simon, Lydia, Philip und Maria für das Korrekturlesen von Teilen oder der ganzen Arbeit.

Liebe Lydia, danke, dass du mich immer wieder daran erinnerst, dass man jede noch so stressige Situation nur einmal erleben darf und deshalb genießen sollte.

Lieber Denis, danke, dass du dir mit so viel Geduld jeglichen Frust anhörst, jeden Erfolg mit mir feierst und mir immer sagst, *du kannst alles und noch viel mehr*. Du holst das Beste in mir heraus und unterstützt mich in allem was ich mir in den Kopf setze. D a n k e.

## Summary

Molecular chaperones are diligent helpers of the cell that ensure a well-balanced proteome by regulating protein production, protein folding, refolding and holding as well as protein degradation. In doing so, molecular chaperones assist proteins throughout their lifetime. Within the proteome, i.e. the entirety of all proteins, a special feature is reserved for the group of intrinsically disordered proteins (IDPs). They inherently lack a distinct three-dimensional structure so that, when unbound, their side chains are unprotected. Thereby, IDPs are able to participate in a wide range of interactions and react sensitively to external changes. At the same time this feature bears a particularly high risk for unfavorable contacts that may in the worst case engender protein aggregation. The importance of molecular chaperones to shelter IDPs from such undesired interactions manifests in yet incurable neurodegenerations such as Alzheimer's or Parkinson's disease. In each of these disorders, there are disease specific IDPs that attach to each other, clump together, and deposit as huge protein aggregates.

With regard to IDP chaperoning, a special role is assigned to the heat shock protein (Hsp) family, as they possess the unique capability of protein holding to protect proteins from undesired interactions. Thus, the binding of Hsps to IDPs gained increasing research interest. So far, mainly the interaction of IDPs, including the Alzheimer's disease related, IDP prime example protein Tau, with individual Hsps has been studied. However, for foldable substrates, it is known that, in addition to their discrete function, Hsps can team up to drive protein turnover. And so also Hsp70 and Hsp90, which together can form the Hsp70/Hsp90 chaperone machinery to particularly prevent protein misfolding. Hence, being on the one side equipped with the marvelous capacity to counteract aggregation *via* the Hsp70/Hsp90 chaperone machinery and observing on the other side the deposition of insoluble Tau aggregates, poses the central question on whether the cellular defense system of the Hsp70/Hsp90 chaperone machinery isn't likewise involved in the chaperoning of Tau.

The Hsp70/Hsp90 chaperone machinery comprises the minimal system of the five proteins Hsp70, Hsp40, Hsp90, Hop and p23. In order to understand the role of each of these proteins in the Hsp70/Hsp90 chaperone machinery mediated Tau chaperoning, its stepwise assembly with distinct intermediate states was reconstituted *in vitro*. The analysis showed that (i) one Hop molecule stabilizes the Hsp90<sub>2</sub> dimer in a V-shaped conformation, (ii) Hsp70, Hop and Hsp90 together form the Hsp70/Hsp90 chaperone machinery comprising the Hsp70<sub>2</sub>:Hop<sub>1</sub>:Hsp90<sub>2</sub> complex, (iii) Tau associates with the preassembled Hsp70/Hsp90 chaperone machinery creating a 710 kDa large (Hsp70<sub>1</sub>:Hop<sub>1</sub>:Hsp90<sub>2</sub>:Tau<sub>1</sub>)<sub>2</sub> dimeric complex and that (iv) the addition of p23 stabilizes the Hsp70/Hsp90 chaperone machinery: Tau interaction generating a stable 750 kDa large (Hsp70<sub>1</sub>:Hop<sub>1</sub>:Hsp90<sub>2</sub>:Tau<sub>1</sub>:p23<sub>1</sub>)<sub>2</sub> complex. (v) By means of the co-chaperone CHIP, which marks proteins for proteasomal degradation, it was further shown that the

(Hsp70<sub>1</sub>:Hop<sub>1</sub>:Hsp90<sub>2</sub>:Tau<sub>1</sub>:p23<sub>1</sub>)<sub>2</sub> complex is no irreversible deadlock but part of a co-chaperone-mediated dynamic equilibrium between protein holding *via* Hop and p23, and protein degradation induced by CHIP. (vi) The Hsp70/Hsp90 chaperone machinery was revealed to control normal as well as abnormal Tau, as pathologically modified, hyperphosphorylated Tau (PTau) equally associated with the Hsp70/Hsp90 chaperone machinery forming Hsp70:Hop:Hsp90:PTau and Hsp70:Hop:Hsp90:PTau:p23 complexes.

Altogether, the Hsp70/Hsp90 chaperone machinery was revealed as interaction partner and thus potential chaperone system for the intrinsically disordered protein Tau. An integrated approach of biochemical and biophysical methods including native page, tryptophane fluorescence, isothermal titration calorimetry, nuclear magnetic resonance, dynamic light scattering, sucrose density gradient centrifugation, chromatography and chemical cross-linking coupled to mass spectrometry was used to describe a detailed model of stepwise machinery assembly accompanied with Tau binding. The knowledge gained about binding sites, conformational changes, stoichiometries and affinities presents novel structural and biochemical insights into the IDP chaperoning by the Hsp70/Hsp90 chaperone machinery. The obtained data thus may serve as fundamental basis for high-resolution structure determination and future research directions deciphering why the Hsp70/Hsp90 chaperone machinery fails to protect against Tau aggregation during disease.

## Publication

Parts of this work have been already published. Excerpts from this publication used in this work encompass chapter 3.1 and parts of chapter 4.1. A detailed list of the adopted items with the corresponding figures in this work can be found in the Appendix (see chapter 7.1).

### 2020 Molecular basis of the interaction of Hsp90 with its co-chaperone Hop

A Lott, J Oroz, M Zweckstetter

*Protein Science* 2020 Oct 19. doi: 10.1002/pro.3969

Author contributions: AL prepared proteins and performed experiments and data analysis. JO performed Hsp90 NMR assignments. AL and MZ designed the project and wrote the paper.

# List of Contents

Acknowledgments.....	III
Summary.....	VI
Publication.....	VIII
List of Figures.....	XII
List of Tables.....	XV
Abbreviations.....	XVI
<b>1 Introduction.....</b>	<b>1</b>
1.1 Proteostasis.....	1
1.1.1 Protein production.....	1
1.1.2 Protein retention.....	4
1.1.3 Protein degradation.....	4
1.2 Molecular chaperones.....	5
1.2.1 Chaperonins.....	5
1.2.2 Heat shock proteins.....	6
1.3 The Hsp70/Hsp90 chaperone machinery.....	7
1.3.1 Hsp70.....	8
1.3.2 Hsp40.....	9
1.3.3 Hsp90.....	11
1.3.4 Hop.....	13
1.3.5 p23.....	14
1.3.6 A structural model of the Hsp70/Hsp90 chaperone machinery.....	15
1.4 Intrinsically disordered proteins.....	17
1.5 IDP-associated proteinopathies.....	17
1.6 The IDP Tau.....	19
1.6.1 Tau physiology.....	19
1.6.2 Tau pathophysiology.....	21
1.6.3 The chaperoning of Tau.....	22
1.7 Aim of this thesis.....	24
<b>2 Material and Methods.....</b>	<b>25</b>
2.1 Material.....	25
2.1.1 Consumables.....	25
2.1.2 Instruments.....	26
2.1.3 Chemicals.....	27
2.1.4 Enzymes.....	29
2.1.5 E. coli competent cells.....	29

2.1.6	Plasmids .....	29
2.1.7	Software .....	29
2.2	General methods.....	30
2.2.1	SDS page.....	30
2.2.2	Native page.....	31
2.2.3	Chromatography .....	32
2.2.4	Concentration determination .....	33
2.3	Protein expression and purification.....	34
2.3.1	Stock solutions.....	35
2.3.2	Cloning.....	36
2.3.3	Transformation and o/n culture .....	38
2.3.4	Purification protocols.....	38
2.4	In vitro complex reconstitution .....	48
2.5	Affinity measurements.....	49
2.5.1	Chemical Assay by gel electrophoresis .....	49
2.5.2	Trp fluorescence.....	50
2.5.3	Isothermal titration calorimetry.....	50
2.6	Nuclear magnetic resonance spectroscopy .....	52
2.6.1	Heteronuclear single quantum coherence (HSQC) .....	53
2.6.2	Transverse relaxation optimized spectroscopy (TROSY) .....	54
2.6.3	Data processing .....	56
2.7	Protein phosphorylation and acetylation.....	57
2.8	Dynamic light scattering.....	57
2.9	Chemical cross-linking.....	59
2.10	Sucrose density gradient centrifugation .....	60
2.11	Molecular weight determination .....	60
2.12	Mass spectrometry.....	61
2.12.1	Identification of phosphorylation sites by LC-MS/MS.....	61
2.12.2	Cross-link analysis by LC-MS/MS .....	61
<b>3</b>	<b>Results .....</b>	<b>63</b>
3.1	Hop stabilizes Hsp90 in a V-shaped conformation .....	63
3.1.1	In vitro reconstitution of the Hsp90:Hop complex.....	63
3.1.2	Hop binds Hsp90's open state with high affinity.....	64
3.1.3	Hop stabilizes Hsp90 in an extended conformation .....	66
3.1.4	Hop's TPR2A-2B domains determine the affinity for the CTD and MD of Hsp90 .....	69
3.1.5	The Hop:Hsp90-CTD interaction is sufficient to induce the V-shaped state .....	71
3.2	The human Hsp70/Hsp90 association decisively relies on the adaptor Hop .....	72
3.2.1	In vitro reconstitution of the Hsp70:Hop:Hsp90 complex.....	72
3.2.2	The Hsp70/Hsp90 chaperone machinery comprises two copies of Hsp70 .....	73
3.3	The Hsp70/Hsp90 chaperone machinery interacts with the intrinsically disordered protein Tau.....	76
3.3.1	Formation of the client-loading complex .....	76

3.3.2	Tau prefers to bind the Hsp70/Hsp90 chaperone machinery over the individual chaperones .....	78
3.3.3	Tau's repeat region is the main interaction site with the Hsp70:Hsp90 complex .....	79
3.3.4	Tau's P2 / R' domains effectively contribute to the Hsp70:Hsp90:Tau interaction .....	81
3.4	The co-chaperone p23 stabilizes the Hsp70:Hsp90:Tau interaction .....	82
3.4.1	In vitro reconstitution of the Hsp70:Hsp90:Tau:p23 complex .....	82
3.4.2	p23 interaction is cooperatively enhanced in the presence of Tau .....	83
3.4.3	Tau's repeat region as the major binding site within the Hsp70:Hsp90:Tau:p23 complex .....	84
3.5	Structural insights into the 750 kDa (Hsp70 <sub>1</sub> :Hop <sub>1</sub> :Hsp90 <sub>2</sub> :Tau <sub>1</sub> :p23 <sub>1</sub> ) <sub>2</sub> complex .....	87
3.5.1	The binding of Tau evokes the dimerization of the Hsp70/Hsp90 chaperone machinery .....	87
3.5.2	A single Tau molecule, embraced in the center of each Hsp70/Hsp90 chaperone machinery, determines the localization of p23 .....	89
3.5.3	A structural model of the dimeric (Hsp70 <sub>1</sub> :Hop <sub>1</sub> :Hsp90 <sub>2</sub> :Tau <sub>1</sub> :p23 <sub>1</sub> ) <sub>2</sub> complex .....	93
3.5.4	Hsp90's charged linker region remains unbound within the Hsp70/Hsp90 chaperone machinery .....	94
3.6	Balance between the assembly and disassembly of the Hsp70/Hsp90 chaperone machinery .....	95
3.7	The Hsp70/Hsp90 chaperone machinery likewise recognizes pathologic Tau .....	97
3.7.1	Post-translationally modified Tau as client of the Hsp70/Hsp90 chaperone machinery .....	97
3.7.2	Pathologic Tau associates with the Hsp70/Hsp90 chaperone machinery similar to normal Tau, but the interaction with Hsp90 alone is lost .....	98
<b>4</b>	<b>Discussion .....</b>	<b>101</b>
4.1	The assembly of the Hsp70:Hsp90 complex .....	101
4.1.1	The Hsp90:Hsp interaction .....	102
4.1.2	The Hsp70:Hsp90 complex .....	104
4.2	The Hsp70/Hsp90 chaperone machinery as a protective shell .....	106
4.3	p23 serves for Tau binding .....	108
4.4	The alternation of Hop and CHIP controls the Hsp70/Hsp90 chaperone machinery:Tau interaction .....	110
4.5	The Hsp70/Hsp90 chaperone machinery:Tau interaction is independent on ATP hydrolysis .....	111
4.6	The role of Hsp40 for Tau binding to Hsp70 .....	112
4.7	Tau chaperoning by the Hsp70/Hsp90 chaperone machinery .....	113
4.8	Pathologic Tau as substrate of the Hsp70/Hsp90 chaperone machinery .....	115
<b>5</b>	<b>Outlook .....</b>	<b>117</b>
<b>6</b>	<b>References .....</b>	<b>118</b>
<b>7</b>	<b>Appendix .....</b>	<b>144</b>
7.1	List of published items .....	144
7.2	Supplementary Information .....	144



## List of Figures

Figure 1 Proteostasis includes the dynamic interplay between protein production, retention and degradation. ....	2
Figure 2 The process of protein folding holds difficulties with the major risk of protein aggregation due to misfolding. ....	2
Figure 3 Energy landscapes of folded and intrinsically disordered proteins. ....	3
Figure 4 The heat shock protein Hsp70. ....	8
Figure 5 The co-chaperone Hsp40. ....	10
Figure 6 The heat shock protein Hsp90. ....	12
Figure 7 The co-chaperone Hop. ....	14
Figure 8 The co-chaperone p23. ....	15
Figure 9 The Hsp70/Hsp90 chaperone machinery in protein folding. ....	16
Figure 10 The proteome includes folded, partially folded and intrinsically disordered proteins. ..	17
Figure 11 Biological role of the intrinsically disordered protein Tau. ....	19
Figure 12 Neurodegeneration is associated with the deposition of insoluble protein aggregates in the patients' brains. ....	21
Figure 13 Selectively <sup>1</sup> H- <sup>13</sup> C labeled Hsp90 at the Ile δ-methyl groups. ....	45
Figure 14 Selectively <sup>15</sup> N-labeled Tau. ....	48
Figure 15 The <sup>15</sup> N- <sup>1</sup> H HSQC pulse sequence selects for covalently bound NH-groups. ....	53
Figure 16 The methyl-TROSY pulse sequence selects for <sup>13</sup> C- <sup>1</sup> H labeled CH-bonds. ....	55
Figure 17 <i>In vitro</i> reconstitution of the Hsp90:Hop complex. ....	63
Figure 18 Hop preferentially binds the open conformation of Hsp90. ....	64
Figure 19 A single Hop molecule binds the Hsp90 dimer with high affinity. ....	65
Figure 20 TROSY NMR of Hsp90 in presence of AMP-PNP. ....	66
Figure 21 TROSY NMR of Hsp90 in presence of Hop. ....	67
Figure 22 Model for the Hsp90 <sub>2</sub> :Hop <sub>1</sub> complex. ....	68
Figure 23 Comparison of the Hsp90 interaction with Hop and Aha1. ....	69
Figure 24 <i>In vitro</i> reconstitution of the Hsp90:Hop112a complex. ....	70
Figure 25 TROSY NMR of Hsp90 in presence of Hop112a. ....	71
Figure 26 <i>In vitro</i> reconstitution of the Hsp70/Hsp90 chaperone machinery. ....	73
Figure 27 TROSY NMR of Hsp90 in the Hsp70/Hsp90 chaperone machinery. ....	74
Figure 28 Hsp70 binding to the Hsp90:Hop complex. ....	75
Figure 29 <i>In vitro</i> reconstitution of the Hsp70/Hsp90 chaperone machinery: Tau interaction. ....	76
Figure 30 Interaction of Tau with individual proteins of the Hsp70/Hsp90 chaperone machinery base. ....	77
Figure 31 Affinity measurements of Tau binding to the Hsp70/Hsp90 chaperone machinery. ...	78
Figure 32 NMR pH titration of <sup>15</sup> N-labeled Tau used to transfer the backbone assignment from pH 6.8 to pH 7.4. ....	79
Figure 33 NMR spectroscopy of Tau binding to the Hsp70:Hop:Hsp90 complex. ....	80

Figure 34 <i>In vitro</i> reconstitution of the interaction of the Hsp70/Hsp90 chaperone machinery with smaller Tau constructs.....	81
Figure 35 <i>In vitro</i> reconstitution of the Hsp70:Hop:Hsp90:Tau:p23 complex.....	82
Figure 36 Interaction of p23 with Hsp70 and Hsp90.....	83
Figure 37 TROSY NMR of Hsp90 in presence of p23.....	84
Figure 38 Influence of p23 binding to the Hsp70:Hop:Hsp90:Tau complex on Tau dynamics....	85
Figure 39 Comparison of Tau interaction with Hsp70, Hsp90 and the Hsp70/Hsp90 chaperone machinery.....	86
Figure 40 Sucrose density gradient and size exclusion chromatography (SEC) of the Hsp70/Hsp90 chaperone machinery in complex with Tau and p23.....	87
Figure 41 Molecular weight determination of the Hsp70/Hsp90 chaperone machinery:Tau complexes.....	88
Figure 42 Cross-linking reaction of the Hsp70/Hsp90 chaperone machinery:Tau complex using DSS and EDC.....	90
Figure 43 Intramolecular cross-link analysis of the Hsp70:Hop:Hsp90:Tau:p23 complex using DSS and EDC.....	91
Figure 44 Intermolecular cross-link analysis of the Hsp70:Hop:Hsp90:Tau:p23 complex cross-linked with DSS.....	92
Figure 45 Model of the dimeric (Hsp70 <sub>1</sub> :Hop <sub>1</sub> :Hsp90 <sub>2</sub> :Tau <sub>1</sub> :p23 <sub>1</sub> ) <sub>2</sub> complex.....	93
Figure 46 TROSY NMR of the Hsp70/Hsp90 chaperone machinery:Tau and machinery:Tau:p23 complexes.....	94
Figure 47 The E3-ubiquitin ligase CHIP dissociates the Hsp70/Hsp90 chaperone machinery....	96
Figure 48 The interaction of the Hsp70/Hsp90 chaperone machinery with phosphorylated and acetylated Tau.....	97
Figure 49 Phosphorylation pattern of Cdk2 kinase on Tau.....	99
Figure 50 <i>In vitro</i> reconstitution of the interaction of the Hsp70/Hsp90 chaperone machinery with pathologic P <sup>Cdk2</sup> Tau.....	100
Figure 51 High affinity interaction sites on Hop for the C-terminal peptides of Hsp70 and Hsp90.....	102
Figure 52 Hop stabilizes Hsp90 in a V-shaped conformation.....	103
Figure 53 Hsp70 and Hsp90 interaction with the TPR domains of Hop.....	104
Figure 54 The Hsp70:Hop:Hsp90 complex comprises two Hsp70 molecules.....	105
Figure 55 Tau binding to the Hsp70/Hsp90 chaperone machinery induces its dimerization.....	107
Figure 56 The (Hsp70 <sub>1</sub> :Hop <sub>1</sub> :Hsp90 <sub>2</sub> :Tau <sub>1</sub> ) <sub>2</sub> dimer is stabilized by p23.....	109
Figure 57 The co-chaperones Hop and CHIP compete for the binding to Hsp70 and Hsp90...110	
Figure 58 Cartoon representation of the Hsp70/Hsp90 chaperone machinery-mediated Tau chaperoning.....	113
Figure 59 Tetrameric states of Hsp90.....	114
Figure 60 Balance between protein retention and degradation of normal Tau and pathologic P <sup>Cdk2</sup> Tau.....	116

Figure A 1 The pET28a cloning vector. ....	148
Figure A 2 The pNG2 cloning vector encoding the protein Tau. ....	149
Figure A 3 Purification of the CHIP protein (tagged: 38.68 kDa; cut: 36.79 kDa) <i>via</i> IMAC (Ni-NTA) and SEC. ....	151
Figure A 4 Purification of the Hop protein (65.09 kDa) <i>via</i> IMAC (Ni-NTA) and SEC.....	151
Figure A 5 Purification of the Hop112a protein (tagged: 43.21 kDa; cut: 41.33 kDa) <i>via</i> IMAC (Ni-NTA) and SEC. ....	152
Figure A 6 Purification of the Hsp40 protein (tagged: 40.26 kDa; cut: 38.38 kDa) <i>via</i> IMAC (Ni-NTA) and SEC. ....	152
Figure A 7 Purification of the Hsp70 protein (tagged: 74.03 kDa; cut: 72.15 kDa) <i>via</i> IMAC (Ni-NTA) followed by tag cleavage, a second IMAC (Ni-NTA) and SEC. ....	152
Figure A 8 Purification of the Hsp90 protein (85.72 kDa) <i>via</i> IMAC (Ni-NTA) and SEC.....	153
Figure A 9 Purification of the Hsp90* protein (96.55 kDa) <i>via</i> IMAC (Ni-NTA) and SEC.....	153
Figure A 10 Purification of the p23 protein (tagged: 21.15 kDa; cut: 19.27 kDa) <i>via</i> IMAC (Ni-NTA) and SEC. ....	153
Figure A 11 Purification of the Tau protein (45.85 kDa) <i>via</i> IEX and SEC. ....	154
Figure A 12 Tau NMR spectra in presence of Hsp90, Hsp70 and p23. ....	154

## List of Tables

Table 1 Examples for proteinopathies associated with IDP aggregation. <sup>264-266</sup> .....	18
Table 2 Consumables with supplier in alphabetical order.....	25
Table 3 Instruments with supplier in alphabetical order.....	26
Table 4 Chemicals with supplier in alphabetical order.....	27
Table 5 Enzymes with supplier in alphabetical order.....	29
Table 6 <i>E. coli</i> competent cells with supplier in alphabetical order.....	29
Table 7 Plasmids with supplier in alphabetical order.....	29
Table 8 Software with developer in alphabetical order.....	29
Table 9 Pipetting scheme for SDS-gels.....	31
Table 10 Column specifications used for IMAC, SEC and IEX. ....	33
Table 11 Characteristics of proteins used in this work.....	34
Table 12 Sequences of the reverse (rvs) and forward (fwd) primer used for Hop112a amplification through PCR.....	36
Table 13 PCR reaction setup and cycling protocol for Hop112a DNA amplification.....	36
Table 14 Reaction setups for DNA restriction and ligation.....	37
Table 15 Experimental protocols for the <i>in vitro</i> reconstitution of the Hsp70/Hsp90 chaperone machinery.....	72
Table 16 In vitro Tau phosphorylation sites using Cdk2 kinase detected by mass spectrometry..	99
Table 17 Reported affinity values of Hop for Hsp70 and Hsp90.....	101
Table 18 Top: Reported affinity values of CHIP for Hsp70 and Hsp90. Bottom: Protein amounts of Hsp70, Hsp90, Hop and CHIP <i>in vivo</i> .....	111
Table A 1 Gene sequences of the proteins used in this work.....	144
Table A 2 Protein sequences of the proteins used in this work.....	150
Table A 3 Selected intra- and intermolecular cross-links within the Hsp70:Hop:Hsp90:Tau:p23 complex cross-linked with disuccinimidyl suberate (DSS).....	155
Table A 4 Selected intra- and intermolecular cross-links within the Hsp70:Hop:Hsp90:Tau:p23 complex cross-linked with 1-ethyl-3-(3-dimethylaminopropyl) carbodiimid (EDC).....	163

## Abbreviations

°C	Degree celsius
A	Absorption
Å	Angstrom
ADP	Adenosine diphosphate
Aha1	Activator of Hsp90 ATPase
Amp	Ampicillin
AMP-PNP	Adenosine $\gamma$ -imidotriphosphate
ATP	Adenosine triphosphate
B	Magnetic field
BCA	Bicinchonin acid
c	Concentration
Cdk	Cyclin dependent kinase
CHIP	Carboxyl terminus of Hsc70-interacting protein
cl	Charged linker
CNS	Central nervous system
COC	Cylin olefin copolymer
CSM	Cross-link spectrum match
CSP	Chemical shift perturbation
CTD	C-terminal domain
cv	Column volume
D	Diffusion coefficient
Da	Dalton
DLS	Dynamic light scattering
DNA	Deoxyribonucleic acid
dNTP	Deoxyribose nucleoside triphosphate
DP domain	Domain rich in aspartates and prolines
DS	Dummy scans
DSS	Disuccinimidyl suberate
DTT	Dithiothreitol
<i>E. coli</i>	Escherichia coli
EDC	1-ethyl-3-(3-dimethylaminopropyl)carbodiimide
EDTA	Ethylenediaminetetraacetic acid
ER	Endoplasmic reticulum
EtOH	Ethanol
F	Fluorescence
FID	Free induction decay
fwd	Forward
g	Gram / gravity

G	Gibbs free energy
GR	Glucocorticoid receptor
GTP	Guanosine triphosphate
h	Hour
H	Enthalpy
HEPES	4-(2-hydroxyethyl)-1-piperazineethanesulfonic acid
HF	High fidelity
His	Histidine
Hop	Hsp organizing protein
Hsp	Heat shock protein
HSQC	Heteronuclear single quantum coherence
I	Intensity / Isoleucine
IDP	Intrinsically disordered protein
IEX	Ion exchange chromatography
Ile	Isoleucine
IMAC	Immobilized metal affinity chromatography
INEPT	Insensitive nuclei enhancement by polarization transfer
IPTG	Isopropyl- $\beta$ -D-thiogalactopyranoside
ITC	Isothermal titration calorimetry
k	Kilo
Kan	Kanamycin
$k_B$	Boltzmann constant
$K_D$	Dissociation equilibrium constant
L	Liter
LB	Luria Broth
LC	Liquid chromatography
LSB	Laemmli sample buffer
M	Molarity
m	Milli
m	Meter
MALS	Multi angle light scattering
MARK	Microtubule affinity regulating kinase
max.	Maximum
MD	middle domain
MHz	Megahertz
min	Minute
Mpa	Megapascal
MS	Mass spectrometry
MW	Molecular weight
n	Nano

NBD	Nucleotide binding domain
NEF	Nucleotide exchange factor
NIH	National Institute of Health
NMR	Nuclear magnetic resonance
NS	Number of scans
NTA	Nitrilotriacetic acid
NTD	N-terminal domain
o/n	Over night
o/w	Over weekend
OD <sub>600</sub>	Optical density at $\lambda=600\text{nm}$
Page	Polyacrylamide gel electrophoresis
PCR	Polymerase chain reaction
pD	pH of deuterated solutions ( $=\text{pH}+0.2$ )
PDB	Protein data bank
pH	Potentia hydrogenii
PMSF	Phenylmethylsulfonylfluoride
PPIase	Peptidyl-prolyl-cis-trans-isomerase
pSEC	Peptide size exclusion chromatography
Q	Heat
R	Universal gas constant
RF	Radio frequency
$R_b$	Hydrodynamic radius
RNA	Ribonucleic acid
rpm	Rounds per minute
RT	Room temperature
rvs	Reverse
S	Entropy
SBD	Substrat binding domain
SD	Superdex
SDS	Sodium dodecyl sulfate
SEC	Size exclusion chromatography
sec	Seconds
Sulfo-NHS	N-hydroxysulfosuccinimide
T	Temperature
$T_2$	Transverse relaxation
TCEP	Tris(2-carboxyethyl)phosphin
TGS buffer	Tris Glycine SDS buffer
TPR	Tetratricopeptide repeat
Tris	Tris(hydroxymethyl)aminomethan
TROSY	Transverse relaxation optimized spectroscopy

Trp	Tryptophane
U	Units
UTP	Uridine triphosphate
UV	Ultraviolet
V	Volume / Volt
v/v	Volume per volume
w/v	Weight per volume
$\beta$ -ME	$\beta$ -Mercaptoethanol
$\epsilon$	Extinction coefficient
$\eta$	Viscosity
$\lambda$	Wavelength
$\mu$	Micro





# 1 Introduction

---

Every single life relies on the impressive phenomenon called proteostasis. Proteostasis implies a well-balanced proteome including the continuous protein production and protein degradation, and in between the regulated protein localization for proper cellular function.<sup>1</sup> Ideally, the whole system can adapt to external influences as needed but given the complexity of proteostasis, errors can occur.<sup>2</sup> Yet incurable human diseases including neurodegenerative disorders demonstrate what happens if proteostasis is no longer maintained.<sup>2-4</sup> Major hallmarks are deposits of insoluble, disease specific protein aggregates causing proteome imbalance.<sup>5</sup> Knowing what proteostasis is, how proteostasis is regulated and how one can therapeutically target key players involved in proteostasis is pivotal for the treatment of the diseases.<sup>6,7</sup>

## 1.1 Proteostasis

In principle, proteostasis is a compound word made up of ‘protein’ and ‘homeostasis’.<sup>2,8,9</sup> It describes the balanced equilibrium of cellular protein amounts, collectively called the proteome. The proteome is not a static condition but rather dynamically varies in composition.<sup>10</sup> Depending on the current state, such as cell proliferation, any kind of stress, heat, infections etc., different proteins and protein levels are needed compared to the resting state.<sup>11-14</sup> Hence, protein quantities must be constantly up- or down-regulated and proteins must be produced and degraded as needed to maintain proteostasis.<sup>15</sup>

On balance, proteins pass through distinct phases involving protein production, protein retention and protein degradation (Figure 1).<sup>1</sup> Each of them contains critical elements that could promote protein aggregation, hence harm proteostasis, and thus need to be carefully controlled.<sup>16</sup>

### 1.1.1 Protein production

Proteins are large peptides that consist of up to thousands of amino acids attached to one another.<sup>17</sup> Each single amino acid has to be incorporated after the other, a process that is called protein translation.<sup>18</sup> The production site is the ribosome, from which plain peptide strands of different lengths are released.<sup>19,20</sup> Depending on their amino acid composition, proteins can adopt a distinct three-dimensional structure including variable folded and less structured regions or be completely disordered (see chapter 1.4).<sup>21</sup>

## Introduction

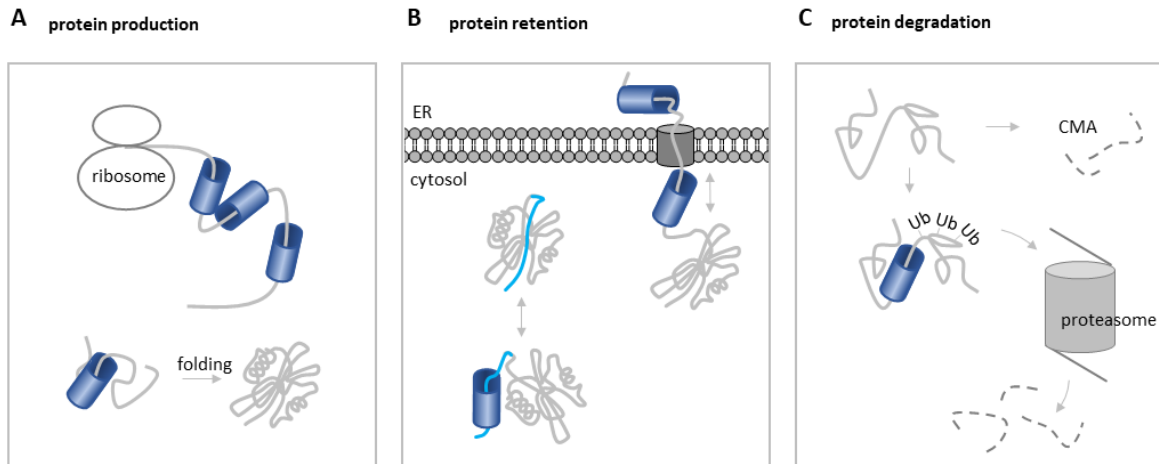


**Figure 1** Proteostasis includes the dynamic interplay between protein production, retention and degradation.

Each process is carefully controlled and regulated by molecular chaperones (blue barrels) that assist proteins (depicted as grey lines) throughout their lifetime.<sup>22</sup> **A** Chaperones promote the protein's native state. In this process they can interact already co-translationally with the newly synthesized peptide chain.<sup>23</sup> **B** Chaperones can hold proteins in the cell awaiting the ligand to bind<sup>24</sup> or assist during protein translocation between cell organelles (e.g. cytosol and endoplasmic reticulum (ER)).<sup>25</sup> **C** If proteins are no longer needed chaperones can initiate their degradation *via* the chaperone mediated autophagy (CMA)<sup>26</sup> or the proteasome that recognizes ubiquitinated (Ub) proteins.<sup>27</sup>

To avoid undesired interactions, both intra- and intermolecular, freshly translated peptide chains should be shielded as soon as possible.<sup>28,29</sup> Especially proteins consisting of rather long peptide chains are exposed to a high risk acquiring inactive conformations or entering unfavorable protein-protein interactions (Figure 2).<sup>8,30</sup>

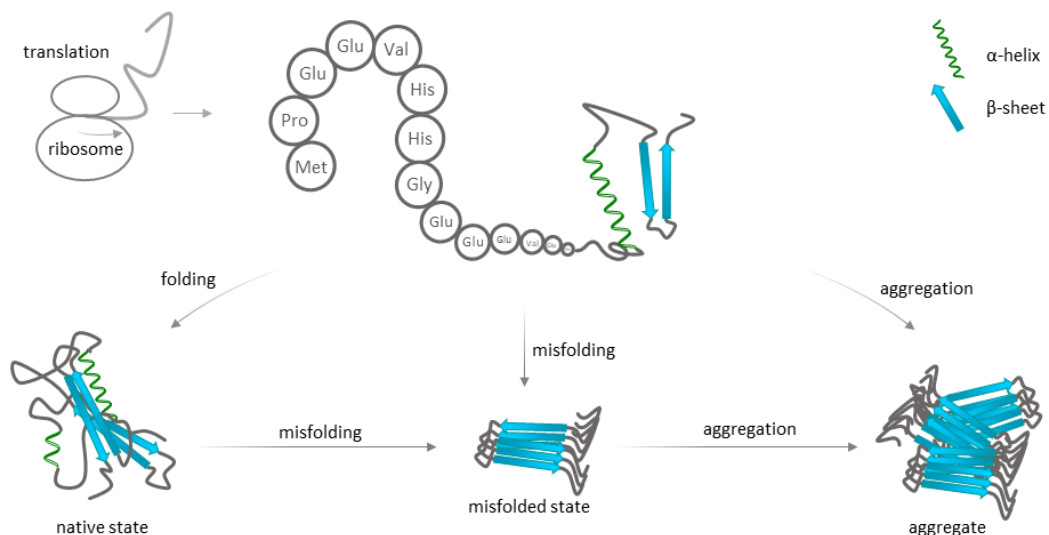


**Figure 2** The process of protein folding holds difficulties with the major risk of protein aggregation due to misfolding.

The amino acid chain produced at the ribosome can locally fold into  $\alpha$ -helices and  $\beta$ -sheets dependent on the respective amino acid composition.<sup>21</sup> The formation of additional intramolecular contacts ideally yields the protein's native state. Undesired interactions may lead to misfolding, which in great measure causes the accumulation of inactive protein aggregates.<sup>31</sup> The specific group of intrinsically disordered proteins (IDPs) is unable to fold and thus is particularly vulnerable for misfolding.<sup>32</sup> The illustration refers to a review from Hipp et al.<sup>8</sup>

## Introduction

In fact, proteins are thought to traverse through a jungle of potential conformations to finally adopt their required, active state.<sup>33</sup> This is best depicted with the proposed metaphor of a folding funnel.<sup>34</sup> Here, the energy landscape signifies multiple local minima with the active state representing the intended minimum (Figure 3A).<sup>35</sup> To avoid that proteins rest within local minima, the cell has developed helper proteins assisting their way out so that different, ideally lower energy states can be acquired. These helper proteins are called molecular chaperones, which literally take the proteins in need of help by their 'hand' and conduct them to their active form.<sup>22,28,36,37</sup> Notable, though functioning as folding catalysts, the chaperones have no effect on the proteins three-dimensional structure.<sup>38</sup>

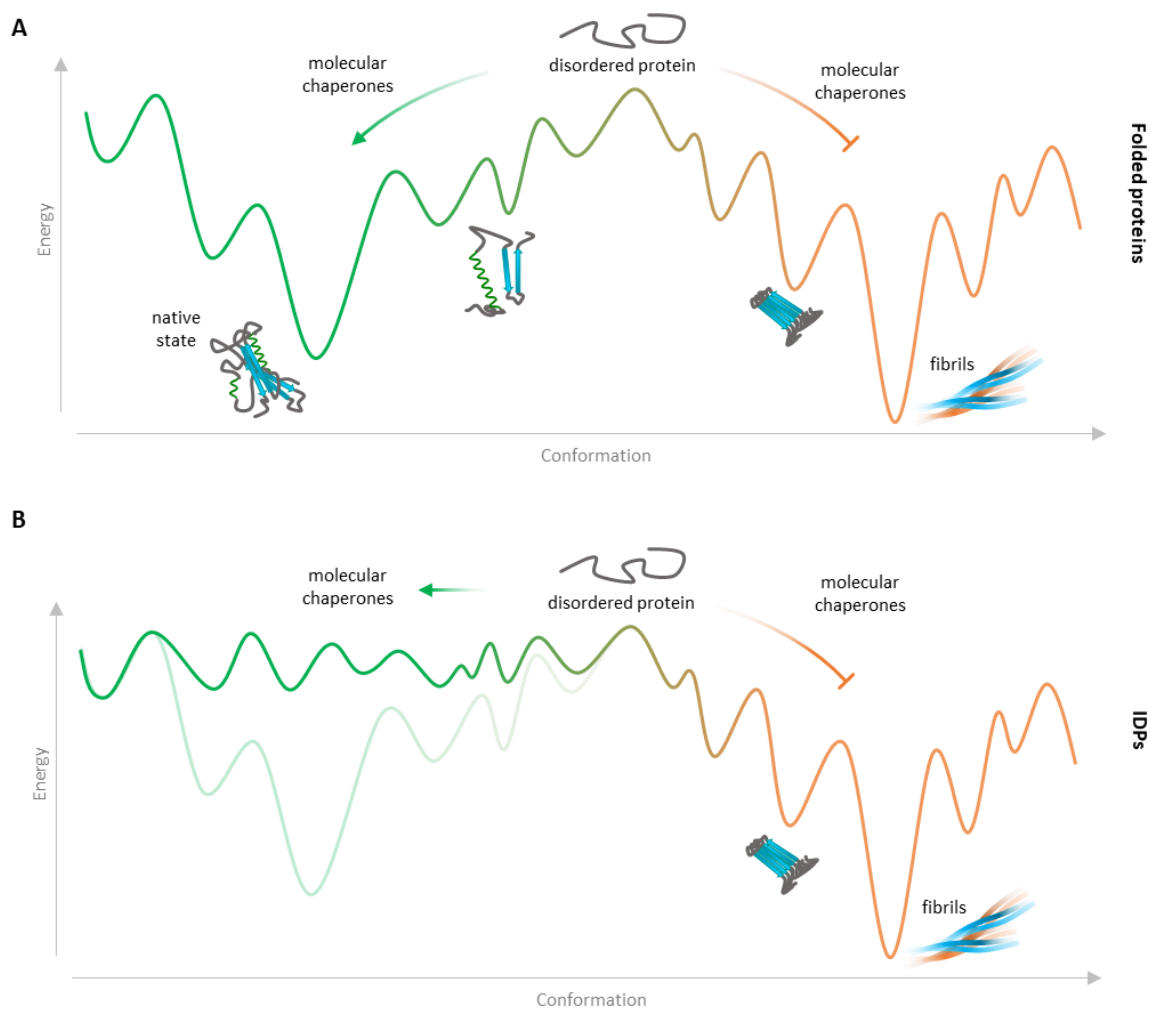


**Figure 3 Energy landscapes of folded and intrinsically disordered proteins.**

**A** A model of the protein folding pathway with multiple local minima.<sup>35</sup> Molecular chaperones help the proteins to navigate towards their native state, by overcoming the free energy barriers that hold them up to follow their downhill path (green line). At the same time they counteract protein aggregation (orange line) to prevent the formation of insoluble fibrils. **B** In the case of intrinsically disordered proteins (IDPs) molecular chaperones are essential to hold the proteins in their unfolded state and prevent undesired contacts. As the unfolded conformations capture (on average) equal energy levels, the aggregation pathway is accessible at any time.<sup>39</sup>

During protein production a special role is to be assigned to intrinsically disordered proteins (IDPs).<sup>40,41</sup> These proteins lack a distinct three-dimensional structure in their unbound state (see chapter 1.4).<sup>42</sup> Being intrinsically disordered, such proteins can adopt multiple conformations, but with on average equal energy (Figure 3B). Due to this property, IDPs pose a particularly high risk for protein aggregation at all times.<sup>32</sup>

### 1.1.2 Protein retention

Once an active protein is produced, it should fulfill its inherent function. Proteins act *via* interactions with other proteins<sup>43</sup>, membranes<sup>44,45</sup> or metal ions.<sup>46</sup> Thereby, they perform diverse tasks, which are crucial for cellular function. However, it is not self-evident that the respective interaction partner is available at the same time or present at the same place. Hence, proteins need to be kept soluble throughout their lifetime awaiting interaction partners to bind.<sup>22</sup> Proceeding from the co-translational support of molecular chaperones to omit undesired interactions<sup>23</sup>, they are likewise assisting proteins while waiting for their action by specifically hiding vulnerable or labile regions.<sup>24</sup> The interaction with chaperones can also hold proteins in an inactive state, which are then activated in the presence of the interacting partner (Figure 1B).<sup>47,48</sup> Besides, molecular chaperones cooperate in intracellular protein translocation, where they unfold proteins on one side of the membrane and refold them on the other side and by that transport proteins between different cell compartments.<sup>25</sup> Since errors can never be ruled out, the refolding capacity of chaperones plays an outstanding role able to break up harmful protein-protein interactions and refold them properly.<sup>49,50</sup> However, if refolding fails or appears to be inefficient, the chaperone network can beyond direct proteins to degradation pathways.<sup>51</sup>

### 1.1.3 Protein degradation

When proteins are no longer needed, irreparably misfolded or of foreign (food/ pathogen) origin, various degradation pathways are available to disassemble the peptide chains into their building blocks from which new proteins can be produced.<sup>52-56</sup> On the one hand the chaperone network can engender the ubiquitination of proteins, tagging them for proteasomal degradation (Figure 1C).<sup>27,57-59</sup> On the other hand, proteins can be dissected *via* chaperone mediated autophagy<sup>26,60</sup>, where proteins are transferred to lysosomes. The acidic environment of the lysosome evokes the denaturation of proteins, upon which numerous proteolytic enzymes can initiate protein degradation.<sup>61</sup>

Evidently, molecular chaperones control the stability of proteins in multiple ways, and thus possess superior function.<sup>22,37,62</sup> So far, ‘molecular chaperones’ was used as a general term synonymous with a large family of helper proteins. However, extensive research revealed a detailed knowledge about different chaperone families, their members and composition, structure and functional mechanisms.

### 1.2 Molecular chaperones

Consistent with the complexity of a cell, the network of molecular chaperones is vast and sophisticated, and itself fine tunable as needed.<sup>63,64</sup> In fact, both prokaryotes and eukaryotes depict molecular chaperones that contribute to a fluent cell metabolism.<sup>65</sup> There are several ways reported to classify chaperones<sup>64,66</sup>, including a distinction between chaperonins and heat shock proteins (Hsps)<sup>67</sup> – two distinct subfamilies that act and function in different ways.

#### 1.2.1 Chaperonins

Chaperonins are huge (~1 MDa in size) donut-like ring structures.<sup>68,69</sup> Two ring layers are stacked on top of each other yielding a cylindrical barrel that is hollow in its center, whereby both rings have individual chaperone activity.<sup>70,71</sup> Each ring of the chaperonin dimers consists of a different number of subunits (dependent on which organism you are looking at)<sup>72</sup>, with each of them capable of binding and hydrolyzing ATP.<sup>73,74</sup>

The bacterial chaperonin (group I) is termed GroEL.<sup>74,75</sup> The structure and function of GroEL is dependent on the co-chaperonin GroES acting as a lid from above or below to enclose substrates inside of the respective GroEL monomer cavity.<sup>71</sup> Substrate trapping and folding is directed by the ingenious decrease of surface hydrophobicity from the hydrophobic port binding hydrophobic regions of unfolded proteins, towards the hydrophilic cavity likely to accelerate protein folding.<sup>76,77</sup> The eukaryotic homologue of GroEL is TRiC (group II) (T-Ring Complex, also known as CCT: chaperone containing TCP-1).<sup>68</sup> Though being structurally highly similar, eukaryotic TRiC lacks a detachable homologue of GroES.<sup>78</sup> Instead, the structure of TRiC includes itself a lid region that seals the barrel upon substrate binding through interdomain rearrangements.<sup>79</sup> The ability to accelerate the folding of substrates within a shielded system is unique.<sup>80</sup> For this reason, chaperonins play a key role in cell proliferation, where protein biosynthesis is particularly high.<sup>81</sup> However, the function of chaperonins is effectively constrained to protein (re-)folding only<sup>80</sup> and thus might have little relevance to the chaperoning of IDPs, which inherently resist protein folding (see chapter 1.4). Here, another chaperone family, the heat shock proteins, comes into play.<sup>82-84</sup>

### 1.2.2 Heat shock proteins

The heat shock proteins (Hsps) are ubiquitous and multifunctional chaperones.<sup>85,86</sup> With regard to their structure and function, the Hsp family is made up of a variety of diverse members that have been historically classified according to their molecular weight.<sup>87</sup> These include Hsp100s, Hsp90s, Hsp70s, Hsp60s and small Hsps (sHsps) depicting masses of ~100 kDa, 90 kDa, 70 kDa, 60 kDa and <40 kDa in their monomeric state.

Hsp100s are unique ‘disaggregases’ in bacteria, yeast and plants<sup>88</sup> capable to unwind protein aggregates after heat stress.<sup>89</sup> However, they do not exist in animals or humans.<sup>88,90</sup> Hsp90 and Hsp70 have been assigned a central role in protein chaperoning.<sup>91-93</sup> They use the energy of ATP hydrolysis to control functional protein turnover being involved in protein (re-)folding<sup>94</sup>, protein activation<sup>77</sup>, transport<sup>95</sup> and degradation<sup>96</sup> as well as the disaggregation of harmful protein deposits.<sup>97,98</sup> Hsp60 represents the subunits of the group I chaperonin rings<sup>74</sup>, and as such is exclusively involved in protein folding. Lastly, small Hsps are likewise present from bacteria to humans and essentially counteract protein aggregation by binding misfolded proteins.<sup>99</sup> They act as holdases awaiting substrate disaggregation wherefore they do not require ATPase activity.<sup>90</sup>

Maintaining soluble proteins to counteract protein aggregation requires stoichiometric concentrations of chaperones relative to the amount of un(-properly) folded proteins.<sup>90</sup> Accordingly, heat shock proteins are present at higher levels when the cell is stressed<sup>86,100</sup>, which among other things can be heat – the stress factor after which they have been named.<sup>87</sup> Elevated levels of chaperones are prompted by the heat shock response causing the release of heat shock transcription factors that induce the expression of heat shock genes.<sup>101,102</sup> The process is termed auto-induction, as under normal, non-stressed conditions these factors are bound by the chaperones and thereby kept in an inactive state.<sup>103-105</sup> However, as soon as the chaperones are increasingly required for protein control due to increased amounts of un-/ misfolded proteins, the transcription factors are automatically released, whereupon they bind DNA and stimulate the expression of additional chaperones.<sup>90,106,107</sup> The adverse process of chaperone downregulation is alike auto-induced, and thus termed auto-inhibition. As soon as the cell has recovered, an excess of chaperones without interaction partner is present. These uncommitted chaperones are able to re-bind the transcription factors holding them back in an inert state.<sup>103,108</sup> Finally, the excess of chaperones can be diminished like all other proteins *via* traditional degradation pathways (see chapter 1.1.3).<sup>109</sup>

Hsp70 and Hsp90 represent the most abundant Hsps in the cell<sup>110,111</sup> and possess the most versatile functions among all members of the chaperone network.<sup>112,113</sup> Their operation mode is adjusted by an additional layer of regulation constructed by a variety of chaperone assistants termed co-chaperones.<sup>114,115</sup> Despite the close resemblance of the prokaryotic and eukaryotic Hsp systems, the eukaryotic network is more complex. In fact, bacterial Hsp70 (DnaK) has only two co-chaperones (DnaJ and the nucleotide exchange factor NEF), Hsp90 (HtpG) has none.<sup>93</sup> In contrast, eukaryotic co-chaperones can be Hsp70-specific (e.g. Hsp40s, NEFs)<sup>114,116</sup>, interact with each Hsp70 and Hsp90 (e.g. Hop, CHIP)<sup>94,96,117</sup> or specifically associate with Hsp90 (e.g. Aha1, Cdc37, Cyp40, FKBP51, FKBP52, p23).<sup>118-122</sup> Thereby, eukaryotic Hsp70 and Hsp90 act through an orchestrated interplay to accomplish diverse, though target-oriented functions.<sup>123</sup> In order to combat protein aggregation, distinct machinery assemblies can recognize protein aggregates<sup>98</sup>, dissolve protein aggregates<sup>97,124</sup>, and direct misfolded proteins to degradation pathways<sup>125,126</sup> – each of which is modulated by co-chaperone diversity. But first of foremost, protein aggregation should not come about at all.<sup>127,128</sup> Along this line, the so called Hsp70/Hsp90 chaperone machinery was suggested as productive folding pathway for proteins to acquire their native state.<sup>57</sup>

### 1.3 The Hsp70/Hsp90 chaperone machinery

Using foldable substrates as model systems, it is known that Hsp70 acts prior to Hsp90.<sup>77,84,117,129,130</sup> Hsp70, credited with decisive function of whether a protein is retained or removed<sup>131</sup>, traps the substrate *via* hydrophobic interactions and may initiate protein (re-)folding<sup>132</sup>, followed by Hsp90 interacting with less hydrophobic, prefolded substrates to finalize protein folding and activation.<sup>77,93,133,134</sup>

The joint action of Hsp70 and Hsp90 for substrate transfer is variably entitled as the Hsp70-Hsp90 chaperone cascade<sup>94</sup>, the foldosome complex<sup>135</sup> or the Hsp70/Hsp90 folding machinery<sup>117</sup> and here further termed as the Hsp70/Hsp90 chaperone machinery.<sup>136</sup> As few as five components are required whilst sufficient for substrate activity *in vitro* and thus full functionality of the Hsp70/Hsp90 chaperone machinery.<sup>137-139</sup> The minimal system includes Hsp70 and Hsp90, the Hsp70-specific co-chaperone Hsp40, the co-chaperone Hop that interacts with both Hsp70 and Hsp90 and the Hsp90-binding co-chaperone p23. In fact, the reduction to these five proteins is based on studies with reticulocyte lysates that were able to reactivate denatured substrates added to them externally.<sup>140-142</sup> The analysis of lysate composition revealed major amounts of Hsp70, Hsp90, and Hop.<sup>142,143</sup> Attempts to reconstitute substrate reactivation *in vitro* to gain mechanistic insights, manifested that beyond, Hsp40 and p23 are essential for same effectiveness.<sup>137,138,144-146</sup> On the basis of this five-component system, various substrates have been demonstrated to depend on Hsp70/Hsp90 cooperation. In contrast to isolated Hsp70 and Hsp90, their tight interplay within the Hsp70/Hsp90 chaperone machinery was shown to uniquely recover the activation of steroid



receptors<sup>138,147</sup>, compose a functional RISC complex (RNA-induced silencing complex)<sup>148</sup>, regulate the activity of the tumor suppressor protein p53<sup>149</sup> or significantly enhance the kinetics of hepatitis B virus reverse transcriptase.<sup>150</sup> Even in context of chaperone inhibition, the system was critical for Hsp90 ATP binding blockage indicating a distinct Hsp90 conformation that is only achieved in the presence of all five proteins.<sup>151</sup> Thus, the orchestrated interplay of Hsp70, Hsp40, Hsp90, Hop and p23 appears pivotal, though its role for IDPs has not been reported so far.

### 1.3.1 Hsp70

In humans, the Hsp70 family encloses up to 13 isoforms<sup>152</sup> each encoded by its specific gene.<sup>153</sup> The Hsp70 variants are present in different cell compartments (cytosol, nucleus, endoplasmic reticulum (ER) and mitochondria) and at different levels depending on cellular needs.<sup>152</sup>

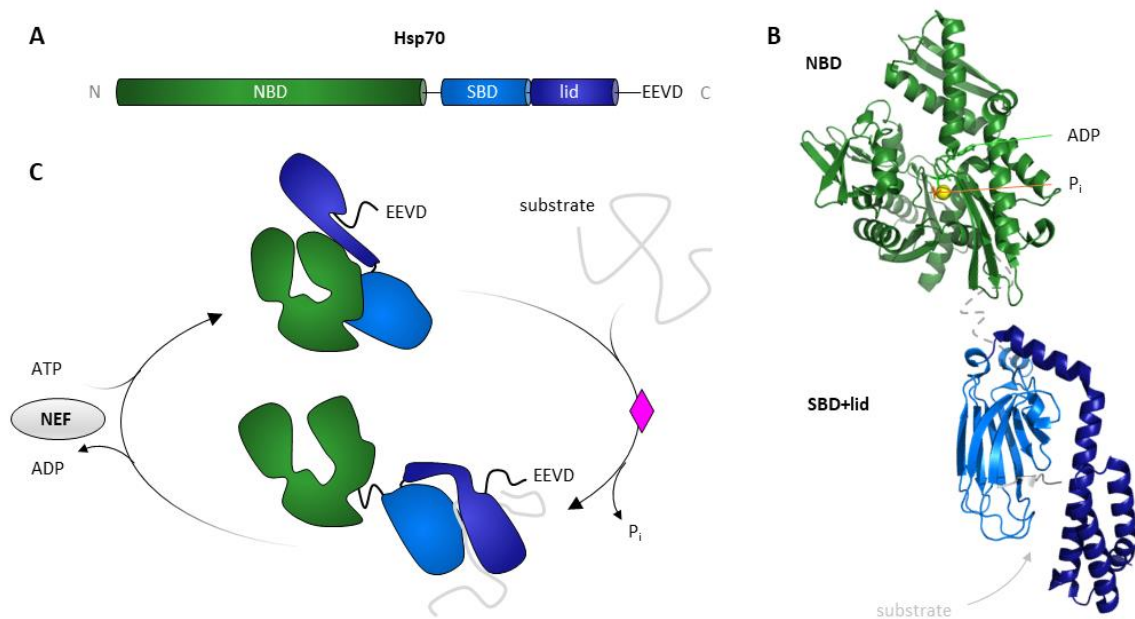


**Figure 4 The heat shock protein Hsp70.**

**A** Domain organization of Hsp70 consisting of the nucleotide binding domain (NBD) and the substrate binding domain (SBD) that includes a lid region.<sup>154</sup> The C-terminal EEVD-motif is necessary for the interaction of Hsp70 with TPR-containing co-chaperones.<sup>92</sup> **B** Assembled structure of the human Hsp70 with the NBD ADP/P<sub>i</sub> bound (PDB code 3atu; the yellow sphere represents the Mg<sup>2+</sup> ion)<sup>157</sup> and SBD-lid closed state (PDB code 4po2; bound substrate peptide is depicted in grey).<sup>158</sup> The linker connecting the NBD and SBD is represented with a grey dotted line. Domains are color coded as in (A). **C** Hsp70 adopts two major conformations: an ATP-bound, lid open conformation, and an ADP/substrate-bound, lid closed conformation, whose interchange is driven by ATP hydrolysis (pink diamond) and a nucleotide exchange factor (NEF).<sup>159</sup>

Hsp70s are monomeric proteins that are composed of an N-terminally located nucleotide binding domain (NBD) and a C-terminally located substrate binding domain (SBD) (Figure 4A).<sup>154</sup> Both domains are connected by a short linker region that allows allosteric changes, which are essential for chaperone function. The NBD of Hsp70 depicts an actin-like fold (Figure 4B).<sup>152,155</sup> It

consists of four subdomains that frame the catalytic center.<sup>152</sup> The SBD consists of two parts including the polypeptide binding cavity depicted as  $\beta$ -sheet sandwich and the  $\alpha$ -helical lid region that closes upon substrate binding.<sup>156</sup> In addition, cytosolic Hsp70s contain a C-terminal EEVD-motif that is necessary for the interaction with TPR-containing co-chaperones like Hop (Figure 4A).<sup>92</sup>

The nucleotide state of the NBD determines the conformation of the SBD, being open in the NBD-ATP state or closed in the NBD-ADP state (Figure 4C).<sup>160</sup> The conversion from ATP to ADP is achieved by ATP hydrolysis that is accelerated in presence of Hsp40.<sup>161</sup> Upon ATP hydrolysis the SBD-lid closes holding the substrate in a high affinity state.<sup>159</sup> It is assumed that the energy released during hydrolysis can break unfavorable bonds, thereby promoting the active form of the substrates.<sup>162,163</sup> To happen repeatedly, ADP is exchanged to ATP by means of nucleotide exchange factors (NEFs) that engender the reopening of the SBD along with substrate release.<sup>164</sup> Repetitive cycles of substrate binding and ATP hydrolysis are believed to initiate or complete protein folding dependent on substrate complexity.<sup>94,131,165</sup> Hsp70 only binds particularly hydrophobic protein segments of five amino acids in length.<sup>166</sup> With progressive folding these patches are buried eventually leaving scattered hydrophobic side chains in need of help.<sup>84</sup> Hereupon, Hsp70 relies on the help of Hsp90 able to recognize broad hydrophobic regions.<sup>94</sup>

### 1.3.2 Hsp40

The importance of Hsp40 on the formation of the Hsp70/Hsp90 chaperone machinery is based on its capability to stimulate the ATPase rate of Hsp70.<sup>161</sup> In fact, Hsp40 stabilizes the Hsp70:ADP state, which in turn is the high affinity conformation for the co-chaperone Hop.<sup>137,167</sup> Beyond, although Hsp70 can recognize substrates on its own, it has been shown how Hsp40 diversity can drive Hsp70 specificity.<sup>114</sup>

Hsp40s are categorized into three classes based on their domain architecture (class A, B and C) (Figure 5A).<sup>87</sup> What they all have in common is the so-called J-domain, a  $\sim 70$  amino acids long  $\alpha$ -helical hairpin structure, wherefore the group of Hsp40s is often termed as J-domain proteins (JDPs) (Figure 5B).<sup>168,169</sup>

In human class A Hsp40s (DnaJA) the J-domain is located at their N-terminus.<sup>152,170</sup> A flexible GF linker rich in glycines and phenylalanines connects this moiety to the two consecutive C-terminal domains of  $\beta$ -sheet conformation (CTDI and CTDI) and the dimerization domain (DD). Class B Hsp40s (DnaJB) are constructed highly similar to members of class A, however uniformly lack an additional zinc finger-like domain inserted in the CTDI of class A Hsp40s.<sup>171</sup> Due to their C-terminal dimerization domain, class A and B Hsp40s exist as triangular homodimers (Figure 5C).<sup>172</sup> In contrast, class C Hsp40s (DnaJC) solely share the J-domain with other JDP

members. It is located in the center of the protein sequence bordered by diverse subdomains strongly varying in sequence and length.<sup>152,170</sup> In general, all Hsp40s that do not fall into class A or B are sorted into class C giving rise to their heterogeneity.<sup>170</sup> In total, the human DNA encodes for up to ~50 different Hsp40s, of which four belong to class A and 13 to class B.<sup>87</sup>

The J-domain is the site of Hsp70 interaction essential for Hsp70 ATPase stimulation.<sup>168</sup> Hsp40s specifically bind the linker region connecting the NBD and SBD of Hsp70 thereby making direct impact on allosteric rearrangements in Hsp70.<sup>159</sup> For class A Hsp40s the exclusive interaction *via* their J-domain is sufficient for ATPase acceleration.<sup>114</sup> However, in the case of class B Hsp40s a more complex two-step mechanism involving an initial Hsp40-CTDI:EEVD-Hsp70 interaction is required, upon which Hsp70 stimulation is achieved *via* the traditional Hsp40-J-domain:linker-Hsp70 association.<sup>114,173</sup>

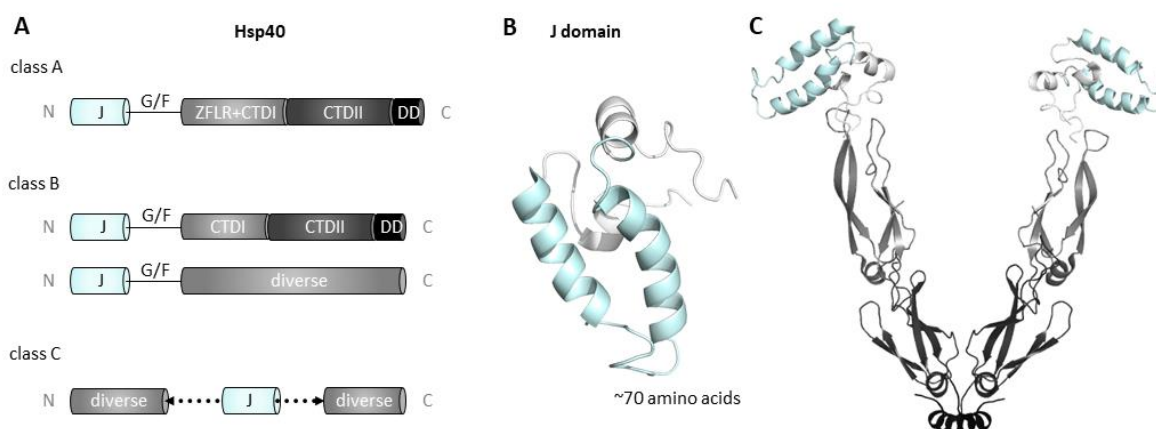


**Figure 5 The co-chaperone Hsp40.**

**A** Domain organization of different members of the Hsp40 family divided into class A, B and C; J – J-domain, G/F – domain rich in glycines and phenylalanines, ZFLR – zinc finger-like region, CTDI and II – C-terminal domain I and II, DD – dimerization domain, diverse – diverse subdomains of any character.<sup>152</sup> **B** Cartoon representation of the ~70 amino acid long, Hsp40 characteristic J-domain (light blue) (PDB code 1hdj).<sup>169</sup> **C** Assembled structure of the human class B Hsp40 active as homodimer (PDB code 1hdj (J-domain)<sup>169</sup>; 3agy (CTDI, CTDII, DD))<sup>172</sup>. Domains are color coded as in (A).

Despite their importance in substrate recognition, the nature of Hsp40:substrate interactions are still unknown.<sup>174,175</sup> Although binding studies revealed that the substrate binding region of class A and B Hsp40s is constrained to CTDI and CTDII<sup>176,177</sup>, it yet remains elusive how or if at all Hsp40s drive substrate selectivity.<sup>152</sup> In any case, Hsp40s interact independently with Hsp70 and the substrate<sup>114</sup> allowing the formation of ternary Hsp40:substrate:Hsp70 complexes<sup>114</sup> as the basis for the substrate delivery from Hsp40 to Hsp70.<sup>174,178</sup>

## 1.3.3 Hsp90

The Hsp90 protein family is comparatively small with so far four classes known including the cytosolic stress-inducible Hsp90 $\alpha$ , the constitutively expressed Hsp90 $\beta$ , the Grp94 (glucose-related protein) located in the ER and the mitochondrial TRAP1 (tumor necrosis factor receptor-associated protein 1) (Figure 6A).<sup>179</sup>

Hsp90s are active as homodimers (Figure 6B).<sup>91,180,181</sup> The molecular structure of cytosolic Hsp90 includes the N-terminal GHKL nucleotide binding domain (NTD) that is conserved in members of the GHKL ATPase superfamily (Gyrase, Hsp90, histidine kinase, and MutL) (Figure 6C).<sup>182,183</sup> The Hsp90 NTD differs from the corresponding NBD domain in Hsp70s based on their distinct, so called Bergerat ATP-binding fold.<sup>182</sup> In Hsp90 this fold is composed of several  $\beta$ -sheets aligned to one another that are framed by  $\alpha$ -helices on the left, right and on top, whereby the latter is inserted into a flexible loop region depicting the ATP lid.<sup>184</sup>

The Hsp90 NTD is connected to the middle domain (MD) *via* a charged linker region (cl) that allows NTD dynamics and thus modulates the chaperone's activity.<sup>119,185-189</sup> The MD is crucial for substrate recognition<sup>113</sup> as well as the ATPase activity of Hsp90 by interacting with the ATP  $\gamma$ -phosphate essential for ATP hydrolysis.<sup>190,191</sup> The C-terminal domain (CTD) is the site of dimerization important for Hsp90 function.<sup>91,181</sup> The CTD ends with a conserved MEEVD-motif, by which they can, similar to Hsp70, recruit TPR-containing co-chaperones.<sup>192,193</sup> Notable, Hsp90 does not exhibit a distinct substrate binding domain.<sup>113,194</sup> Clients commonly expose broad hydrophobic regions that occupy various, client-specific interaction sites spanned throughout Hsp90's NTD and MD.<sup>84,195</sup>

Despite TRAP1 and Grp94 only have ~45% and ~60% sequence similarity to the cytosolic paralogues, they exhibit high structural analogy mainly differing in length and domain composition.<sup>91</sup> Grp94 represents the longest Hsp90 isoform<sup>196</sup>, with an extended N-terminal sequence and a conserved C-terminal KDEL signal peptide, whereby the latter is responsible for the localization of Grp94 to the ER.<sup>91</sup> Otherwise, Grp94 exhibits all four domains including the NTD, cl, MD and CTD. TRAP1 in turn is the smallest Hsp90 member due to the absent of the cl region and a shorter CTD.<sup>196</sup> Similar to Grp94, TRAP1 contains an N-terminal signal sequence that directs the protein to mitochondria, which is cleaved off after translocation and thus not present in the active protein.<sup>91</sup>

All Hsp90 paralogues share their active form as homodimers, which is crucial for their function.<sup>91</sup> As dimers, they consist of two specific ATP binding sites located in the NTD, which have been shown to function cooperatively by lowering the dissociation rate of the opposite nucleotide.<sup>118,183</sup> Despite, for ATP hydrolysis it is not necessary that both NTDs are nucleotide-bound.<sup>183</sup>

## Introduction

ATP hydrolysis is accomplished through large conformational rearrangements that direct the Hsp90 dimer from an apo-extended to a closed ATP hydrolysis active form (Figure 6B).<sup>181</sup> Dimer closure is essential for ATP hydrolysis enabling the interaction of the Hsp90 MD with the ATP  $\gamma$ -phosphate, without which the phosphate cannot be cleaved off.<sup>190,191</sup> Human Hsp90s mainly adopt the extended conformation and spend only a fraction of seconds in the ATP-bound, closed state that is directly re-opened upon ATP hydrolysis.<sup>197,198</sup> Notable, an additional subordinate nucleotide binding site has been proposed in the CTDs of Hsp90 that is less specific in ATP binding (binds also GTP and UTP) and opens up only when the NTDs are occupied.<sup>199,200</sup> So far, however, no information is available on their function for Hsp90 chaperone activity.

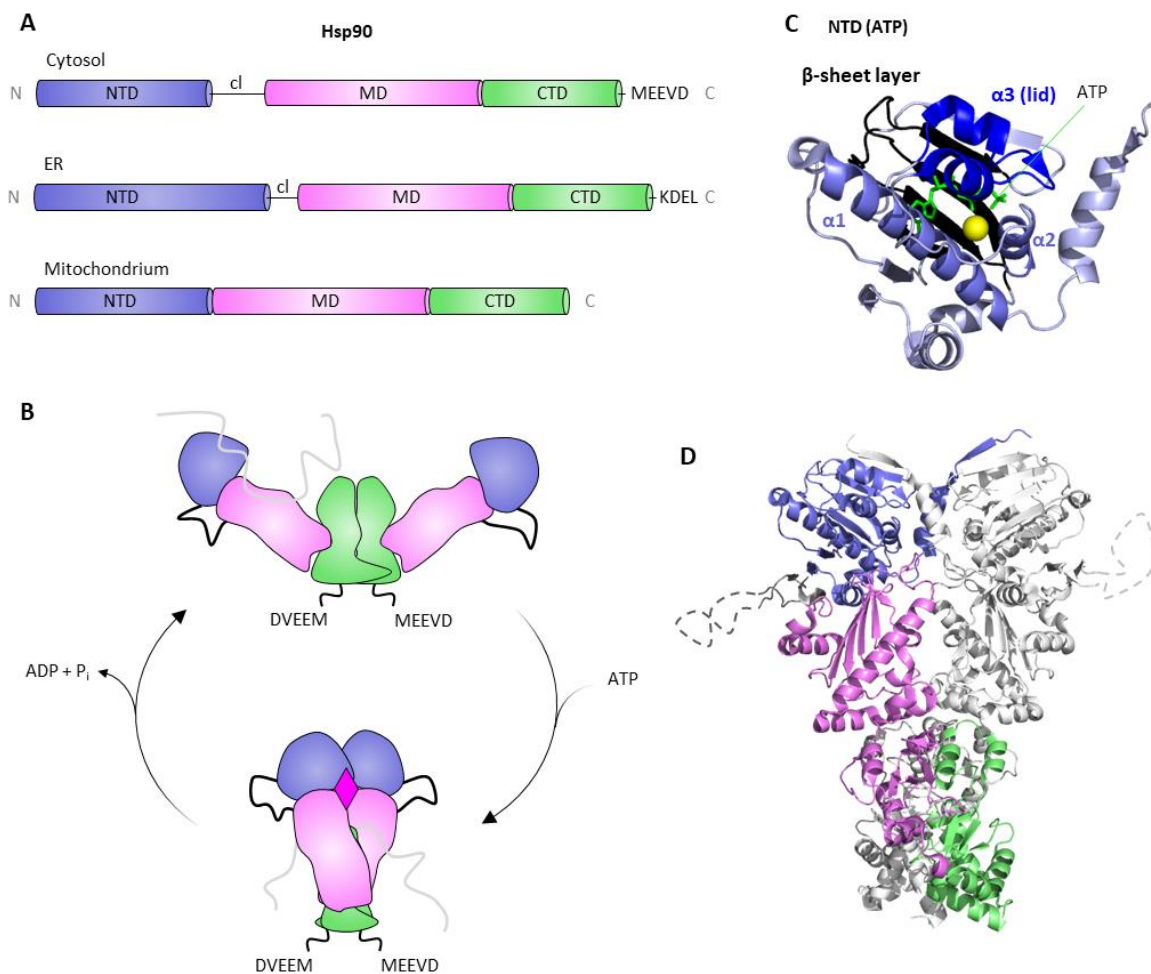


**Figure 6 The heat shock protein Hsp90.**

**A** Domain organization of different members of the Hsp90 family located in the cytosol, endoplasmic reticulum (ER) and mitochondrion consisting of an N-terminal domain (NTD), a charged linker region (cl), a middle domain (MD) and a C-terminal dimerization domain (CTD) as indicated.<sup>91</sup> The C-terminal MEEVD-motif of cytosolic Hsp90 is necessary for the interaction with TPR-containing co-chaperones.<sup>192,193</sup> The C-terminal KDEL-motif retains Hsp90s in the ER.<sup>91</sup> **B** Hsp90s are active as homodimers that cycle from an open nucleotide free through a closed nucleotide bound state whose interchange is driven by ATP binding and hydrolysis (pink diamond).<sup>181</sup> The substrate is considered to bind at any stage.<sup>84,195</sup> **C** Structure of the human Hsp90-NTD in its ATP (green) bound state (PDB code 5fwk; the yellow sphere represents the Mg<sup>2+</sup> ion).<sup>119</sup> The different components of its GHKL ATPase domain are highlighted with the  $\beta$ -sheet layer (black) framed by the helices  $\alpha$ 1 (left, marine),  $\alpha$ 2 (right, marine) and  $\alpha$ 3-lid (top, blue).<sup>182</sup> **D** Structure of full-length closed human cytosolic Hsp90 (PDB code 5fwk; the absent cl-region is depicted as grey dotted line).<sup>119</sup> For clarity, the domains of only one monomer arm are color coded as in (A).

## Introduction

Consistent with their predominant open conformation<sup>198</sup>, human Hsp90s are exceptionally slow in terms of ATP hydrolysis activity.<sup>179</sup> In fact, cytosolic Hsp90 requires ~10 min to hydrolyze one ATP molecule – this is ten times as slow as bacterial Hsp90.<sup>179</sup> However, eukaryotic Hsp90 can compensate for the rather low intrinsic ATPase activity by means of the vast network of co-chaperones.<sup>201-204</sup> These bind and stabilize distinct conformations of Hsp90 guiding the chaperone from the open to the closed conformation.<sup>181</sup> Thereby, co-chaperones can accelerate the ATPase activity of Hsp90 (e.g. Aha1)<sup>201,202</sup> or inhibit ATP hydrolysis (e.g. Hop and p23)<sup>205-207</sup> to await the substrate to bind. The Hsp90 cycle of ATP binding and hydrolysis are thought to be essential for substrate folding.<sup>208</sup> However, it is not yet clear whether folding takes place bound to Hsp90 (similar to chaperonins) (see chapter 1.2.1) or after release from Hsp90 (similar to Hsp70s)<sup>209</sup> (see chapter 1.3.1) or how Hsp90's ATP hydrolysis driven conformational changes achieve substrate folding at all.<sup>136</sup>

With regard to intrinsically disordered clients, Hsp90 can beyond act as holdase – an exceptional function that is independent on ATP hydrolysis.<sup>93</sup> The holding activity of Hsp90 is suggested to prevent protein aggregation and is thus particularly important for the chaperoning of IDPs.<sup>84,210</sup> So far the holdase activity of Hsp90 has been described independent on the presence of Hsp70 and co-chaperones.<sup>93</sup> It therefore remains to be investigated what role the Hsp70/Hsp90 chaperone machinery as well as Hsp90 ATPase activity bears upon IDP chaperoning.

### 1.3.4 Hop

A unique role is attributed to the co-chaperone Hop (Hsp organizing protein), which can simultaneously bind to both Hsp70 and Hsp90.<sup>117,211</sup> Hop favors the Hsp70-ADP state, i.e. substrate bound form.<sup>167</sup> Thereby, Hop may initiate Hsp70/Hsp90 chaperone machinery assembly preferentially in the presence of substrates. In contrast, on the side of Hsp90, Hop interacts with the apo state with no effect on the ATP affinity for Hsp90.<sup>206</sup>

Hop belongs to the group of tetratricopeptide repeat domain (TPR) containing co-chaperones (Figure 7A).<sup>212</sup> TPR domains are constructed by a minimum of three TPR motifs, each of which depicting a helix-turn-helix structure made up of ~34 amino acids (Figure 7B).<sup>213</sup> Hop contains three of such TPR domains separated by two aspartate-proline rich (DP) segments arranged as TPR1-DP1-TPR2A-TPR2B-DP2 multi-domain protein.<sup>207</sup> Although no structure of full-length Hop is reported so far, it is assumed to be a highly dynamic protein without interdomain contacts.<sup>117</sup> Merely the linker region connecting the TPR2A-2B domains is suggested to be particularly rigid and holds both domains in a fixed orientation to one another (Figure 7C).<sup>207</sup> Hop associates *via* its TPR domains with the EEVD-motifs at the C-termini of Hsp70 and Hsp90.<sup>192,193</sup> In this way, it acts as an adaptor bridging both chaperone systems.<sup>211</sup> Interaction studies revealed the TPR1 domain as the main interaction site for Hsp70, whereas the interaction with Hsp90 is

## Introduction

preserved for the TPR2A domain.<sup>193,207,214</sup> However, despite its interaction with both Hsp70 and Hsp90, Hop is solely reported to inhibit the ATPase activity of Hsp90 retaining the chaperone in an extended, hydrolysis inactive state.<sup>206,207</sup> While doing so, Hop is assumed to preorganize Hsp90's NTDs in their ATP-bound form holding Hsp90 in a V-shaped conformation.<sup>215</sup> In association with Hsp90, Hop's DP segments and especially DP2 were shown to be important for client activation *in vivo*.<sup>207</sup> Hence, altogether, Hop acts as a joint to link Hsp70 and Hsp90<sup>117,129</sup>, concurrently regulates Hsp90 ATPase activity<sup>207</sup> and beyond, possesses impact on substrate modulation.<sup>207</sup> Notable, to date there are conflicting evidences for both monomeric and dimeric human Hop.<sup>215,216</sup> Since the corresponding dimerization interface is however located within Hop's TPR2A domain<sup>216</sup>, it remains unclear to what extent a dimeric Hop might interact with Hsp90 and/or the Hsp70/Hsp90 chaperone machinery.

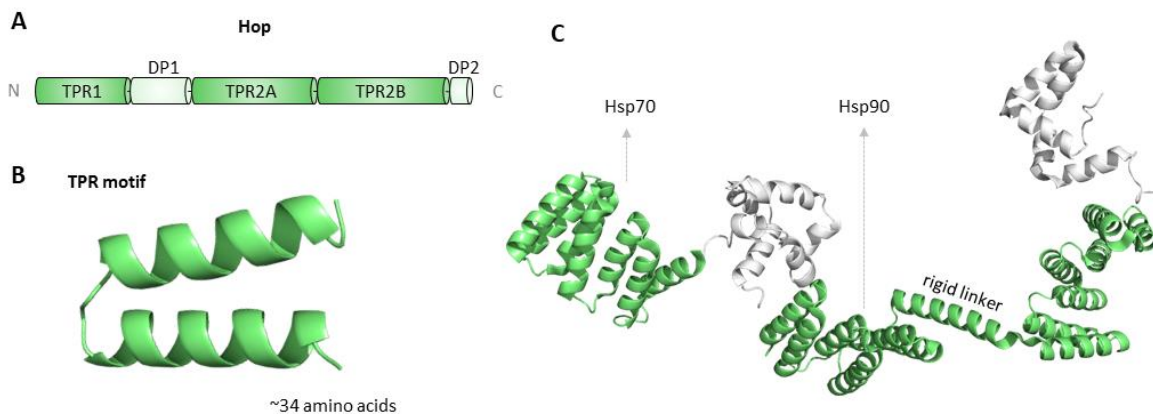


**Figure 7 The co-chaperone Hop.**

**A** Domain organization of Hop including three tetratricopeptide repeat (TPR) domains (TPR1, TPR2A and TPR2B) and two DP domains (DP1 and DP2) rich in aspartates and prolines.<sup>207</sup> **B** Cartoon representation of the ~34 amino acid long TPR motif (PDB code 1elw). Three of such make up a TPR domain.<sup>213</sup> **C** Assembled structure of Hop depicted as dynamic molecule with the rigid linker as sole stiff connector (PDB code 1elw (TPR1), 2llv (yeast DP1), 3uq3 (yeast TPR2A-2B), 2llw (yeast DP2)).<sup>193,207</sup> In addition, the structure of human TPR2A is deposited in the PDB (PDB code 1elr).<sup>193</sup> Domains are color coded as in (A). The main interaction site with Hsp70 (TPR1) and Hsp90 (TPR2A) are indicated.<sup>207</sup>

### 1.3.5 p23

p23 is best-known as an Hsp90 co-chaperone that, similarly to Hop, inhibits the chaperone's ATPase activity.<sup>217,218</sup> It preferably interacts with the closed, ATP-bound state of Hsp90<sup>205,219,220</sup> contacting both monomers at the NTD and MD region.<sup>122,221,222</sup> Yet it remains unclear whether Hsp90 inhibition is achieved by p23 blocking Hsp90 interdomain contacts necessary for ATP hydrolysis<sup>122</sup> or by preventing the dissociation of ADP and Pi after hydrolysis.<sup>221</sup>

p23 is active as a monomer.<sup>205</sup> Human p23 consists of a single domain that forms a globular core arranged as two opposing  $\beta$ -sheet layers.<sup>223</sup> The last approximately 35 C-terminal residues are of unstructured character depicting a disordered, highly acidic tail (Figure 8A, B).<sup>224</sup> In the absence of interaction partners the tail is suggested to stabilize the p23 core and partly adopt  $\alpha$ -helical



conformation.<sup>225</sup> Intriguingly, the adaptation of secondary structure is lost upon Hsp90 binding<sup>225</sup>, though regained in the presence of a substrate, where the p23 tail and in particular the reformed  $\alpha$ -helix possesses essential impact for client interaction bound to Hsp90.<sup>48,226</sup>

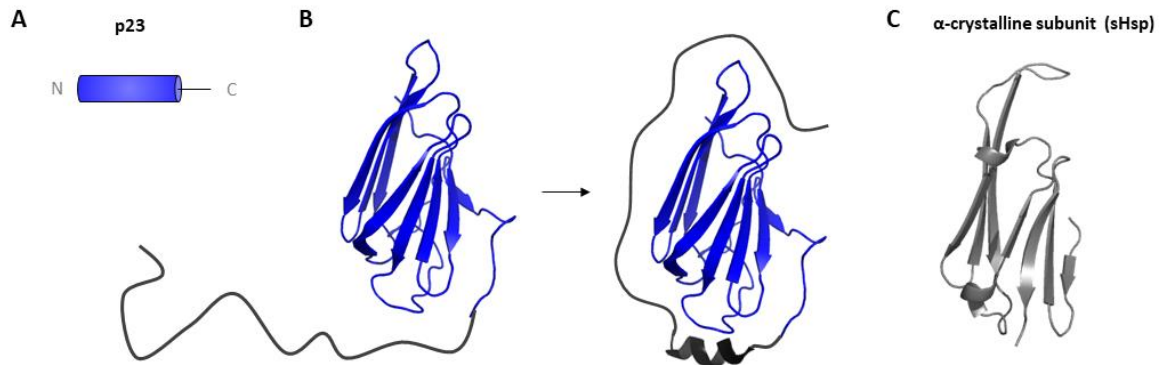


**Figure 8 The co-chaperone p23.**

**A** Domain organization of human p23 consisting of an N-terminal globular domain and a C-terminal tail.<sup>218</sup> **B** Assembled structure of p23 including the protein core made up of two opposing  $\beta$ -sheet layers (PDB code 1ejf)<sup>223</sup> and the unstructured C-terminal tail.<sup>225</sup> In the apo state, the tail region possesses  $\alpha$ -helical propensity to stabilize the p23 core.<sup>225</sup> The same  $\alpha$ -helix is used to interact with substrates bound to Hsp90.<sup>48</sup> Domains are color coded as in (A). **C** Cartoon representation of the  $\alpha$ -crystalline subunit of sHsps (PDB code 2wj7)<sup>227</sup>, which is structurally related to the p23 core.

Much has already been learned about the p23 function for Hsp90 regulation<sup>122,205,221,228</sup>, but little is known about its additional intrinsic, i.e. Hsp90 independent, ability to interact with non-native substrates.<sup>229-231</sup> In this process, p23 plays a role in the prevention of protein aggregation related to sHsps. The relationship is based on the structural similarity of the hydrophobic core of p23 and the crystalline subunit of sHsps (Figure 8C).<sup>232</sup> Thereby, the p23's globular domain might be particularly important for the holding of unfolded, intrinsically disordered proteins.<sup>98,233</sup> For substrate binding however, full-length p23 has been found to be required including the C-terminal tail<sup>48,223,224,234</sup>, whereby the individual domains were self-insufficient to bind the substrate. It is thus likely to be the interplay between the C-terminal tail and the core essential for p23 activity.<sup>224</sup> So far, these assumptions are however mainly based on speculation and experimental evidence for the function of p23 in IDP holding is yet to be demonstrated.

### 1.3.6 A structural model of the Hsp70/Hsp90 chaperone machinery

With regard to the Hsp70/Hsp90 chaperone machinery, the determination and analysis of individual intermediate complexes has already provided deep insights into the synergistic interplay of Hsp70, Hsp40, Hsp90, Hop and p23.<sup>47,48,117,130,215</sup> At the outset of this study several reports describing the synergistic interplay between Hsp70 and Hsp90 were revealing though highly diverse and inconsistent.<sup>117,215,216,235</sup> Most recently the full Hsp70/Hsp90 chaperone machinery cycle has been demonstrated with the highest resolution to date for the Hsp-substrate paragon, the



glucocorticoid receptor (GR)<sup>47,48</sup>, giving substantial progress in the understanding of the underlying molecular mechanisms that enable the cooperation of Hsp70 and Hsp90 chaperone systems. On this basis, the Hsp70/Hsp90 chaperone machinery assembles in stages during which different sub-complexes are established (Figure 9). Their sequential buildup is launched with Hsp70 that traps the substrate *via* hydrophobic interactions.<sup>132</sup> Hsp40 assists in substrate binding able to capture Hsp70 clients and stabilize the substrate:Hsp70 interaction.<sup>114</sup> Hop serves as an adaptor between the two chaperones able to bind simultaneously to both Hsp70 and Hsp90.<sup>211</sup> In this way the synergistic interplay for Hsp70/Hsp90 cooperation is established *via* substrate:Hsp70:Hop:Hsp90 complexes to which Hsp40 is no longer bound.<sup>47</sup> Lastly, p23 is described to stabilize the Hsp90:substrate interaction<sup>236</sup> contributing to the formation of Hsp90:substrate:p23 complexes finalizing the substrate transfer onto Hsp90 through the release of Hsp70 and Hop.<sup>48,117,235,237</sup> Along this line, the simultaneous binding of Hsp90 to p23 and Hop has been precluded in several previous studies, since both co-chaperones prefer different conformations of Hsp90.<sup>130,167,238</sup>

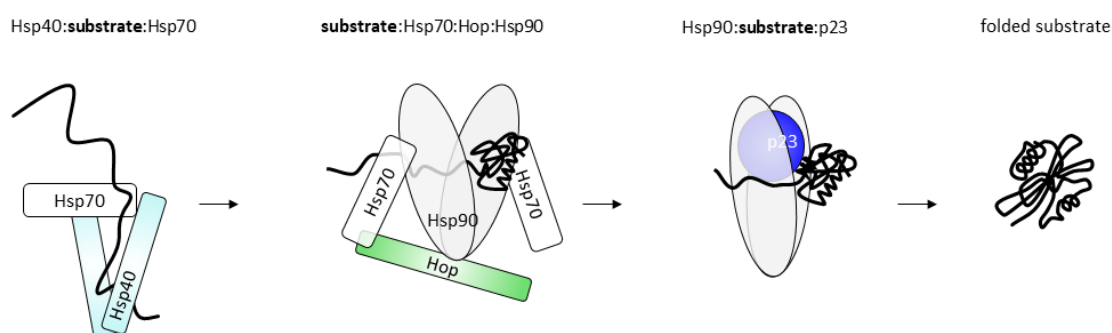


**Figure 9 The Hsp70/Hsp90 chaperone machinery in protein folding.**

The substrate is trapped by Hsp70 with the help of Hsp40.<sup>114</sup> Hop bridges Hsp70 and Hsp90 to form the substrate:Hsp70:Hop:Hsp90 complex.<sup>47</sup> p23 binding is accompanied with the release of Hsp70 and Hop yielding a stable Hsp90:substrate:p23 complex.<sup>48</sup> The illustration was created based on the most recent model from Wang et al.<sup>47</sup> with 3.57 Å and 2.56 Å of resolution for the substrate:Hsp70:Hop:Hsp90 and Hsp90:substrate:p23 complex, respectively.

The model in Figure 9 presents the cooperative work of Hsp70 and Hsp90 that promotes protein folding. Thus, the Hsp70/Hsp90 chaperone machinery represents a pathway that actively protects proteins against misfolding and aggregation. On the other side, there are numerous diseases caused by protein aggregation initiated by the misfolding of the very specific type of IDPs (see chapter 1.5).<sup>239,240</sup> Even though for different IDPs the direct interaction with the individual Hsp70 and Hsp90 has been demonstrated<sup>84,241,242</sup>, yet, there is no data available on whether both Hsps likewise work together for IDP chaperoning. Along this line, it remains unknown whether a Hsp70/Hsp90 chaperone machinery:IDP interaction might counteract IDP misfolding.

## 1.4 Intrinsically disordered proteins

Intrinsically disordered proteins (IDPs) are distinguished from globular, folded proteins, as they inherently lack a stable native structure (Figure 10).<sup>243</sup> Their disordered character is intrinsic, i.e. sequence-dependent with an amino acid chain of low complexity and only few hydrophobic residues.<sup>244,245</sup> IDPs are highly dynamic proteins that, when unbound, tumble around many different conformations (Figure 3).<sup>41</sup> The capability of IDPs to interchange between different conformations gives rise to a complex network of interactions.<sup>246</sup> Although it is a common feature of IDPs to be disordered in the apo (i.e. unbound) state, they can adopt distinct secondary structures in association with an interaction partner.<sup>21</sup>

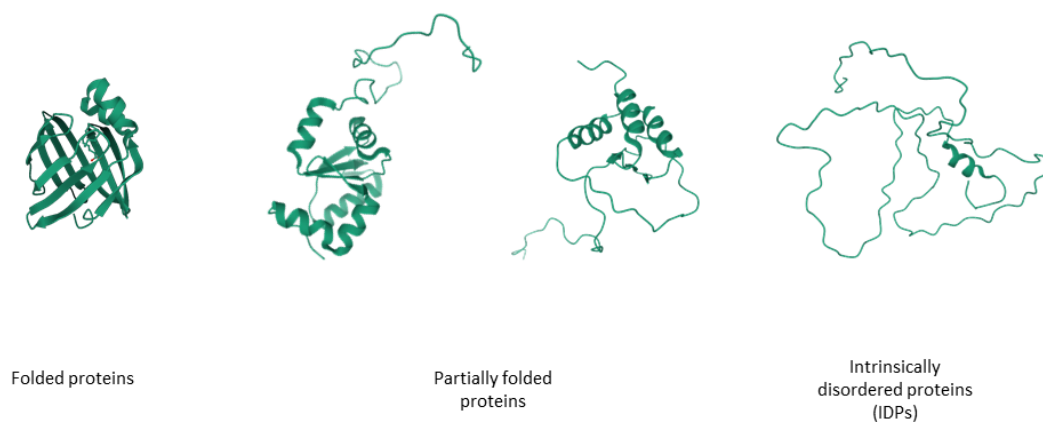


**Figure 10** The proteome includes folded, partially folded and intrinsically disordered proteins.

PDB code from left to right: 1fe3, 2mxn, 2lm0, 6xry.<sup>247-250</sup>

Disordered proteins and regions appear all over the cell signifying their functional diversity and indispensability.<sup>251-255</sup> IDPs are substantially important being highly sensitive for subtle environmental changes, which include changes in pH, temperature or ionic strength.<sup>256-258</sup> Especially the regions that are not involved in the interaction and remain constantly unbound can sense external changes to regulate the protein's binding behavior.<sup>259</sup> However, despite their indispensability, IDPs carry great drawback, as due to their disordered nature the risk for protein misfolding and aggregation is particularly high (Figure 3).<sup>260</sup>

## 1.5 IDP-associated proteinopathies

Proteinopathies are diseases characterized by protein aggregation.<sup>261</sup> The event of protein aggregation is typically initiated by the formation of abnormal protein structures with high potential for self-attachment.<sup>262</sup> In the case of IDPs, distinct regions can adopt  $\beta$ -sheet conformation facilitating their stacking and eventually generating insoluble fibrillar aggregates.<sup>263</sup> The large

## Introduction

number of IDP-associated proteinopathies exemplifies how diverse the pathologic consequences of protein aggregation can be (Table 1).<sup>264-266</sup> Hereby, the diseases are classified according to disease-specific proteins that undergo fibrillation.

The biggest group encompasses the tauopathies with the intrinsically disordered protein Tau as pathologic marker.<sup>266-268</sup> Tau itself demonstrates the classic conception of an IDP being naturally unstructured, possessing high conformational plasticity, thereby being able to associate with versatile interaction partners and thus fulfilling vital biological function (see chapter 1.6).<sup>84,242,254,257,269</sup> On the other hand, it is found in numerous diseases deposited in insoluble protein aggregates, in which many copies of Tau have accumulated (Table 1).<sup>264-266</sup>

Among all tauopathies, the Alzheimer's disease is the most prevalent form with Tau forming insoluble protein deposits in the patients' brains.<sup>270</sup> Worldwide approximately 40 million people are suffering from Alzheimer's disease, the most common cause of dementia<sup>271,272</sup>. Affected people first express behavioral problems, the most prominent of which is subtle, though steadily increasing forgetfulness.<sup>273</sup> Descending memory accompanies with confusion, irritability and depression, followed by the gradual impairment of cognitive skills. Ultimately, the loss of basic bodily functions may lead to death.<sup>274</sup>

**Table 1** Examples for proteinopathies associated with IDP aggregation.<sup>264-266</sup>

Disease	Aggregated IDP / protein with intrinsically disordered regions	Class of proteinopathy
Alzheimer's disease	Tau Amyloid- $\beta$	Tauopathy Amyloidosis
Amyotrophic lateral sclerosis	FUS TDP-43	FUS-proteinopathy
Argyrophilic grain dementia	Tau	Tauopathy
Corticobasal degeneration	Tau	Tauopathy
Dementia pugilistica	Tau	Tauopathy
Diffuse NFT with calcification	Tau	Tauopathy
Fronto-temporal dementia	Tau FUS	Tauopathy FUS-proteinopathy
Lewy body disease	$\alpha$ -synuclein	Synucleinopathy
Multiple system atrophy	$\alpha$ -synuclein	Synucleinopathy
Parkinson's disease	$\alpha$ -synuclein	Synucleinopathy
Pick's disease	Tau	Tauopathy
Progressive subcortical gliosis	Tau	Tauopathy
Progressive supranuclear palsy	Tau	Tauopathy
Tangle only dementia	Tau	Tauopathy

Tau as a central player has driven research to reveal considerable knowledge about its physiological and pathological role, thus allowing to understand the link between Tau aggregation on a cellular level and cognitive impairments on the holistic level.

## 1.6 The IDP Tau

Tau is an IDP being naturally disordered in its native state.<sup>257,275,276</sup> The protein sequence includes the classic characteristics to resist protein folding presenting a high number of prolines and glycines (known as helix-breaker) and only a few hydrophobic residues (Table A 2). It is encoded by a single gene, wherefrom six different isoforms of Tau are expressed throughout the central nervous system (CNS) generated *via* alternative splicing.<sup>277</sup> The longest isoform of Tau (2N4R) consists of 441 amino acids in length posing two N-terminal inserts (N1, N2), a proline rich region (P1, P2) and four repeat domains (R1-R4 plus R') (Figure 11A).<sup>254</sup>

### 1.6.1 Tau physiology

The intrinsically disordered amino acid chain of Tau can be roughly divided into two modules: the N-terminally located 'projection domain' and the microtubule binding region (MTBR) that is involved in the interaction of Tau with microtubules (Figure 11A).<sup>278,279</sup>

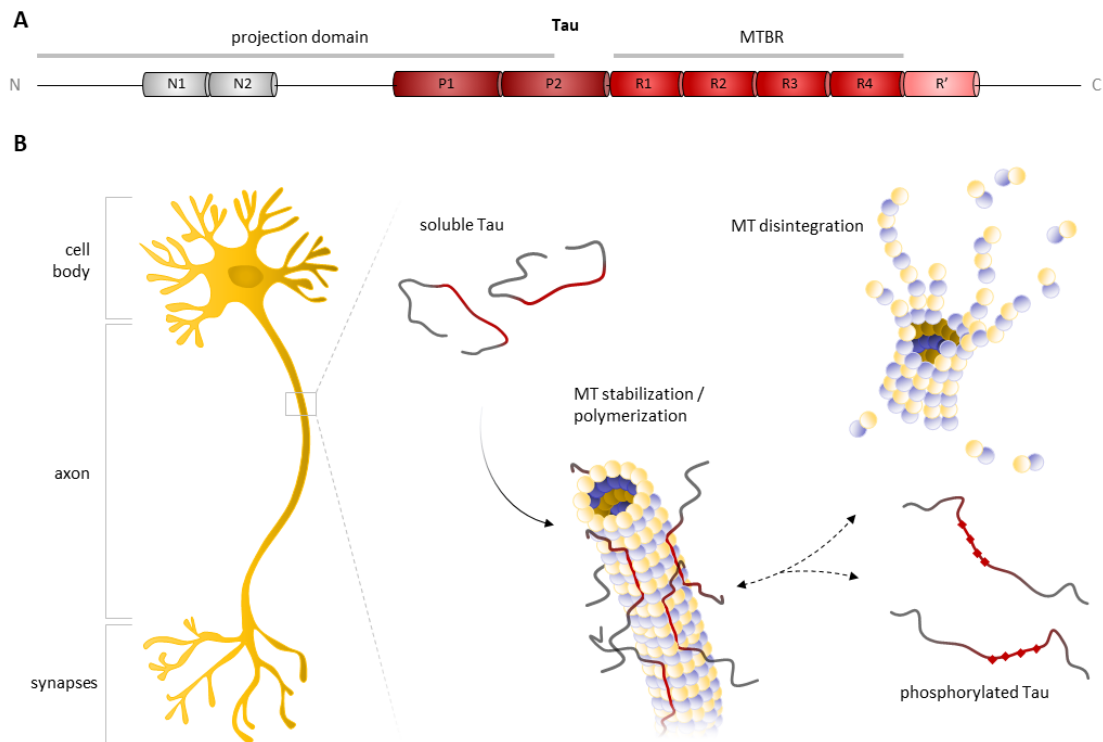


**Figure 11 Biological role of the intrinsically disordered protein Tau.**

**A** Domain organization of the longest isoform of Tau (2N4R) including two N-terminal inserts N1 and N2, two proline rich segments P1 and P2 and the repeat region R1-R4 and R'.<sup>254</sup> Tau interacts *via* its microtubule binding region (MTBR) with microtubules.<sup>287</sup> **B** *In vivo* Tau is primarily located in the axons of neurons where it serves for microtubule stabilization and polymerization.<sup>281,283,284</sup> Upon phosphorylation Tau dissociates from microtubules.<sup>288</sup>

## Introduction

Microtubuli are part of the cytoskeleton and thus responsible for cell stability. They are conceivable as vast rail network responsible for the active protein transport through the cell.<sup>280</sup> Upon binding, Tau does not only stabilize microtubules but also acts as spacer arm inside of microtubule bundles.<sup>281,282</sup> In neuronal cells, Tau is primarily localized in the axons<sup>283</sup> and, due to its ability to promote microtubule assembly<sup>284</sup>, it does not only play a key role in axonal transport<sup>285</sup> but also in the outgrowth of axons<sup>254</sup>, both fundamentally important for the formation of synaptic conjunctions, i.e. neuronal communication (Figure 11B).<sup>286</sup>

### *Post-translational modifications of Tau*

*In vivo*, Tau function is regulated by post-translational modifications among which phosphorylation, acetylation, N-acetyl glucosaminylation, glycosylation, methylation as well as truncation have been directly linked to Tau pathology.<sup>254,289</sup> Notably, in most cases it was suggested that the site and excess of the modification might be detrimental rather than the modification as such.<sup>254</sup>

The regulation of Tau by means of phosphorylation is particularly delicate.<sup>290</sup> On the one hand, Tau phosphorylation is vital provoking the detachment of Tau from microtubules, which is important for the dynamic assembly and disassembly of microtubule structures as well as for the movement of transporters along microtubuli (Figure 11B).<sup>288</sup> In great measure however, phosphorylation correlates with Tau pathology, as hyperphosphorylated Tau deposits into large helical filaments.<sup>254,291,292</sup> Along this line, different kinases were found to introduce specific phosphorylation patterns on Tau.<sup>254</sup> In specific, phosphorylation clusters in the MTBR flanking regions targeted by serine/threonine kinases are commonly observed in Alzheimer's disease and other tauopathies and thus of high therapeutic interest.<sup>293</sup> The direct link between Tau hyperphosphorylation and Tau toxicity has been approached from various perspectives including the dislocation from neuronal axons<sup>294</sup>, altered degradation<sup>295</sup>, enhanced aggregation<sup>296</sup> or varied binding to interaction partners<sup>121</sup>, yet, however, remains a matter of debate.

Besides, Tau acetylation at lysine residues in the MTBR and the MTBR flanking regions has been found in association with altered Tau protein turnover. Dependent on the acetylation site, Tau degradation was inhibited or facilitated directly correlating with increased or decreased Tau levels, respectively.<sup>297-299</sup> Other post-translational modifications of Tau including N-acetyl glucosaminylation, glycosylation and methylation are correlated with Tau pathology by blocking or facilitating the phosphorylation of Tau<sup>254,300</sup> or by stabilizing the structure of Tau aggregates.<sup>301</sup> Beyond, non-enzymatic modifications such as isomerization are suggested to promote Tau aggregation.<sup>121</sup> Lastly, the truncation of Tau has been proposed to foster Tau pathology with the truncated constructs eventually having increased aggregation potential.<sup>254</sup>

## 1.6.2 Tau pathophysiology

Tau pathology is associated with the aggregation of hyperphosphorylated Tau.<sup>291</sup> The process of Tau aggregation has been extensively studied in the last decades, so far however yielding only models of the aggregation pathway. Most recent representations include the nucleation-elongation mechanism<sup>254</sup> facilitated by the adoption of an abnormal conformation that initially leads to the formation of Tau oligomers.<sup>268,302-304</sup> As it is usually the case for all types of IDP-interactions (see chapter 1.4), the self-association of Tau molecules is likewise associated with changes in secondary structure.<sup>263</sup> Extensive Tau oligomerization eventually depicts long stretches of  $\beta$ -sheet conformation that circularly twist to paired helical filaments termed as neurofibrillary tangles.<sup>305</sup>

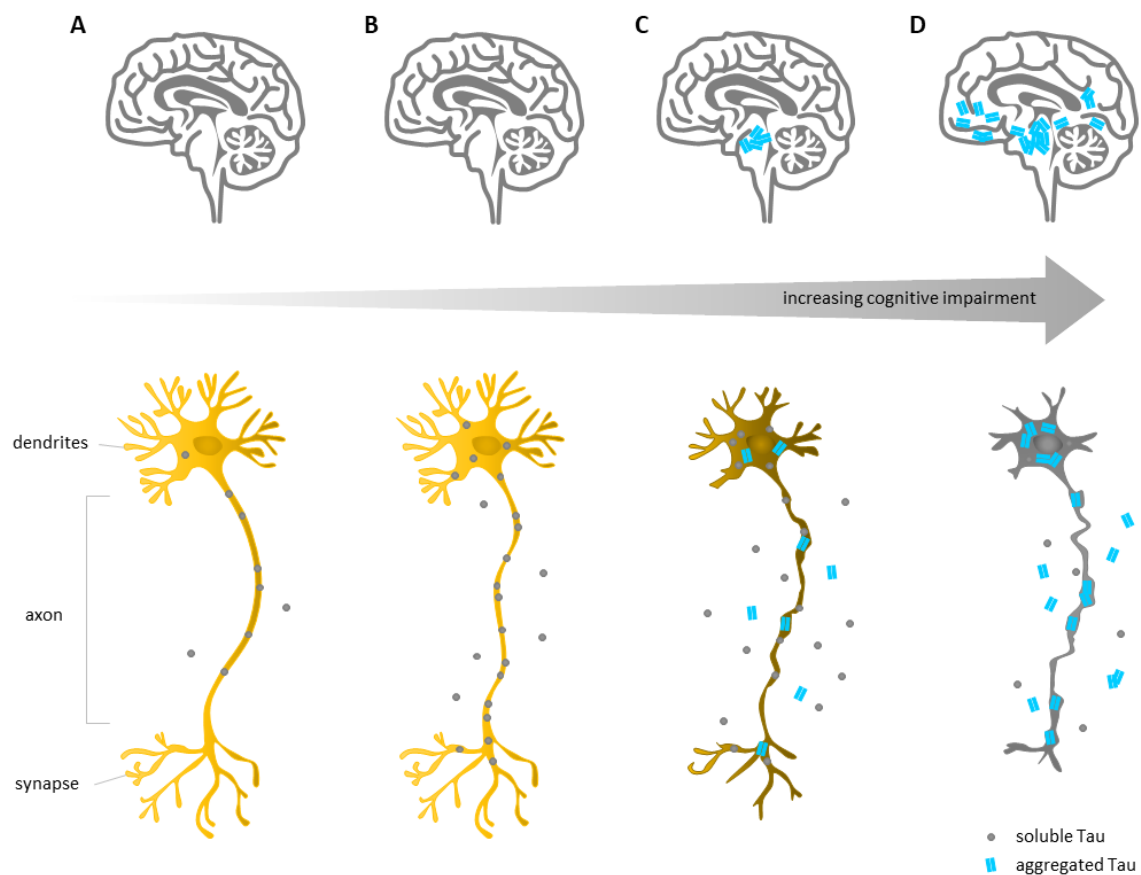


**Figure 12 Neurodegeneration is associated with the deposition of insoluble protein aggregates in the patients' brains.**

The proposed model of the progress in Alzheimer's disease is illustrated. **A** The healthy brain depicts well outgrown neurons with physiological Tau production and secretion. **B-D** Increasing Tau levels engender the formation of Tau aggregates. The accumulation of such insoluble Tau deposits causes neuronal cell death accompanied with the loss of synaptic connections. At advanced stages, more and more areas of the brain are affected, which increasingly impair the patient's cognitive skills. The illustration was created in the style of a report from Sato et al.<sup>316</sup>

On a molecular level, the repeat region which is physiologically involved in the interaction with microtubules, equally features the core of Tau fibrils.<sup>306-308</sup> The core is surrounded by the highly flexible, unbound termini of Tau conceivable as 'fuzzy coat' that is suggested to be important for the stabilization of Tau fibrils.<sup>309,310</sup>

Different Tau strains have been assigned to different tauopathies according to the Tau isoform that undergoes aggregation. Eventually, the number of repeat domains (4R as shown in Figure 11 and 3R lacking the R2 domain) classifies the diseases into 4R (e.g. progressive supranuclear palsy), 3R (e.g. Pick's disease) and 4R+3R tauopathies (e.g. Alzheimer's disease).<sup>254</sup> The sequestration of Tau molecules into these insoluble structures engenders Tau toxicity considered on the basis on both loss-of-function<sup>311</sup> and gain-of-function principles<sup>312,313</sup> with decreasing amounts of soluble Tau and increasingly toxic Tau oligomers, respectively. In either case, the aggregation of Tau causes microtubule disintegration due to decreasing stabilization by Tau.<sup>314</sup> The ultimate collapse of the cytoskeleton disrupts the active transport of molecules, impairs axonal stability and thus evokes synaptic dysfunction.<sup>315</sup>

With the progression of the disease Tau fibrils expand inside and outside of neurons affecting more and more areas of the brain (Figure 12).<sup>316</sup> Along this line, the concept of Tau spreading has emerged suggesting the neuron-to-neuron propagation of Tau aggregates.<sup>317</sup> The prion-like spreading hypothesis includes the 'infection' of originally normal Tau by abnormal states facilitating their incorporation into Tau fibrils. In particular seeding experiments support this concept through an accelerated aggregation profile in the presence of Tau aggregates (seeds).<sup>318</sup>

It is known that Tau dysfunction drives neurodegeneration depriving the patient's memory, its independence and ultimately its life.<sup>319</sup> However, in sporadic tauopathies, such as Alzheimer's disease, the underlying mechanism that triggers Tau pathology is not known.<sup>254</sup>

### 1.6.3 The chaperoning of Tau

The central question of which system prevents Tau aberration in healthy people draws back the attention to the cell's defense system of molecular chaperones. Being aware of the particularly high risk to aggregate, the cell has to be cautious especially with IDPs.<sup>240</sup> In these cases, the capability of protein holding by Hsp70 and Hsp90 becomes all the more essential to protect the protein from undesired interactions.<sup>136,320</sup>

Indeed, consistent with the chaperoning of IDPs in general, Tau has been evidenced as a substrate of both Hsp70 and Hsp90.<sup>84,242</sup> In agreement with Hsp70 acting prior to Hsp90 (see chapter 1.3), binding studies revealed a slightly higher affinity of Tau for Hsp70 ( $K_D = 2.9 \mu\text{M}$ )<sup>321</sup> than for Hsp90 ( $K_D = 4.8 \mu\text{M}$ ).<sup>84</sup> Based on interaction studies with the individual chaperones, both Hsps interact with residues located in Tau's repeat region. Consistent with the commonly known substrate binding behavior of Hsp70 and Hsp90 (see chapter 1.3.1 and 1.3.3), Hsp70 targets two short patches flanking Tau's R2 domain<sup>242</sup>, whereas the binding of Hsp90 involves a broad region including the whole MTBR of Tau.<sup>84</sup> On the side of the chaperones, yet there are no structural data available on the Hsp70: Tau complex. In contrast, the Hsp90: Tau

## Introduction

interaction has revealed an extended binding site on Hsp90 spanning from the MD throughout the NTD.<sup>84</sup> Compared to globular proteins the interaction of Hsp90 with Tau as intrinsically disordered substrate was found to be independent on the nucleotide state of Hsp90<sup>84</sup> and accordingly did not affect Hsp90's ATPase rate.<sup>121</sup>

With regard to the large number of eukaryotic co-chaperones (see chapter 1.2.2), various Hsp: Tau:co-chaperone complexes have been studied in order to draw conclusions about their function and relation to Tau aggregation. The involvement of the FKBP51 (FK506 binding protein 51 kDa) PPIase was found to promote Tau aggregation<sup>322</sup> suggested to be caused by an increased cis-trans isomerization of proline residues in Tau facilitated on Hsp90 that acts as a scaffolding element.<sup>121</sup> In contrast, the co-chaperone, E3-ubiquitin ligase CHIP (carboxyl terminus of Hsc70-interacting protein) is involved in the ubiquitination of Tau tagging the proteins bound to Hsp70 or Hsp90 for proteasomal degradation (see chapter 1.1.3).<sup>295,323</sup>

Although other co-chaperone functions in relation to Tau remain to be investigated, the interaction with both Hsp70 and Hsp90 has been directly linked to Tau chaperoning. Both chaperones have been proven to promote Tau function by assisting Tau's association with and polymerization of microtubules<sup>324</sup>, as well as induce Tau degradation.<sup>295,321,323</sup> Beyond, the interaction with Hsp70 is involved in the disaggregation of Tau aggregates.<sup>325</sup> Hence, Tau is not simply left to its own devices but is controlled and regulated by both Hsp70 and Hsp90. However, with respect to their synergistic function as part of the Hsp70/Hsp90 chaperone machinery, yet it is unclear, whether Hsp70 and Hsp90 act separately, successively or even simultaneously on Tau – let alone if or how they act on IDPs to prevent protein aggregation at all.



## 1.7 Aim of this thesis

On the one hand, the cell holds a gigantic network of molecular chaperones that maintain proteostasis through an orchestrated interplay (see chapter 1.1 and 1.2). In particular, the collaboration of Hsp70 and Hsp90 in the Hsp70/Hsp90 chaperone machinery fosters the protein's native state and thus actively combats protein misfolding and aggregation (see chapter 1.3). On the other hand, there are multiple diseases caused by protein aggregation involving the displacement of intrinsically disordered proteins (IDPs) into insoluble deposits (see chapter 1.4 and 1.5). Since no data on the direct interaction of the Hsp70/Hsp90 chaperone machinery with IDPs are available to date, it is not known whether the Hsp cooperation fails during disease, or whether it is of no use to IDPs at all.

At the outset of this work, much has been learned about the structural and functional basis of the Hsp70/Hsp90 cooperation, however, largely restricted to the chaperone's role in protein folding<sup>57,77</sup> and activation.<sup>47</sup> The reason for this is that the substrate models were so far limited to foldable proteins with secondary and tertiary structure elements, whose folding state is controlled by the tight interplay of Hsp70 and Hsp90. However, the specific group of IDPs that are intrinsically incapable to fold get left out from these results and the insights obtained with folded clients should be applied to IDPs with caution.

To that effect, the work of this thesis was designed to get deeper insights into the role of the Hsp70/Hsp90 chaperone machinery:IDP interaction with the Alzheimer's disease related, intrinsically disordered protein Tau (see chapter 1.6) used as client model.

In specific, it was aimed to reveal which role the synergistic interplay of Hsp40, Hsp70, Hsp90, Hop and p23 plays for Tau chaperoning, and whether Hsp70 and Hsp90 act successively, concomitantly or after all completely independent of each other. On this basis, a stepwise approach was anticipated generating distinct intermediate states in the machinery pathway to shed light into the structural and functional relevance of each of the five components for the Hsp70/Hsp90 chaperone machinery mediated chaperoning of Tau.

Although there have been numerous reports on the Hsp70/Hsp90 chaperone machinery (in combination with foldable substrates), no consistent picture was apparent for the preassembly of the Hsp70/Hsp90 chaperone machinery prior to substrate binding. The described complexes were inconclusive differing in composition<sup>117,130,215,216,235</sup>, spatial arrangement<sup>207,215</sup> and structure<sup>117,130,215</sup>, in turn demanding an own detailed analysis along with the stepwise *in vitro* reconstitution of each interjacent protein-protein interaction.

## 2 Material and Methods

---

### 2.1 Material

In this section all consumables (Table 2), instruments (Table 3), chemicals (Table 4), enzymes (Table 5), bacterial cells (Table 6), plasmids (Table 7) and software (Table 8) used for the experiments and data analysis are listed.

#### 2.1.1 Consumables

**Table 2 Consumables with supplier in alphabetical order.**

Consumable	Supplier
0.2 – 1000 $\mu$ L pipet tips	Eppendorf
10 / 25 mL pipet tips	Cellstar
14 mL polypropylene round-bottom-tubes	FALCON
5 mL pipet tips	Sarstedt
C18 column	Dr. Maisch GmbH
Dialysis hose	Spectrum Labs
Disposable cuvettes	BRAND
Disposable cyclic olefin copolymer (COC) cuvettes	Wyatt Technology
HiLoad 16/600 Superdex 75 pg	GE Healthcare
HiLoad 26/600 Superdex 200 pg	GE Healthcare
HiLoad 26/600 Superdex 75 pg	GE Healthcare
Membrane filter	Merck Millipore
Mini-PROTEAN TGX Precast Protein Gel	Bio-Rad Laboratories
Mono S 10/100 GL	GE Healthcare
NMR tubes	Shigemi Inc.
PCR clean-up Gel extraction Kit	Macherey-Nagel
PCR reaction tube	Molecular Biology Products
PD-10 column	Thermo Scientific
Pipets	Eppendorf
Plasmid DNA purification Kit	Macherey-Nagel
Reaction tubes (1.5 / 2 / 5 mL)	Star lab products
Reaction tubes (15 / 50 mL)	Cellstar
Slide-A-Lyzer dialysis cassettes	Thermo Scientific
Superdex 200 10/300 GL	GE Healthcare
Syringes	Braun
Ultramicro Suprasil quartz cuvettes	Hellma
Vivaspin concentrators	Sartorius

## Material and Methods

Vortex Genie	Scientific Industries
--------------	-----------------------

### 2.1.2 Instruments

**Table 3 Instruments with supplier in alphabetical order.**

<b>Instrument</b>	<b>Supplier</b>
45-Ti rotor	Beckman Coulter
5424R centrifuge	Eppendorf
5810R centrifuge	Eppendorf
ÄKTAmicro	GE Healthcare
ÄKTA Pure	GE Healthcare
ÄKTAprime Plus	GE Healthcare
Avance 800 MHz spectrometer	Bruker
Avance 800 MHz spectrometer (cryoprobe)	Bruker
Avance 900 MHz spectrometer (cryoprobe)	Bruker
Avanti JXN-26 centrifuge	Beckman Coulter
BioSpectrometer	Eppendorf
Cary Eclipse Fluorescence Spectrophotometer	Agilent Technologies
Duomax 1030 Gel shaker	Heidolph Instruments
DynaPro NanoStar	Wyatt Technology
EmulsiFlex C3 French Press	AVESTIN
FA-45-6-30 rotor	Eppendorf
GelDoc™ XR+	Bio-Rad Laboratories
Gradient Master™	BioComp Instruments
Heratherm incubator	Thermo Scientific
JA 25.50 rotor	Beckman Coulter
JLA-8.1000 rotor	Beckman Coulter
KS 4000 i control incubator	IKA
MicroCal PEAQ-ITC Automated	Malvern Panalytical
Microwave	Sharp
Multitron Pro incubator	INFORS HT
NanoDrop 2000/2000c	Thermo Scientific
Optima XPN80 ultracentrifuge	Beckman Coulter
Orbitrap Fusion Lumos Tribrid	Thermo Scientific
PCR labcycler	Sensquest
pH-meter	Mettler Toledo
PowerPac™ Basic Power Supply	Bio-Rad Laboratories
Purelab flex	Veolia
Q Exactive™ HF-X Hybrid Quadrupole-Orbitrap	Thermo Scientific
Rotating Mixer	JP Selecta
Scales	Sartorius

## Material and Methods

Sonicator <i>Sonoplus</i>	Bandelin
Sub-Cell GT Agarose Gel Electrophoresis Systems	Bio-Rad Laboratories
SW 60 Ti	Beckman Coulter
ThermoMixer <i>comfort</i>	Eppendorf
UltiMate 3000 UHPLC	Thermo Scientific
Water bath	GFL

### 2.1.3 Chemicals

**Table 4 Chemicals with supplier in alphabetical order.**

Chemical	Supplier
[ <sup>2</sup> H- <sup>12</sup> C]-glucose	Sigma-Aldrich
10 x CutSmart buffer	New England Biolabs
10 x TG buffer	Bio-Rad Laboratories
10 x TGS buffer	Bio-Rad Laboratories
<sup>15</sup> N-ammonium chloride <sup>15</sup> NH <sub>4</sub> Cl	Cambridge Isotope Laboratories
1-ethyl-3-(3-dimethylaminopropyl)carbodiimide hydrochloride EDC	Thermo
2-(N-morpholino)ethanesulfonic acid MES	Sigma-Aldrich
2-ketobutyric acid-4 [ <sup>13</sup> C],3,3-[D <sub>2</sub> ] sodium salt	NMR-Bio
4-(2-hydroxyethyl)-1-piperazineethanesulfonic acid HEPES	Sigma-Aldrich
6 x DNA loading dye	Thermo Fisher
Acrylamide 30%	SERVA Electrophoresis
Adenosine 5 <sup>1</sup> -(β,γ-imido)triphosphate lithium salt hydrate AMP-PNP	Sigma-Aldrich
Adenosine 5 <sup>1</sup> -diphosphate sodium salt ADP	Sigma-Aldrich
Adenosine 5 <sup>1</sup> -triphosphate disodium salt hydrate ATP	Sigma-Aldrich
Agarose	Bio-Rad Laboratories
Ammonium persulfate APS	Sigma-Aldrich
Ammonium sulfate (NH <sub>4</sub> ) <sub>2</sub> SO <sub>4</sub>	Sigma-Aldrich
Ampicillin sodium salt	Sigma-Aldrich
Bactotryptone	BD
BenchMark protein ladder	Thermo Fisher
Boric acid (H <sub>3</sub> BO <sub>3</sub> )	Sigma-Aldrich
Bovine serum albumin BSA	Sigma-Aldrich
Bromophenol blue sodium salt	Sigma-Aldrich
Cobalt(II) chloride hexahydrate (CoCl <sub>2</sub> ·6H <sub>2</sub> O)	Carl Roth
cOmplete™ EDTA-free Protease Inhibitor Cocktail	Sigma-Aldrich
Copper(II) chloride dihydrate (CuCl <sub>2</sub> ·2H <sub>2</sub> O)	Sigma-Aldrich
Deuterium oxide D <sub>2</sub> O	Eurisotop
Disodium hydrogen phosphate (Na <sub>2</sub> HPO <sub>4</sub> )	Carl Roth
Disuccinimidyl suberate DSS	Thermo Fisher

## Material and Methods

DL-Dithiothreitol DTT	Sigma-Aldrich
Ethanol ROTISOLV HPLC Gradient Grade	Carl Roth
Ethylene glycol-bis( $\beta$ -aminoethyl ether)-N,N,N',N'-tetraacetic acid EGTA	Carl Roth
Ethylenediaminetetraacetic acid EDTA	Sigma-Aldrich
FastGene Q-Stain	NIPPON Genetics
GeneRuler 1 kb Plus	Thermo Fisher
Glycerol	Carl Roth
Hydrochloric acid (HCl)	Sigma-Aldrich
Imidazole	Sigma-Aldrich
IPTG	Carl Roth
Iron(III) chloride hexahydrate ( $\text{FeCl}_3 \cdot 6\text{H}_2\text{O}$ )	Merck Millipore
Isopropanol	Sigma-Aldrich
Kanamycin sulfate	Sigma-Aldrich
Ligase Buffer	New England Biolabs
Magnesium chloride hexahydrate ( $\text{MgCl}_2 \cdot 6\text{H}_2\text{O}$ )	Sigma-Aldrich
Manganese(II) chloride tetrahydrate ( $\text{MnCl}_2 \cdot 4\text{H}_2\text{O}$ )	Merck Millipore
Midori Green DNA Stain	NIPPON Genetics
N-hydroxysulfosuccinimide Sulfo-NHS	Thermo
Niacinamide	Sigma-Aldrich
Nickel(II) chloride hexahydrate ( $\text{NiCl}_2 \cdot 6\text{H}_2\text{O}$ )	Thermo Fisher
Ni-NTA Agarose beads	Qiagen
Phenylmethyl sulfonyl fluoride PMSF	Carl Roth
Phusion Mastermix	Thermo
Pierce™ BCA Protein Assay Kit	Thermo Fisher
Potassium chloride KCl	Sigma-Aldrich
Potassium hydroxide KOH	Merck Millipore
Potassium phosphate monobasic ( $\text{KH}_2\text{PO}_4$ )	Sigma-Aldrich
Protein standard mix 15-600 kDa	Sigma-Aldrich
Pyridoxine hydrochloride	Sigma-Aldrich
Riboflavin	Sigma-Aldrich
Sodium chloride (NaCl)	Sigma-Aldrich
Sodium dodecyl sulfate SDS	Merck Millipore
Sodium hydroxide (NaOH)	Merck Millipore
Streptomycin sulfate	Carl Roth
Sucrose	Merck Millipore
Tetramethylethylenediamine TEMED	Thermo Fisher
Thiamine hydrochloride	Sigma-Aldrich
Tris(2-carboxyethyl)phosphine hydrochloride TCEP	Sigma-Aldrich
Tris(hydroxymethyl)aminomethane	Thermo Fisher
Yeast extract	Sigma-Aldrich
Zinc chloride ( $\text{ZnCl}_2$ )	Honeywell Fluka
$\beta$ -Mercaptoethanol $\beta$ -ME	Sigma-Aldrich

## Material and Methods

### 2.1.4 Enzymes

Table 5 Enzymes with supplier in alphabetical order.

Enzyme	Supplier
Cdk2/CyclinA2 kinase	Thermo Fisher
CREB binding protein CBP acetyltransferase	Enzo Biochem Inc.
DNAse I	AppliChem
Lysozyme	Sigma-Aldrich
MARK2 kinase	provided by the Madelkow lab, DZNE Bonn
NheI-HF	New England Biolabs
p300 acetyltransferase	Enzo Biochem Inc.
Phusion DNA Polymerase	Thermo
RNAse A	AppliChem
Shrimp Alkaline Phosphatase	New England Biolabs
T <sub>4</sub> DNA Ligase	New England Biolabs
Thrombin protease	Sigma-Aldrich
XhoI	New England Biolabs

### 2.1.5 *E. coli* competent cells

Table 6 *E. coli* competent cells with supplier in alphabetical order.

Bacterial cells	Supplier
<i>E. coli</i> BL21 (DE3)	Invitrogen
<i>E. coli</i> Rosetta2 (DE3)	Novagen
<i>E. coli</i> XL2 blue	Agilent Technologies

### 2.1.6 Plasmids

Table 7 Plasmids with supplier in alphabetical order.

Plasmid	Supplier
pET28a	Novagen
pNG2-Tau	provided by the Madelkow lab, DZNE Bonn

### 2.1.7 Software

Table 8 Software with developer in alphabetical order.

Software	Developer
Adobe Illustrator CS5.1	Adobe Inc.
ChemDraw v19.1.1.21	PerkinElmer

## Material and Methods

DYNAMICS	Wyatt Technology
EMBOSS Needle Pairwise Sequence Alignment tool	EMBL's European Bioinformatics Institute
EndNote X7.8	Thomson Reuters
Expasy ProtParam	Swiss Institute of Bioinformatics
ImageJ v1.53e	National Institutes of Health, USA
Inkscape v0.92	Free Software Foundation, Inc.
MicroCal PEAQ-ITC Analysis software	Malvern Panalytical
Office 365	Microsoft
PyMOL™ v2.0.4	Schrodinger
SnapGene Viewer v5.2.4	GSL Biotech LLC
Sparky v1.4	NMRFAM
TopSpin	Bruker
xVis Crosslink Analysis Webserver	Gene Center Munich

## 2.2 General methods

### 2.2.1 SDS page

SDS page analysis is particularly useful to identify the purity of a protein solution. For SDS page, proteins are fully denatured (by heat and reducing agents) and given uniform charge according to the length of their amino acid chain (by the detergent SDS). In this way, the components of a sample are separated exclusively according to their molecular weight. The shorter the amino acid chain the faster it moves through the gel and the further down it is located.

#### *5 x LSB (Laemmli Sample Buffer)*

156.25 mM Tris pH 6.8  
5 % (w/v) SDS  
25 % (v/v) Glycerol  
0.1 % (w/v) Bromophenol Blue  
5 % (v/v)  $\beta$ -ME

#### *10 x TGS Running Buffer*

25 mM Tris pH 8.3  
250 mM Glycine  
0.1 % (w/v) SDS

Sample preparation for SDS page analysis was adjusted for each analysis step.

#### *Protein purification*

In order to analyze expression yields, whole cell extracts ( $V = 300/OD_{600}$ ) were spun down for 1 min at 4°C with max. speed (5424R). The pellet was resuspended in 20  $\mu$ L H<sub>2</sub>O and mixed with 5  $\mu$ L of 5 x LSB. After cell lysis 3  $\mu$ L of sample were mixed with 17  $\mu$ L H<sub>2</sub>O and 5  $\mu$ L of 5 x

## Material and Methods

LSB. In the case of SEC elution fractions, 20  $\mu\text{L}$  of sample were mixed with 5  $\mu\text{L}$  of 5 x LSB. 8  $\mu\text{L}$  of each sample were loaded on the gel.

### *Sucrose density gradient centrifugation*

20  $\mu\text{L}$  of the sample were mixed with 5  $\mu\text{L}$  of 5x LSB. 15  $\mu\text{L}$  were loaded on the gel.

SDS gels with constant acrylamide content were self-made. The pipetting scheme is listed in Table 9. Gradient gels were purchased from Bio-Rad Laboratories (Mini-Protean TGX precast gels). Prior to gel loading, the samples were boiled for 5 min at 95°C and spun down for 30 sec at 4°C with max. speed (5424R). 3  $\mu\text{L}$  of BenchMark Protein Ladder were loaded as protein standard for size classification. SDS gels were run in 1 x TGS running buffer at 180 V until completion and stained with FastGene Q Stain for at least 1 h.

**Table 9 Pipetting scheme for SDS-gels.**

The indicated volumes are sufficient for two gels.

stock solution	separating gel			stacking gel
	15 %	12 %	8 %	
ddH <sub>2</sub> O	2.296 mL	3.3 mL	4.696 mL	3.4 mL
30 % Acrylamide	5 mL	4 mL	2.6 mL	830 $\mu\text{L}$
1.5 M Tris <b>pH 8.8</b>	2.5 mL			
1.5 M Tris <b>pH 6.8</b>				630 $\mu\text{L}$
10 % SDS	100 $\mu\text{L}$			50 $\mu\text{L}$
10 % APS	100 $\mu\text{L}$			40 $\mu\text{L}$
TEMED	4 $\mu\text{L}$			5 $\mu\text{L}$

### 2.2.2 Native page

In contrast to the sample analysis by SDS page (see chapter 2.2.1), native page is performed under non-denaturing conditions and thus allows the separation of proteins in their native, i.e. active state. Here, the proteins' shape and charge are decisive for their running behavior in the gel. Thereby, protein-protein interactions can be investigated – ideally giving rise to a complex band distinct from the unbound proteins.

#### *1 x Native Sample Buffer*

62.5 mM Tris pH 6.8  
40 % (v/v) Glycerol  
0.01 % (w/v) Bromophenol Blue

#### *10 x TG Running Buffer*

25 mM Tris pH 8.3  
192 mM Glycine



## Material and Methods

Samples analyzed by native page were mixed 1:1 with 1 x native sample buffer. 2-3  $\mu\text{g}$  were loaded on the gel. For native page 7.5 % precast gels (Mini-Protean TGX) were used, running at 110 V for 1.5 - 2.5 h. Control lanes containing the individual proteins served for band assignment.

### 2.2.3 Chromatography

#### *Immobilized metal affinity chromatography (IMAC)*

His<sub>6</sub>-tagged proteins were purified by affinity chromatography using nickel-charged resin with immobilized Nickel-nitrilotriacetic acid (Ni-NTA). The resin was filled into PD-10 columns and equilibrated with 7 cv of H<sub>2</sub>O and 7 cv of lysis buffer without reducing agent prior to each run. The whole supernatant of the centrifuged cell lysate was loaded and purified with gravity flow. Proteins were eluted with imidazole competing for Ni-binding. After each purification the resin was washed with 7 cv of H<sub>2</sub>O and stored in 20 % EtOH at 4°C. After every third purification the resin was stripped with 2 cv of 500 mM EDTA pH 8.5, washed with 7 cv of H<sub>2</sub>O and recharged with 7 cv of 500 mM NiCl<sub>2</sub>.

#### *Size exclusion chromatography (SEC)*

Size exclusion chromatography (SEC) was used to separate proteins according to their size and shape. The smaller and more compact a protein is, the slower it runs through the column and the later it elutes. SEC runs were performed on an ÄKTA Pure or ÄKTAprime Plus purification system. Prior to any SEC run the column was equilibrated with 1 cv of H<sub>2</sub>O and 1 cv of buffer. A maximum of half of the loop volume was used as sample volume. The sample was either filtered or centrifuged before loading in order to remove any precipitated content out of the solution. For storage the column was washed with 1 cv of 1 M NaOH/NaCl and 1 cv of 0.1 M HCl with 1 cv of H<sub>2</sub>O in between each washing step and stored in 20 % EtOH at RT.

#### *Ion exchange chromatography (IEX)*

Cation exchange chromatography was used to purify proteins according to their charge based on the principle that the negatively charged resin binds proteins with a net positive charge (cations), i.e. any protein whose isoelectric point is above the pH of the buffer system. IEX runs were performed on an ÄKTA Pure or ÄKTAprime Plus purification system. Prior to each run the column was washed with 5 cv of H<sub>2</sub>O, 5 cv of buffer A and 5 cv of buffer B and equilibrated with 5 cv of buffer A. The supernatant of the centrifuged cell lysate was desalted by dialysis and filtered before loading. Bound proteins were eluted with increasing salt concentration competing for resin binding. For storage the column was washed with 2 cv of 2 M NaCl, 4 cv of 1 M NaOH, 2 cv of 2 M NaCl and 4 cv of H<sub>2</sub>O and stored in 20% EtOH at RT.

Specifications for columns used in this work are listed in Table 10.

**Table 10** Column specifications used for IMAC, SEC and IEX.

	Column	Matrix material	CV	Max. pressure
IMAC	PD-10	Agarose	4–12 mL	-
SEC	HiLoad 26/600 Superdex200 pg	Agarose-dextran	320 mL	0.3 Mpa
	Superdex 200 10/300 GL	Agarose-dextran	24 mL	1.5 Mpa
	HiLoad 26/600 Superdex75 pg	Agarose-dextran	320 mL	0.3 Mpa
	HiLoad 16/600 Superdex75 pg	Agarose-dextran	120 mL	0.3 Mpa
IEX	Mono S 10/100 GL	Polystyrene/divinyl benzene	8 mL	4 Mpa

#### 2.2.4 Concentration determination

##### *Absorption measurement at 280 nm*

The concentration of proteins that contain tryptophane residues in their primary sequence was determined at RT by absorption measurement at  $\lambda=280$  nm using the NanoDrop 2000/2000c. 2  $\mu$ L of protein solution were loaded for data acquisition. Protein concentration was calculated according to the Lambert-Beer law with  $c = \frac{A_{280}}{\epsilon \cdot d}$ , whereby  $A_{280}$  is the absorption value at  $\lambda=280$  nm,  $\epsilon$  the protein's extinction coefficient and  $d$  the optical path length.

##### *Pierce<sup>TM</sup> BCA Protein Assay*

###### *Working Reagent*

24.5 mL Reagent A  
0.5 mL Reagent B

For proteins with low absorption at  $\lambda=280$  nm, protein concentration was determined based on the bicinchonin acid (BCA) assay including two reactions. First  $\text{Cu}^{2+}$  ions are reduced to  $\text{Cu}^+$  by the peptide bonds of the proteins. Then BCA chelates the reduced  $\text{Cu}^+$  ions in a 2:1 ratio that gives the sample a purple color with an absorption maximum at  $\lambda=562$  nm. The extent of coloring is directly dependent on the amount of protein in solution: the more peptide bonds, the higher the amount of reduced  $\text{Cu}^+$  ions that can be complexed.

For absorption measurements two appropriate dilutions of the protein solution were prepared in the range of  $\sim 0 - 2$  mg/mL each in 100  $\mu$ L final volume. 2 mL of working reagent were added. The samples were incubated for 30 min at 37°C followed directly by absorption measurement at  $\lambda=562$  nm. In order to produce a standard curve, the same protocol was performed in parallel with a serial dilution of bovine serum albumin (BSA) with 100  $\mu$ L of 0 – 2 mg/mL BSA

## Material and Methods

diluted in H<sub>2</sub>O. The standard curve was created with Excel by plotting the BSA absorption value at  $\lambda=562$  nm (y-axis) against the BSA protein concentration (x-axis) giving the linear function:  $y = mx + c$ . With y as the experimentally determined absorption values of the sample of interest, the protein concentration was determined by solving the equation for x (taking into account the preceding dilution factor). The final protein concentration was set as the average of both dilutions.

### 2.3 Protein expression and purification

As the substrate Tau is predominantly present in the cytosol<sup>326</sup>, this study is confined to the cytosolic isoforms Hsp70 and Hsp90 $\beta$ , for convenience hereafter denoted as Hsp70 and Hsp90. In accordance with various previous studies and reviews<sup>57,91,181</sup>, the isoforms of Hsp70 and Hsp90 were considered as interchangeable.

The gene construct of full-length human CHIP was thankfully received from the lab of Laura J Blair at the University of South Florida. The DNA of full-length human Hop, Hsp40, Hsp70, Hsp90, p23, Tau and the Tau constructs K18 and K32 were already available in the lab. Gene and protein sequences used in this work are listed in the Appendix in Table A 1 and Table A 2 including the respective cloning vector and the used restriction sites. The corresponding vector maps are shown in Figure A 1 and Figure A 2. Selected protein characteristics are compiled in Table 11.

**Table 11 Characteristics of proteins used in this work.**

Protein characteristics of recombinantly expressed CHIP, Hop, the Hop construct Hop112a, Hsp40, Hsp70, Hsp90 $\beta$ , p23, Tau and the Tau constructs K18 and K32 – in alphabetical order. Specifications refer to the purified proteins in their final state (tags were cut as indicated).<sup>327</sup>

Protein	MW [kDa]	Theoretical pI	$\epsilon \left[ \frac{\text{L}}{\text{mol} \cdot \text{cm}} \right]$	Number of		
				amino acids	Trp	Cys
CHIP <sub>cut</sub>	36.79	5.69	28880	322	2	8
Hop	65.09	6.78	48710	566	1	11
Hop112a <sub>cut</sub>	41.33	6.28	33810	358		5
Hsp40 <sub>cut</sub>	38.38	8.66	21890	343	1	4
Hsp70 <sub>cut</sub>	72.15	5.53	33350	662	2	5
Hsp90 $\beta$	85.72	5.11	57760	747	4	6
p23 <sub>cut</sub>	19.27	4.36	30480	166	5	5
Tau	45.85	8.24	7450	441	-	2
K18	13.81	9.73	1490	130		
K32	21.03	10.09	2980	198		

## Material and Methods

Proteins were either self-produced (CHIP, Hop, Hop112a, Hsp40, Hsp70, unlabeled and isotopically labeled Hsp90 (Hsp90 and Hsp90\*, respectively), p23 and unlabeled Tau) or thankfully received from the group's technician S. Cima-Omori (isotopically labeled Tau, K18 and K32). The expression and purification protocol of each self-produced protein is described in 2.3.4 (in alphabetical order).

### 2.3.1 Stock solutions

Stock solutions were sterile filtered and stored at -20°C if not otherwise indicated.

#### *LB medium*

10 g bactotryptone, 5 g yeast extract, 10 g NaCl solubilized in 1 L H<sub>2</sub>O, pH 7.4 (autoclaved; stored at 4°C)

#### *M9 minimal medium (1 L)*

100 mL 10x M9 medium, 10 mL 100x trace elements, 1 mL 1000x vitamins, 1 mM MgSO<sub>4</sub>, 4 g Glucose (<sup>2</sup>H labeled as required), 1 g NH<sub>4</sub>Cl (<sup>15</sup>N labeled as required) → sterile filter, add 0.3 mM CaCl<sub>2</sub>

10x M9 medium (1 L): 60 g Na<sub>2</sub>HPO<sub>4</sub>, 30 g KH<sub>2</sub>PO<sub>4</sub>, 5 g NaCl (autoclaved; stored at RT)

100x trace elements (1 L): 5 g EDTA, 0.8 g FeCl<sub>3</sub>, 0.05 g ZnCl<sub>2</sub>, 0.01 g CuCl<sub>2</sub>, 0.01 g CoCl<sub>2</sub>, 0.01 g H<sub>3</sub>BO<sub>3</sub>, 1.6 mg MnCl<sub>2</sub>, pH 7.0 (stored at RT)

1000x vitamins (500 mL): 0.5 g riboflavin, 0.5 g niacinamide, 0.5 g pyridoxine monohydrate, 0.5 g thiamine

<i>Ampicillin</i>	100 mg/mL in H <sub>2</sub> O
<i>DNAse</i>	1 mg/mL in 10 mM Tris pH 7.6, 150 mM NaCl, 1 mM MgCl <sub>2</sub> , 50% glycerol
<i>DTT</i>	1 M in H <sub>2</sub> O
<i>IPTG</i>	1 M in H <sub>2</sub> O
<i>Kanamycin</i>	30 mg/mL in H <sub>2</sub> O
<i>Lysozyme</i>	100 mg/mL in 10 mM Tris pH 8.4
<i>PMSF</i>	100 mM in Isopropanol
<i>RNAse</i>	1 mg/mL in 10 mM Tris pH 8, 1 mM EDTA

### 2.3.2 Cloning

The shorter Hop construct Hop112a was generated by insertion of a premature stop codon through polymerase chain reaction (PCR) and was subsequently cloned into the target vector *via* restriction and ligation.

#### PCR

The premature stop codon was introduced through PCR using the forward and reverse primer shown in Table 12. The PCR reaction setup and cycling protocol is listed in Table 13.

**Table 12 Sequences of the reverse (rvs) and forward (fwd) primer used for Hop112a amplification through PCR.**  
NheI (GCTAGC) and XhoI (CTCGAG) restriction sites are highlighted in grey.

Primer	Sequence 3' → 5'
Hop112a_fwd	GAAGCTAGCATGGAGCAGGTCAATGAG
Hop112a_rvs	GTACCTCGAGCTACAGCCGCTCTTGC

**Table 13 PCR reaction setup and cycling protocol for Hop112a DNA amplification.**

The Phusion Mastermix contains 0.04 U/μL Phusion High Fidelity DNA Polymerase in 2 x HF buffer including 1.5 mM MgCl<sub>2</sub> and 400 μM of each dNTP. Full-length Hop DNA served as template.

PCR setup		Cycling protocol			
Component	V [μL]	Temperature [°C]	Duration	Cycles	
template DNA	1	98	1.5 min	1	Initial denaturation
Primer fwd [10 μM]	2.5	98	30 sec	35	Denaturation
Primer rvs [10 μM]	2.5	72	30 sec		Annealing
2x Phusion Mastermix	20	72	40 sec		Elongation
ddH <sub>2</sub> O	14	72	10 min	1	Final Extension
total	40 μL	4	∞	1	Storage

The amplified Hop112a DNA was purified *via* agarose gel electrophoresis (1.5 % gel w/v with 0.0015 % (v/v) Midori Green DNA Stain). 40 μL of the PCR reaction were mixed with 8 μL of 6 x DNA loading dye. 5 μL of GeneRuler 1 kb Plus was loaded for size classification. The gel was run for 1 h at RT with 70 V. The desired band was cut out under UV-light and extracted using the PCR clean-up Gel extraction Kit. The DNA was eluted in 30 μL warm H<sub>2</sub>O.

#### Restriction and Ligation

The purified Hop112a DNA was restricted with the restriction enzymes NheI-HF and XhoI using the restriction protocol shown in Table 14. The sample was incubated for 1 h at 37°C

## Material and Methods

followed by enzyme inactivation at 65°C for 20 min. The restricted DNA was purified *via* agarose gel electrophoresis (1.5 % gel w/v with 0.0015 % (v/v) Midori Green DNA Stain). 50 µL from restriction digest were mixed with 10 µL of 6 x DNA loading dye. 5 µL of GeneRuler 1 kb Plus was loaded for size classification. The gel was run for 1 h at RT with 70V. The desired band was cut out under UV-light and extracted using the PCR clean-up Gel extraction Kit. The DNA was eluted in 30 µL warm H<sub>2</sub>O.

Before ligation, the target vector pET28a (previously digested with the same restriction enzymes) was dephosphorylated in order to prevent self-ligation. The sample was incubated for 30 min at 37°C with 1 µL of Shrimp Alkaline Phosphatase followed by enzyme inactivation at 65°C for 15 min. The ligation reaction of the restricted Hop112a DNA with pET28a was performed with a vector:insert mass ratio of 1:1 as shown in Table 14. The sample was incubated for 15 min at 37°C followed by 1 h at RT and o/n at 16°C. The next day the enzyme was inactivated at 65°C for 10 min.

**Table 14 Reaction setups for DNA restriction and ligation.**

DNA restriction		DNA ligation		
Component	V [µL]	Component	V [µL]	m [ng]
10x CutSmart buffer	5	1:1		50
DNA	x (as much as possible)	T <sub>4</sub> DNA Ligase	1	
NheI-HF	1	Ligase buffer	1	
XhoI	1			
total	50 µL	total	10 µL	

### *Plasmid amplification and sequencing*

5 µL of the ligated product was transformed into 100 µL of *E. coli* XL2 blue competent cells. After 30 min incubation on ice, the cells were permeabilized for 45 sec at 42°C, cooled down for 2 min on ice, resuspended in 900 µL LB medium and shaken for 1 h at 37°C with 210 rpm. Bacteria were harvested for 1 min with max. speed, resuspended in 200 µL of the supernatant and plated onto an LB Agar plate including 30 µg/mL of Kanamycin for selection. Cells were grown o/n at 37°C. The next day a single colony was picked and incubated o/n at 37°C shaking at 225 rpm in 5 mL LB medium including 30 µg/mL of Kanamycin for selection.

Plasmid DNA was extracted according to the Plasmid DNA purification Kit. The DNA was eluted in 30 µL warm H<sub>2</sub>O. DNA concentration was measured at RT by absorption measurement at λ=280 nm using the NanoDrop 2000/2000c. 15 µL including 1089 ng of plasmid were sent to Seqlab Goettingen to verify the DNA sequence. Results were analyzed with the EMBOSS Needle Pairwise Sequence Alignment tool.<sup>328</sup>

## Material and Methods

### 2.3.3 Transformation and o/n culture

1  $\mu\text{L}$  of the recombinant vector was added to 50  $\mu\text{L}$  of *E. coli* competent cells\*. After 30 min incubation on ice, the cells were permeabilized for 45 sec at 42°C, cooled down for 2 min on ice, resuspended in 450  $\mu\text{L}$  LB medium and shaken for 1 h at 37°C with 210 rpm. 200  $\mu\text{L}$  of the transformed cells were plated onto an LB Agar plate including the respective antibiotic agent for selection\*. Cells were grown either o/n at 37°C or o/w at 25°C.

For 1 L protein expression, a single colony was picked and incubated in 25 mL LB medium containing the respective antibiotic agent for selection\*. Bacteria were enriched while shaking o/n at 37°C with 210 rpm.

### 2.3.4 Purification protocols

The protocols were either established by myself, with students supervised by me or received from colleagues as indicated on top of each section in *italic*.

---

\* see individual production protocols for specifications in chapter 2.3.4.

## Material and Methods

### 2.3.4.1 CHIP *established by A. Lott*

<i>Lysis buffer</i>	20 mM Tris pH 8.0 500 mM NaCl 10 mM Imidazole 5 mM $\beta$ -ME	<i>Elution buffer</i>	20 mM Tris pH 8.0 500 mM NaCl 500 mM Imidazole 5 mM $\beta$ -ME
<i>Thrombin buffer</i>	20 mM Tris pH 8.0 100 mM KCl 5 mM $\beta$ -ME	<i>SEC buffer</i>	25 mM HEPES pH 7.4 100 mM KCl 5 mM MgCl <sub>2</sub> 1 mM TCEP

CHIP was overexpressed in 2 x 1 L LB medium (30  $\mu$ g/mL Kanamycin) shaking o/n at 20°C with 110 rpm in *E. coli* BL21(DE3) induced at OD<sub>600</sub> = 0.6 with 0.1 mM IPTG. Cells were harvested for 25 min at 4°C with 7500 rpm (JLA-8.1000 rotor), resuspended in up to 40 mL lysis buffer plus 1  $\mu$ M PMSF and 1 tablet of protease inhibitor (w/o EDTA), flash-frozen in liquid nitrogen and stored o/n at -20 °C. The next day the bacteria were thawed in hot tap water and lysed by sonication on ice (5 min in total with 20 sec pulses interrupted by 10 sec breaks, 50 % amplitude). Cell debris was spun down for 30 min at 4°C with 10000 g (5424R centrifuge).

The supernatant including the His<sub>6</sub>-tagged CHIP was further purified by IMAC with gravity flow. Therefore, 12 mL equilibrated Ni-NTA Agarose beads were gently shaken with the lysed supernatant of 1 L protein expression for 30 min at 4°C. Unspecifically bound proteins were washed off with 5 cv of lysis buffer. The remaining proteins including the His<sub>6</sub>-tagged CHIP were eluted with 2 cv of elution buffer. After o/n dialysis in thrombin buffer at 4°C (dialysis hose: 3.5 kDa cutoff) possible precipitations were spun down for 30 min at 4°C with 9000 rpm (FA-45-6-30). The protein solution was concentrated down to 5.5 mL (concentrator pores: 10 kDa cutoff; FA-45-6-30) followed by His<sub>6</sub>-tag cleavage with 74 NIH units of thrombin protease per 1 mg protein gently shaking o/n at 4°C. The next day the sample was filtered (pore size: 0.45  $\mu$ m) in order to remove any precipitated contents out of the solution. 5.5 mL of sample were purified *via* SEC (SD75 26/600, 10 mL loop, 1 mL/min). Peak fractions were pooled and concentrated up to ~250  $\mu$ M (concentrator pores: 5 kDa cutoff; FA-45-6-30). Protein concentration was determined by absorption measurement at  $\lambda$  = 280 nm. Aliquots of 20  $\mu$ L were flash-frozen in liquid nitrogen and stored at -80 °C.

An exemplary purification analysis of human CHIP is presented in Figure A 3.



## Material and Methods

### 2.3.4.2 Hop *established by A. Lott*

<i>Lysis buffer</i>	20 mM Tris pH 8.0 500 mM NaCl 10 mM Imidazole 3 mM $\beta$ -ME	<i>Elution buffer</i>	20 mM Tris pH 8.0 500 mM NaCl 500 mM Imidazole 3 mM $\beta$ -ME
<i>SEC buffer</i>	25 mM HEPES pH 7.4 100 mM KCl 5 mM MgCl <sub>2</sub> 1 mM TCEP		

Hop was overexpressed in 1 L LB medium (30  $\mu$ g/mL Kanamycin) shaking o/n at 20°C with 110 rpm in *E. coli* Rosetta2 (DE3) induced at OD<sub>600</sub> = 0.7 with 0.1 mM IPTG. Cells were harvested for 25 min at 4°C with 7500 rpm (JLA-8.1000 rotor), resuspended in up to 20 mL lysis buffer plus 1  $\mu$ M PMSF and 1 tablet of protease inhibitor (w/o EDTA), flash-frozen in liquid nitrogen and stored for one week at -20 °C. For cell lysis bacteria were thawed in hot tap water and fresh 3 mM  $\beta$ -ME were added as reducing agent. After sonication on ice (5 min in total with 20 sec pulses interrupted by 10 sec breaks, 40 % amplitude) cell debris was spun down for 30 min at 4°C with 22000 rpm (JA 25.50).

The supernatant including the His<sub>6</sub>-tagged Hop was further purified by IMAC with gravity flow. Therefore, 4 mL equilibrated Ni-NTA Agarose beads were gently shaken with the lysed supernatant of 1 L protein expression for 30 min at 4°C. Unspecifically bound proteins were washed off with 5 cv of lysis buffer. The remaining proteins including the His<sub>6</sub>-tagged Hop were eluted with 2 cv of elution buffer.

After o/n dialysis in SEC buffer at 4°C (dialysis hose: 8-10 kDa cutoff) the protein solution was concentrated down to 10 mL (concentrator pores: 30 kDa cutoff; FA-45-6-30) and centrifuged for 15 min at 4°C with 8000 rpm (FA-45-6-30) in order to remove any precipitated contents out of the solution. Two runs of SEC were performed with each 5 mL of sample (SD75 26/600, 10 mL loop, 2 mL/min). Peak fractions were pooled and concentrated up to ~250  $\mu$ M (concentrator pores: 10 kDa cutoff; FA-45-6-30). Protein concentration was determined by absorption measurement at  $\lambda$  = 280 nm. Aliquots of 25  $\mu$ L were flash-frozen in liquid nitrogen and stored at -80 °C.

An exemplary purification analysis of human Hop is presented in Figure A 4.

## Material and Methods

### 2.3.4.3 Hop112a *established by G. Butnariu under the supervision of A. Lott*

<i>Lysis buffer</i>	20 mM Tris pH 8.0 500 mM NaCl 10 mM Imidazole 3 mM $\beta$ -ME	<i>Elution buffer</i>	20 mM Tris pH 8.0 500 mM NaCl 500 mM Imidazole 3 mM $\beta$ -ME
<i>Thrombin buffer</i>	25 mM Tris pH 8.0 100 mM NaCl 3 mM $\beta$ -ME	<i>SEC buffer</i>	25 mM HEPES pH 7.4 150 mM NaCl 1 mM DTT

Hop112a was overexpressed in 2 x 1 L LB medium (30  $\mu$ g/mL Kanamycin) shaking o/n at 20°C with 110 rpm in *E. coli* Rosetta2 (DE3) induced at OD<sub>600</sub> = 0.7 with 0.1 mM IPTG. Cells were harvested for 25 min at 4°C with 7500 rpm (JLA-8.1000 rotor), resuspended in up to 40 mL lysis buffer plus 1  $\mu$ M PMSF and 1 tablet of protease inhibitor (w/o EDTA), flash-frozen in liquid nitrogen and stored at -80 °C. For cell lysis bacteria were thawed in hot tap water and fresh 3 mM  $\beta$ -ME were added as reducing agent. After sonication on ice (5 min with 30 % amplitude, 2 min 50%, 2 min 55%, each with 20 sec pulses interrupted by 10 sec breaks) cell debris was spun down for 30 min at 4°C with 22000 rpm (JA 25.50).

The supernatant including the His<sub>6</sub>-tagged Hop112a was further purified by IMAC with gravity flow. Therefore, 8 mL equilibrated Ni-NTA Agarose beads were gently shaken with the lysed supernatant of 1 L protein expression for 30 min at 4°C. Unspecifically bound proteins were washed off with 10 cv of lysis buffer. The remaining proteins including the His<sub>6</sub>-tagged Hop112a were eluted with 2 cv of elution buffer. After o/n dialysis in thrombin buffer at 4°C (dialysis hose: 8-10 kDa cutoff) the His<sub>6</sub>-tag was cleaved off with 148 NIH units of thrombin protease per 1 mg protein gently shaking o/n at 25°C. The next day thrombin protease was inactivated with 500  $\mu$ M PMSF. After o/n dialysis in SEC buffer at 4°C (dialysis hose: 0.5-1 kDa cutoff), the sample was concentrated down to 5 mL (concentrator pores: 10 kDa cutoff; FA-45-6-30), centrifuged for 15 min at 4°C with 8000 rpm (FA-45-6-30) in order to remove any precipitated contents out of the solution and purified *via* SEC (SD75 26/600, 10 mL loop, 2 mL/min). Peak fractions were pooled and dialyzed o/n in storage buffer (25 mM HEPES pH 7.4/ 100 mM KCl/ 5 mM MgCl<sub>2</sub>/ 1 mM TCEP) at 4°C (dialysis hose: 0.5-1 kDa cutoff). The next day the protein solution was concentrated up to ~220  $\mu$ M (concentrator pores: 10 kDa cutoff; FA-45-6-30). Protein concentration was determined by absorption measurement at  $\lambda$  = 280 nm. Aliquots of 50  $\mu$ L were flash-frozen in liquid nitrogen and stored at -80 °C.

An exemplary purification analysis of the Hop112a construct is presented in Figure A 5.

## Material and Methods

### 2.3.4.4 Hsp40 *established by A. Lott*

<i>Lysis buffer</i>	10 mM HEPES pH 7.5 500 mM NaCl 10 mM Imidazole 6 mM $\beta$ -ME	<i>Elution buffer</i>	20 mM Tris pH 8.0 500 mM NaCl 500 mM Imidazole 6 mM $\beta$ -ME
<i>Thrombin buffer</i>	20 mM Tris pH 8.0 100 mM NaCl 6 mM $\beta$ -ME	<i>SEC buffer</i>	25 mM HEPES pH 7.4 100 mM KCl 5 mM MgCl <sub>2</sub> 1 mM TCEP

Hsp40 was overexpressed in 1 L LB medium (30  $\mu$ g/mL Kanamycin) shaking o/n at 20°C with 110 rpm in *E. coli* Rosetta2 (DE3) induced at OD<sub>600</sub> = 0.7 with 0.1 mM IPTG. Cells were harvested for 30 min at 4°C with 7500 rpm (JLA-8.1000 rotor), resuspended in up to 20 mL lysis buffer plus 1  $\mu$ M PMSF and 1 tablet of protease inhibitor (w/o EDTA), flash-frozen in liquid nitrogen and stored at -80 °C. For cell lysis bacteria were thawed in hot tap water and fresh 6 mM  $\beta$ -ME were added as reducing agent. After sonication on ice (2 x 5 min in total with 20 sec pulses interrupted by 10 sec breaks, 45 % amplitude) cell debris was spun down for 30 min at 4°C with 22000 rpm (JA 25.50).

The supernatant including the His<sub>6</sub>-tagged Hsp40 was further purified by IMAC with gravity flow. Therefore, 4 mL equilibrated Ni-NTA Agarose beads were gently shaken with the lysed supernatant of 1 L protein expression for 30 min at 4°C. Unspecifically bound proteins were washed off with 5 cv of lysis buffer. The remaining proteins including the His<sub>6</sub>-tagged Hsp40 were eluted with 2 cv of elution buffer. After o/n dialysis in thrombin buffer at 4°C (dialysis hose: 0.5-1 kDa cutoff) possible precipitations were spun down for 20 min at 4°C with 6000 rpm (FA-45-6-30). The His<sub>6</sub>-tag was cleaved off with 74 NIH units of thrombin protease per 1 mg protein gently shaking o/n at 4°C. The next day thrombin protease was inactivated with 500  $\mu$ M PMSF. After dialysis in SEC buffer (dialysis hose: 0.5-1 kDa cutoff) for two days at 4°C, the sample was concentrated down to 5 mL (concentrator pores: 10 kDa cutoff; FA-45-6-30), filtered (pore size: 0.2  $\mu$ m) in order to remove any precipitated contents out of the solution and purified *via* SEC (SD75 26/600, 10 mL loop, 1.8 mL/min). Peak fractions were pooled and concentrated up to ~250  $\mu$ M (concentrator pores: 10 kDa cutoff; FA-45-6-30). Protein concentration was determined by absorption measurement at  $\lambda$  = 280 nm. Aliquots of 25  $\mu$ L were flash-frozen in liquid nitrogen and stored at -80 °C.

An exemplary purification analysis of human Hsp40 is presented in Figure A 6.

## Material and Methods

### 2.3.4.5 Hsp70 *received from A. Savastano*

<i>Lysis buffer</i>	20 mM Tris pH 8.0 500 mM NaCl 10 mM Imidazole 6 mM $\beta$ -ME	<i>Elution buffer</i>	20 mM Tris pH 8.0 500 mM NaCl 250 mM Imidazole 6 mM $\beta$ -ME
<i>Thrombin buffer</i>	20 mM Tris pH 8.0 150 mM NaCl 1 mM DTT	<i>SEC buffer</i>	25 mM HEPES pH 7.4 100 mM KCl 5 mM MgCl <sub>2</sub> 1 mM TCEP

Hsp70 was overexpressed in 1 L LB medium (30  $\mu$ g/mL Kanamycin) shaking for 4 h at 37°C with 110 rpm in *E. coli* Rosetta2 (DE3) induced at OD<sub>600</sub> = 0.8 with 1 mM IPTG. Cells were harvested for 25 min at 4°C with 7500 rpm (JLA-8.1000 rotor), resuspended in up to 20 mL lysis buffer plus 1  $\mu$ M PMSF, 1 tablet of protease inhibitor (w/o EDTA), 1 mg/mL lysozyme, 10  $\mu$ g/mL RNase and 10  $\mu$ g/mL DNase, flash-frozen in liquid nitrogen and stored at -20 °C. For cell lysis bacteria were thawed in hot tap water and fresh 6 mM  $\beta$ -ME were added as reducing agent. After sonication on ice (5 min in total with 20 sec pulses interrupted by 10 sec breaks, 30 % amplitude) cell debris was spun down for 30 min at 4°C with 22000 rpm (JA 25.50).

The supernatant including the His<sub>6</sub>-tagged Hsp70 was further purified by IMAC with gravity flow. Therefore, 6 mL equilibrated Ni-NTA Agarose beads were gently shaken with the lysed supernatant of 1 L protein expression for 30 min at 4°C. Unspecifically bound proteins were washed off with 10 cv of lysis buffer. The remaining proteins including the His<sub>6</sub>-tagged Hsp70 were eluted with 2 cv of elution buffer. During o/n dialysis in thrombin buffer at 4°C (dialysis hose: 3.5-5 kDa cutoff) the His<sub>6</sub>-tag was cleaved off with 80  $\mu$ L of thrombin protease (stock: 74 NIH units/ $\mu$ L). The next day a second IMAC was performed in order to extract the cleaved fraction only. The flow through and wash fraction (2 cv lysis buffer) were pooled and concentrated down to 5 mL (concentrator pores: 30 kDa cutoff; FA-45-6-30). The sample was centrifuged for 20 min at 4°C with 7900 rpm (FA-45-6-30) in order to remove any precipitated contents out of the solution and purified *via* SEC (SD75 26/600, 10 mL loop, 0.75 mL/min). Peak fractions were pooled and concentrated up to ~300  $\mu$ M (concentrator pores: 30 kDa cutoff; FA-45-6-30). Protein concentration was determined by absorption measurement at  $\lambda$  = 280 nm. Aliquots of 25  $\mu$ L were flash-frozen in liquid nitrogen and stored at -80 °C.

An exemplary purification analysis of human Hsp70 is presented in Figure A 7.

## Material and Methods

### 2.3.4.6 Hsp90 *received from J. Oroz*

<i>Lysis buffer</i>	20 mM Tris pH 8.0 500 mM NaCl 10 mM Imidazole 6 mM $\beta$ -ME	<i>Elution buffer</i>	20 mM Tris pH 8.0 500 mM NaCl 250 mM Imidazole 6 mM $\beta$ -ME
<i>SEC buffer</i>	10 mM HEPES pH 7.5 500 mM KCl 0.5 mM DTT	<i>Storage buffer</i>	25 mM HEPES pH 7.4 100 mM KCl 5 mM MgCl <sub>2</sub> 1 mM TCEP

Hsp90 was overexpressed in 2 x 1 L LB medium (30  $\mu$ g/mL Kanamycin) shaking for 4 h at 37°C with 110 rpm in *E. coli* Rosetta2 (DE3) induced at OD<sub>600</sub> = 1.1 with 1 mM IPTG. Cells were harvested for 25 min at 4°C with 7500 rpm (JLA-8.1000 rotor), resuspended in up to 40 mL lysis buffer plus 1  $\mu$ M PMSF and 1 tablet of protease inhibitor (w/o EDTA), flash-frozen in liquid nitrogen and stored at -80 °C. For cell lysis bacteria were thawed in hot tap water and fresh 6 mM  $\beta$ -ME were added as reducing agent. After sonication on ice (5 min in total with 20 sec pulses interrupted by 10 sec breaks, 60 % amplitude) cell debris was spun down for 30 min at 4°C with 22000 rpm (JA 25.50).

The supernatant including the His<sub>6</sub>-tagged Hsp90 was further purified by IMAC with gravity flow. Therefore, 5 mL equilibrated Ni-NTA Agarose beads were gently shaken with the lysed supernatant of 2 L protein expression for 30 min at 4°C. Unspecifically bound proteins were washed off with 10 cv of lysis buffer. The remaining proteins including the His<sub>6</sub>-tagged Hsp90 were eluted with 3 cv of elution buffer.

The protein solution was concentrated down to 5 mL (concentrator pores: 30 kDa cutoff; FA-45-6-30), centrifuged for 20 min at 4°C with 8000 rpm (FA-45-6-30) in order to remove any precipitated contents out of the solution and purified *via* SEC (SD200 26/600, 10 mL loop, 2 mL/min). Peak fractions were pooled and dialyzed o/n in storage buffer at 4°C (dialysis hose: 3.5-5 kDa cutoff). The next day the protein solution was concentrated up to ~200  $\mu$ M (concentrator pores: 30 kDa cutoff; FA-45-6-30). Protein concentration was determined by absorption measurement at  $\lambda$  = 280 nm. Aliquots of 25  $\mu$ L were flash-frozen in liquid nitrogen and stored at -80 °C.

An exemplary purification analysis of human Hsp90 is presented in Figure A 8.

### 2.3.4.7 Hsp90\* *received from J. Oroz*

For NMR experiments, Hsp90 was produced perdeuterated with selectively labeled [ $^1\text{H}$ - $^{13}\text{C}$ ]-isoleucine  $\delta$ -methyl groups (Figure 13), for clarity here denoted as Hsp90\*. Hsp90\* was produced in *E. coli* BL21(DE3) growing in M9 minimal medium (99%  $\text{D}_2\text{O}$ ) including [ $^2\text{H}$ - $^{12}\text{C}$ ]-glucose as the sole source of carbon. The cells were allowed to stepwise adapt to the deuterated medium, beginning with 5 mL of LB medium (30  $\mu\text{g}/\text{mL}$  Kanamycin) inoculated with a single colony shaking o/n at 37°C with 220 rpm. The next day bacterial growth was continued in 5 mL of M9 minimal medium (30  $\mu\text{g}/\text{mL}$  Kanamycin) in 100 %  $\text{H}_2\text{O}$ . At saturation  $\text{H}_2\text{O}$  was gradually substituted with  $\text{D}_2\text{O}$  by transferring 200  $\mu\text{L}$  of the previous culture into fresh 5 mL of M9 minimal medium (30  $\mu\text{g}/\text{mL}$  Kanamycin) in 33 %  $\text{D}_2\text{O}$ , 66 %  $\text{D}_2\text{O}$  and 99 %  $\text{D}_2\text{O}$ . Finally, the volume was scaled up to 100 mL and then to 1 L of M9 minimal medium (30  $\mu\text{g}/\text{mL}$  Kanamycin) in 99 %  $\text{D}_2\text{O}$  and bacteria were enriched at 37°C shaking with 110 rpm. One hour before induction ( $\text{OD}_{600} = 0.6$ ) the metabolic precursor for selective [ $^1\text{H}$ - $^{13}\text{C}$ ]- Ile  $\delta$ -methyl groups labeling 2-ketobutyric acid-4 [ $^{13}\text{C}$ ],3,3-[ $\text{D}_2$ ] sodium salt was added. At  $\text{OD}_{600} = 0.8$  Hsp90\* overexpression was induced with 0.5 mM IPTG and continued o/n at 37 °C shaking with 110 rpm.

Hsp90\* was purified similarly as unlabeled Hsp90 (see chapter 2.3.4.6). An exemplary purification analysis of human Hsp90\* is presented in Figure A 9.

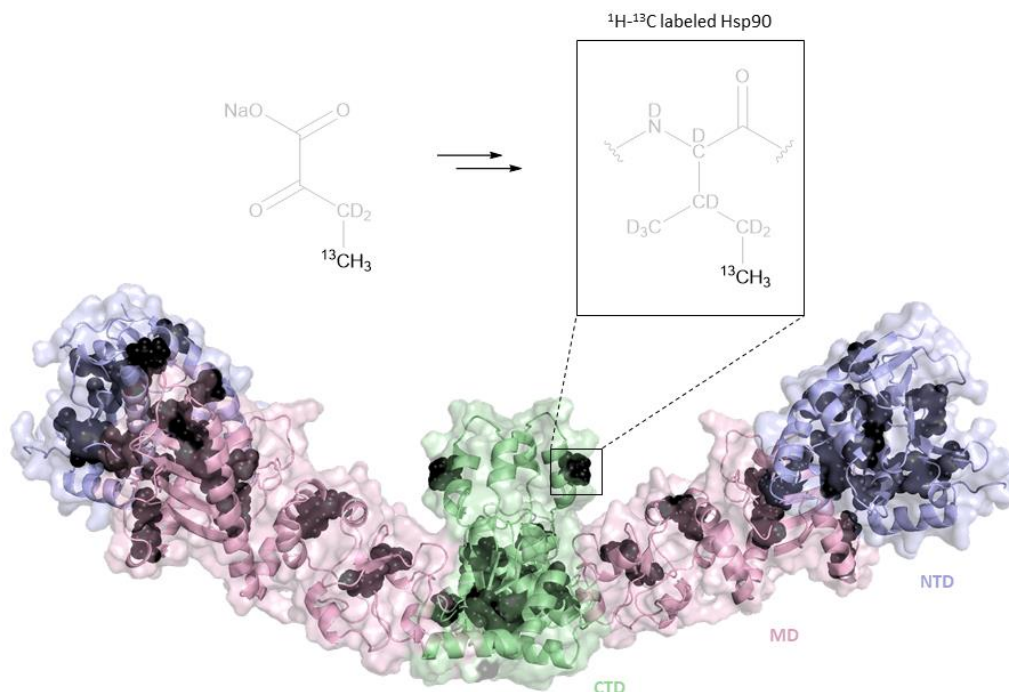


**Figure 13** Selectively  $^1\text{H}$ - $^{13}\text{C}$  labeled Hsp90 at the Ile  $\delta$ -methyl groups.

Front view of the open structure of Hsp90 shown as cartoon (N-terminal domain (NTD, light blue), middle domain (MD, light pink) and C-terminal domain (CTD, light green)).<sup>121</sup> Isoleucines are highlighted in black spheres. The metabolic precursor 2-ketobutyric acid-4 [ $^{13}\text{C}$ ],3,3-[ $\text{D}_2$ ] sodium salt was used for site specific isotope labeling.<sup>329</sup> Zoom in shows Hsp90 isoleucines selectively [ $^1\text{H}$ ,  $^{13}\text{C}$ ] labeled at the  $\delta$ -methyl groups in an otherwise fully deuterated protein.

## Material and Methods

### 2.3.4.8 p23 established by A. Lott

<i>Lysis buffer</i>	20 mM Tris pH 8.0 500 mM NaCl 10 mM Imidazole 6 mM $\beta$ -ME	<i>Elution buffer</i>	20 mM Tris pH 8.0 500 mM NaCl 500 mM Imidazole 6 mM $\beta$ -ME
<i>Thrombin buffer</i>	20 mM Tris pH 8.0 100 mM NaCl 6 mM $\beta$ -ME	<i>SEC buffer</i>	25 mM Tris pH 7.0 100 mM NaCl 1 mM DTT

p23 was overexpressed in 1 L LB medium (30  $\mu$ g/mL Kanamycin) shaking o/n at 20°C with 110 rpm in *E. coli* Rosetta2 (DE3) induced at OD<sub>600</sub> = 0.6 with 0.1 mM IPTG. Cells were harvested for 30 min at 6°C with 7500 rpm (JLA-8.1000 rotor), resuspended in up to 20 mL lysis buffer plus 1  $\mu$ M PMSF and 1 tablet of protease inhibitor (w/o EDTA), flash-frozen in liquid nitrogen and stored at -80 °C. For cell lysis bacteria were thawed in hot tap water and fresh 6 mM  $\beta$ -ME were added as reducing agent. After sonication on ice (5 min with 30 % amplitude, 2 min 45%, each with 20 sec pulses interrupted by 10 sec breaks) cell debris was spun down for 30 min at 6°C with 22000 rpm (JA 25.50).

The supernatant including the His<sub>6</sub>-tagged p23 was further purified by IMAC with gravity flow. Therefore, 8 mL equilibrated Ni-NTA Agarose beads were gently shaken with the lysed supernatant of 1 L protein expression for 30 min at 4°C. Unspecifically bound proteins were washed off with 10 cv of lysis buffer. The remaining proteins including the His<sub>6</sub>-tagged p23 were eluted with 2 cv of elution buffer. The protein solution was concentrated down to 2.5 mL (concentrator pores: 10 kDa cutoff; FA-45-6-30) followed by o/n dialysis in thrombin buffer at 4°C (dialysis hose: 3.5-5 kDa cutoff). The next day the His<sub>6</sub>-tag was cleaved off with 37 NIH units of thrombin protease per 1 mg protein gently shaking for 1 h at RT. Thrombin protease was inactivated with 500  $\mu$ M PMSF. After o/n dialysis in SEC buffer at 4°C (dialysis hose: 3.5-5 kDa cutoff), the sample was centrifuged for 20 min at 4°C with 8000 rpm (FA-45-6-30) in order to remove any precipitated contents out of the solution and purified *via* SEC (SD75 16/600, 5 mL loop, 1.8 mL/min). Peak fractions were pooled and concentrated up to ~500  $\mu$ M (concentrator pores: 10 kDa cutoff; FA-45-6-30). The protein solution was dialyzed o/w in storage buffer (25 mM HEPES pH 7.4/ 100 mM KCl/ 5 mM MgCl<sub>2</sub>/ 1 mM TCEP) at 4°C (dialysis hose: 3.5-5 kDa cutoff). Protein concentration was determined by absorption measurement at  $\lambda$  = 280 nm. Aliquots of 200  $\mu$ L were flash-frozen in liquid nitrogen and stored at -80 °C.

An exemplary purification analysis of human p23 is presented in Figure A 10.

## Material and Methods

### 2.3.4.9 Tau *received from S. Cima-Omori*

<i>Lysis buffer</i>	20 mM MES pH 6.8 1 mM EGTA 0.2 mM MgCl <sub>2</sub> 5 mM DTT	<i>Dialysis buffer</i>	20 mM MES pH 6.8 1 mM EDTA 2 mM DTT
<i>Buffer A / B</i>	20 mM MES pH 6.8 50 mM / 1 M NaCl 1 mM EDTA 2 mM DTT	<i>SEC buffer</i>	25 mM HEPES pH 7.4 100 mM KCl 5 mM MgCl <sub>2</sub> 1 mM TCEP

Flash-frozen *E. coli* BL21 (DE3) bacterial pellets from 6 L Tau expression stored at -80°C were thankfully received from the group's technician S. Cima-Omori. For cell lysis bacteria were thawed in hot tap water, resuspended in 180 mL ice cold lysis buffer plus 1 mM PMSF, 5 tablets of protease inhibitor (w/o EDTA), 1 mg/mL lysozyme and 10 µg/mL DNase and stirred for 20 min at 4°C to obtain a homogeneous solution. Cells were lysed *via* French press on ice (two rounds for complete disruption), 500 mM NaCl were added and the lysate was boiled in a water bath for 20 min at 98°C. After cooling down the solution for 10 min on ice, cell debris and precipitated proteins were spun down by ultracentrifugation for 40 min at 4°C with 127000 g (45-Ti). Nucleic acids were precipitated by adding 20 mg streptomycin per 1 mL supernatant. The sample was gently shaken for 15 min at 4°C followed by centrifugation for 30 min at 4°C with 15000 g (FA-45-6-30). Tau was extracted by ammonium sulfate precipitation with 0.361 g (NH<sub>4</sub>)<sub>2</sub>SO<sub>4</sub> per 1 mL supernatant (again 15 min incubation at 4°C and 30 min centrifugation at 4°C with 15000 g (FA-45-6-30)). The pellet including the Tau protein was resuspended in dialysis buffer plus 0.1 mM PMSF and dialyzed o/n in 4 L dialysis buffer plus 0.1 mM PMSF at 4°C (dialysis cassette: 3.5 kDa cutoff).

The next day the dialyzed sample was filtered (pore size: 0.22 µm) and further purified by cation exchange chromatography (MonoS 10/100, 2 mL/min). Unspecifically bound proteins were washed off with 5 cv of buffer A plus 0.1 mM PMSF. The remaining proteins including Tau were eluted with increasing salt concentration (linear gradient 0-60% buffer B plus 0.1 mM PMSF within 15 cv). The fractions of interest were pooled and concentrated down to 5 mL (concentrator pores: 5 kDa cutoff; FA-45-6-30). The sample was centrifuged for 20 min at 4°C with 9000 g (FA-45-6-30) and purified two times *via* SEC (SD75 26/600, 10 mL loop, 2 mL/min). Peak fractions of both runs were pooled and concentrated up to ~1 M (concentrator pores: 5 kDa cutoff; FA-45-6-30). Protein concentration was determined with the Pierce<sup>TM</sup> BCA Protein Assay Kit. Aliquots of 20 µL were flash-frozen in liquid nitrogen and stored at -80 °C.

An exemplary purification analysis of human Tau is presented in Figure A 11.



## Material and Methods

Isotopically labeled Tau was produced in M9 minimal medium including  $^{15}\text{NH}_4\text{Cl}$  as the only source of nitrogen to generate uniformly  $^{15}\text{N}$ -labeled Tau (Figure 14). The purification protocol corresponds to that described above for unlabeled Tau.

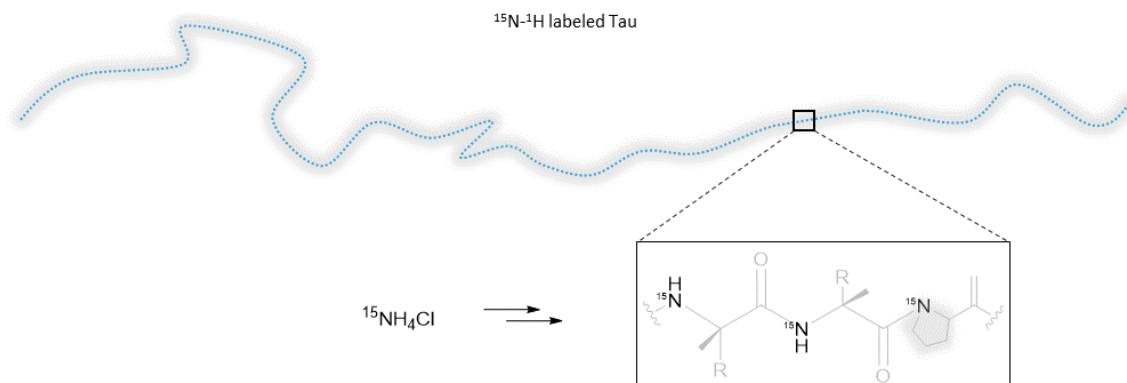


**Figure 14 Selectively  $^{15}\text{N}$ -labeled Tau.**

For NMR experiments Tau was produced uniformly  $^{15}\text{N}$ -labeled. Accordingly labeled ammonium chloride was added as the only source of nitrogen. Zoom in shows the backbone of Tau  $^{15}\text{N}$ -labeled at the nitrogen of each peptide group (highlighted in black). By this expression technique proline residues are invisible in  $^{15}\text{N}$ - $^1\text{H}$  correlation NMR spectra as they lack the hydrogen at the backbone nitrogen (shaded in grey).

## 2.4 *In vitro* complex reconstitution

### *Reaction Buffer*

25 mM HEPES pH 7.4  
100 mM KCl  
5 mM  $\text{MgCl}_2$   
1 mM TCEP

If not already present as such, proteins were dialyzed o/n in 1 L reaction buffer slowly stirring at  $4^\circ\text{C}$  (dialysis hose: 0.5-1 kDa cutoff). Complex formation was followed *via* titration by mixing the proteins of interest in a molar ratio of 1:x, whereby 1 refers to 2.5-10  $\mu\text{M}$  of titrant A in a final volume of 10  $\mu\text{L}$  (applied concentrations are specified in the respective figure legends). Each titration point was set up as individual experiment. When indicated, the nucleotides ATP, AMP-PNP or ADP were added in excess to a final concentration of 5 mM. For complex analyses the proteins Hsp70, Hop, Hsp90, Tau and p23 were mixed in a molar ratio of 1:1:1:5:5 in reaction buffer. Samples were incubated for 45 min at  $25^\circ\text{C}$  gently shaking with 350 rpm and analyzed by native page (see chapter 2.2.2).

Relative band intensities were quantified using ImageJ, whereby the mean intensity of the band of interest was background subtracted and divided by the intensity of the reference band for normalization. Errors represent the standard deviation from three independent experiments.

## 2.5 Affinity measurements

The dissociation equilibrium constant  $K_D$  characterizes the affinity of two interaction partners A and B for each other - the higher the affinity the stronger the interaction. Thus, by measuring the  $K_D$  between two molecules one can estimate which interactions are more likely than others – a highly valuable information regarding the incredible amounts of interaction partners within a biological cell. The following estimations are described for a single site binding model.<sup>350</sup>

Affinity measurements are based on the premise that at equilibrium the rate of binding is equal to the rate of dissociation. Along this line, the  $K_D$  for a reversible, bimolecular binding reaction  $A + B \rightleftharpoons AB$  is defined as:

$$K_D = \frac{A_{\text{free}} \cdot B_{\text{free}}}{AB} \quad 1$$

As  $A_{\text{free}} = A_{\text{total}} - AB$  (and the same holds true for  $B_{\text{free}}$ ), it is sufficient to measure the concentration of AB in order to calculate the  $K_D$ , whereby the signal one obtains upon binding must be directly proportional to the concentration of AB. If the experimental setup further allows to hold the concentration of A below the  $K_D$  (ideally 10 x lower) virtually all B is free at any experimental point, implying  $B_{\text{free}} = B_{\text{total}}$ . This yields the classic expression for a hyperbolic binding curve with:

$$AB = \frac{A_{\text{total}} \cdot B_{\text{total}}}{B_{\text{total}} + K_D} \quad 2$$

### 2.5.1 Chemical Assay by gel electrophoresis

Native page was used to determine the amount of complex formed as the intensity of the complex band. Complexes were formed as described in 2.4. The affinity was measured between the Hsp70:Hop:Hsp90 complex (molecule A) in a molar ratio of 1:1:1 and the substrate Tau (molecule B). The concentration of A was fixed at 0.8  $\mu\text{M}$ . The intensity of the complex band AB was followed upon increasing concentrations of B ranging from 0 – 64  $\mu\text{M}$ .

The intensity I of AB was quantified as described in 2.4. The normalized mean intensity of AB (y-axis) was plotted against  $B_{\text{total}}$  (x-axis) at each respective titration point. Data were fitted using the solver function in Excel according to the equation  $I = I_{\text{max}} \cdot \frac{B_{\text{total}}}{B_{\text{total}} + K_D}$ , whereby  $I_{\text{max}} = 1$  due to normalization. Errors represent the standard deviation from three independent experiments (Hsp70:Hop:Hsp90:Tau) or the standard deviation of the fit (Hsp70:Hop:Hsp90:Tau+AMP-PNP) with  $\text{stdv of fit} = \sqrt{\frac{\sum(I - I_{\text{obs}})^2}{n-2}}$ , with  $I_{\text{obs}}$  as the detected band intensity and n as the number of data points.

### 2.5.2 Trp fluorescence

The intrinsic tryptophane (Trp) fluorescence of a protein A can likewise be used for affinity measurements if the fluorescence intensity changes upon binding with partner B. In such cases the change in fluorescence intensity is directly proportional to the amount of AB complex formed.

This technique was used to reproduce the affinity measurements between Hsp90 (molecule A) and Tau (molecule B) reported in literature<sup>84</sup>. Therefore, 160  $\mu$ L of Hsp90: Tau complex were prepared as described in 2.4 in a molar ratio of 1:10 with 5  $\mu$ M of Hsp90. The binding profile was measured from back to forth with stepwise dilution of Tau by exchanging 20  $\mu$ L of Hsp90: Tau with 20  $\mu$ L of Hsp90 only. Fluorescence spectra were recorded on an Agilent Cary Eclipse fluorescence spectrophotometer with  $\lambda_{\text{excitation}} = 295$  nm and  $\lambda_{\text{emission}} = 302\text{-}398$  nm. The maximum emission values within  $\lambda = 340\text{-}355$  nm (y-axis) were averaged from three measurement cycles and plotted against  $B_{\text{total}}$  (x-axis) at each respective titration point. Data were fitted using the solver function in Excel according to the equation  $F = F_{\text{max}} \cdot \frac{B_{\text{total}}}{B_{\text{total}} + K_D}$ , whereby  $F_{\text{max}} = 1$  due to normalization. The error represents the standard deviation of the fit with  $\text{stdv of fit} = \sqrt{\frac{\sum(I - I_{\text{obs}})^2}{n-2}}$ , with  $I_{\text{obs}}$  as the detected band intensity and n as the number of data points.

### 2.5.3 Isothermal titration calorimetry

By isothermal titration calorimetry (ITC) one determines the heat that is released or consumed upon the interaction of two binding partners.<sup>331</sup> The raw data are plotted as the differential power in  $\mu$ cal/sec needed (endothermic) or retained (exothermic) to maintain isothermal conditions between the reference and the sample cell. The integral of each spike yields the heat Q absorbed or evolved at each respective titration point. The final ITC binding isotherms are presented in the derivative format depicting the differential heat  $\frac{dQ}{dB_{\text{total}}}$  per injection in kcal/mol, i.e. the change of heat (dQ) with the change of total molecule B concentration ( $dB_{\text{total}}$ ) in the sample cell. The change of heat is directly proportional to the change of AB concentration (dAB) as:

$$dQ = dAB \cdot \Delta H^0 \cdot V_0 \quad 3$$

with  $\Delta H^0$  and  $V_0$  as the molar binding enthalpy and the cell volume at each titration point, respectively. Commonly, in ITC the concentration of A is in the range of or above the  $K_D$  of the binding reaction. Hence, a substantial amount of B exists as AB so that  $B_{\text{free}}$  is no longer equal to  $B_{\text{total}}$  as introduced in 2.5. In such cases, applying  $A_{\text{free}} = A_{\text{total}} - AB$  and  $B_{\text{free}} = B_{\text{total}} - AB$  in Eq. 1 gives the quadratic formula  $0 = ax^2 + bx + c$  (Eq. 4) that can be solved for AB with  $AB_{1/2} = \frac{-b \pm \sqrt{b^2 - 4ac}}{2a}$ , whereby the only real root is Eq. 5, as the maximum concentration of AB is

limited to the concentration of  $A_{\text{total}}$  and  $B_{\text{total}}$ . Differentiation and rearrangement yields  $dAB$  as the change of the amount of AB complex with respect to the variation of  $B_{\text{total}}$  (Eq. 6).

$$0 = AB^2 - (A_{\text{total}} + B_{\text{total}} + K_D) \cdot AB + A_{\text{total}} \cdot B_{\text{total}} \quad 4$$

$$AB = \frac{A_{\text{total}} + B_{\text{total}} + K_D - \sqrt{(A_{\text{total}} + B_{\text{total}} + K_D)^2 - 4 \cdot A_{\text{total}} \cdot B_{\text{total}}}}{2} \quad 5$$

$$\frac{dAB}{dB_{\text{total}}} = \frac{1}{2} + \frac{1 - \left(1 + \frac{B_{\text{total}}}{A_{\text{total}}} + \frac{K_D}{A_{\text{total}}}\right) \cdot \frac{1}{2}}{\sqrt{\left(1 + \frac{B_{\text{total}}}{A_{\text{total}}} + \frac{K_D}{A_{\text{total}}}\right)^2 - 4 \cdot \frac{B_{\text{total}}}{A_{\text{total}}}}} \quad 6$$

Substituting Eq. 6 into Eq. 3 yields the classical Wiseman-isotherm used to fit the experimentally determined differential heat from which the  $K_D$  can be determined:

$$\frac{dQ}{dB_{\text{total}}} = \left( \frac{1}{2} + \frac{1 - \left(1 + \frac{B_{\text{total}}}{A_{\text{total}}} + \frac{K_D}{A_{\text{total}}}\right) \cdot \frac{1}{2}}{\sqrt{\left(1 + \frac{B_{\text{total}}}{A_{\text{total}}} + \frac{K_D}{A_{\text{total}}}\right)^2 - 4 \cdot \frac{B_{\text{total}}}{A_{\text{total}}}}} \right) \cdot \Delta H^0 \cdot V_0 \quad 7$$

ITC is the only technique that beyond gives insights into the thermodynamic character of a binding reaction, as the free energy  $\Delta G$  (Eq. 8) as well as the entropy  $\Delta S$  (Eq. 9) can further be calculated with:

$$\Delta G = -R \cdot T \cdot \ln\left(\frac{1}{K_D}\right) \quad 8$$

$$\Delta G = \Delta H - T \cdot \Delta S \quad 9$$

where  $R$  is the universal gas constant and  $T$  is the temperature. This information yields the driving force of a particular interaction, as an entropically driven binding reaction is of rather hydrophobic character, whereas enthalpically driven binding reactions are based on hydrogen bondings, salt bridges and van der Waals forces.<sup>332</sup>

Affinity measurements by ITC were performed at 25°C on a Microcal PEAQ-ITC automated machine. Prior to each experiment, proteins were dialyzed o/n into the same buffer (25 mM HEPES pH 7.4/ 100 mM KCl/ 5 mM MgCl<sub>2</sub>/ 1 mM TCEP; degassed) at 4°C (dialysis hose: 0.5-1 kDa cutoff). The sample cell was filled with 320  $\mu\text{L}$  of 8  $\mu\text{M}$  Hsp90, the syringe contained 120  $\mu\text{L}$  of 50-80  $\mu\text{M}$  Hop or Hop112a as indicated. Each binding reaction was conducted with 18

injections à 2 µL in 150 sec intervals – an initial 0.4 µL injection was applied to minimize artifacts from the first injection. The latter was neglected in curve fitting. The sample cell was constantly stirred with 750 rpm throughout the experiment.

The experimentally determined differential heat  $\frac{dQ}{dB_{total}}$  (y-axis) was plotted against the molar ratio of  $\frac{B_{total}}{A_{total}}$  (x-axis) displaying a sigmoidal saturation curve, whereby  $\frac{B_{total}}{A_{total}} = \frac{B_{syr} \cdot i \cdot V_{inj}}{A_0 \cdot V_0}$  with  $B_{syr}$  as the concentration of molecule B in the syringe,  $i$  the injection number,  $V_{inj}$  the injection volume, and  $A_0$  and  $V_0$  the concentration of molecule A in the sample cell and the sample cell volume at time point 0, respectively. With the ratio of  $\frac{B_{total}}{A_{total}}$  on the x-axis, the inflection point of the sigmoidal titration curve marks the switch from an excess of unbound molecules A to an excess of unbound molecules B in the sample cell. Hence, assuming full activity of both interaction partners, at the inflection point the amounts of unbound A and B are close to zero, revealing the stoichiometry of the AB complex. Data were fitted according to Eq. 7 using the Malvern software package. Errors represent the standard deviation from three independent experiments.

## 2.6 Nuclear magnetic resonance spectroscopy

Nuclear magnetic resonance (NMR) is a broadly used technique yielding information about the chemical environment of atomic nuclei. These naturally randomly orientated nuclei can interact with and align to a magnetic field  $B_0$ . If  $B_0 \neq 0$  the nuclei align either with or against the magnetic field, whereby each nucleus precesses around  $B_0$  with its own frequency (Larmor frequency). By applying a radio frequency (RF) pulse to the system, the nuclei can be flipped off the alignment to  $B_0$ . As they continue to precess, they realign to  $B_0$  shortly after.

In NMR one usually measures systems with a large number of nuclei giving rise to a total magnetization. In the equilibrium state this magnetization is aligned to  $B_0$ , defined as the z-axis. By the application of the RF pulse the magnetization is tilted towards the xy-plane (detector plane). The magnitude of the NMR signal, the so called free induction decay (FID), observed in the detector plane declines with nuclei realignment to  $B_0$ . As each nuclei experiences a unique chemical environment arising from its surrounding electrons, the nuclei are shielded differently from the magnetic field. A higher electron density results in a lower local magnetic field wherefore the nucleus precesses with a lower frequency, i.e. at lower chemical shift. As the chemical shift varies with changes in the chemical environment, NMR is particularly valuable to observe protein-protein interactions giving insights into the binding site and conformational rearrangements at an atomic level of resolution.

Due to nucleus-specific frequency ranges, one can choose which nuclei to observe. Beyond, nucleus-nucleus interactions (*via* covalent bonding or *via* space) can be selectively filtered by certain pulse sequences.

### 2.6.1 Heteronuclear single quantum coherence (HSQC)

#### *NMR Buffer (HSQC)*

25 mM HEPES pH 7.4  
 100 mM KCl  
 5 mM MgCl<sub>2</sub>  
 1 mM TCEP  
 0.02 % NaN<sub>3</sub>  
 5 % D<sub>2</sub>O

The <sup>15</sup>N-<sup>1</sup>H heteronuclear single quantum coherence (HSQC) pulse sequence (Figure 15)<sup>333</sup> was used to select for covalently bound NH-groups, as they are found in peptide bonds. After proton excitation (direct dimension), the magnetization is transferred to the nitrogen (indirect dimension) and then back to the proton for detection. The transfer of magnetization was accomplished *via* an INEPT element (insensitive nuclei enhancement by polarization transfer). It refers to <sup>15</sup>N as an insensitive nuclei compared to <sup>1</sup>H. The INEPT time length  $\Delta$  defined the selection for the NH-groups as  $\Delta = \frac{1}{2J_{\text{NH}}}$ , whereby  $J_{\text{NH}}$  is the coupling constant between covalently bound nitrogen-proton nuclei.

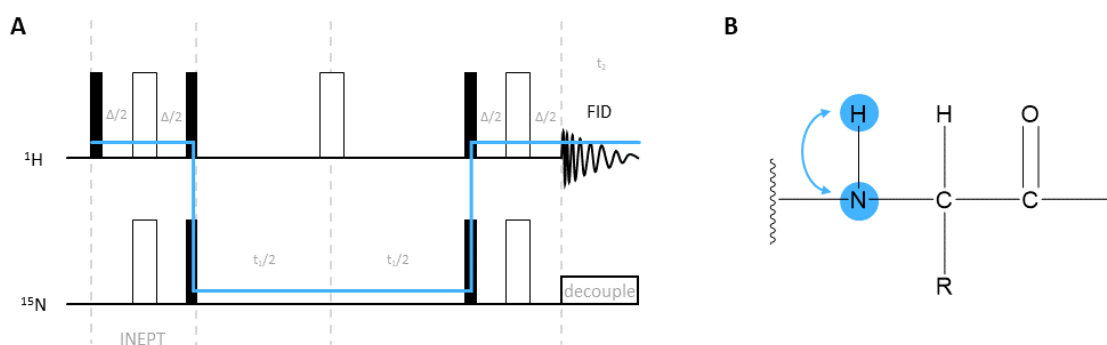


**Figure 15** The <sup>15</sup>N-<sup>1</sup>H HSQC pulse sequence selects for covalently bound NH-groups.

**A** Simplified representation of the HSQC pulse sequence including a <sup>1</sup>H- (direct) and <sup>15</sup>N- (indirect) dimension.<sup>333</sup> 90° and 180° pulses are indicated with black and white bars, respectively. The magnetization is transferred from proton to nitrogen *via* an INEPT element of a defined length  $\Delta = \frac{1}{2J_{\text{NH}}}$ . The second 180° pulse (<sup>1</sup>H dimension) is applied at the center of the evolution time  $t_1$  to refocus <sup>1</sup>H chemical shift evolution. A reverse-INEPT element transfers the magnetization back to proton. During FID acquisition for time  $t_2$  the nuclei are decoupled to simplify the spectrum. The blue line indicates the pathway of magnetization. **B** Zoom-in into a protein backbone with the two in the <sup>15</sup>N-<sup>1</sup>H HSQC experiment observed nuclei highlighted in blue.

## Material and Methods

Two dimensional  $^{15}\text{N}$ - $^1\text{H}$  HSQC spectra were recorded of  $^{15}\text{N}$ -labeled Tau (Figure 14) to get insights into its backbone dynamics when interacting with the Hsp70/Hsp90 chaperone machinery. Due to Tau's dynamic nature as IDP, the frequency variations of the backbone NH-groups are rather small leading to strong signal overlaps. Hence, to reduce thermal motions, NMR experiments were acquired at 5°C on a Bruker Avance 900 MHz spectrometer (proton frequency) equipped with a TCI cryogenic probe. For peak assignment transfer, 20  $\mu\text{M}$  of Tau were measured in NMR buffer (HSQC) with increasing pH from 6.8 to pH 7.4 with a step size of 0.2 on a Bruker Avance 800 MHz spectrometer (proton frequency) equipped with a TCI cryogenic probe. For interaction studies, 24  $\mu\text{M}$  of Tau were measured in NMR buffer (HSQC) as titration experiment with increasing amounts of Hsp70 (1:0, 1:4), Hsp90 (1:0, 1:4), Hsp70:Hsp90 in a molar ratio of 1:1:1 (1:0, 1:0.2, 1:1, 1:2), Hsp70:Hsp90:p23 in a molar ratio of 1:1:1:5 (1:0, 1:0.2, 1:2) and p23 (1:0, 1:10).

16 dummy scans were applied for sample equilibration followed by 32 (pH titration) or 40 (protein titration) number of scans used for data acquisition with in total 2048 points in the direct dimension and 512 points in the indirect dimension.

### 2.6.2 Transverse relaxation optimized spectroscopy (TROSY)

#### *NMR Buffer (TROSY)*

25 mM HEPES pD 7.6  
100 mM KCl  
5 mM  $\text{MgCl}_2$   
1 mM TCEP  
99 %  $\text{D}_2\text{O}$

One of the drawbacks in NMR is that the signal intensities decline with increasing molecular weight due to reducing transverse relaxation rates ( $T_2$ ). On a simplistic view it follows high molecular weight, fast relaxation, low signal. Along this line, new pulse programs have been optimized for large molecules with short  $T_2$ , termed transverse relaxation optimized spectroscopy (TROSY). The TROSY pulse sequence takes advantage of the different decay rates of the total magnetization, prevents their mixing throughout the pulse sequence and thereby preserves slowly relaxing signal components resulting in significant improvement of spectra quality.<sup>334</sup>

In specific, the  $^{13}\text{C}$ - $^1\text{H}$  methyl-TROSY pulse sequence (Figure 16) was used to select for covalently bound  $^{13}\text{C}$ - $^1\text{H}$  labeled CH-groups.<sup>335</sup> After proton excitation, the pulse sequence transfers magnetization from proton (direct dimension) to carbon (indirect dimension) and then back to proton for detection. The magnetization transfer was accomplished by a  $90^\circ$  pulse in the indirect dimension after time  $\Delta$  adjusted for the selection for the CH-groups as  $\Delta = \frac{1}{2J_{\text{CH}}}$ , whereby  $J_{\text{CH}}$  is the coupling constant between covalently bound carbon-proton nuclei.

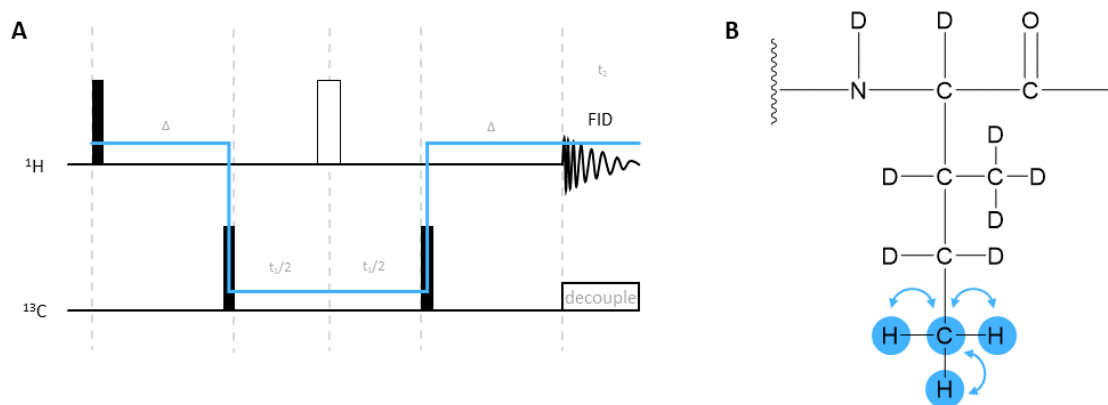


**Figure 16** The methyl-TROSY pulse sequence selects for  $^{13}\text{C}$ - $^1\text{H}$  labeled CH-bonds.

**A** Simplified representation of the methyl-TROSY pulse sequence including a  $^1\text{H}$ - (direct) and  $^{13}\text{C}$ - (indirect) dimension.<sup>335</sup>  $90^\circ$  and  $180^\circ$  pulses are indicated with black and white bars, respectively. The magnetization is transferred from proton to carbon *via* a  $90^\circ$  pulse after time  $\Delta = \frac{1}{2J_{\text{CH}}}$ . A  $180^\circ$  pulse ( $^1\text{H}$  dimension) is applied at the center of the evolution time  $t_1$  to refocus  $^1\text{H}$  chemical shift evolution. The magnetization is transferred back to proton by another  $90^\circ$  pulse. During FID acquisition for time  $t_2$  the nuclei are decoupled to simplify the spectrum. The blue line indicates the pathway of magnetization. **B** Zoom-in into the amino acid chain with  $^{13}\text{C}$ - $^1\text{H}$ -labeled isoleucine  $\delta$ -methyl groups highlighted in blue in an otherwise perdeuterated protein.

Two dimensional methyl-TROSY spectra were recorded of  $^{13}\text{C}$ - $^1\text{H}$ -labeled Hsp90 (Figure 13) to follow its dynamics during Tau chaperoning as part of the Hsp70/Hsp90 chaperone machinery. In large, folded proteins, methyl groups of side chains are particularly favorable spectroscopic targets due to their threefold symmetry with three identical  $^1\text{H}$  spins and due to the higher flexibility of side chains compared to the protein backbone, both contributing to increased signal intensity. Accordingly, by means of side-chain specific isotopic labeling, only the  $\delta$ -methyl groups of Hsp90's isoleucine residues were  $^{13}\text{C}$ -labeled and thus NMR active (see chapter 2.3.4.7).

In order to suppress unfavorable sources of relaxation such as dipole-dipole interactions caused by surrounding protons, Hsp90 was otherwise produced perdeuterated. Prior to the NMR experiment all proteins were dialyzed in NMR buffer (TROSY) for proton deuterium exchange. NMR experiments were acquired at  $25^\circ\text{C}$  on a Bruker Avance 900 MHz spectrometer (proton frequency) equipped with a TCI cryogenic probe.  $50\ \mu\text{M}$  of Hsp90 were measured as titration experiment with increasing amounts of Hop (1:0, 1:0.2, 1:0.5, 1:1), Hop112a (1:0, 1:1, 1:10), Hsp70 (1:0, 1:1), Hsp70:Hop in a molar ratio of 1:1 (1:0, 1:1), Hsp70:Hop:Tau in a molar ratio of 1:1:5 (1:0, 1:1), p23 (1:0, 1:5) and Hsp70:Hop:Tau:p23 in a molar ratio of 1:1:5:5 (1:0, 1:1).

100 dummy scans (DS) were applied for sample equilibration followed by 80 number of scans (NS) used for data acquisition with in total 2048 points in the direct dimension and 256 points in the indirect dimension. NMR experiments in presence of AMP-PNP were acquired at  $25^\circ\text{C}$  on a Bruker Avance 800 MHz spectrometer (proton frequency) in NMR buffer (TROSY) including 10 mM KCl with 32 DS and 136 NS.



## 2.6.3 Data processing

Spectra were processed with TopSpin including zero-filling up to 4096 and 2048 data points in the direct and indirect dimension, respectively. The intensity scaling factor was set at equal level for all spectra of one titration experiment. Baselines were adjusted for both dimensions. Spectra were analyzed with Sparky.<sup>336</sup> Data were further processed in Excel. Peak intensity ratios were plotted as  $\frac{I}{I_0}$ , whereby  $I_0$  is the peak intensity of the reference spectrum, and  $I$  the intensity of the respective titration point. The intensity values from Tau-HSQC spectra were averaged over three residues for profile smoothing assuming that three adjacent side chains of an IDP experience similar changes upon ligand binding. Error bars were calculated from the signal to noise ratio with error  $\left(\frac{I}{I_0}\right) = \frac{I}{I_0} \cdot \sqrt{\left(\frac{1}{SN_0}\right)^2 + \left(\frac{1}{SN}\right)^2}$ , whereby  $SN_0$  and  $SN$  is the signal to noise ratio of the peak in the reference spectrum and the titration point, respectively. The weighted average chemical shift perturbations (CSPs) were calculated according to:

$$\text{CSP}(\text{Tau}) = \sqrt{\left(\Delta H^2 + \left(\frac{\Delta N}{5}\right)^2\right) * \frac{1}{2}} \quad \text{CSP}(\text{Hsp90}) = \sqrt{\left(\Delta H^2 + \left(\frac{\Delta C}{7}\right)^2\right) * \frac{1}{2}} \quad 10$$

with  $\Delta H$ ,  $\Delta N$  and  $\Delta C$  as the peak chemical shift in the proton, nitrogen and carbon dimension, respectively. Different weighting factors for  $^{15}\text{N}$  and  $^{13}\text{C}$  were used compared to  $^1\text{H}$  accounting for different chemical shift sensitivities.<sup>337</sup> The CSP threshold was set to the CSP standard deviation times 1.5.

Structures were displayed with PyMol.<sup>338</sup>

## 2.7 Protein phosphorylation and acetylation

### *Phosphorylation Reaction Buffer*

25 mM HEPES pH 7.4  
 100 mM KCl  
 5 mM MgCl<sub>2</sub>  
 1 mM TCEP  
 5 mM EGTA  
 1 mM PMSF  
 12.5 mM ATP

### *Acetylation Reaction Buffer*

25 mM HEPES pH 7.4  
 100 mM KCl  
 5 mM MgCl<sub>2</sub>  
 1 mM TCEP  
 5 mM EGTA  
 0.5 mM PMSF  
 20  $\mu$ M Acetyl-CoA

Phosphorylation and acetylation reactions were performed in 100  $\mu$ L reaction buffer with 200  $\mu$ M of protein. The protein was phosphorylated with serine/threonine protein kinases using 0.02 mg/mL of the Cdk2/CyclinA2 kinase or 4  $\mu$ mol/L of MARK2. Protein acetylation was conducted with the acetyltransferase CREB-binding protein (CBP) or p300, each used with a final concentration of 0.028 mg/mL. Samples were incubated for 16 h at 30°C gently shaking at 350 rpm. The next day the enzymes were inactivated through boiling for 20 min at 95°C. Note that the boiling step is only applicable for the modifications of IDPs, as those remain active after heating. The denatured proteins were centrifuged for 30 min at 4°C with max. speed (5424R centrifuge). The supernatant including the phosphorylated or acetylated protein was taken off. Aliquots of 25  $\mu$ L were flash-frozen in liquid nitrogen and stored at -20 °C.

## 2.8 Dynamic light scattering

Light scattering (LS) is based on the phenomenon that upon irradiation small particles or molecules such as proteins deflect i.e. scatter the incoming light. In solution these particles move and tumble according to Brownian motion so that the scattered light fluctuates over time. The record of these dynamic fluctuations is termed ‘dynamic light scattering’ (DLS). Dependent on the speed of movement, which in turn depends on the size of the molecule, the fluctuations are stronger or weaker: the smaller a protein, the faster it moves and the stronger the fluctuation of the scattered light.

In DLS one measures these fluctuations at sequential time points to follow the decay of correlation compared to time point 0.<sup>339</sup> Small particles with fast movements lose the correlation fast, whereas large particles that move slower keep the correlation for a longer time. Mathematically this is expressed in the intensity correlation function  $G(\tau)$  (Eq. 11), with  $I(t)$  as the total scattering intensity at the time point  $t$  (angle brackets denote averaged values at the respective time points).

## Material and Methods

Using the Siegert relation the exponential decay of Eq. 11 can be fitted with Eq. 12:

$$G(\tau)_{\text{obs}} = \langle I(t) \cdot I(t+\tau) \rangle \quad 11$$

$$G(\tau)_{\text{fit}} = b + \beta \cdot (e^{-\Gamma\tau})^2 \quad 12$$

with  $b$  as the baseline,  $\beta$  as an instrument's constant and  $\Gamma$  as the decay rate. The experimentally determined  $\Gamma$  is directly related to the particles diffusion coefficient with:

$$D = \frac{\Gamma}{q^2} \quad 13$$

whereby  $q = \frac{4\pi n}{\lambda_0} \sin\left(\frac{\theta}{2}\right)$ , with  $n$  as the refractive index of the solvent,  $\lambda_0$  the wavelength of the light in vacuum and  $\theta$  the angle of the detected scattered light. Herefrom the hydrodynamic radii  $R_h$  of the proteins of interest, i.e. the radii of the proteins including their hydrate shell can be derived *via* the Stokes-Einstein equation (Eq. 14):

$$R_h = \frac{k_B \cdot T}{6 \cdot \pi \cdot \eta \cdot D} \quad 14$$

with  $k_B$  as the Boltzmann constant,  $T$  the temperature and  $\eta$  the solvent viscosity. Note that the calculated  $R_h$  only corresponds to the radius of a hypothetical sphere that moves at the same speed as the particle of interest.

DLS measurements were acquired at 25°C in 4  $\mu\text{L}$  disposable COC cuvettes using a DynaPro NanoStar instrument with a detector positioned at a 90° angle with respect to the incident light. Samples were irradiated with a monochromatic laser with a wavelength of 662 nm (100% power, auto-attenuation turned off). 20  $\mu\text{L}$  of 5-10  $\mu\text{M}$  of sample were prepared as described in 2.4 and 2.7 in 25 mM HEPES pH 7.4/ 100 mM KCl/ 5 mM MgCl<sub>2</sub>/ 1 mM TCEP. Hsp90 was transferred to its closed conformation by incubation for 1.5 h at 40°C in 25 mM HEPES pH 7.4/ 100 mM KCl/ 5 mM MgCl<sub>2</sub>/ 1 mM TCEP/ 5 mM AMP-PNP/ 1 M (NH<sub>4</sub>)<sub>2</sub>SO<sub>4</sub> prior to mixing with Hop. Ten cycles of data acquisition with 5 sec of acquisition time and 30 sec of spacing were set per measurement. Errors represent the standard deviation from three measurements.

DLS data were analyzed with the DYNAMICS software package. As larger molecules scatter light more strongly, the intensity distribution profiles were selected in search for higher oligomers or aggregated molecules. Mass distribution profiles were chosen to investigate the proportions of molecules relative to their mass. The individual decay rates  $\Gamma_i$  of  $n$  differently sized particles in the sample were derived using Eq. 12, whereby the obtained intensity correlation function displays the sum of the decay of all particles in the sample, so that  $e^{-\Gamma\tau}$  was substituted by  $\sum_{i=1}^n G_i(\Gamma) \cdot e^{-\Gamma_i\tau}$ .

## 2.9 Chemical cross-linking

<i>DSS stock</i>	<i>Reaction Buffer</i>
100 mM in DMSO	25 mM HEPES pH 7.4
<i>EDC stock</i>	100 mM KCl
1 M in H <sub>2</sub> O	5 mM MgCl <sub>2</sub>
<i>Sulfo-NHS stock</i>	1 mM TCEP
2 M in H <sub>2</sub> O	

Chemical cross-linking was used to firmly attach protein residues with one another that are in close proximity to each other. Protein complexes were cross-linked with either disuccinimidyl suberate (DSS) or 1-ethyl-3-(3-dimethylaminopropyl) (EDC) depicting an 11.4 Å long and a zero-length linker arm, respectively (according to the manufacturers specifications). DSS cross-links primary amines including lysine residues and the N-terminus of proteins; EDC cross-links primary amines with carboxylic acids, i.e. lysines and N-termini with aspartates or glutamates (Figure 42A). To increase the efficiency of EDC coupling, the latter included a two-step reaction with sulfo-N-hydroxysulfosuccinimide (Sulfo-NHS) used in a molar ratio of 1:2.5 for EDC:Sulfo-NHS. All cross-linking reactions were performed in reaction buffer.

For small scale tests, in order to define the appropriate cross-linker concentration, the complexes were prepared as described in 2.4 with 10 µM of Hsp70. After complex formation, increasing amounts of cross-linker were added ranging from 0 – 4 mM of DSS and 1.25 – 80 mM of EDC (with 3.125 – 200 mM Sulfo-NHS). Each cross-linker concentration point was set up as individual experiment.

Cross-linking reactions in large scale for subsequent purification by sucrose density gradient centrifugation (see chapter 2.10) were performed with 35 µM of Hsp70 each in the Hsp70:Hsp90 (1:1:1), Hsp70:Hsp90:Hop (1:1:1:5) and Hsp70:Hsp90:Hop:tau (1:1:1:5:5) complex. A cross-linker concentration of 1 mM and 10 mM were used for DSS and EDC (with 25 mM Sulfo-NHS), respectively. Samples cross-linked by DSS (*EDC*) were incubated for 30 min (*60 min*) at 25°C gently shaking at 350 rpm. The reactions were quenched with 20 mM Tris pH 7.4 followed by 10 min incubation at RT prior to the next analysis step.

## 2.10 Sucrose density gradient centrifugation

In density gradient centrifugation proteins are sorted according to their sedimentation behavior. The density of the gradient increases from top to bottom so that a protein continues to settle down as long as the density of the protein is higher than the density of the solvent. Protein separation can be achieved based on their molecular weight as large and heavy molecules travel faster than small, light proteins. Hence, if the centrifugation is stopped at a suitable time, the proteins will be distributed along the density gradient depending on their speed of sedimentation.

Density gradients were prepared in 4 mL of 25 mM HEPES pH 7.4/ 100 mM KCl/ 5 mM MgCl<sub>2</sub>/ 1 mM TCEP with 10 – 25 % sucrose. Therefore, 2 mL of each 10 % and 25 % sucrose in buffer were prepared separately, filtered and stacked bottom up with the lower density solution on top. Gradients were mixed with the Gradient Master™ and stored for 30 min at 4°C prior to use. 50 µL of sample with ~1 mg total protein amount were loaded per gradient. The samples were centrifuged for 16 h at 4°C with 38000 rpm (SW 60 Ti). The next day fractions of 200 µL were taken off from top down and analyzed by SDS page (see chapter 2.2.1).

## 2.11 Molecular weight determination

The molecular weight (MW) i.e. the mass of the protein complexes was determined according to their SEC elution volume (see chapter 2.2.3). Complexes were reconstituted as described in chapter 2.4 and cross-linked as described in chapter 2.9. Prior to SEC the samples were purified *via* sucrose density gradient centrifugation as described in 2.10. 200 µL of the peak fraction from the sucrose density gradient centrifugation were loaded onto the SEC column (SD200 10/300, 500 µL loop, 0.8 mL/min) equilibrated in 25 mM HEPES pH 7.4/ 100 mM KCl/ 5 mM MgCl<sub>2</sub>/ 1 mM TCEP. 200 µL of 30 mg/mL protein standard mix (15-600 kDa) were used for size classification.

The corresponding reference line was created with Excel by plotting the elution volume (y-axis) against the logarithmic of the molecular weight (x-axis) giving the linear function:  $y = mx + c$ . With  $y$  as the experimentally determined elution volumes, the molecular weights were determined by solving the equation for  $x$ . Error bars represent the width of the elution peaks at half height.

## 2.12 Mass spectrometry

In mass spectrometry (MS) one can detect the mass-to-charge ratio ( $m/z$ ) of proteins. The general principle relies on the acceleration of gaseous, ionized molecules whereupon they are separated according to their  $m/z$  ratio. These presorted ionized molecules (MS1) can be further fragmented and analyzed by a second round of MS (MS2) – in combination termed tandem mass spectrometry (MS/MS). The sample can be priorly fractionated by liquid chromatography (LC), which is then referred to as LC-MS/MS. By LC-MS/MS one can identify the mass of each sequential fragment of the molecule allowing to ascertain the amino acid chain sequence, sites of post-translational modifications or cross-linked residues.

### 2.12.1 Identification of phosphorylation sites by LC-MS/MS

Following Tau phosphorylation *in vitro* (see chapter 2.7), the respective phosphorylation sites were determined by LC-MS/MS. Sample preparation and data analysis were thankfully performed by Dr. P. Kuan-Ting (MPI-BPC, in the group of Prof. Dr. Henning Urlaub, Department of Bioanalytical Mass Spectrometry), hereafter emphasized in *italic*. 20  $\mu\text{L}$  of 20  $\mu\text{M}$  PTau were forwarded for LC-MS/MS analysis.

*The experimental procedure included o/n protein digestion with trypsin protease followed by sample analysis by LC-MS/MS using an UltiMate 3000 HPLC system (C18 column self-packed, 75  $\mu\text{m}$   $\times$  30 cm) coupled to an Orbitrap Fusion Lumos Tribrid mass spectrometer. LC-MS/MS data were analyzed using MaxQuant<sup>340</sup> searching against the human Tau sequence. Phosphopeptide intensities were normalized to the intensity sum of all detected Tau peptides.*

### 2.12.2 Cross-link analysis by LC-MS/MS

After complex formation (see chapter 2.4), cross-linking (see chapter 2.9) and sucrose density gradient centrifugation (see chapter 2.10), the cross-linked sites within the Hsp70:Hsp90:Tau:p23 complex were identified by LC-MS/MS. The peak fractions of six or three gradients of the same kind were pooled of samples cross-linked with DSS and EDC, respectively. Further sample preparation for the analysis by LC-MS/MS was gratefully conducted by Dr. M. Ninov (MPI-BPC, in the group of Prof. Dr. Henning Urlaub, Department of Bioanalytical Mass Spectrometry), hereafter emphasized in *italic*.

*The experimental procedure included o/n protein digestion with trypsin protease followed by peptide size exclusion chromatography (pSEC, 3.2/300 column) using an ÄKTAmicro system for the enrichment of the cross-linked peptides with subsequent sample analysis by LC-MS/MS using an UltiMate 3000 UHPLC system*

## Material and Methods

*(C18 column self-packed, 75  $\mu\text{m}$   $\times$  30 cm) coupled to an Q Exactive<sup>TM</sup> HF-X Hybrid Quadrupole-Orbitrap mass spectrometer. Raw data were analyzed using pLink<sup>341</sup> searching against a customized protein database comprising the sequences of Hsp70, Hop, Hsp90, Tau and p23. MS data were evaluated manually and classified for unambiguous and unique detected cross-link spectrum matches (CSMs).*

Unique CSMs were further filtered for a minimum of 3 detections (i.e. hits) and a minimal confidence score of 5 % of the max. score value. CSMs that fulfilled these requirements are hereafter denoted as ‘selected cross-links’ including intra- and intermolecular cross-links. Intramolecular distance measurements from C $\alpha$  to C $\alpha$  of the respective residues were determined within Hsp70 (PDB code: 5aqz<sup>342</sup> and 4po2<sup>158</sup>), Hop (PDB code: 1elw<sup>193</sup> and 1elr<sup>193</sup>), Hsp90 (PDB code: 5fwk<sup>119</sup>) and p23 (PDB code: 1ejf<sup>223</sup>) using PyMOL.<sup>338</sup> Tau as an IDP was neglected in this analysis round. The measured values refer exclusively to the listed structures deposited in the PDB; interdomain cross-links including different PDB files were not taken into account. Distance plots were generated with Excel.

Cross-link network plots were created with the xVis Crosslink Analysis Webserver.<sup>343</sup> Intermolecular cross-links were color coded according to their confidence score using Inkscape.

### 3 Results

Despite the number of studies describing the preassembly of the Hsp70/Hsp90 chaperone machinery including the Hsp90:Hop and Hsp70:Hop:Hsp90 interaction<sup>117,130,207,215,216,235</sup>, there were inconsistencies regarding the structural arrangement that needed clarification (see chapter 1.7). In order to obtain a defined picture within the applied system, initially chaperone:co-chaperone interactions preceding substrate binding were investigated in greater detail.

#### 3.1 Hop stabilizes Hsp90 in a V-shaped conformation

##### 3.1.1 *In vitro* reconstitution of the Hsp90:Hop complex

The interaction of Hsp90 and Hop was first studied by native page (Figure 17A) designed as titration experiment using a constant amount of Hsp90 and varying the concentrations of Hop. Both proteins appeared homogenous on the gel each showing a single protein band (Figure 17A, marked with Hsp90 and Hop, respectively). An additional band emerged with increasing concentrations of Hop along with the disappearance of unbound Hsp90, signifying complex formation (Figure 17A, labeled as Hsp90:Hop). Simultaneously, a set of additional bands became visible on the gel that however did not sense the presence of Hop in a concentration dependent manner, and thus could be ascribed to impurities.

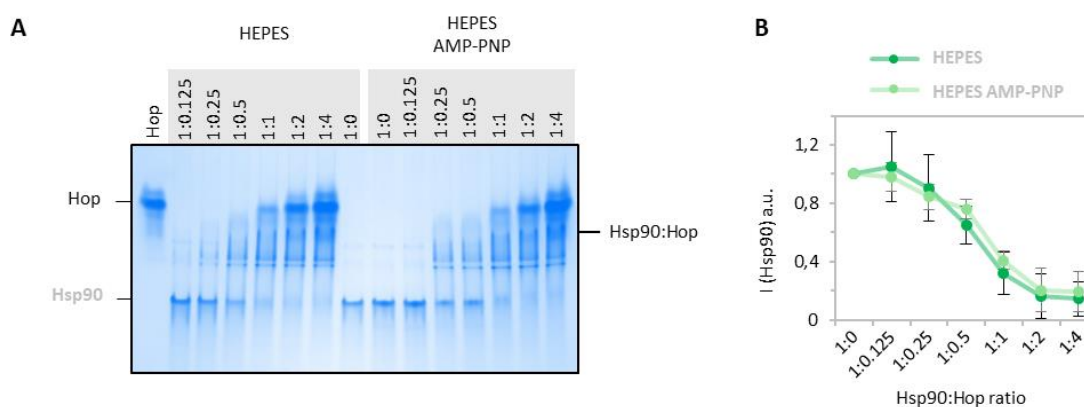


**Figure 17** *In vitro* reconstitution of the Hsp90:Hop complex.

**A** Native page analysis of Hop binding to Hsp90 in absence and presence of AMP-PNP (1.25  $\mu$ M Hsp90). Increasing concentrations of Hop reduce the amount of unbound Hsp90. **B** Quantitative analysis of the band intensity of free Hsp90 in (A).



## Results

As Hop has been shown to interact in the initial states of Hsp90's ATP-hydrolysis cycle<sup>206,344,345</sup>, it was further tested whether the presence of AMP-PNP (which is a non-hydrolysable ATP analog) has an effect on the Hsp90:Hop association. Taking benefit of the isolated localization on the gel, the reduction of unbound Hsp90 was compared in presence and absence of AMP-PNP. Quantitative analysis showed Hsp90 association in either case (Figure 17B).

### 3.1.2 Hop binds Hsp90's open state with high affinity

Size exclusion chromatography (SEC) revealed that Hsp90 adopts a more compact conformation in presence of AMP-PNP indicated by the later elution volume (Figure 18A). The interaction of Hop with the nucleotide-free and AMP-PNP bound state of Hsp90 was confirmed by SEC showing peak shifts to earlier elution volumes referring to higher molecular weights in both cases. However, the peak height of unbound Hop indicated a preference towards the nucleotide free, open state of Hsp90. This observation was assured by SDS page analysis of the peak fractions showing less free Hop in absence of AMP-PNP (Figure 18B).

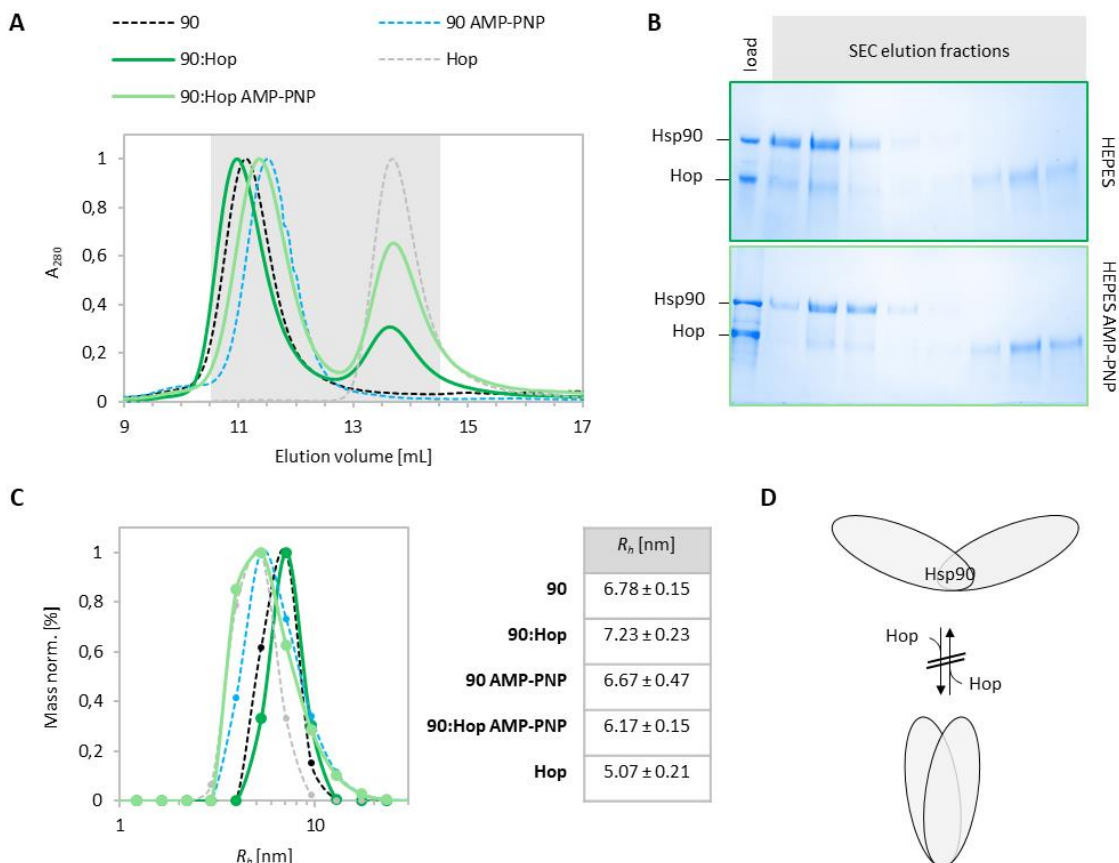


**Figure 18 Hop preferentially binds the open conformation of Hsp90.**

**A** Size exclusion chromatograms of the Hsp90<sup>open</sup>:Hop (90:Hop; dark green) and Hsp90<sup>closed</sup>:Hop (90:Hop AMP-PNP; light green) complexes. Reference elution chromatograms of Hsp90<sup>open</sup> (90; black), Hsp90<sup>closed</sup> (90 AMP-PNP; blue) and Hop are shown for comparison. The grey square highlights the fractions analyzed by SDS page analysis in (B). **B** SDS page analysis (7.5 % gel) of the elution fractions from (A) affirms less free Hop in absence of AMP-PNP. **C** DLS measurements of Hsp90, Hop and the Hsp90:Hop complex in absence and presence of AMP-PNP (same color code as in (A), 5  $\mu$ M each). Determined hydrodynamic radii  $R_h$  are listed on the right. **D** Cartoon representation indicating that Hop binding neither drives an open-close nor a close-open change of Hsp90.

## Results

Consistent with complex formation, the hydrodynamic radius  $R_b$  of the open Hsp90 increased with the addition of Hop (Figure 18C). The increased  $R_b$  gave evidence for Hop not driving an open-close change of Hsp90. The  $R_b$  of the closed Hsp90 decreased in presence of Hop, which could be ascribed to the distinct amount of unbound Hop as observed by SEC. Beyond, it pointed out that Hop is neither driving a close-open change of Hsp90 upon binding (Figure 18D). Due to Hop's preference for the open state of Hsp90, the Hsp90:Hop interaction was further characterized in the absence of AMP-PNP.

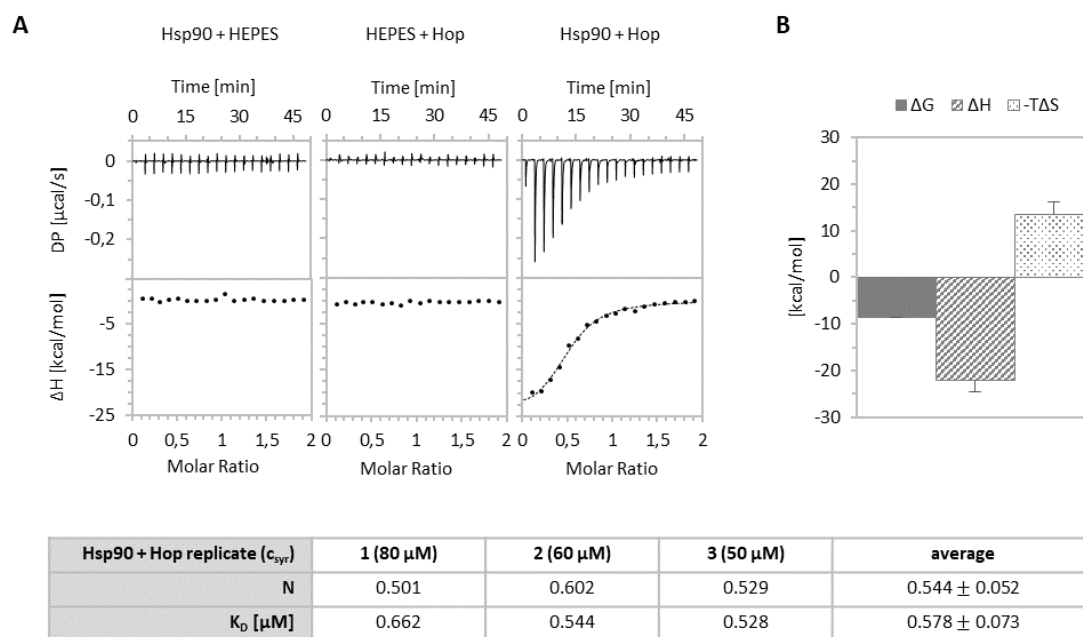


**Figure 19 A** single Hop molecule binds the Hsp90 dimer with high affinity.

**A** Isothermal titration calorimetry (ITC) measurement of Hop binding to Hsp90 fitted to a single binding site model. Negative controls are shown for comparison. The obtained stoichiometry (N) and dissociation constants ( $K_D$ ) are listed from three independent measurements with  $c_{\text{syrr}}$  as the concentrations of Hop in the syringe. **B** Thermodynamic analysis of the Hsp90:Hop association including  $\Delta G$  (Gibbs free energy),  $\Delta H$  (binding enthalpy) and  $\Delta S$  (entropy times T (temperature)).

The affinity of Hop to Hsp90 was measured using isothermal titration calorimetry (ITC) (Figure 19A). The determined  $K_D = 0.578 \pm 0.073 \mu\text{M}$  was in agreement with previous affinity measurements from literature.<sup>216</sup> The stoichiometry of  $N = 0.544 \pm 0.052$  indicated an Hop:Hsp90 molar ratio of 1:2 where one Hop molecule binds to an Hsp90 dimer. In addition, thermodynamic analysis of the Hsp90:Hop interaction revealed that Hop binding involves conformational changes and the formation of hydrogen bonds indicated by a negative entropy ( $\Delta S$ ) and enthalpy ( $\Delta H$ ), respectively (Figure 19B).

## Results

### 3.1.3 Hop stabilizes Hsp90 in an extended conformation

Next, NMR spectroscopy was used for a structural characterization of the Hsp90:Hop complex at an atomic level of resolution. To overcome the NMR molecular size limit due to relaxation-dependent line broadening (see chapter 2.6.2), the advantage of site-specific isotope labeling was taken.<sup>329</sup> On that account, Hsp90 was produced with exclusively [<sup>1</sup>H, <sup>13</sup>C] labeled Ile- $\delta$ -methyl groups in an otherwise fully deuterated protein (Figure 13). The peak assignment of the isoleucine resonances was thankfully adapted from a former colleague who defined 44 out of 48 Ile- $\delta$ -methyl groups (four residues located in Hsp90's C-terminus are absent).<sup>121</sup> Transverse relaxation optimized spectroscopy of methyl-groups (methyl-TROSY) has been already successfully used in the past to study Hsp90 dynamics in solution.<sup>84,121,221,346</sup> The reference spectrum of Hsp90 alone depicted 48 signals for in total 96 isoleucines of the Hsp90 dimer signifying that the isoleucines of both monomers are identical and thus their resonances overlapped (Figure 20A). A control experiment, in which AMP-PNP was titrated to Hsp90 confirmed an intact Hsp90 suitable for NMR studies. In the respective 2D methyl-TROSY spectrum, signal perturbations were only observed for residues located in Hsp90's N-terminal domain highlighting the nucleotide binding site as previously described (Figure 20).<sup>221</sup>

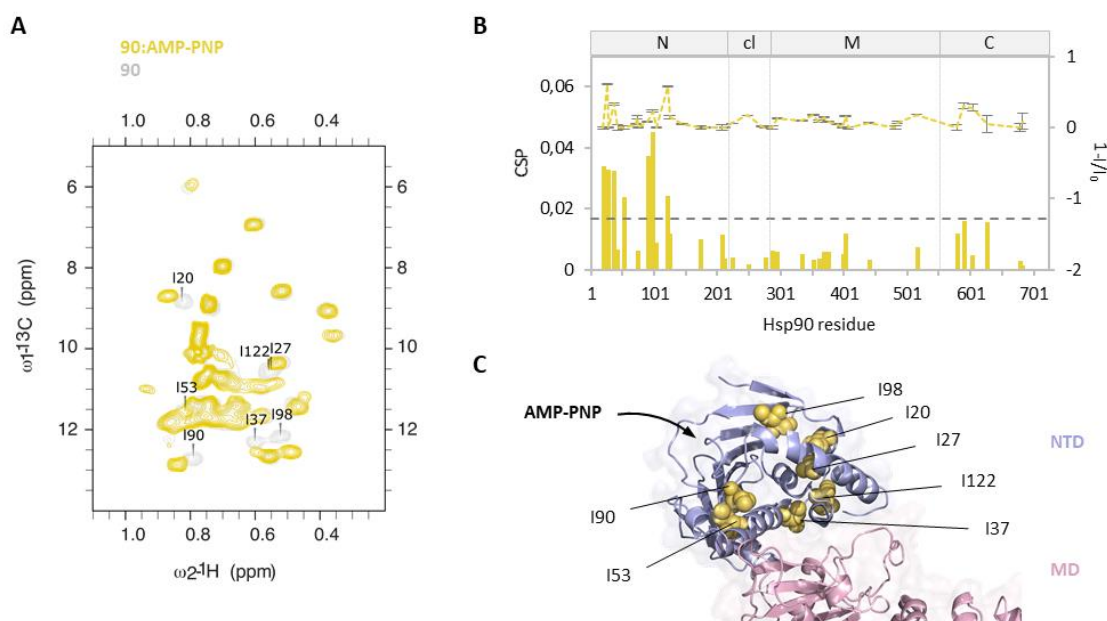


**Figure 20 TROSY NMR of Hsp90 in presence of AMP-PNP.**

**A** 2D <sup>13</sup>C-<sup>1</sup>H methyl-TROSY spectra of Hsp90 in absence (grey) and presence (yellow) of AMP-PNP (1:40). Perturbed residues are labeled. **B** Residue-specific chemical shift perturbations (CSP; bars) and peak intensities ( $1-I/I_0$ ; lines) of Hsp90's isoleucine  $\delta$ -methyl groups observed in (A).  $I_0$  is the signal intensity of the Hsp90 reference. Error bars were calculated based on NMR signal-to-noise ratio. Hsp90 domains are depicted on top and represented with dotted lines (N – N-terminal domain, cl – charged linker, M – middle domain, C – C-terminal domain). **C** Isoleucine residues that sensed the presence of AMP-PNP are highlighted in yellow spheres on the structure of Hsp90 (N-terminal domain (NTD), light blue), middle domain (MD), light pink).

## Results

Accordingly, 2D methyl-TROSY spectra of Hsp90 were recorded in the presence of Hop. Peak broadening as well as chemical shift changes were already observed at substoichiometric concentrations (Figure 21). Corresponding to previous findings, where Hop interacted *via* its TPR2A domain with the C-terminal MEEVD peptide of Hsp90<sup>207</sup>, major signal perturbations were observed for residues located in Hsp90's CTD. At an Hsp90:Hop molar ratio of 1:0.5 a distinct amount of Hsp90:Hop complex was formed giving rise to a second set of NMR peaks. The Hop-bound state of Hsp90 was only detected for residues located in its N-terminal and middle domain including I20, I90, I287 and I334. This suggested that Hop directly interacts with the C-terminal domain of Hsp90 engendering relaxation-dependent loss of signal. In addition, the Hsp90-CTD:Hop interaction induces a conformational change in the chaperone's N-terminal and middle domain, which are not bound by Hop and thus detectable. At the endpoint of the titration, 70-80 % of the signal intensities aroused from the Hop-bound state. Passing a 50:50 distribution of the intensities from unbound and bound state signified that Hop binding induces a symmetrical conformational change in both Hsp90 monomers. Hence, consistent with the 2:1 ratio for Hsp90:Hop obtained by ITC, the NMR analysis indicated an allosteric communication between the two Hsp90 monomers induced by the binding of a single Hop molecule.

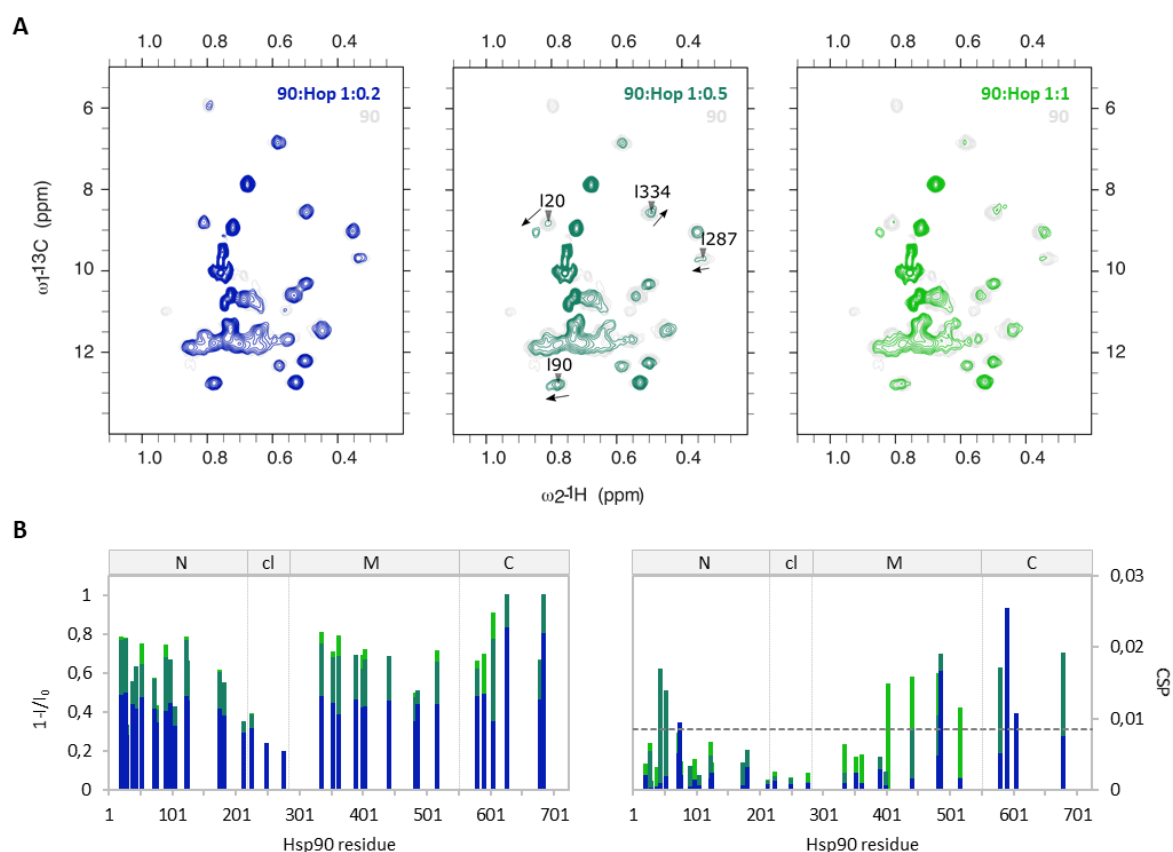


**Figure 21 TROSY NMR of Hsp90 in presence of Hop.**

**A** 2D <sup>13</sup>C-<sup>1</sup>H methyl-TROSY spectra of Hsp90 in presence of increasing concentrations of Hop (1:0.2 blue, 1:0.5 dark green, 1:1 green; black arrows mark the observed peak splitting between the free and the bound state of Hsp90 for I20, I90, I287, I334). The reference spectrum of Hsp90 alone is shown for comparison (grey). **B** Peak intensity ( $1-I/I_0$ ) and chemical shift perturbation (CSP) plots from (A). Hsp90 domains are depicted on top and represented with dotted lines within each graph.

## Results

Isoleucine residues depicting distinct chemical shift perturbations (CSPs) including I43, I53, I403, I440, I482, I485, I516, I590, I604 and I679 were mapped on a previously generated open structure of Hsp90 (Figure 22).<sup>121</sup> Two major regions, located in the MD-CTD and MD-NTD interface, appeared to sense the presence of Hop. Most strikingly, the perturbed isoleucine methyl groups within the MD-CTD interface enclosed two parts of Hsp90 facing each other (marked with green lines). Either Hop binds within this MD-CTD interface thereby blocking the closure of Hsp90. Or Hop induces the closure of the MD-CTD interface stabilizing Hsp90 in a V-shaped conformation, whereby additional contacts with Hop's TPR2B domain stabilize the Hsp90:Hop association. Either scenario would be in agreement with the function Hop inhibiting the ATPase activity of Hsp90.<sup>207</sup>

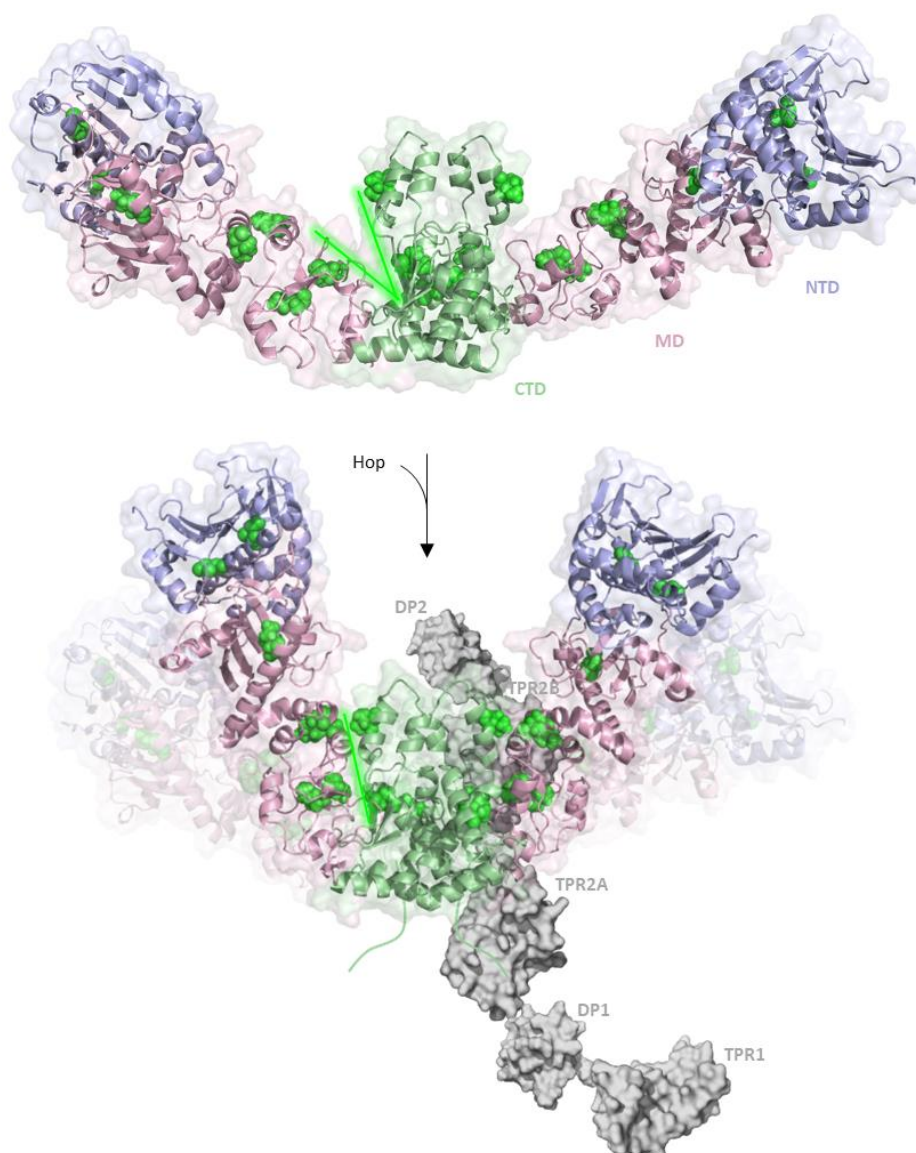


**Figure 22 Model for the Hsp90<sub>2</sub>:Hop<sub>1</sub> complex.**

Front view of the open conformation of Hsp90 shown as cartoon. (N-terminal domain (NTD, light blue), middle domain (MD, light pink) and C-terminal domain (CTD, light green)).<sup>121</sup> Isoleucine residues affected upon the addition of Hop are highlighted in green spheres. NMR signal perturbations in Figure 21A can be best ascribed to a V-shaped Hsp90:Hop complex, whereby Hop binding is directed by the interaction of Hop's TPR2A domain with the C-terminus of Hsp90 (Hop is shown as surface in grey). The MD-CTD interface that is closed upon Hop binding is highlighted with green lines.



## Results

For comparison, the same isoleucines were mapped on the closed conformation of Hsp90 (Figure 23).<sup>119</sup> Notable, in contrast to what has been shown for the Hsp90:Aha1 interaction, which promotes Hsp90 closure<sup>346</sup>, none of the perturbed Ile-methyl groups was located in the dimer interface in between the two opposite NTDs giving further evidence for Hop not driving an open-close change. Beyond, it became apparent that in the closed conformation of Hsp90 the perturbed residues within the MD-CTD interface are embedded within the dimer interface, hence not accessible. In combination with the preference of Hop for the open state of Hsp90 observed by SEC and DLS (Figure 18), the increased interaction could thus be based on a broader interaction interface for Hop when Hsp90 is open.

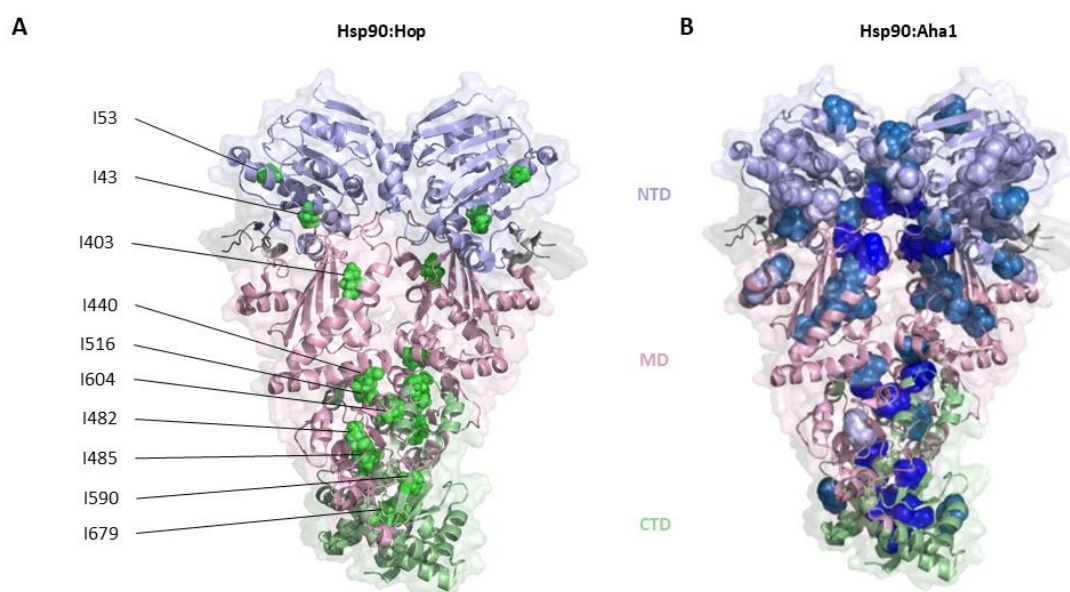


**Figure 23 Comparison of the Hsp90 interaction with Hop and Aha1.**

**A, B** Side view of the closed conformation of Hsp90 (N-terminal domain (NTD, light blue), middle domain (MD, light pink) and C-terminal domain (CTD, light green) (PDB: 5fwk).<sup>119</sup> Isoleucine residues affected upon the addition of Hop (A) are highlighted in green spheres. Aha1-perturbed isoleucines (B) are highlighted as shown in literature<sup>346</sup> (dark blue: strongly affected  $I/I_0 = 0.0-0.4$ , middle blue:  $I/I_0 = 0.4-0.7$ , light blue:  $I/I_0 = 0.7-1.0$ ). In contrast to Aha1, Hop does not induce an open-close change of Hsp90 based on the unperturbed Hsp90 dimer interface.

### 3.1.4 Hop's TPR2A-2B domains determine the affinity for the CTD and MD of Hsp90

To further specify the nature of Hop binding to Hsp90, a shorter Hop construct comprising only TPR1, DP1 and TPR2A was produced (Figure 24A). The new construct, termed Hop112a, is sterically unable to bind the MD-CTD interface while it is bound to the C-terminus of Hsp90 *via* TPR2A. Hence, observing NMR signal perturbations of the same Hsp90 residues as with full-length Hop would approve the V-shaped Hsp90:Hop conformation. The analysis of complex formation by native page signified the Hsp90:Hop112a association based on the appearance of an additional band with increasing concentrations of Hop112a (Figure 24B). Quantitative analysis of the intensity of the unbound Hsp90 however revealed that the Hsp90:Hop112a interaction was

## Results

greatly reduced compared to full-length Hop, whereby the preference for the apo over the AMP-PNP bound Hsp90 was slightly more pronounced (Figure 24C). To that effect, a ten times lower binding affinity was measured by ITC ( $K_D = 3.587 \pm 1.072 \mu\text{M}$ , Figure 24D). Notable, thermodynamic analysis indicated less conformational changes upon binding compared to the full-length Hop (Figure 19B and Figure 24D). Despite, the stoichiometry of the Hsp90:Hop112a complex was similarly ascertained to a molar ratio of 2:1, where one Hop112a molecule binds to an Hsp90 dimer.

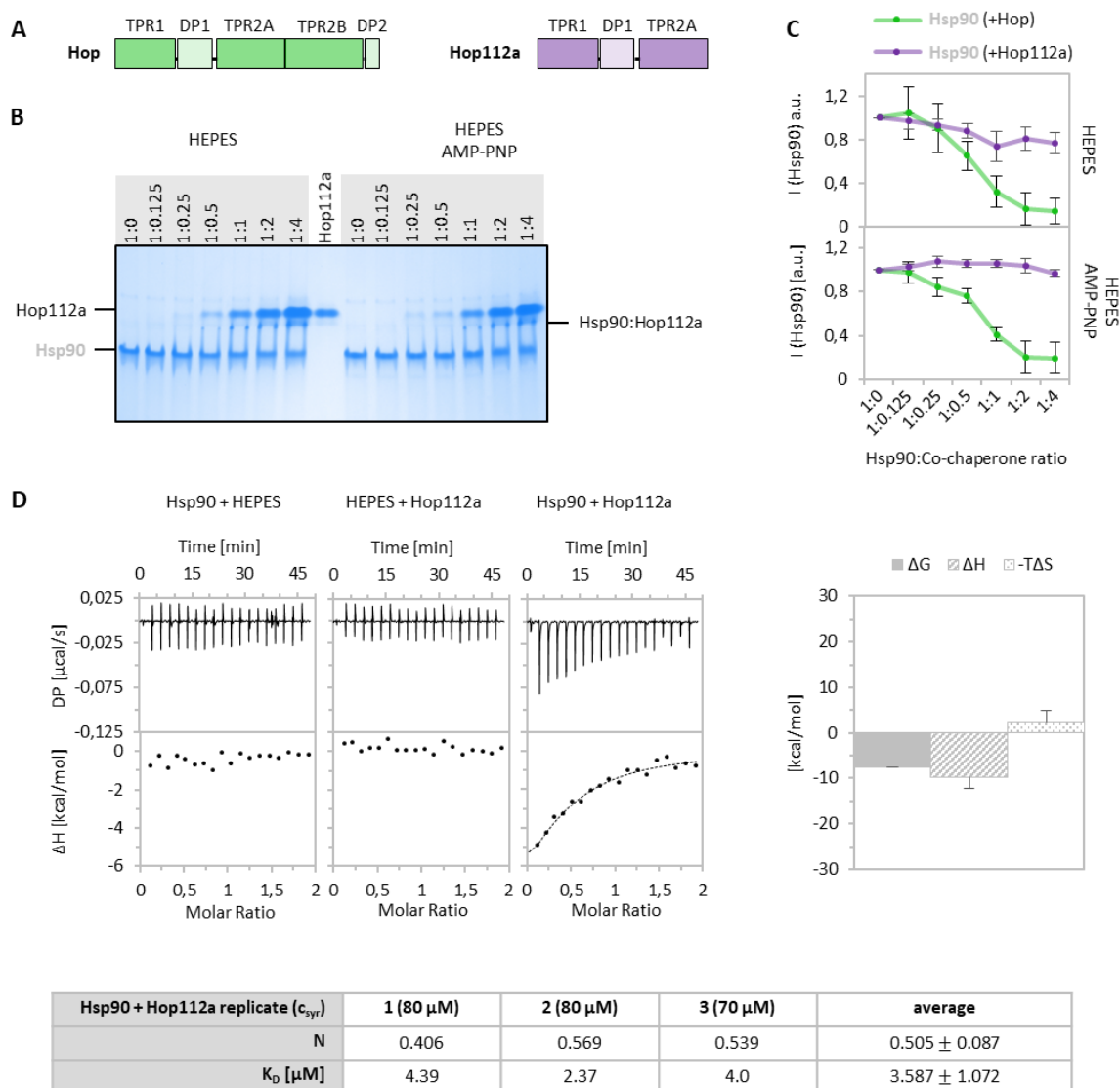


**Figure 24** *In vitro* reconstitution of the Hsp90:Hop112a complex.

**A** Domain organization of Hop and Hop112a. **B** Native page analysis of Hop112a binding to Hsp90 in absence and presence of AMP-PNP (1.25  $\mu\text{M}$  Hsp90). **C** Quantitative analysis of the band intensity of free Hsp90 in (B). Reduction of Hsp90 caused by Hop is shown for comparison. **D** Left: Isothermal titration calorimetry (ITC) measurement of Hop112a binding to Hsp90 fitted to a single binding site model. Negative controls are shown for comparison. The obtained stoichiometry (N) and dissociation constants ( $K_D$ ) are listed from three independent measurements with  $c_{\text{Hsp90}}$  as the concentrations of Hop112a in the syringe. Right: thermodynamic analysis of the Hsp90:Hop112a association including  $\Delta G$  (Gibbs free energy),  $\Delta H$  (binding enthalpy) and  $\Delta S$  (entropy times T (temperature)).

## Results

### 3.1.5 The Hop:Hsp90-CTD interaction is sufficient to induce the V-shaped state

Consistent with the reduced binding affinity, ten times higher amounts of Hop112a were required to detect similar changes in the Hsp90 2D methyl-TROSY spectrum as with full-length Hop (Figure 25). Distinct chemical shift perturbations were detected for similar Ile-methyl groups as for Hsp90:Hop located in the MD-CTD interface of Hsp90 (I482, I579, I590 and I604). Notable, the affected region was slightly smaller compared to the one sensed by full-length Hop. Beyond, at the endpoint of the titration, as much as 50 % of the signal intensities of Hsp90's NTD and middle domain remained in the unbound state. This indicated that only one monomer arm of Hsp90 was affected by Hop112a. This in turn was in agreement with less conformational changes presumed from the ITC experiment (Figure 24D). Although signal perturbations of residues within Hsp90's NTD (I43, I72) were observed likewise in presence of Hop112a, no peak splitting, i.e. distinct resonances of the Hop112a-bound state of Hsp90 were detected suggesting only a sparse population of the Hsp90:Hop112a complex.

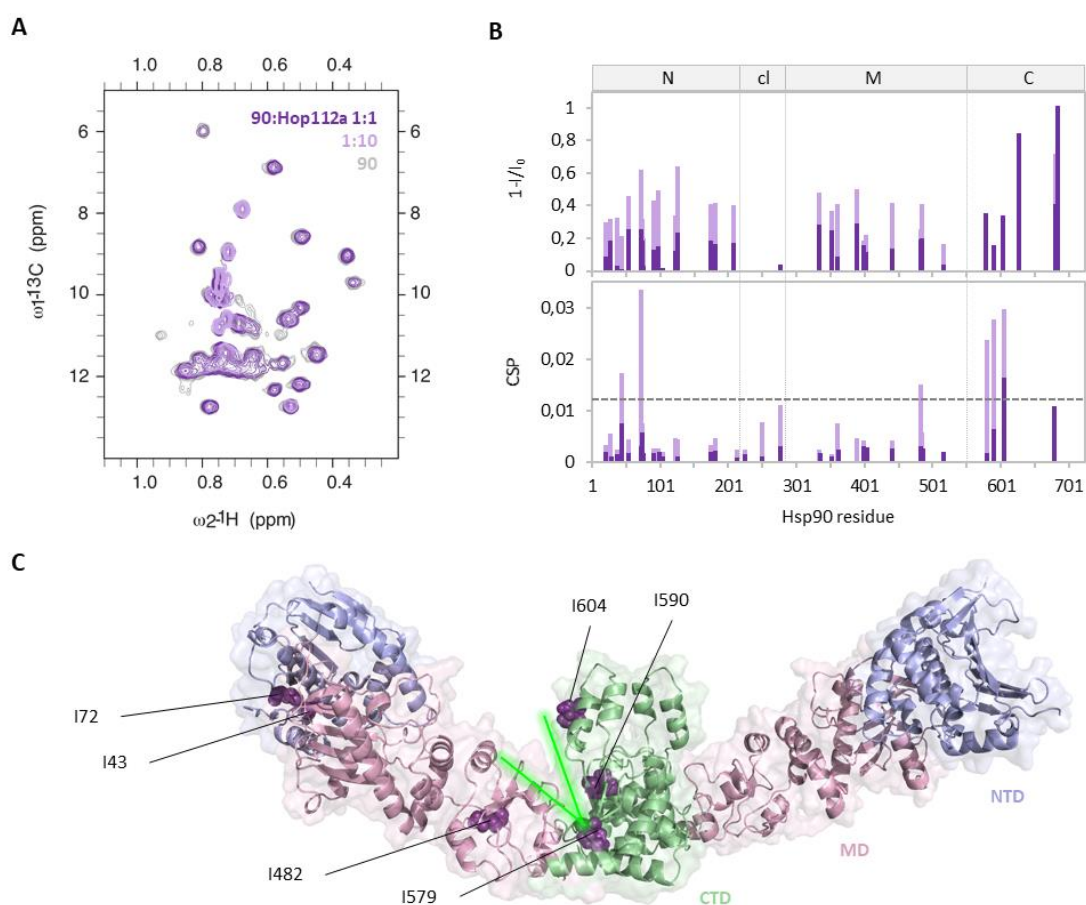


**Figure 25 TROSY NMR of Hsp90 in presence of Hop112a.**

**A** 2D  $^{13}\text{C}$ - $^1\text{H}$  methyl-TROSY spectra of Hsp90 in presence of increasing concentrations of Hop112a (1:1 dark purple, 1:10 light purple). The reference spectrum of Hsp90 alone is shown for comparison (grey). **B** Peak intensity ( $1-I/I_0$ ) and chemical shift perturbation (CSP) plots from (A). Hsp90 domains are depicted on top and represented with dotted lines within each graph. **C** Front view of the open conformation of Hsp90 shown as cartoon. (N-terminal domain (NTD, light blue), middle domain (MD, light pink) and C-terminal domain (CTD, light green)).<sup>121</sup> Isoleucine residues affected upon the addition of Hop112a are highlighted in purple spheres. The MD-CTD interface that is closed upon Hop112a binding is highlighted with green lines.



## Results

Taken together, the NMR data showed that the binding of Hop to the C-terminus of Hsp90 is sufficient to induce the rearrangement of the Hsp90 arms towards the V-shaped state with conformational changes in the chaperone's NTD and middle domain. Beyond, the presence of Hop's TPR2B-DP2 domains strongly contribute to the stabilization of the Hsp90:Hop complex as well as the allosteric communication between the two Hsp90 arms allowing a symmetrical rearrangement upon Hop binding.

### 3.2 The human Hsp70/Hsp90 association decisively relies on the adaptor Hop

The association of Hsp70 with the Hsp90:Hop complex forms the Hsp70/Hsp90 chaperone machinery – a prerequisite for successful substrate transfer from Hsp70 onto Hsp90. In line with the structural determination of the Hsp70/Hsp90 chaperone machinery several reports (Table 15) addressed the *in vitro* reconstitution of the Hsp70:Hop:Hsp90 complex prior to substrate binding.<sup>117,130,215,235</sup> The experimental procedures commonly stated protein concentrations in the low  $\mu\text{M}$  range and included ATP and Hsp40 during protein incubation. However, due to variations in the applied protein ratios as well as buffer conditions, the minimal requirements for an intact machinery association were reinvestigated.

**Table 15 Experimental protocols for the *in vitro* reconstitution of the Hsp70/Hsp90 chaperone machinery.**

70 – Hsp70, 90 $\alpha$  – Hsp90 $\alpha$ , y40A – yeast Hsp40 class A, 40B – Hsp40 class B. The concentration c is specified for the Hsp90 protein used for complex reconstitution.

	c [ $\mu\text{M}$ ]	Molar ratio	Buffer composition
70:Hop:90 $\alpha$ :y40A <sup>215</sup>	10	2:2:1:0.02	20 mM Tris, pH 7.5/ 50 mM KCl/ 0.05 % $\beta$ -OG/ 0.2 mM ATP/ 5 mM MgCl <sub>2</sub>
70:Hop:90 $\alpha$ :y40A <sup>235</sup>	1	1:1:1:0.3	30 mM HEPES, pH 7.5/ 50 mM KCl/ 1 mM DTT/ 0.2 mM ATP-Mg
70:Hop:90 $\alpha$ :y40A <sup>130</sup>	10	1.5:1.5:1:0.2	30 mM HEPES, pH 7.5/ 50 mM KCl/ 2 mM DTT/ 0.4 mM ATP/ 5 mM MgCl <sub>2</sub> / 10 % Glycerol/ 0.05 % $\beta$ -OG
70:Hop:90 $\alpha$ :40B <sup>117</sup>	5	2.4:2.8:1:0.4	20 mM HEPES, pH 7.5/ 50 mM KCl/ 1 mM DTT/ 5 mM MgCl <sub>2</sub> / 1 mM ADP

#### 3.2.1 *In vitro* reconstitution of the Hsp70:Hop:Hsp90 complex

Native page was used to follow complex formation based on the appearance of an additional band corresponding to the formed complex and/or the attenuation of the bands of the free proteins. At an arbitrarily defined protein concentration of 5  $\mu\text{M}$ , a molar ratio of 1:1:1 yielded efficient amount of the Hsp70:Hop:Hsp90 complex along with minimal excess of unbound proteins (Figure 26A). In accordance with previous studies<sup>130,347-349</sup>, purified Hsp70 was present as

## Results

multimeric sample featuring monomers and higher oligomers. With regard to chaperone function only the monomeric fraction is suggested to be functionally active.<sup>347,348</sup> Along this line, only the Hsp70 monomer band disappeared in presence of Hop and Hsp90 implying that single Hsp70 molecule(s) are incorporated into the Hsp70/Hsp90 chaperone machinery. Control experiments revealed that the presence of AMP-PNP or ADP, holding the chaperones in their ATP- or ADP state, had no effect on complex formation. Beyond, no Hsp40 was needed for the Hsp70:Hsp90 interaction.

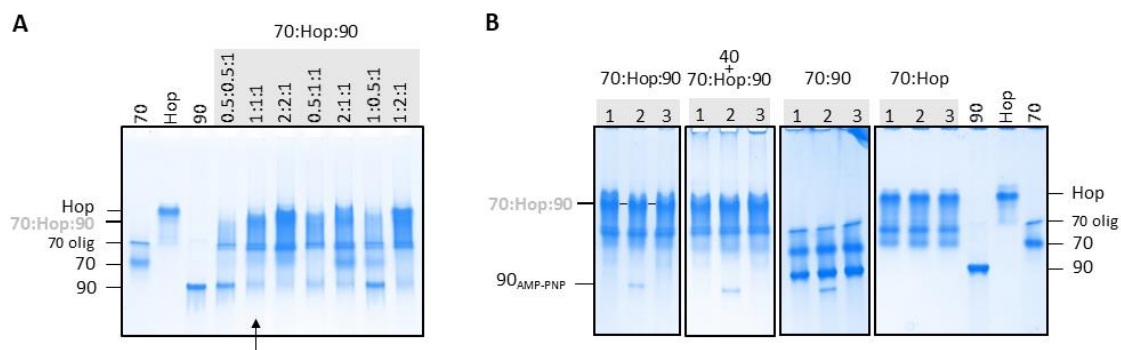


**Figure 26** *In vitro* reconstitution of the Hsp70/Hsp90 chaperone machinery.

**A** Native page analysis of the formation of the Hsp70:Hsp90 complex. The black arrow indicates the most suitable molar ratio of 1:1:1 (5  $\mu$ M Hsp90) resulting in efficient amount of Hsp70:Hsp90 complex along with the least amount of free proteins. Hsp70, Hsp70 oligomers and Hsp90 are abbreviated as “70”, “70 olig.” and “90”, respectively. **B** Native page analysis investigating the influence of nucleotides (1 – no nucleotide, 2 – +AMP-PNP, 3 – +ADP) and Hsp40 for individual protein-protein interactions each at 1:1 molar ratio (25  $\mu$ M each, except Hsp40 (10  $\mu$ M)).

### 3.2.2 The Hsp70/Hsp90 chaperone machinery comprises two copies of Hsp70

No direct interaction between Hsp70 and Hsp90 could be observed by native page. Hop was found to be necessary to recruit the free Hsp70 monomers and Hsp90 dimers forming the Hsp70:Hsp90 complex (Figure 26). Although no additional band was visible for the Hsp70:Hsp90 complex, the interaction was attributed to the decreased free Hsp70 amount in presence of Hop – the corresponding complex band might be overlapping with the bands of the unbound proteins.

Analogously to the Hsp90:Hop interaction, 2D  $^{13}\text{C}$ - $^1\text{H}$  methyl-TROSY NMR spectra were acquired of isotopically labeled Hsp90 as part of the Hsp70/Hsp90 chaperone machinery. At an equimolar ratio of Hsp70, Hop and Hsp90 the signals of most Ile-methyl groups of the unbound Hsp90 were broadened beyond detection, indicating completion of the Hsp70:Hsp90 complex (Figure 27). Chemical shift perturbations were further induced for residues within Hsp90’s N-terminal (I37, I75), middle (I334, I352) and C-terminal domain (I579, I627, I683) when compared to the Hsp90:Hop interaction. This suggested that either Hsp70 displays a direct interaction with Hsp90 after recruitment *via* Hop, or Hsp70 binding to Hop induces a

## Results

conformational change in Hsp90. In either way, Hsp70 interacts with Hsp90 once the Hsp90:Hop complex is formed. Hsp90 signal perturbations were observed as well in presence of Hsp70 only, however rather unspecific as compared to when Hop is present, and weak considering that no Hsp70:Hsp90 complex was detected by native page. Notable, no precipitation was observed after the measurement. Hence, based on the attenuation of NMR signals from Hsp90's free state far beyond 50%, the Hsp70:Hop action on Hsp90 likewise must occur symmetrically. Mapping the perturbed residues on the V-shaped Hsp90:Hop structure (see chapter 3.1.3) a broad binding pocket located within Hsp90's NTD and MD became apparent (Figure 28A). Consistent with the most recent structure of an Hsp70:Hop:Hsp90:GR client loading complex<sup>47</sup>, the observed signal perturbations in Hsp90 thus could be ascertained to two Hsp70 molecules, whereby only one Hsp70 is bound *via* Hop (Figure 28B).

Noteworthy, even as part of the Hsp70:Hop:Hsp90 complex, NMR signals belonging to Hsp90's charged linker region persisted, suggesting that this region remains unbound and highly flexible (see chapter 3.5.4).

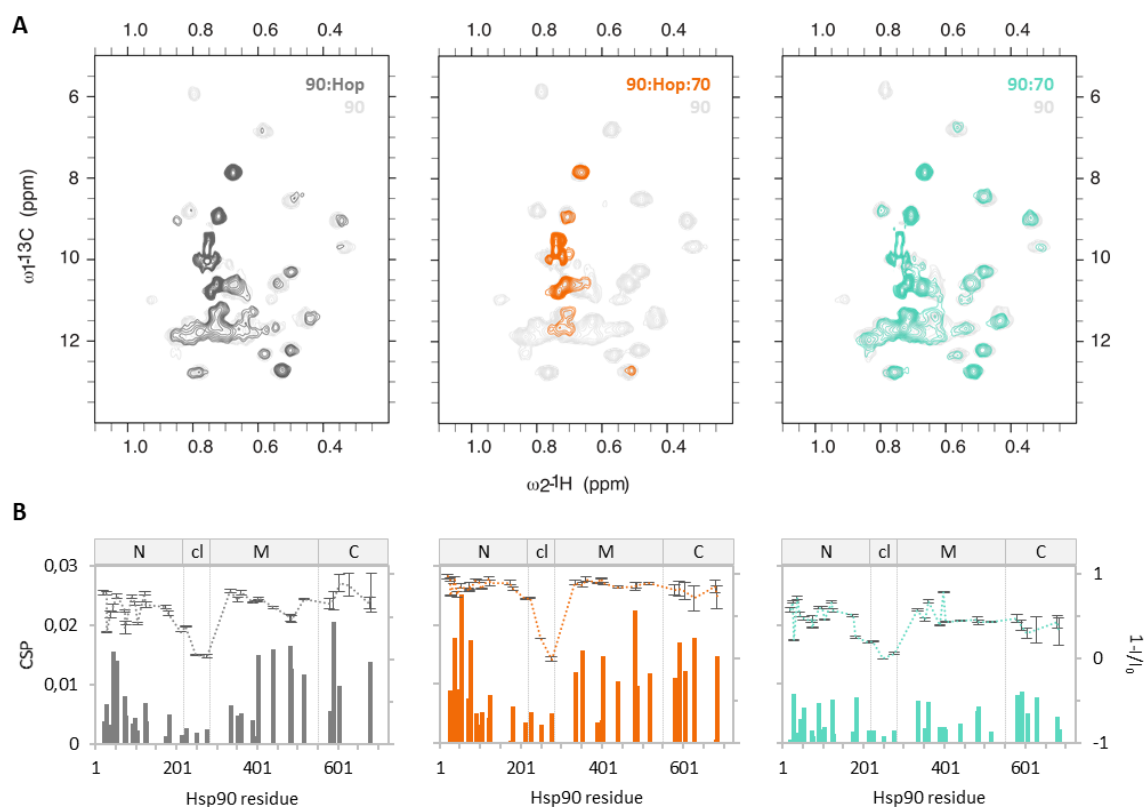


**Figure 27 TROSY NMR of Hsp90 in the Hsp70/Hsp90 chaperone machinery.**

**A** 2D  $^{13}\text{C}$ - $^1\text{H}$  methyl-TROSY spectra of Hsp90 in presence of Hop only (grey), Hop and Hsp70 (orange), and Hsp70 only (turquoise) – (molar ratios 1:1, 50  $\mu\text{M}$  Hsp90). The reference of Hsp90 alone is shown in each spectrum in light grey for comparison. **B** Residue-specific chemical shift perturbations (CSP; bars) and peak intensities ( $1-I/I_0$ ; lines) of Hsp90's isoleucine  $\delta$ -methyl groups observed in (A); same color coding.  $I_0$  is the signal intensity of the Hsp90 reference. Error bars were calculated based on NMR signal-to-noise ratio. Hsp90 domains are depicted on top of each plot and represented with dotted lines (N – N-terminal domain, cl – charged linker, M – middle domain, C – C-terminal domain).

## Results

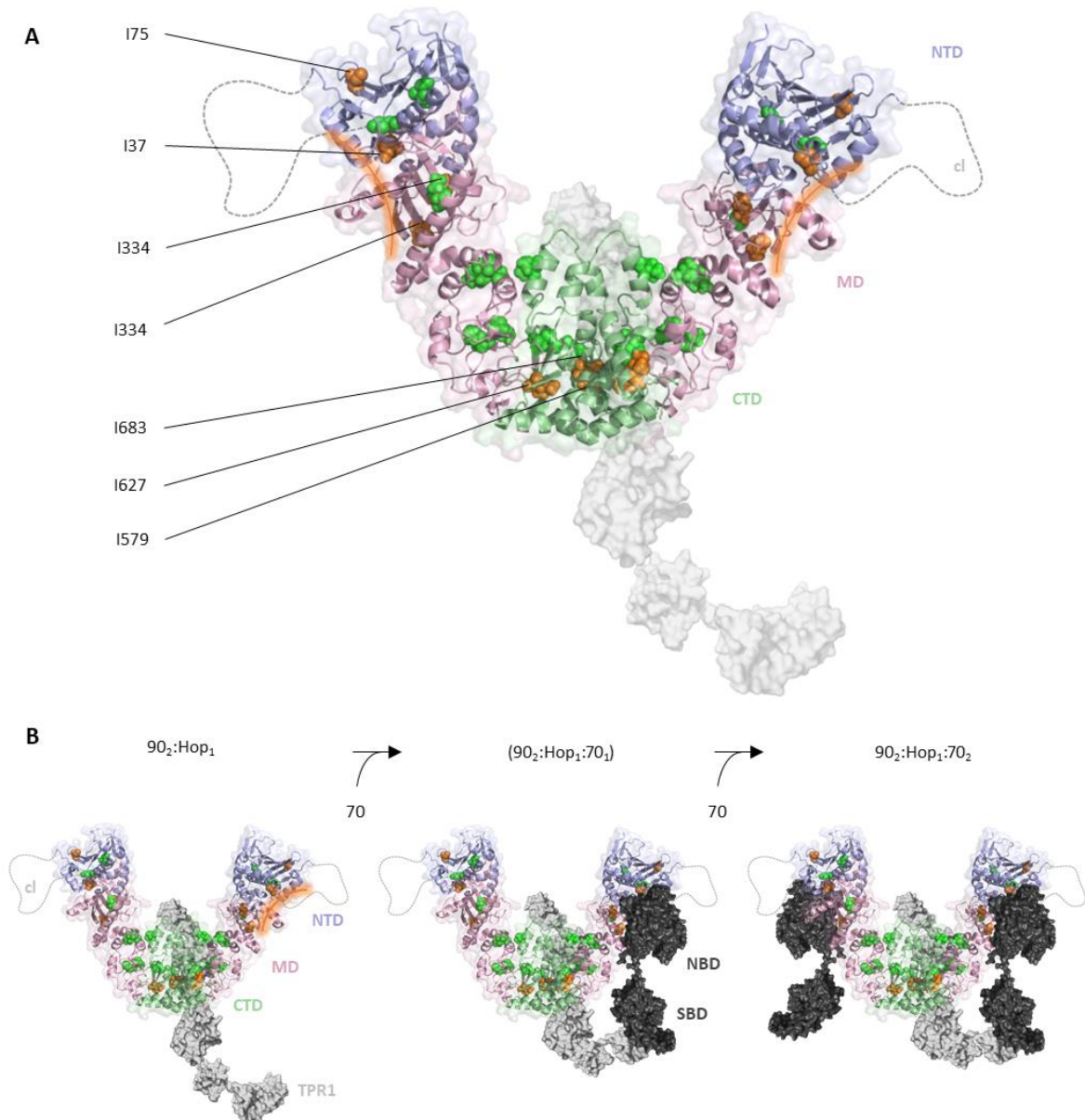


**Figure 28 Hsp70 binding to the Hsp90:Hop complex.**

**A** Front view of the V-shaped Hsp90:Hop complex depicted as cartoon (NTD purple; cl grey; MD pink; CTD green) (see chapter 3.1). Affected isoleucine residues are highlighted in light green (Hsp90:Hop) and orange (Hsp90:Hop:Hsp70) and represented as spheres. Perturbations observed in the NMR spectra in Figure 27A highlight the potential binding site of Hsp70 in Hsp90's NTD and MD (marked with an orange line). Hop is depicted with a grey surface. **B** One Hsp70 molecule binds *via* its SBD to Hop's TPR1 domain.<sup>192</sup> The second Hsp70 molecule may bind Hsp90 Hop-independent. Hsp70 is depicted with a black surface.

### 3.3 The Hsp70/Hsp90 chaperone machinery interacts with the intrinsically disordered protein Tau

#### 3.3.1 Formation of the client-loading complex

Proceeding from an assembled Hsp70/Hsp90 chaperone machinery, it was further investigated whether the intrinsically disordered protein (IDP) Tau does interact with the Hsp70:Hsp90 complex. Indeed, with increasing concentrations of Tau an additional band appeared on the native gel along with the reduction of the Hsp70:Hsp90 band – indicative for the formation of an Hsp70:Hsp90:Tau complex (Figure 29). Similar to what is already known for folded substrates as for example the glucocorticoid receptor (GR)<sup>47,235</sup>, this was the first evidence that a so called ‘client-loading complex’ does exist also for an IDP. Effectively, a dynamic equilibrium between the free proteins, the Hsp70/Hsp90 chaperone machinery and the client-loading complex could be observed, which, with an excess of Tau, could be pushed towards the Hsp70:Hsp90:Tau complex.

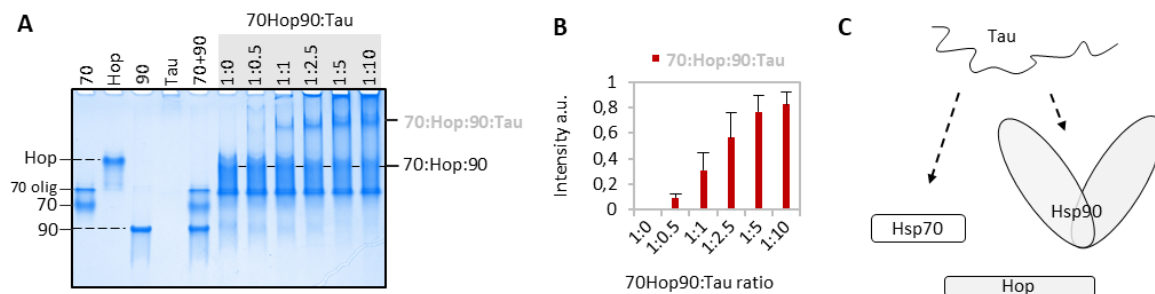


**Figure 29** *In vitro* reconstitution of the Hsp70/Hsp90 chaperone machinery: Tau interaction.

**A** Native page analysis of the Hsp70:Hsp90 complex (1:1:1 molar ratio; 5  $\mu$ M Hsp90) interacting with the intrinsically disordered substrate Tau (0-50  $\mu$ M). Increasing concentrations of Tau pushed the equilibrium towards the Hsp70:Hsp90:Tau complex. Hsp70, Hsp70 oligomers and Hsp90 are abbreviated as “70”, “70 olig.” and “90”, respectively. **B** Quantitative analysis of the band intensity of the Hsp70:Hsp90:Tau complex. **C** Cartoon representation of Tau interacting with components of the Hsp70/Hsp90 chaperone machinery base.

Control experiments showed that Tau interacts *via* Hsp70 and Hsp90, but it does not bind to Hop (Figure 30A). The quantification of the unbound chaperones with stepwise addition of Tau further manifested that Tau preferably binds to Hsp70 (Figure 30B). As Hsp40 was proposed to play a role in client binding to Hsp70<sup>110</sup> it was further tested whether the addition of Hsp40 may enhance the Hsp70:Tau interaction. According to native page, Hsp40 had no effect on the amount of the Hsp70:Tau complex, though the presence of AMP-PNP appeared beneficial in either case (Figure 30D, lanes 2). When incubating Tau with both Hsp70 and Hsp90 (without Hop) a broad band appeared on the gel (Figure 30E, marked with a bracket on the left). Due to the simultaneous strong reduction of free Hsp70, this band was in part attributed to an Hsp70:Tau complex. In

## Results

addition, a minor fraction of Hsp70:Tau:Hsp90 complex potentially provoked band smearing. Altogether, the interaction of Tau with the Hsp70/Hsp90 chaperone machinery was proven to be independent on Hsp40 and the chaperones' nucleotide-state (Figure 30E).

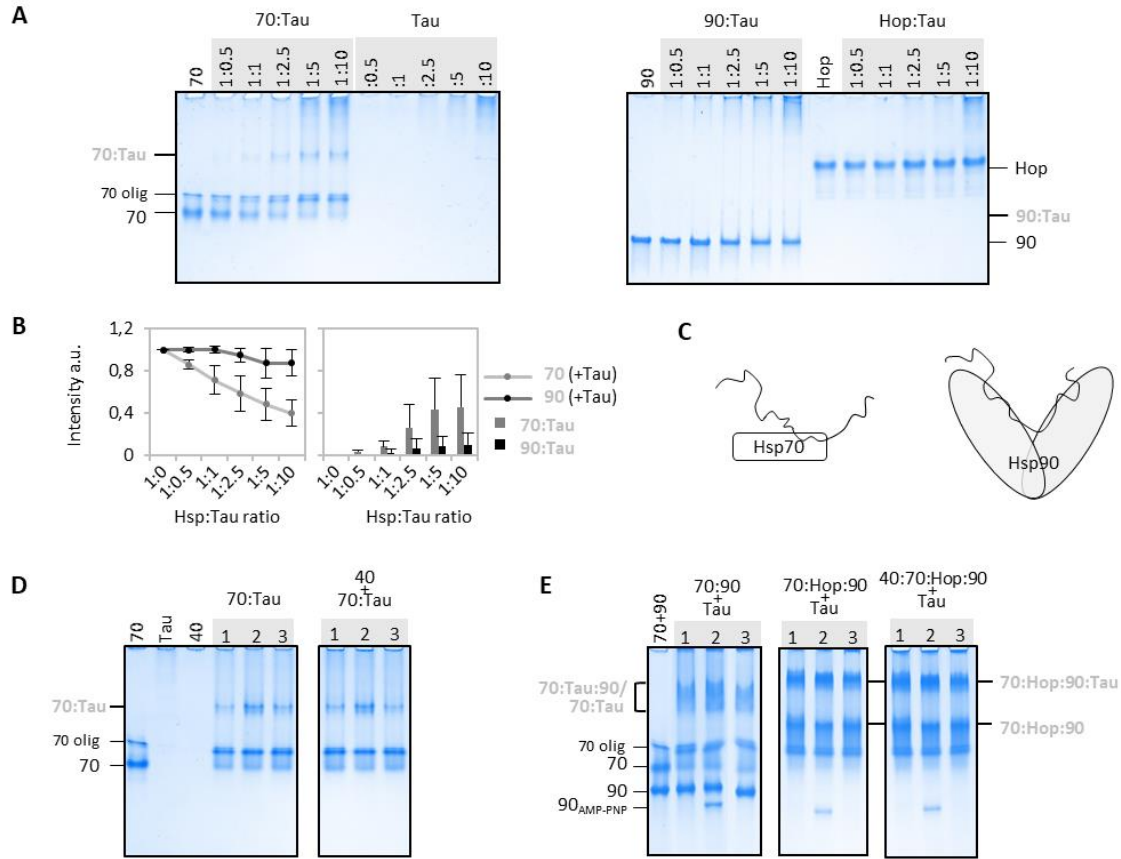


**Figure 30 Interaction of Tau with individual proteins of the Hsp70/Hsp90 chaperone machinery base.**

**A** Native page analysis of the interaction between Tau (2.5-50  $\mu$ M) and Hsp70, Hsp90 and Hop (5  $\mu$ M each). Protein-protein interactions are observed for Hsp70:Tau and Hsp90:Tau based on intensity loss of the chaperone bands along with the appearance of a new band corresponding to the respective Tau:chaperone complex with increasing concentrations of Tau. Hsp70, Hsp70 oligomers and Hsp90 are abbreviated as “70”, “70 olig.” and “90”, respectively. **B** Quantitative analysis of the band intensity of the chaperones Hsp70 and Hsp90 alone (left) and the Hsp70:Tau and Hsp90:Tau complexes (right) with increasing concentrations of Tau. **C** Cartoon representation of Tau interacting with Hsp70 and Hsp90 taking into account the binding of Tau's repeat region to both chaperones.<sup>84,242</sup> **D**, **E** Native page analysis showing no influence of Hsp40 and nucleotides (1 – no nucleotide, 2 – +AMP-PNP, 3 – +ADP) on the Hsp70:Tau, Hsp70:Tau:Hsp90 and the Hsp70:Hop:Hsp90:Tau interaction (25  $\mu$ M each, except Hsp40 (10  $\mu$ M) and Tau (125  $\mu$ M)).



## Results

### 3.3.2 Tau prefers to bind the Hsp70/Hsp90 chaperone machinery over the individual chaperones

With regard to the isolated Hsp70:Hsp90:Tau complex band, the Tau affinity towards the Hsp70/Hsp90 chaperone machinery base was determined by quantifying the corresponding band intensity. Compared to the Tau interaction with individual Hsp70 or Hsp90 known from literature (and reaffirmed for Hsp90:Tau), Tau showed with a  $K_D = 1.31 \pm 0.07 \mu\text{M}$  an increased affinity for the Hsp70:Hsp90 complex than for the individual chaperones (Figure 31). As the addition of AMP-PNP neither had an effect on Tau's affinity to the Hsp70:Hsp90 complex, the following experiments were performed in the absence of nucleotides.

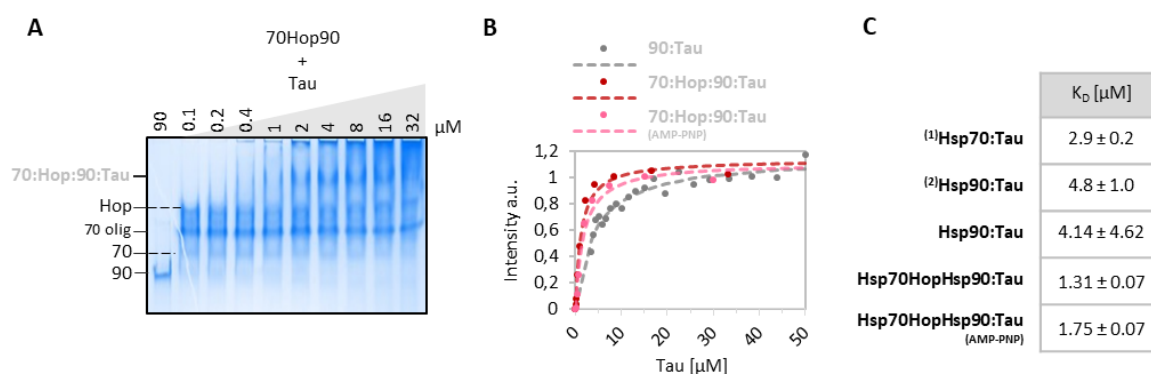


**Figure 31** Affinity measurements of Tau binding to the Hsp70/Hsp90 chaperone machinery.

**A** Native page analysis of Tau interacting with the Hsp70:Hsp90 complex (1:1:1 molar ratio;  $0.4 \mu\text{M}$  Hsp90). Hsp70, Hsp70 oligomers and Hsp90 are abbreviated as “70”, “70 olig.” and “90”, respectively. **B** Normalized intensities of the Hsp90:Tau (grey; Trp quenching) and the Hsp70:Hsp90:Tau complex in the absence (red; native gel in (A)) and the presence of AMP-PNP (rose; native gel in Supplementary data) plotted against the Tau concentration of the respective titration point. **C** Tau affinities for Hsp70, Hsp90 and the Hsp70/Hsp90 chaperone machinery base (1)<sup>321</sup> (2)<sup>84</sup>.

## Results

### 3.3.3 Tau's repeat region is the main interaction site with the Hsp70:Hsp90 complex

NMR spectroscopy was used to monitor the Tau dynamics in presence of the Hsp70/Hsp90 chaperone machinery. 2D  $^{15}\text{N}$ - $^1\text{H}$  correlation spectra were recorded of uniformly  $^{15}\text{N}$ -labeled Tau (Figure 14) – a technique that has already been widely used to ascertain interaction sites on Tau.<sup>84,242,350</sup> In order to drive residue-specific conclusion about the interaction site, the knowledge about which peak belongs to which backbone NH-group is fundamental. The backbone assignment of Tau was available at pH 6.8.<sup>257</sup> The assignment was transferred by pH titration to pH 7.4 – the buffer conditions in which all previous results were performed in (Figure 32).

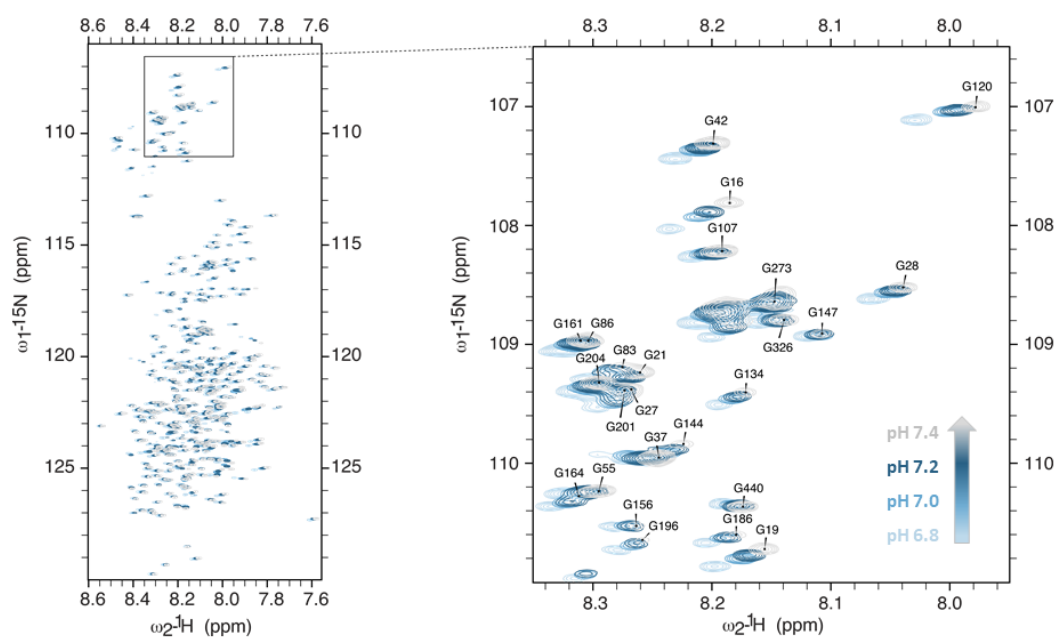
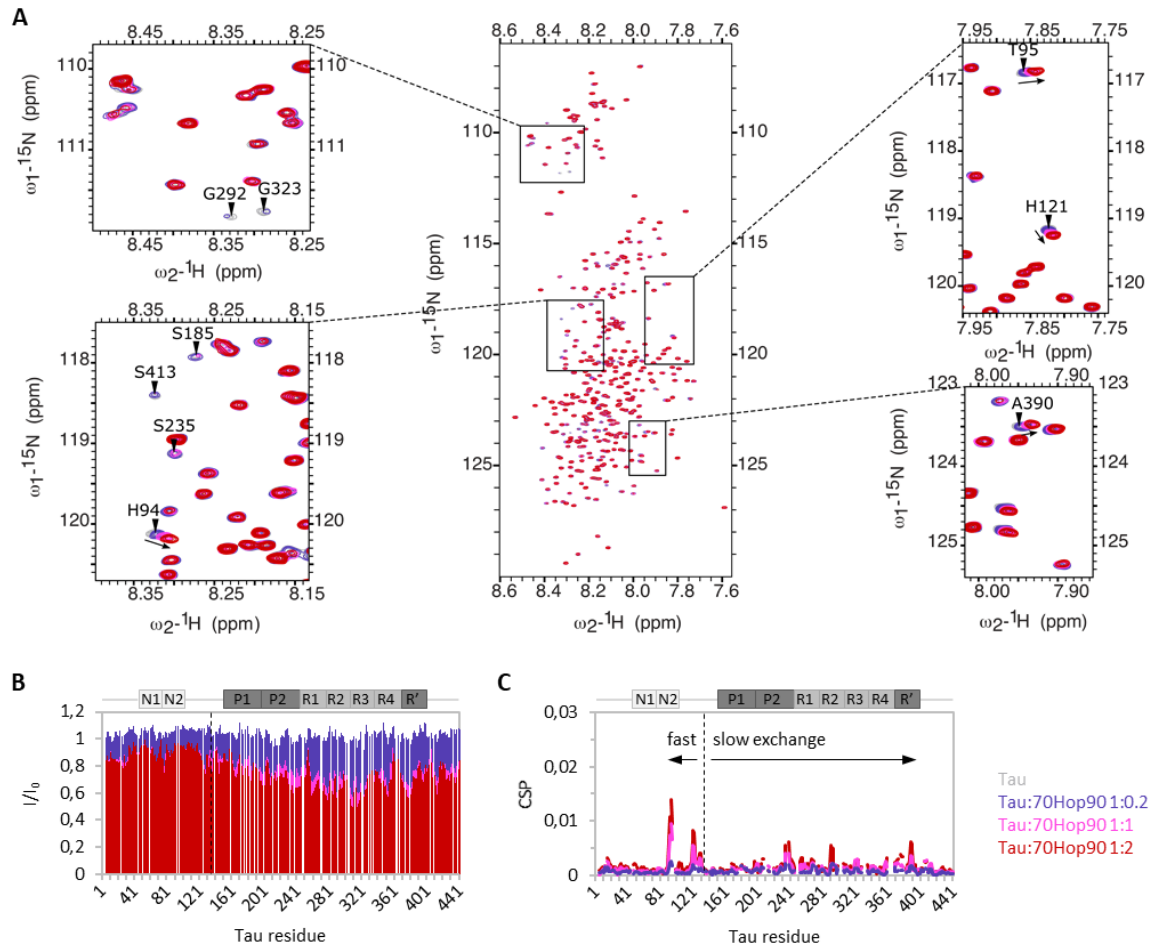


Figure 32 NMR pH titration of  $^{15}\text{N}$ -labeled Tau used to transfer the backbone assignment from pH 6.8 to pH 7.4.

In line with the ascertained interaction of Tau with the Hsp70/Hsp90 chaperone machinery, the stepwise addition of the Hsp70:Hsp90 complex resulted in changes in the Tau spectrum signifying the interaction (Figure 33A). Sequence-specific analysis showed that a large part of Tau, ranging from the proline-rich region P1/P2 to the flanking R' region, was strongly broadened along with only few chemical shift perturbations (Figure 33B, C). Because such alterations are characteristic for residues interacting in a slow exchange regime, i.e. high affinity, the data show that Tau's central part including the repeat region is the main interaction site with the Hsp70:Hsp90 complex. In comparison, chemical shift changes, which are characteristic for fast-to-intermediate exchange and thus lower affinity, were more dominant for residues preceding the proline rich region. The N- and C-terminal residues of Tau were not affected upon the addition of the Hsp70:Hsp90 complex, hence remained unbound.



## Results



**Figure 33 NMR spectroscopy of Tau binding to the Hsp70:Hsp90 complex.**

**A**  $^{15}\text{N}$ - $^1\text{H}$  HSQC spectra of Tau alone and with increasing amounts of the Hsp70:Hsp90 (1:1:1 molar ratio) complex. Titration experiments of Tau with the preformed Hsp70:Hsp90 complex (termed 70Hop90) in molar ratios of 1:0.2 (purple), 1:1 (pink) and 1:2 (red) were acquired. **B**, **C** NMR interaction profiles depicting the intensity changes (**B**) and the chemical shift perturbations (**C**) observed in (**A**) (same color code as in (**A**)).  $I_0$  is the intensity of Tau cross peaks in the absence of binding partners (grey spectrum in **A**). Tau domains are marked above each plot.

## Results

### 3.3.4 Tau's P2 / R' domains effectively contribute to the Hsp70:Hsp90:Tau interaction

As Tau's central part was ascertained as the main interaction site with the Hsp70/Hsp90 chaperone machinery (Figure 33), it was further tested whether Tau's repeat region alone is sufficient to evoke binding to the Hsp70:Hsp90 complex. To this end, the Tau construct K18 was produced containing only repeats R1-R4 (Figure 34). Native page analysis revealed an additional band that emerged with increasing concentrations of K18. Simultaneously only the band of the free Hsp70 decreased, whereas the amount of Hsp70:Hsp90 complex remained unchanged. This suggested that the repeat region of Tau alone does not evoke an equally strong interaction with the Hsp70/Hsp90 chaperone machinery as full-length Tau. Following that, a second, longer Tau construct, termed K32, which comprises the repeats R1-R4 as well as the neighboring regions P2 and R' (Figure 34) was used. In this case a similar result was obtained as with full-length Tau: an additional, more intense band appeared with increasing concentrations of K32 while the band corresponding to the Hsp70:Hsp90 complex decreased. The proline-rich region P2 and the pseudo-repeat region R' thus contribute to a stable interaction between Tau and the Hsp70/Hsp90 chaperone machinery.

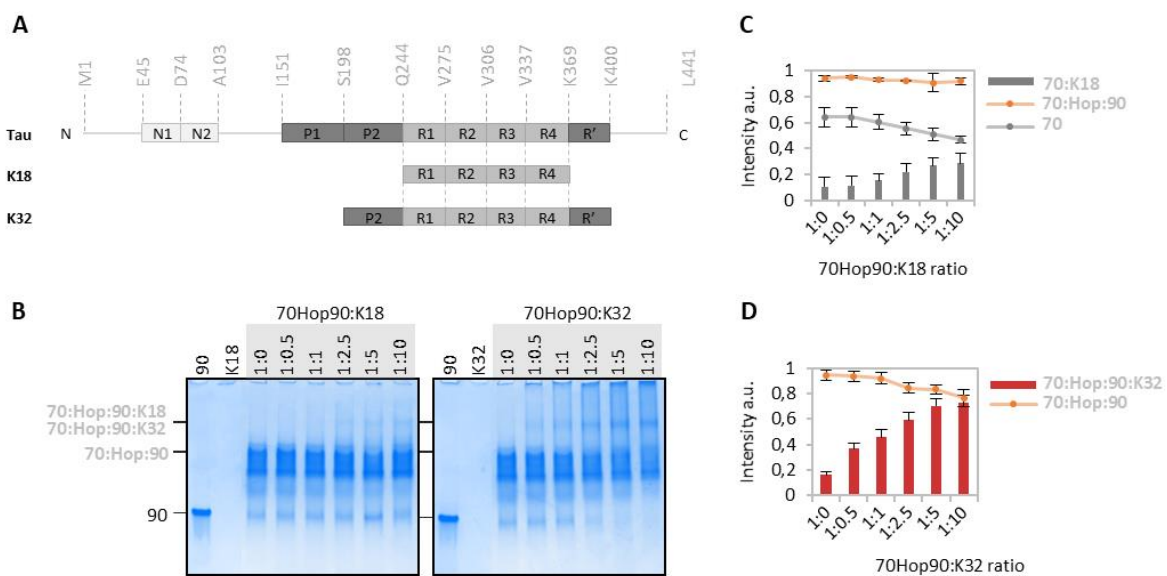


**Figure 34** *In vitro* reconstitution of the interaction of the Hsp70/Hsp90 chaperone machinery with smaller Tau constructs.

**A** Domain organization of Tau, K18 and K32.<sup>351</sup> **B** Native page analysis of the Hsp70:Hsp90 complex interacting with K18 (left) and K32 (right) – 5  $\mu$ M of Hsp90 were loaded as reference. **C**, **D** Quantitative analysis of the band intensities from (B) of the Hsp70:K18 complex (grey bars), the Hsp70:Hsp90 complex (orange line), Hsp70 (grey line) and the Hsp70:Hsp90:K32 complex (red bars).

### 3.4 The co-chaperone p23 stabilizes the Hsp70:Hop:Hsp90:Tau interaction

#### 3.4.1 *In vitro* reconstitution of the Hsp70:Hop:Hsp90:Tau:p23 complex

To complete the list of minimal components that are reported for a functional Hsp70/Hsp90 chaperone machinery, the co-chaperone p23 was added to the Hsp70:Hop:Hsp90 and Hsp70:Hop:Hsp90:Tau complex (Figure 35).

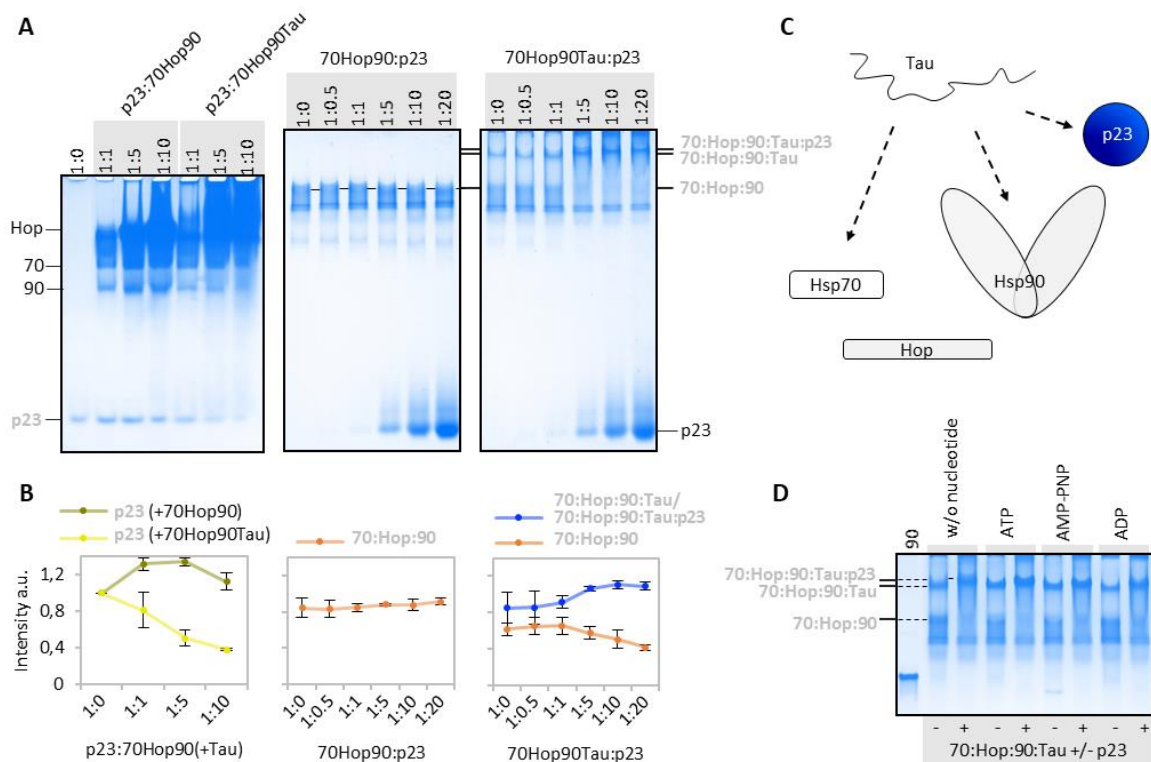


**Figure 35** *In vitro* reconstitution of the Hsp70:Hop:Hsp90:Tau:p23 complex.

**A** Native page analysis of the interaction between p23 and the Hsp70:Hop:Hsp90 complex in absence and presence of Tau (70:Hop:90:Tau molar ratio of 1:1:1:5). Left panel: fixed p23 concentration at 2.5  $\mu$ M; middle and right panel: fixed Hsp70:Hop:Hsp90:(Tau) concentration at 5  $\mu$ M Hsp90. Hsp70 and Hsp90 are abbreviated as “70” and “90”, respectively. **B** Quantitative analysis of band intensities from (A). Left plot: band intensity of p23 with increasing amounts of the Hsp70:Hop:Hsp90 complex in the absence (+70Hop90; olive) and presence (+70Hop90Tau; yellow) of Tau; middle and right plot: band intensities of the Hsp70:Hop:Hsp90 (orange), Hsp70:Hop:Hsp90:Tau / Hsp70:Hop:Hsp90:Tau:p23 complexes (blue) with increasing amounts of p23. Because the bands of the 4-component Hsp70:Hop:Hsp90:Tau and 5-component Hsp70:Hop:Hsp90:Tau:p23 complexes are very close, they were analyzed together. **C** Cartoon representation of the 5-component Hsp70:Hop:Hsp90:Tau:p23 interaction. **D** In the presence of Tau, native page analysis demonstrates that the formation of a stable Hsp70:Hop:Hsp90:Tau:p23 complex (mixed in a ratio of 1:1:1:5:5) is independent of the presence of the nucleotides ATP, AMP-PNP or ADP; (-) and (+) indicate the absence and presence of p23, respectively.

In native page, increasing amounts of p23 had no effect on the level of the Hsp70:Hop:Hsp90 tau complex in absence of Tau suggesting no interaction (Figure 35A, B middle panel). In contrast, when Tau was present, the binding of p23 to the Hsp70:Hop:Hsp90:Tau complex was observed (Figure 35A, B right panel). The corresponding complex band was located

## Results

slightly above the band of the Hsp70:Hsp90:Tau complex. Along with the formation of the 5-component Hsp70:Hsp90:Tau:p23 complex, the concentration of the Hsp70:Hsp90 complex decreased signifying that p23 stabilizes the Hsp70/Hsp90 chaperone machinery in its Tau-bound form. In this line, monitoring the amount of free p23, an interaction with the Hsp70/Hsp90 chaperone machinery was only detected in the presence of Tau (Figure 35A, B left panel). The addition of different nucleotides showed no effect on the Hsp70:Hsp90:Tau:p23 interaction (Figure 35D).

### 3.4.2 p23 interaction is cooperatively enhanced in the presence of Tau

Interaction studies with the individual chaperones in both the absence and presence of Tau further showed that p23 interacts with Hsp90 but not with Hsp70 (Figure 36). The interaction of p23 with Hsp90 was cooperatively enhanced in the presence of Tau, as the amount of free Hsp90 was greatly reduced compared to the addition of p23 only.

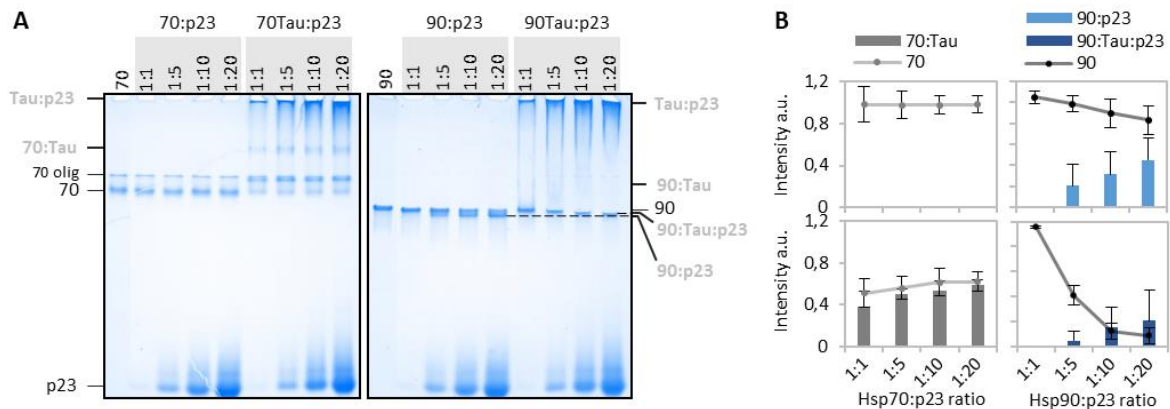


**Figure 36 Interaction of p23 with Hsp70 and Hsp90.**

**A** Native page analysis of the interaction between p23 and the chaperones Hsp70 and Hsp90 (5  $\mu$ M each) in the absence and presence of Tau (25  $\mu$ M). **B** Left: quantitative analysis displays a constant amount of free Hsp70 independent of the p23 concentration precluding a direct interaction between Hsp70 and p23. Right: quantitative analysis points out the cooperative binding of p23 to Hsp90 in the presence of Tau.

NMR experiments demonstrated the p23 binding site on Hsp90 (Figure 37). Main signal perturbations were detected for residues in the middle domain of Hsp90 located in close proximity to the NTD including I295, I361 and I403. The perturbed residues were mapped on the closed structure of Hsp90 as suggested from previous studies.<sup>48,181,221</sup> The residues I361 and I403 of each Hsp90 monomer faced each other, which could place p23 in between the dimer interface, thereby preventing the ATP hydrolysis of Hsp90.<sup>205</sup> In contrast, I295 is located at the outer side of Hsp90's MD, which could sense the presence of p23 due to conformational change of the NTD-MD arrangement upon p23 binding. Consistent with the high amounts of p23 that were necessary for

## Results

the Hsp90:p23 interaction observed by native page (Figure 36), quantification analysis of the respective peak intensities and chemical shift perturbations were characteristic for an intermediate exchange regime, i.e. moderate affinity (Figure 37B). In combination, this suggested that Tau acts as an additional binding partner for p23 in the Hsp70/Hsp90 chaperone machinery decisively increasing p23 binding.

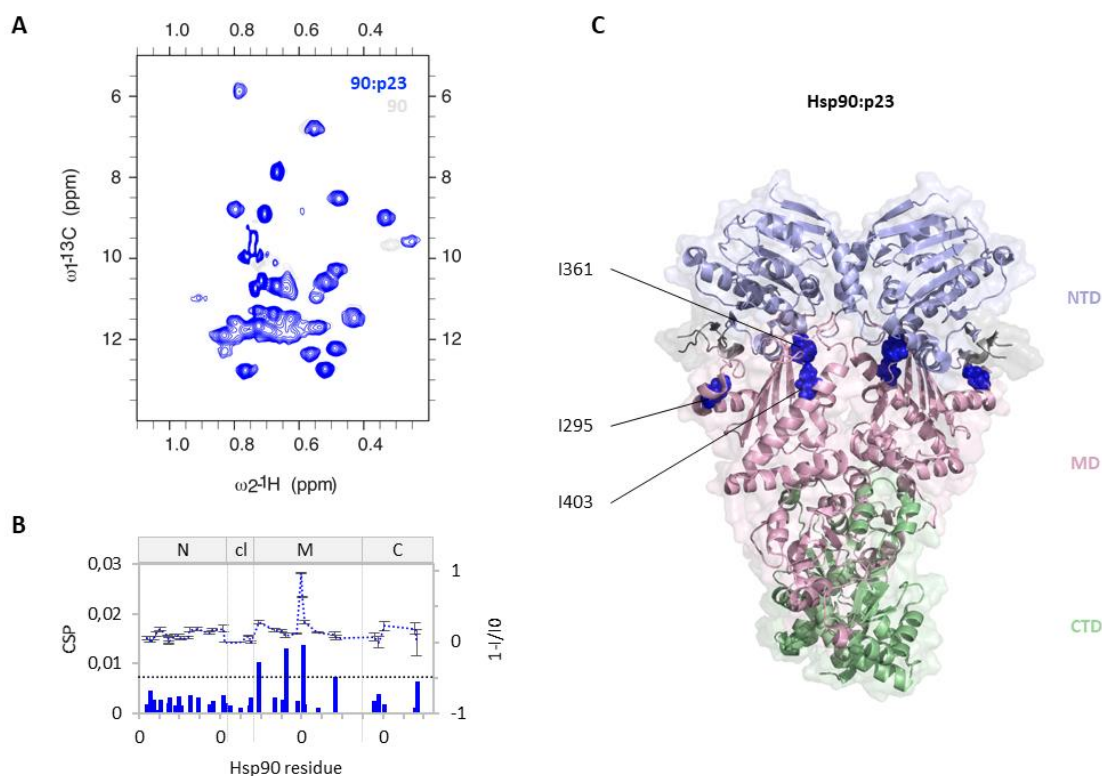


**Figure 37 TROSY NMR of Hsp90 in presence of p23.**

**A** 2D  $^{13}\text{C}$ - $^1\text{H}$  methyl-TROSY spectra of Hsp90 in absence (grey) and presence of p23 (blue, molar ratio 1:5, 50  $\mu\text{M}$  Hsp90). **B** Residue-specific chemical shift perturbations (CSP; bars) and peak intensities ( $1-I/I_0$ ; lines) of Hsp90's isoleucine  $\delta$ -methyl groups observed in (A).  $I_0$  is the signal intensity of the Hsp90 reference. Error bars were calculated based on NMR signal-to-noise ratio. Hsp90 domains are depicted on top of each plot and represented with dotted lines (N – N-terminal domain, cl – charged linker, M – middle domain, C – C-terminal domain). **C** Side view of the closed conformation of Hsp90 (N-terminal domain (NTD, light blue), middle domain (MD, light pink) and C-terminal domain (CTD, light green) (PDB: 5fwk).<sup>119</sup> Isoleucine residues affected upon the addition of p23 are highlighted in blue spheres.

### 3.4.3 Tau's repeat region as the major binding site within the Hsp70:Hsp90:Tau:p23 complex

Tau dynamics within the Hsp70:Hsp90:Tau:p23 complex were further followed by NMR spectroscopy. As described before (see chapter 3.3.3), 2D  $^{15}\text{N}$ - $^1\text{H}$  correlation spectra of isotopically labeled Tau were recorded in the absence and the presence of the Hsp70:Hsp90 complex together with p23 (Figure 38A). A few changes in Tau's peak positions were observed, but most resonances did not sense the presence of p23. Quantitative analysis showed that the residue-specific peak broadening profiles with and without p23 were highly similar (Figure 38B),



## Results

whereas residues within the P2 domain of Tau depicted distinct chemical shift perturbations upon the addition of p23 (Figure 38C).

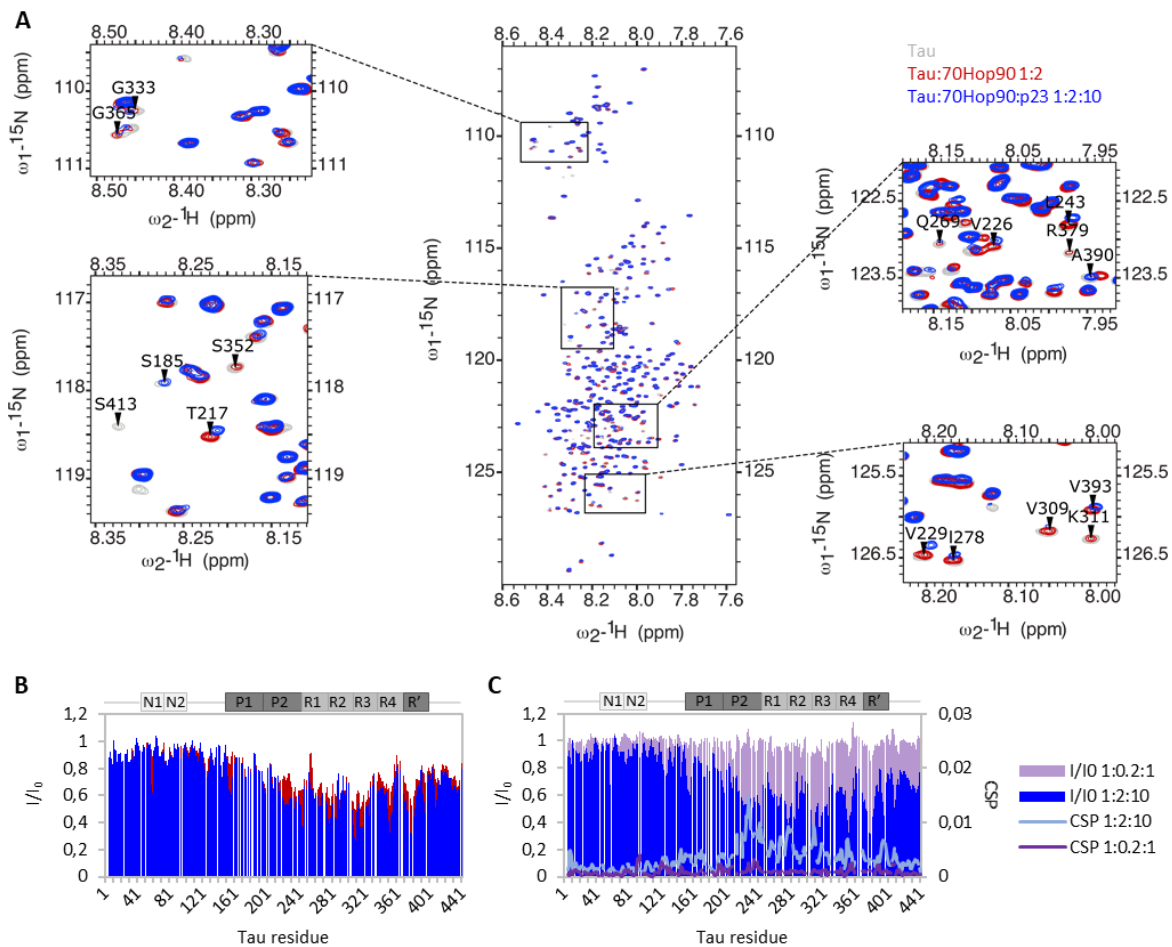


**Figure 38** Influence of p23 binding to the Hsp70:Hsp90:Tau complex on Tau dynamics.

**A**  $^{15}\text{N}$ - $^1\text{H}$  HSQC spectra of Tau alone (grey) and in the presence of the Hsp70:Hsp90 complex (1:1:1) without (red) and with a ten-fold excess of p23 (blue). **B** Residue-specific peak intensity changes derived from (A; same color code).  $I_0$  is the intensity of Tau cross peaks in the absence of binding partners (grey spectrum in A). **C** Chemical shift changes (lines) in Tau upon addition of Hsp70:Hsp90 and p23 with Tau:Hsp70:Hsp90:p23 molar ratios of 1:0.2:1 (purple) and 1:2:10 (blue). Peak intensity changes (bars) are shown for comparison. Tau domains are marked above each plot.

The comparison of Tau's interaction profile of the Hsp70/Hsp90 chaperone machinery with the ones of Hsp70 and Hsp90 alone highlighted that not only the same binding region but also the same residues of Tau are involved in both interactions (Figure 39A). Hsp70 binding involves four dominant dips in the intensity profile of Tau, in presence of Hsp90 the binding region is broader and includes five major dips. All five dips are similarly present in the interaction profile of Tau within the Hsp70:Hsp90:Tau and the Hsp70:Hsp90:Tau:p23 complex, whereby the presence of p23 appears to strengthen the interaction of Tau with the Hsp70/Hsp90 chaperone machinery. Sequence-specific analysis of the five central amino acids of each dip overlapped with previous NMR studies of the Tau:Hsp90 complex (Figure 39B)<sup>84</sup>, though included additionally residues of the R4 and R' region in case of the Tau:Hsp70 interaction.<sup>242</sup> Separate titrations of Tau

## Results

with p23 alone proved that p23 can directly bind to Tau (Figure 39C). The distinct chemical shift changes observed for the Hsp70:Hsp90:Tau:p23 interaction thus might also be aroused from the binding of p23 to Tau molecules not bound to the Hsp70/Hsp90 chaperone machinery.

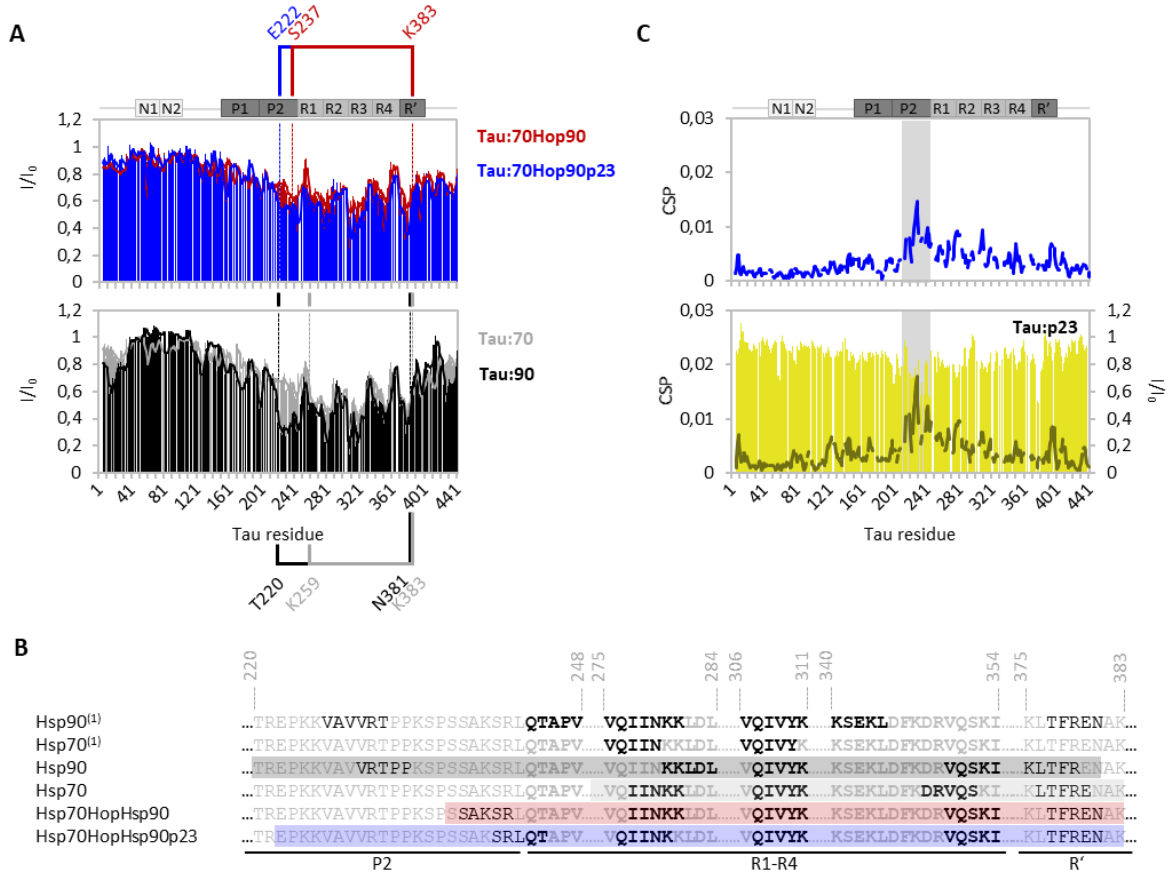


**Figure 39 Comparison of Tau interaction with Hsp70, Hsp90 and the Hsp70/Hsp90 chaperone machinery.**

**A** NMR peak intensity changes of Tau upon the addition of the Hsp70/Hsp90 chaperone machinery in presence (blue) and absence (red) of p23 (from Figure 38B), and in presence of Hsp70 (grey) and Hsp90 (black) only. Corresponding spectra are shown in Figure A 12. Main interaction sites are marked with brackets in the respective color code. **B** Key section of the Tau sequence involved in chaperone interaction ranging from the P2 to the R' region. The repeat region R1-R4 is highlight in bold. The five central amino acids of each interaction dip are highlighted in black. <sup>(1)</sup> are taken from the literature.<sup>84,242</sup> Binding sites are colored according to (A) **C** Top: Chemical shift changes of Tau upon addition of Hsp70:Hsp90 and p23 (from Figure 38C). Bottom: NMR interaction profile of Tau upon p23 addition (10-fold molar excess) yielding a distinct chemical shift perturbation plot with the maximum perturbations within Tau's P2 region. Peak intensity changes (bars) are shown for comparison. Tau domains are marked above each plot.

### 3.5 Structural insights into the 750 kDa (Hsp70<sub>1</sub>:Hop<sub>1</sub>:Hsp90<sub>2</sub>:Tau<sub>1</sub>:p23<sub>1</sub>)<sub>2</sub> complex

#### 3.5.1 The binding of Tau evokes the dimerization of the Hsp70/Hsp90 chaperone machinery

To gain insights into the stoichiometry of the Hsp70:Hop:Hsp90:Tau:p23 interaction, multi-angle light scattering (MALS) analysis was anticipated to determine its molecular weight (MW). Accurate MW determination by MALS requires the presence of a monodisperse sample, i.e. particles of same character. As a 5-fold excess of Tau and p23 was required to shift the equilibrium towards the Hsp70:Hop:Hsp90:Tau:p23 complex (Figure 35A), the latter needed to be purified from the unbound proteins or potential subcomplexes achieved by sucrose density gradient centrifugation (Figure 40A).

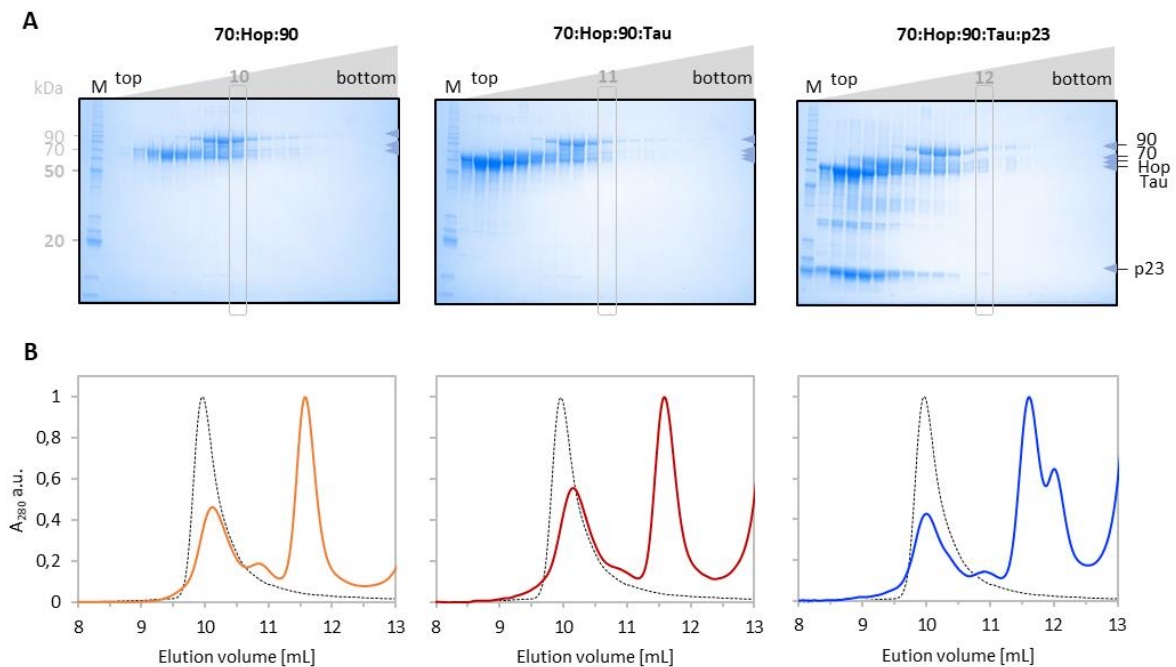


**Figure 40** Sucrose density gradient and size exclusion chromatography (SEC) of the Hsp70/Hsp90 chaperone machinery in complex with Tau and p23.

**A** SDS-page analysis (8-16 % gradient gels; BioRad) of the Hsp70:Hop:Hsp90, Hsp70:Hop:Hsp90:Tau and Hsp70:Hop:Hsp90:Tau:p23 complexes after sucrose density gradient purification (10-25 % sucrose). Fractions of interest are highlighted with a grey square and used for the subsequent SEC run. **B** SEC analysis of the fractions highlighted in (A): Hsp70:Hop:Hsp90 in orange, Hsp70:Hop:Hsp90:Tau in red and Hsp70:Hop:Hsp90:Tau:p23 in blue (Shodex column 30/50; Wyatt). The elution chromatogram of Hsp90 is shown for comparison (black dashed line).

Fractions containing the proteins of interest were further analyzed by MALS. A batch injection was unsuccessful due to the high sensibility of the instrument. In contrast, SEC-MALS, which included a size exclusion chromatography prior to the MALS measurement, guaranteed a stable environment yielding reliable results. However, compared to Hsp90 alone, no higher molecular weight complex based on earlier elution volume could be observed (Figure 40B).



## Results

Unfortunately, all proteins eluted separately in the respective elution chromatogram either due to too high forces during the SEC run, or due to dilution effects resulting in the dissociation of the complex. Control experiments without p23 and Tau showed the same behavior for the Hsp70:Hop:Hsp90:Tau and the Hsp70:Hop:Hsp90 complexes (Figure 40B).

To counteract the dissociation of the individual proteins, chemical cross-linking was used to stabilize the Hsp70:Hop:Hsp90:Tau:p23 complex. Following the same experimental procedure additional bands appeared at higher molecular weights in the SDS page analysis of the sucrose density gradient fractions (Figure 41A).

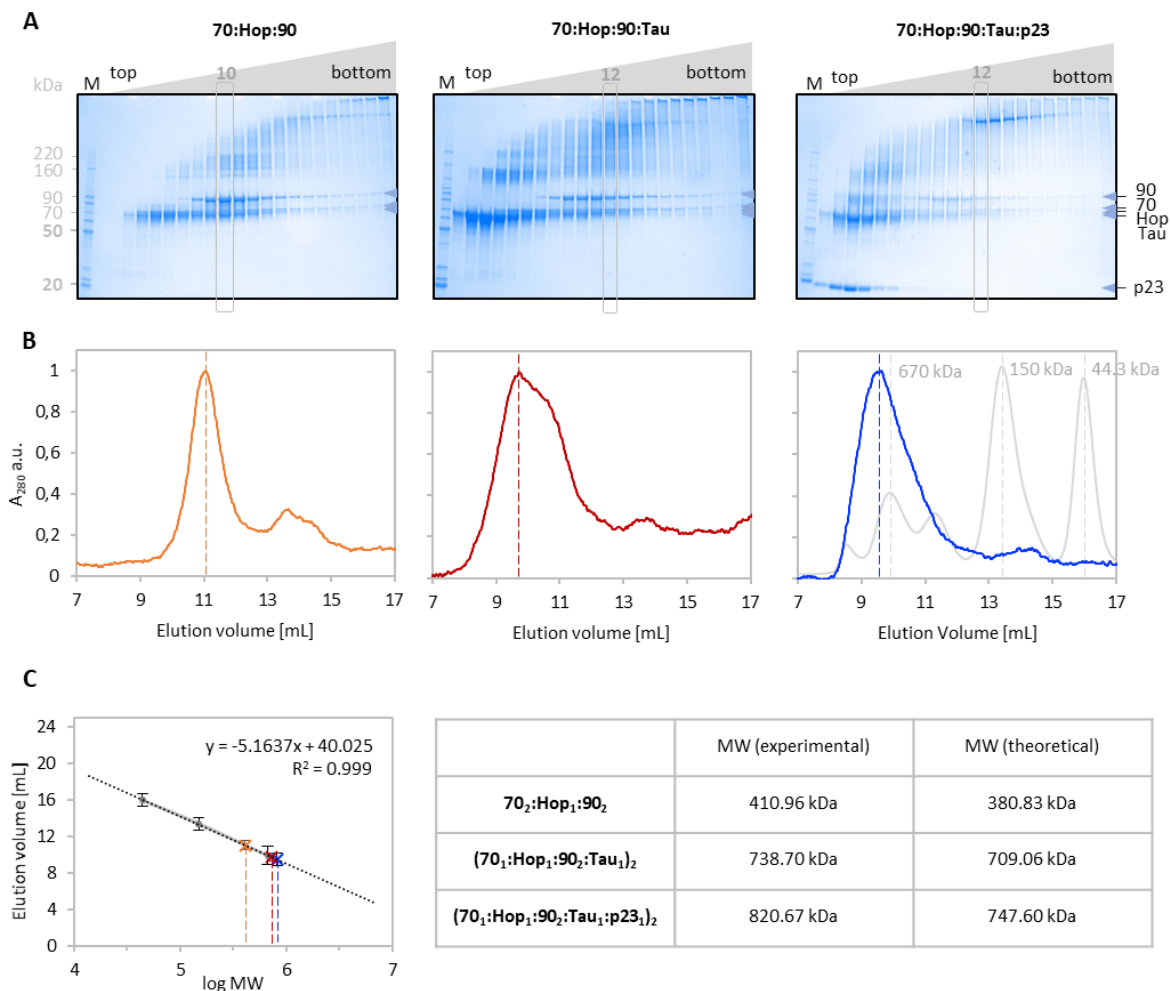


**Figure 41 Molecular weight determination of the Hsp70/Hsp90 chaperone machinery:Tau complexes.**

**A** SDS-page analysis (4-15 % gradient gels; BioRad) of the cross-linked Hsp70:Hop:Hsp90, Hsp70:Hop:Hsp90:Tau and Hsp70:Hop:Hsp90:Tau:p23 complexes after sucrose density gradient purification (10-25 % sucrose). Fractions of interest are highlighted with a grey square and used for the subsequent SEC run. **B** SEC analysis of the fractions highlighted in (A): Hsp70:Hop:Hsp90 in orange, Hsp70:Hop:Hsp90:Tau in red and Hsp70:Hop:Hsp90:Tau:p23 in blue (SD200 10/30). The elution chromatogram of the protein standard mix is shown for comparison. Dashed lines mark the respective peak maxima. **C** Linear reference line of the protein standard mix (grey). The logarithmic molecular weight (log MW) is plotted against the elution volume to determine the molecular weight of the Hsp70:Hop:Hsp90, Hsp70:Hop:Hsp90:Tau and Hsp70:Hop:Hsp90:Tau:p23 complexes (same color code as in (B)). The theoretical masses of each complex are listed for comparison.

## Results

In the subsequent SEC chromatogram the fraction of interest showed up as one individual peak signifying successful cross-linking reaction (Figure 41). Due to unreliable MW determination by MALS at low protein concentrations, the complex size was estimated according to its elution volume. On the basis of a protein standard, the determined mass of ~821 kDa was close to the molecular weight of a dimeric (Hsp70<sub>1</sub>:Hop<sub>1</sub>:Hsp90<sub>2</sub>:Tau<sub>1</sub>:p23<sub>1</sub>)<sub>2</sub> protein complex (747.6 kDa; V<sub>e</sub> = 9.5 mL), taking into account the additional mass of the DSS cross-linker (~0.37 kDa). Without p23, the elution volume corresponded to a mass of ~739 kDa, which is best in agreement with again a dimeric (Hsp70<sub>1</sub>:Hop<sub>1</sub>:Hsp90<sub>2</sub>:Tau<sub>1</sub>)<sub>2</sub> protein complex (709.06 kDa; V<sub>e</sub> = 9.7 mL). Consistent with the previously mentioned equilibrium between the Tau bound and unbound Hsp70/Hsp90 chaperone machinery, the machinery:Tau peak depicted a shoulder at later elution volumes that could be attributed to a co-purified Hsp70:Hop:Hsp90 complex. Indeed, for the sample including Hsp70:Hop:Hsp90 only, a single peak at this elution volume was observed. The much smaller elution volume of V<sub>e</sub> = 11 mL could be ascribed to a monomeric Hsp70<sub>2</sub>:Hop<sub>1</sub>:Hsp90<sub>2</sub> protein complex (380.83 kDa) with a calculated mass of ~411 kDa. Notable, the data suggested two Hsp70 molecules bound within the Hsp70:Hop:Hsp90 complex, whereas in the machinery:Tau complexes only one Hsp70 was attached to each machinery monomer.

Taken together, the analysis demonstrated that the addition of Tau induces the formation of a dimeric Hsp70/Hsp90 chaperone machinery. An antiparallel orientated dimer could further allow the Hsp70 molecule of one machinery to compete for the second binding site on Hsp90 of the opposite machinery.

### 3.5.2 A single Tau molecule, embraced in the center of each Hsp70/Hsp90 chaperone machinery, determines the localization of p23

The cross-linking of the Hsp70:Hop:Hsp90:Tau:p23 complex has been further studied in more detail by mass spectrometry (in collaboration with the lab of Prof. H. Urlaub). Identifying the residues that are involved in intra- and intermolecular cross-links could give further insights into the spatial orientation of the proteins within the Hsp70:Hop:Hsp90:Tau:p23 complex. Two different cross-linkers, disuccinimidyl suberate (DSS) and 1-ethyl-3-(3-dimethylaminopropyl) carbodiimide hydrochloride (EDC), were tested and compared.

## Results

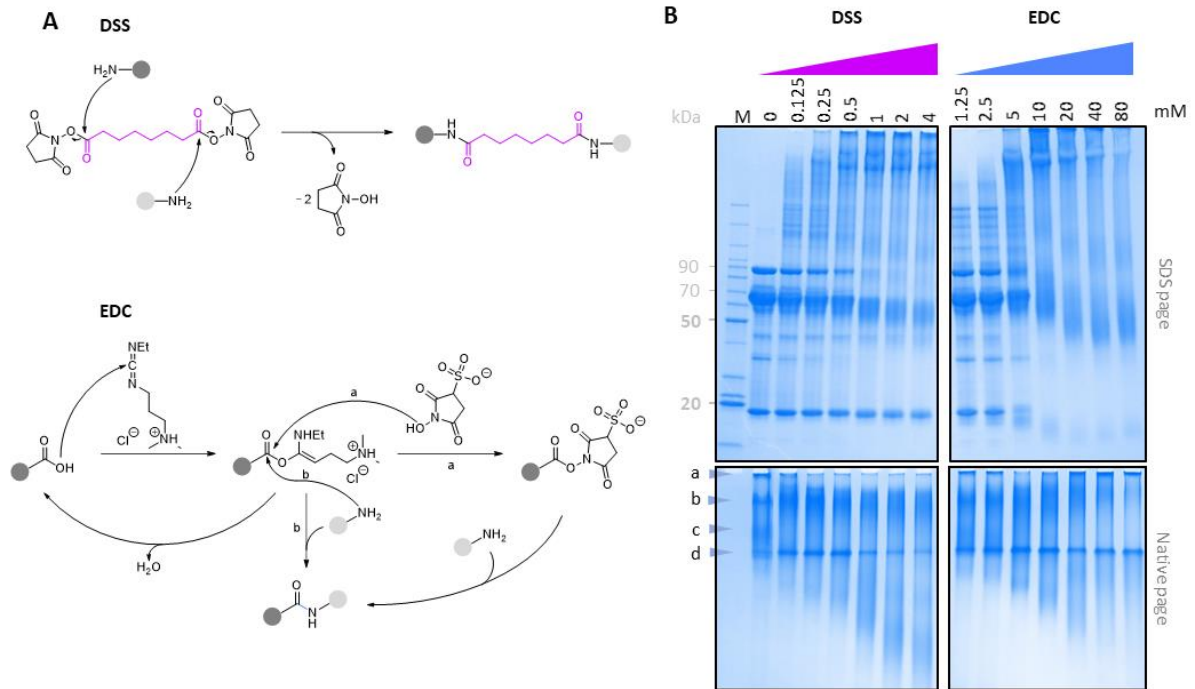


**Figure 42 Cross-linking reaction of the Hsp70/Hsp90 chaperone machinery: Tau complex using DSS and EDC.**

**A** Reaction mechanism of disuccinimidyl suberate (DSS) and 1-ethyl-3-(3-dimethylaminopropyl) carbodiimide hydrochloride (EDC) cross-linking primary amines, and primary amines with carboxylic acids, respectively. **B** SDS (top; 4–20 % gradient gel) and native page (bottom; 7.5 % gel) analysis of the Hsp70:Hsp90:Tau:p23 complex incubated with increasing concentrations of cross-linker. Bands of interest are marked in the native gel: Tau (a), Hsp70:Hsp90:Tau:p23 (b), Hsp70:Hsp90 (c) and Hsp70 oligomers (d).

Cross-linker titration analyzed by SDS page revealed high molecular weight bands signifying the successful reaction in both cases (Figure 42B). The main difference was that more p23 molecules were cross-linked by the use of EDC compared to DSS. Notable, native page analysis of the same samples indicated that increasing concentrations of both cross-linkers concomitantly promoted the formation of smaller sub-complexes trailing a reducing amount of the complex of interest. Finally, a protein:DSS molar ratio in the range of 1:25 to 1:50 (i.e. 0.125 – 0.25 mM DSS for 5  $\mu$ M of Hsp90) yielded the maximum amount of Hsp70:Hsp90:Tau:p23 complex, without detectable Hsp70:Hsp90 complex and minor amounts of side products. For EDC the same applied with ten times the amount of cross-linker.

Following that, the Hsp70:Hsp90:Tau:p23 complex was purified *via* sucrose density gradient purification as described above. The peak fractions were pooled and measured by mass spectrometry<sup>†</sup>. In total, 2070 and 4460 unique cross-link spectra matches (CSMs) could be identified for DSS and EDC, respectively (Figure 43A, Table A 3, Table A 4). First, intramolecular cross-links were analyzed on the basis of the 3D structures of the individual proteins available in

<sup>†</sup> MS experiments and cross-link analyses were gratefully conducted by Dr. M. Ninov (MPI-BPC, in the group of Prof. Dr. Henning Urlaub, Department of Bioanalytical Mass Spectrometry).

## Results

the PDB (Hsp90 – 5fwk; Hsp70<sup>NBD</sup> – 5aqz; Hsp70<sup>SBD</sup> – 4po2; Hop<sup>TPR1</sup> – 1elw; Hop<sup>TPR2A</sup> – 1elr; p23 – 1ejf).<sup>119,158,193,223,342</sup> According to the lengths of the cross-linker (Figure 43B) a distance threshold was set to 29.4 Å for DSS (= 2 x 6 Å for the lysine side chains + 11.4 Å linker arm + 6 Å for backbone flexibility) and 17 Å for EDC (= 6 Å for the lysine side chain + 5 Å for the carboxylic acid side chain + 6 Å for backbone flexibility)<sup>352</sup>, whereby the distances were measured from C $\alpha$  to C $\alpha$  of the cross-linked residues. For DSS 96.08 % of the selected intramolecular cross-links appeared below that threshold signifying reliable results (Figure 43C). In contrast, for EDC only 64.22 % were detected within the threshold manifesting a distinct amount of false-positive cross-links. Notable, Tau was neglected in this analysis round as Tau is intrinsically disordered, i.e. unstructured in solution. Beyond, distance measurements of p23 were not included in the DSS analysis, as the cross-linked residues were not present in the structure deposited in the PDB.

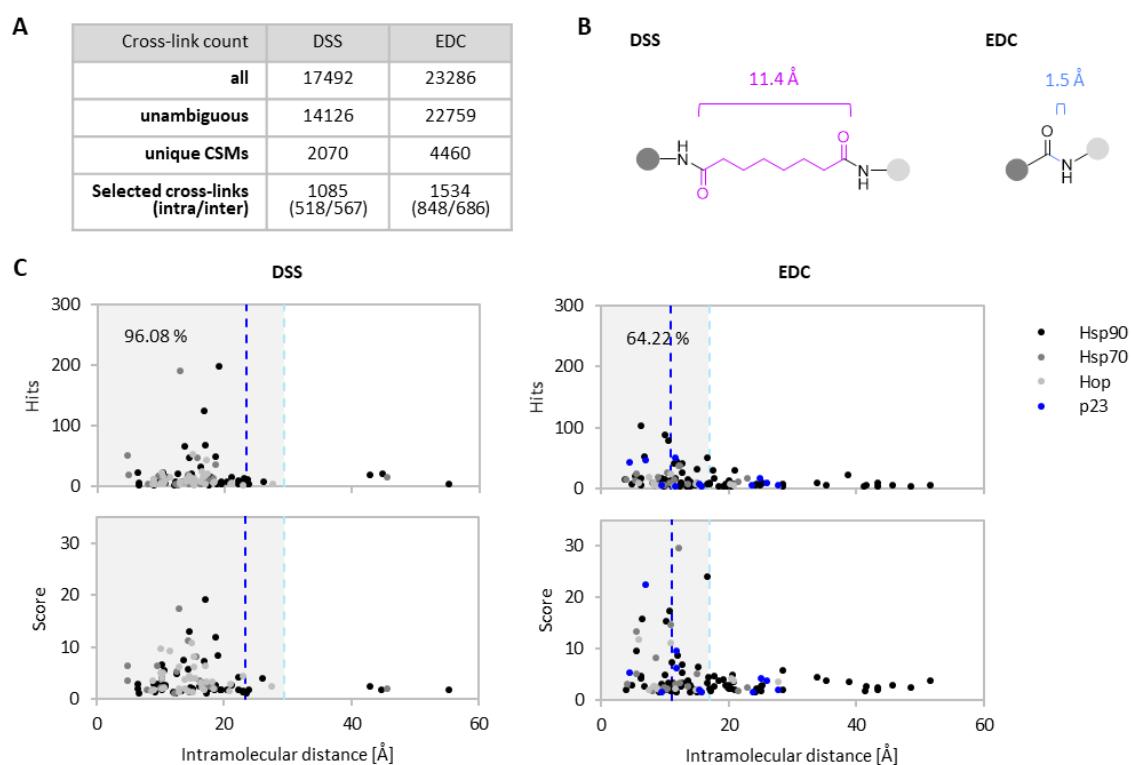


**Figure 43 Intramolecular cross-link analysis of the Hsp70:Hop:Hsp90:Tau:p23 complex using DSS and EDC.**

**A** Starting from 17492 identified DSS cross-links (*EDC*: 23286), 14126 could be unambiguously assigned (22759), whereby 2070 were unique (4460). Setting a threshold of as few as three hits and at least 5% of the maximum score, 1085 DSS cross-links were finally selected for structural analysis (*EDC*: 1534). **B** Length of the cross-linker arm from DSS and EDC (Thermo Scientific<sup>TM</sup>). **C** Distance measurements of intramolecular cross-links within Hsp70, Hop, Hsp90 and p23. 96.08 % and 64.22 % of the measured distances fell below the set threshold of 29.4 Å and 17 Å for DSS and EDC, respectively. The blue lines mark the thresholds without (dark) and with (light) additional 6 Å for the flexibility of the backbone.<sup>352</sup>

Based on the reliable intramolecular cross-link data, the intermolecular cross-links with DSS were examined in more detail (Figure 44). The connections between two proteins were analyzed and classified according to their confidence score (Figure 44B). This allowed the determination of regions that are in close proximity within the Hsp70/Hsp90 chaperone machinery. As expected

## Results

from the NMR experiments described above, the majority of Tau cross-links with Hsp70 and Hsp90 were located around the repeat region (see chapter 3.3). Although Tau contacts were found throughout the complete sequences of the chaperones, major cross-links were located in Hsp70's SBD close to the linker region connecting Hsp70's NBD and SBD, and in Hsp90's N- and C-terminal domain. Beyond, as part of the Hsp70/Hsp90 chaperone machinery, Tau's repeat region showed intense cross-linking with the two termini of Hop. Altogether this suggested that Tau is bound to the Hsp70/Hsp90 chaperone machinery in a way that all three components (Hsp70-SBD, Hop and Hsp90 termini) are associated with the substrate.

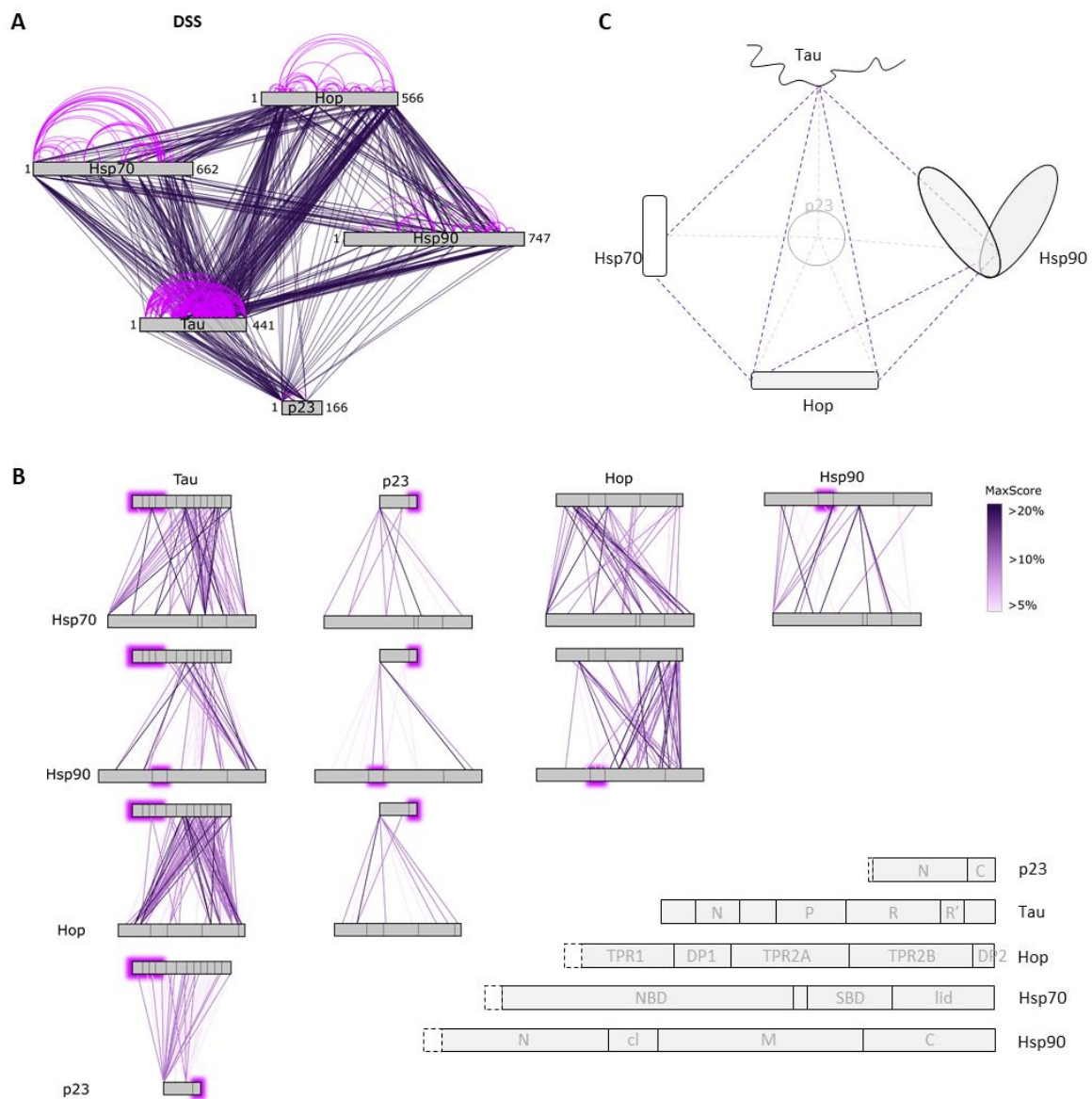


**Figure 44 Intermolecular cross-link analysis of the Hsp70:Hsp90:Tau:p23 complex cross-linked with DSS.**

**A** Network plot of the Hsp70:Hsp90:Tau:p23 complex including intra- (pink) and intermolecular cross-links (purple). **B** Intermolecular cross-link analysis between two proteins within the Hsp70/Hsp90 chaperone machinery: Tau complex. The contact lines are color coded based on their confidence score, whereby confidence correlates with darkness. Protein domains are indicated on the bottom right. Uncross-linked regions are highlighted with a blurred pink box. **C** Cartoon representation of the major intermolecular cross-links from (B) connecting Tau with Hsp70's SBD, Hsp90's C-terminus, both Hop termini and p23.

## Results

The analysis of the cross-links in between Hop and Hsp70/Hsp90 further revealed that Hop's TPR1 domain, which is located at its N-terminus, is in close proximity to Hsp70's SBD, whereas Hop's C-terminal domains TPR2B and DP2 were located next to Hsp90's middle and C-terminal domain. Both observations were in agreement with previous interaction studies of Hop with the chaperones (see chapter 3.1).<sup>207</sup> Consistent with the Hsp70:Hop:Hsp90 binding interface determined by NMR (see chapter 3.2), few direct cross-links between Hsp70 and Hsp90 indicated that, within the Hsp70/Hsp90 chaperone machinery, Hsp70-NBD and -SBD are close to Hsp90's N-terminal and middle domain, respectively. Although p23 cross-links were detected with all proteins, the majority of these cross-links were of low confidence, wherefore the localization of p23 within the DSS cross-linked Hsp70/Hsp90 chaperone machinery could not be specified with high accuracy. Most strikingly however, p23 co-localized with Tau on each protein signifying Tau as the major interaction site for p23 in the Hsp70:Hop:Hsp90:Tau:p23 complex. Beyond, in contrast to the Hsp90-NTD/MD:p23 interaction described in literature and reaffirmed by NMR (Figure 37)<sup>48,221</sup>, high confidence cross-links with Hsp90's CTD were detected (Figure 44), which in combination with the dimeric model of the  $(\text{Hsp70}_1:\text{Hop}_1:\text{Hsp90}_2:\text{Tau}_1:\text{p23}_2)_2$  complex supported the proposed antiparallel orientated dimer. Eventually, cross-links were solely found with the globular domain of p23, signifying its relationship to sHsps in binding non-native proteins *via* their  $\beta$ -sheet core to prevent protein aggregation.<sup>353</sup>

### 3.5.3 A structural model of the dimeric $(\text{Hsp70}_1:\text{Hop}_1:\text{Hsp90}_2:\text{Tau}_1:\text{p23}_1)_2$ complex

The combination of molecular weight determination by SEC (see chapter 3.5.1), the cross-link analysis by LC-MS/MS (see chapter 3.5.2) and preceding data describing the Hsp90:Hop and Hsp70:Hop:Hsp90 interaction (see chapter 3.1 and 3.2) allowed to follow a structural model of the Hsp70/Hsp90 chaperone machinery in association with Tau and p23 (Figure 45).

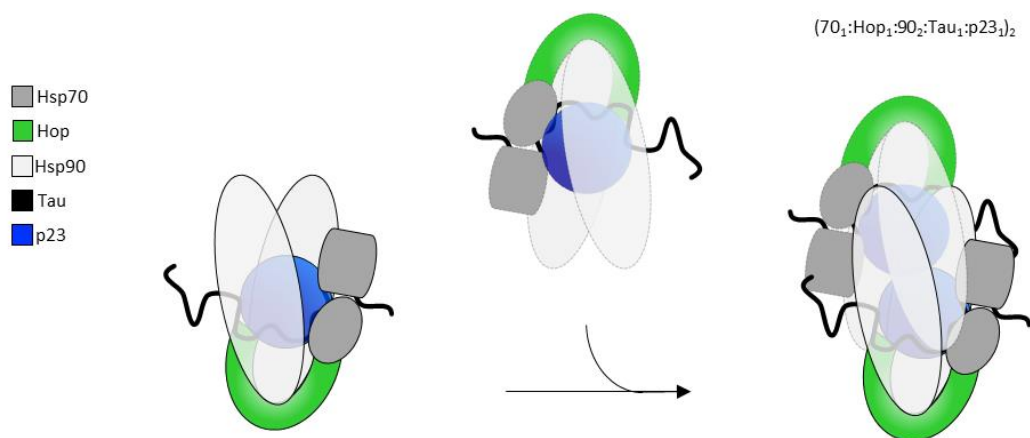


**Figure 45 Model of the dimeric  $(\text{Hsp70}_1:\text{Hop}_1:\text{Hsp90}_2:\text{Tau}_1:\text{p23}_1)_2$  complex.**

Cartoon representation of the Hsp70/Hsp90 chaperone machinery interacting with Tau and p23 taking into account the positioning of p23 determined *via* Tau. Protein arrangement is based on LC-MS/MS cross-link analysis as well as molecular weight determination by SEC (Figure 41, Figure 44).



## Results

Hop would be located at the C-terminus of Hsp90 embracing the chaperone from bottom up. Tau could be placed top down in between the two Hsp90 monomer arms, thereby accessing simultaneously both termini of Hop. The binding of Tau triggers the dimerization of the Hsp70/Hsp90 chaperone machinery along with the dissociation of one Hsp70 molecule. The remaining Hsp70 would be attached at one side of Hsp90 being associated with Hsp90's NTD/middle domain, Hop's TPR1 domain and Tau's central region. The localization of the co-chaperone p23 could be directed by Tau and the antiparallel orientation of the (Hsp70<sub>1</sub>:Hop<sub>1</sub>:Hsp90<sub>2</sub>:Tau<sub>1</sub>:p23<sub>1</sub>)<sub>2</sub> protein complex (Figure 45).

### 3.5.4 Hsp90's charged linker region remains unbound within the Hsp70/Hsp90 chaperone machinery

NMR spectroscopy is a powerful technique to follow protein dynamics in solution, but it reaches its limits with increasing molecular weight of the protein of interest (see chapter 2.6.2). Consequently, strong line broadening was observed for Hsp90 as part of the at least 307 kDa large Hsp70:Hop:Hsp90 complex compared to the unbound 171 kDa Hsp90 dimer (see chapter 3.2, Figure 27). Methyl-TROSY spectra were also recorded of <sup>13</sup>C-<sup>1</sup>H Ile-methyl group labeled Hsp90 as part of the Hsp70:Hop:Hsp90:Tau and Hsp70:Hop:Hsp90:Tau:p23 complexes (Figure 46A). The addition of Tau and p23 further contributed to the reduction of Hsp90 peak intensities, which in turn signified their association generating higher molecular weight complexes.

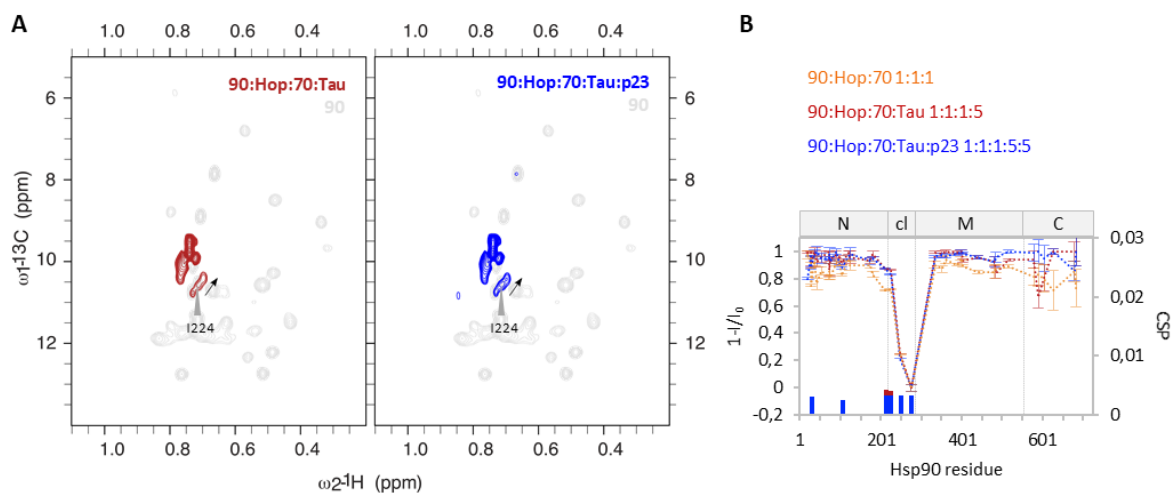


**Figure 46 TROSY NMR of the Hsp70/Hsp90 chaperone machinery: Tau and machinery: Tau:p23 complexes.**

**A** 2D <sup>13</sup>C-<sup>1</sup>H methyl-TROSY spectra of Hsp90 in presence of the Hsp70:Hop:Hsp90:Tau and Hsp70:Hop:Hsp90:Tau:p23 complexes – (molar ratios 1:1:1:5(:5), 50  $\mu$ M Hsp90). The black arrow marks the signal splitting of I224. The reference of Hsp90 alone is shown in each spectrum in light grey for comparison. **B** Residue-specific peak intensities (1-I/I<sub>0</sub>; lines) and chemical shift perturbations (CSP; bars) of Hsp90's isoleucine  $\delta$ -methyl groups observed in (A and Figure 27A); same color coding. I<sub>0</sub> is the signal intensity of the Hsp90 reference. Error bars were calculated based on NMR signal-to-noise ratio. Hsp90 domains are depicted on top and represented with dotted lines (N – N-terminal domain, cl – charged linker, M – middle domain, C – C-terminal domain).

Most strikingly, in all cases only little line broadening and few chemical shift changes were observed for the charged linker (cl) region of Hsp90 (Figure 46B). For residue I224, which is located in the cl region close to the NTD, peak splitting was detected upon the addition of Tau indicating a conformational change or binding event within this region. Beyond that, the NMR analysis demonstrated that Hsp90's charged linker remains unbound and highly mobile within the Hsp70/Hsp90 chaperone machinery: Tau complex.

### 3.6 Balance between the assembly and disassembly of the Hsp70/Hsp90 chaperone machinery

A balanced protein homeostasis precludes a dynamic equilibrium between protein production, retention and degradation (see chapter 1.1). Proteins can be guided towards proteasomal degradation *via* a direct interaction of Hsp70 and Hsp90 with the E3-ubiquitin ligase CHIP (carboxyl terminus of Hsc70-interacting protein).<sup>295,354</sup> CHIP is a functional counterpart of Hop competing for the binding to Hsp70 and Hsp90 *via* the TPR domain.<sup>207,355</sup> In this line, it was further investigated whether the interplay of Hop and CHIP can ensure a continuous cycle of machinery buildup and breakdown when Tau and/or p23 are present.

Native page demonstrated the disintegration of the Hsp70:Hop:Hsp90: Tau complex already at sub-stoichiometric concentrations of CHIP (Figure 47A, D). Consistent with the competition of CHIP and Hop for binding to Hsp70/Hsp90, the release of Hop was observed with increasing CHIP concentrations (Figure 47E). Comparison with the native page behavior of individual Hsp70:CHIP and Hsp90:CHIP complexes in either the presence or absence of Tau further suggested that CHIP-mediated disintegration of the Hsp70:Hop:Hsp90: Tau complex leads to Hsp70:CHIP, Hsp70:CHIP: Tau, Hsp90:CHIP and Hsp90:CHIP: Tau subcomplexes (Figure 47B). The breakdown of the Tau: machinery complex was delayed in the presence of p23 (Figure 47C). The retarding effect of p23 against CHIP-mediated disintegration is in agreement with the stabilizing function of p23 for the Hsp70:Hop:Hsp90: Tau interaction (Figure 47B). Thus, by interacting with either Hop or CHIP, Hsp70 and Hsp90 could maintain a dynamic equilibrium between the assembly and disassembly of the Hsp70/Hsp90 chaperone machinery (Figure 47F).

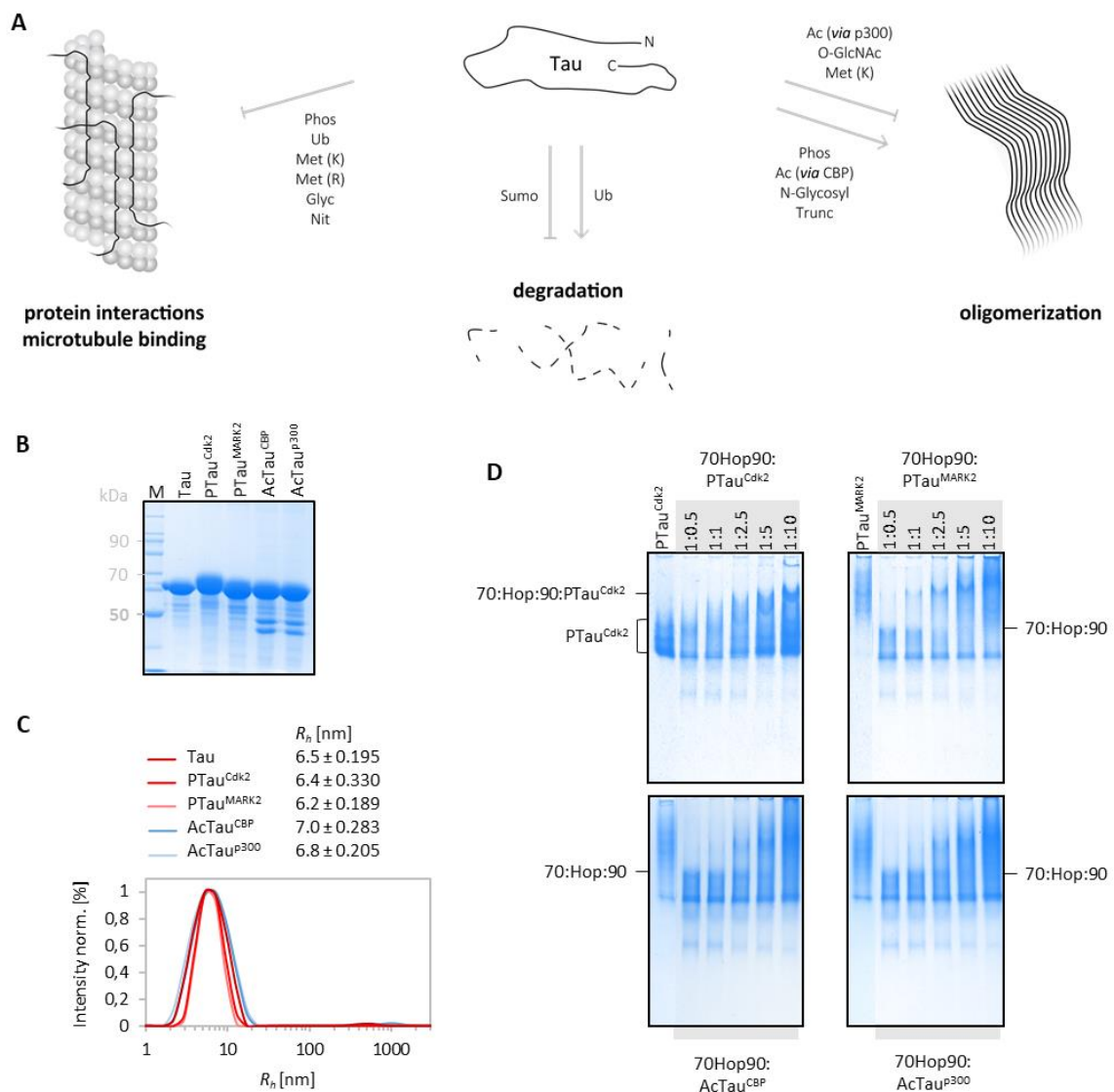




### 3.7 The Hsp70/Hsp90 chaperone machinery likewise recognizes pathologic Tau

#### 3.7.1 Post-translationally modified Tau as client of the Hsp70/Hsp90 chaperone machinery

*In vivo*, Tau has been found with various post-translational modifications that regulate Tau function and dysfunction (Figure 48A).<sup>254,289</sup> As both phosphorylation and acetylation are linked to pathologic Tau aggregation and neurotoxicity<sup>297,299,356</sup>, the role of the Hsp70/Hsp90 chaperone machinery for pathologically modified Tau was further examined.



## Results

Tau was phosphorylated or acetylated *in vitro* by two different kinases (Cdk2 and MARK2) and acetyltransferases (CBP and p300) generating distinct modification patterns on Tau.<sup>297,298,357,358</sup> In SDS-page only the phosphorylated Tau using Cdk2 (PTau<sup>Cdk2</sup>) showed a shift to higher molecular weight signifying the addition of phospho-groups (Figure 48B). Instead native page analysis revealed that Tau was heterogeneously modified in all reactions (Figure 48D). Acetylation or phosphorylation did not promote Tau oligomerization or aggregation *in vitro* as no large particles corresponding to higher oligomers or aggregates were detected by DLS (Figure 48C). In agreement with previous studies on Tau, the protein remained monomeric with hydrodynamic radii in the range of 6.2-7.0 nm.<sup>257,359</sup>

Native page analysis demonstrated that the Hsp70/Hsp90 chaperone machinery likewise recognizes the post-translationally modified Tau. The amount of the Hsp70:Hsp90 complex decreased with increasing substrate concentrations in all cases indicative for the formation of Hsp70:Hsp90:PTau/AcTau complexes (Figure 48D). The Tau heterogeneity however complicated the analysis of complex formation by native page due to band smearing. Only the Hsp70:Hsp90:PTau<sup>Cdk2</sup> complex appeared separately on the gel and thus was selected for further analysis.

### 3.7.2 Pathologic Tau associates with the Hsp70/Hsp90 chaperone machinery similar to normal Tau, but the interaction with Hsp90 alone is lost

In collaboration with the lab of Prof. H. Urlaub, mass spectrometry was used to detect the sites of phosphorylation that were introduced *in vitro* by Cdk2<sup>‡</sup> (Table 16). As expected, Cdk2 generated a phosphorylation pattern in Tau, which accumulated in the proline-rich region and the C-terminus of Tau – similar to what is observed in Alzheimer's disease (Figure 49).<sup>293,360,361</sup> In particular, the phosphorylation epitopes recognized by the antibodies AT8, AT180 and PHF1, which are used to detect phosphorylated Tau species in Alzheimer's disease<sup>362</sup>, were modified *in vitro* signifying PTau<sup>Cdk2</sup> as pathologically modified Tau.

---

<sup>‡</sup> MS experiments and P-site analysis was gratefully performed by Dr. P. Kuan-Ting (MPI-BPC, in the group of Prof. Dr. Henning Urlaub, Department of Bioanalytical Mass Spectrometry).

## Results

**Table 16** *In vitro* Tau phosphorylation sites using Cdk2 kinase detected by mass spectrometry.

#Phosphorylation site	Intensity	Localization probability
T175	27.63	1
T181	25.30	0.999
S199	26.78	0.922
S202	22.27	0.724
T205	30.37	0.999
T205	26.78	0.999
T217	23.45	0.936
T220	23.74	0.724
T231	24.14	0.999
S235	24.14	0.969
T245	26.47	1
S262	27.20	0.971
T263	27.82	0.991
S396	24.58	1
S400	23.36	0.815
T403	25.05	0.581
S404	24.13	0.911
S422	24.22	0.999
S435	21.79	0.839

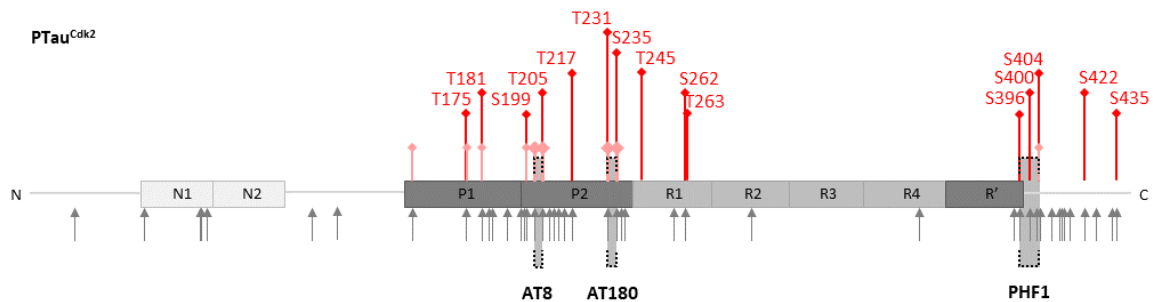


**Figure 49** Phosphorylation pattern of Cdk2 kinase on Tau.

Grey arrows depict main phosphorylation sites on Tau extracted from brains of patients with Alzheimer's disease.<sup>293</sup> Tau phosphorylation sites of Cdk2 reported in literature are shown in light red.<sup>360</sup> Red bars show phosphorylation sites of Cdk2 detected by mass spectrometry listed in Table 16 with a minimum localization probability  $\geq 0.75$ . Experimentally detected phospho-Tau antibody epitopes (AT8 (S202 and T205), AT180 (T231 and S235) and PHF1 (S396 and S404)) from paired helical filaments are marked in black brackets.<sup>362</sup>

The  $\text{PTau}^{\text{Cdk2}}$  interaction with the Hsp70/Hsp90 chaperone machinery was further analyzed in absence and presence of p23 (Figure 50A, B). Quantitative analysis showed that comparable amounts of Hsp70:Hsp90:PTau<sup>Cdk2</sup> complex were formed as with unmodified Tau, and p23 likewise associated generating an Hsp70:Hsp90:PTau<sup>Cdk2</sup>:p23 complex (Figure 50C, D). In control experiments PTau<sup>Cdk2</sup> showed less interaction with Hsp90 alone, whereas the binding to Hsp70 was independent on the phosphorylation of Tau (Figure 50E, F). The decreased interaction of PTau for Hsp90 is in agreement with previous NMR studies.<sup>121</sup> The finding that PTau<sup>Cdk2</sup>

## Results

efficiently binds to the Hsp70/Hsp90 chaperone machinery, but not to Hsp90 alone, suggested that Tau chaperoning by Hsp90 including CHIP-mediated degradation is inaccessible for pathologically modified Tau.

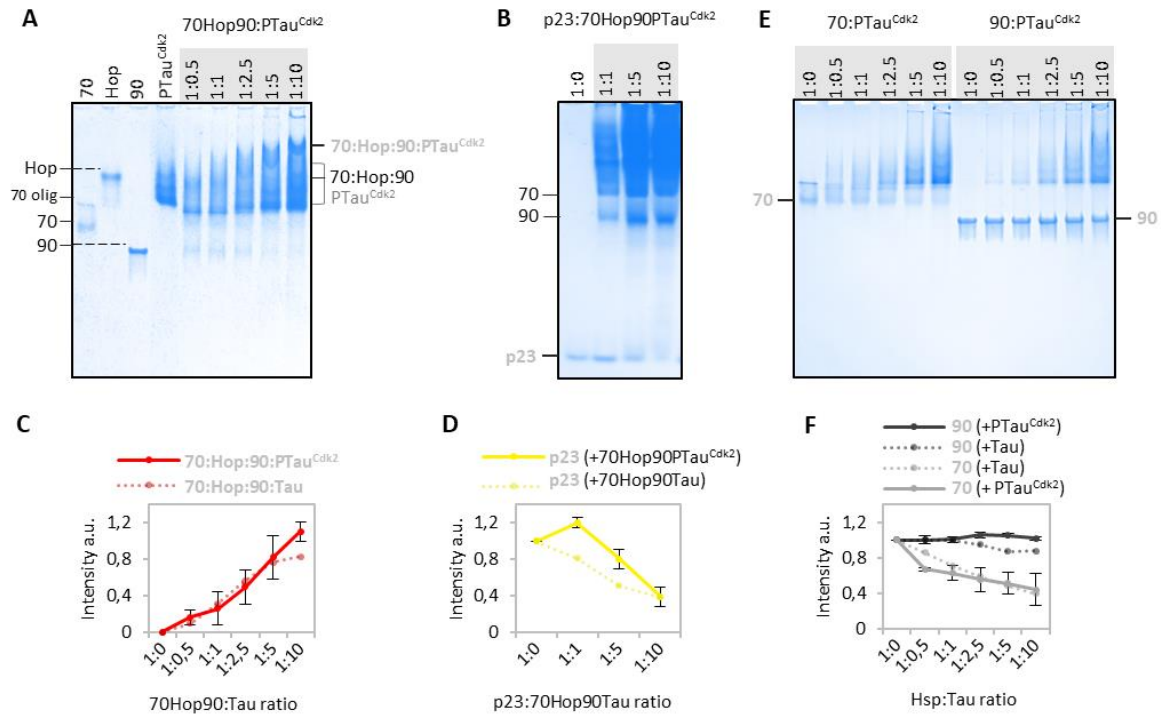


**Figure 50** *In vitro* reconstitution of the interaction of the Hsp70/Hsp90 chaperone machinery with pathologic PTau<sup>Cdk2</sup>. **A, B** Native page analysis of the Hsp70:Hsp90:PTau<sup>Cdk2</sup> (A) and Hsp70:Hsp90:PTau<sup>Cdk2</sup>:p23 interaction (B). **C, D** Quantitative analysis of the band intensities of the Hsp70:Hsp90:PTau<sup>Cdk2</sup> complex (in A) and unbound p23 (in B). **E** Native page analysis of PTau<sup>Cdk2</sup> interacting with the chaperones Hsp70 and Hsp90. **F** Band intensities of Hsp70 and Hsp90 with increasing concentrations of PTau<sup>Cdk2</sup> (in E). For comparison, the data of the respective interactions with unmodified Tau are shown in dashed lines.

## 4 Discussion

---

Hsp70 and Hsp90 represent two central hubs that control a vital balance between protein retention and degradation. In addition to their discrete functions, both chaperones can band together synergistically acting as part of the Hsp70/Hsp90 chaperone machinery. Being part of the intriguing complex network of chaperones and co-chaperones, the Hsp70/Hsp90 chaperone machinery is suggested to retain proteins in the cell.<sup>57</sup> With regard to numerous lethal diseases including neurodegenerative disorders, where proteins accumulate beyond harmful concentrations, the Hsp70/Hsp90 chaperone machinery thus became the central focus of proteostasis research.<sup>2-4</sup>

### 4.1 The assembly of the Hsp70:Hop:Hsp90 complex

The core of the Hsp70/Hsp90 chaperone machinery is formed by the Hsp70:Hop:Hsp90 complex. A broad spectrum of affinity measurements has been already used to identify which chaperone is bound first by Hop.<sup>137,214,216,363-365</sup> Intriguingly, affinity measurements using the C-terminal EEVD peptides of Hsp70 and Hsp90 (further termed Hsp70-C/Hsp90-C) revealed a higher affinity of Hop for Hsp70-C ( $K_D = 3.47 \pm 0.83 \mu\text{M}$ ) than for Hsp90-C ( $K_D = 6.43 \pm 0.17 \mu\text{M}$ ), which however could be ascribed to twice as many binding sites available for Hsp70-C (TPR1 and TPR2B) compared to Hsp90-C (TPR2A) (Table 17, Figure 51).<sup>207</sup> Considering the average dissociation constants from measurements using full-length proteins, Hop in turn tends to bear a higher affinity for Hsp90 ( $K_D = 0.41 \mu\text{M}$ ) than for Hsp70 ( $K_D = 0.87 \mu\text{M}$ ) (Table 17). It was further shown that the affinity of Hop for Hsp70 is increased in the presence of Hsp90 ( $K_D = 0.25 \mu\text{M}$ ) indicating a distinct Hop conformation within the Hsp90:Hop complex that promotes the binding to Hsp70.<sup>137</sup> In contrast, the interaction of Hop with Hsp90 was not affected by Hsp70. Hence, Hsp70:Hop and Hsp90:Hop complexes may indeed form to an equal extent, but once an Hsp90:Hop complex is formed, Hsp70 readily associates generating the ternary Hsp70:Hop:Hsp90 complex.

**Table 17 Reported affinity values of Hop for Hsp70 and Hsp90.**

Hsp70 - 70, Hsp90 - 90, C-terminal peptides - 70C and 90C). Affinity values were taken from literature determined by (1) antibody precipitation with subsequent gel quantification<sup>137</sup>, (2) ITC<sup>216</sup>, (3) SPR<sup>214</sup>, (4) ITC<sup>364</sup>, (5) fluorescence polarization assay<sup>363</sup> and (6) fluorescence polarization assay<sup>365</sup>.

	$K_D$ [ $\mu\text{M}$ ]				$K_D$ (average) [ $\mu\text{M}$ ]
Hop:70	1.3 <sup>(1)</sup>		$0.43 \pm 0.15$ <sup>(3)</sup>		<b><math>0.87 \pm 0.44</math></b>
Hop:70C	$2.64 \pm 0.13$ <sup>(5)</sup>	4.3 <sup>(6)</sup>			<b><math>3.47 \pm 0.83</math></b>
90Hop:70	0.25 <sup>(1)</sup>				
Hop:90	0.09 <sup>(1)</sup>	$0.69 \pm 0.04$ <sup>(2)</sup>	$0.29 \pm 0.02$ <sup>(3)</sup>	$0.58 \pm 0.07$ <sup>(4)</sup>	<b><math>0.41 \pm 0.24</math></b>
Hop:90C	$6.26 \pm 0.87$ <sup>(5)</sup>	6.6 <sup>(6)</sup>			<b><math>6.43 \pm 0.17</math></b>

## Discussion



**Figure 51 High affinity interaction sites on Hop for the C-terminal peptides of Hsp70 and Hsp90.**

The TPR1/TPR2B and TPR2A domains of Hop represent the high affinity sites for the C-terminal peptides Hsp70-C and Hsp90-C, respectively.<sup>207</sup> Domain organization of Hop is color coded as in Figure 7.

### 4.1.1 The Hsp90:Hop interaction

In a first step to decipher the construction of the Hsp70/Hsp90 chaperone machinery, the Hsp90:Hop interaction was characterized in greater detail. The obtained data (Figure 19) indicated that Hsp90 and Hop interact in a 2:1 molar ratio signifying one Hop molecule binding an Hsp90 dimer. Though this was in contrast to previous findings where Hop has been described as dimer, and also suggested to bind as a dimer to Hsp90<sup>137,216,366</sup>, the observed Hsp90<sub>2</sub>:Hop<sub>1</sub> complex was in agreement with results depicting Hop as a monomer – both as unbound protein and as part of the Hsp90:Hop complex.<sup>117,215,344,367</sup>

Hop is known to interact with Hsp90 in the early stages of the hydrolysis cycle<sup>206,344,345</sup>, i.e. with the open conformation. In line with this, Hop was found to preferably bind to the open state of Hsp90 (Figure 18A, B). Consistent with the inhibition of Hsp90's ATPase activity due to impeded Hsp90 closure<sup>206</sup>, Hop did not promote an open-close change of Hsp90 (Figure 18C). The combined data rather suggested that Hop induces a symmetric conformational rearrangement stabilizing Hsp90 in a V-shaped conformation (Figure 22). In this model Hop is arranged with respect to Hsp90 in a way that the high affinity TPR2A domain of Hop interacts with the CTD of Hsp90.<sup>207</sup> Thereby, Hop's TPR2B domain contacts Hsp90's CTD-MD junction, whereas Hop's TPR1 domain remains unbound, hence accessible for subsequent Hsp70 binding (Figure 52). Notably, the Hsp90:Hop association was confined to the TPR domains of Hop. An interaction with Hop's DP domains was not detected so far.<sup>207</sup>

With regard to the orientation of Hop, the domain architecture depicted in Figure 52 is inconsistent with a previous cryo-EM model where Hop's TPR1 domain was placed in between the two Hsp90 arms.<sup>215</sup> However, the ten-fold reduction in binding affinity upon TPR2B removal suggested an additional interaction *via* TPR2B that stabilizes the Hsp90:Hop complex (Figure 24D). With data of increasing resolution becoming available, the same lab recently revoked their findings and localized the TPR2B domain close to the Hsp90 dimer interface.<sup>47</sup> Site-specific NMR interaction studies between the Hsp90-MD and a TPR2A-TPR2B construct of Hop further supported a direct Hsp90-MD:Hop-TPR2B interaction.<sup>207</sup>

## Discussion

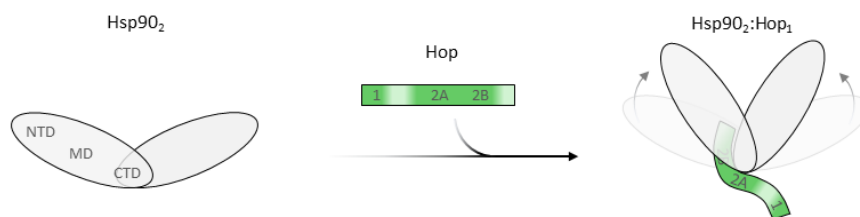


**Figure 52 Hop stabilizes Hsp90 in a V-shaped conformation.**

The TPR2A-TPR2B domains of Hop (denoted as 2A and 2B) interact with Hsp90's CTD and CTD-MD junction, respectively.

Although the proposed V-shaped structure differed from a previous Hsp90:Hop model, where Hsp90 was ascertained to be in its semi-closed, ADP-bound state<sup>117</sup>, a V-shaped Hsp90:Hop structure has also been proposed by low resolution cryo-EM.<sup>215</sup> In this model the N-terminal domains of Hsp90 were rotated inward by 90° representing the ATP-bound state. Similarly, a conformational change in Hsp90's NTD-MD interface was observed by NMR upon the addition of Hop, independent on the presence of a nucleotide (Figure 21). This suggested that the binding to the Hsp90-CTD is sufficient to transform Hsp90's NTDs into their nucleotide-bound state. Indeed, a cross-talk between the Hsp90 domains (NTD and CTD) has been proposed previously.<sup>368</sup> Consistent with these findings, the  $k_{on}$  and  $k_{off}$  rates of ATP binding to Hsp90 were shown to be increased in the presence of Hop while the overall affinity remained unchanged.<sup>206,216</sup>

As it was shown that only one Hop molecule interacts with the Hsp90 dimer (Figure 19), the symmetric change induced by full-length Hop (Figure 21) further implied an allosteric communication not only within the different Hsp90 domains, but also in between the two Hsp90 monomers. Consistent with a reduced conformational change observed by ITC in presence of Hop112a, which lacked the C-terminal TPR2B-DP2 motif (see chapter 3.1.4), only one arm of the Hsp90 dimer was arranged to the V-shaped state (Figure 25). Thus, the additional interaction *via* TPR2B appeared to be essential to drive the allosteric communication between the two Hsp90 arms. Taken together, the TPR2A:CTD interaction might be sufficient for the inter-domain cross-talk necessary for the rotation of the NTD, whereas the TPR2B:CTD-MD interaction may be required for the inter-monomer communication accounting for the V-shaped Hsp90:Hop complex.

In context with Hsp90 ATPase measurements it has been shown that only the combined TPR2A-2B Hop construct can inhibit the ATPase activity of Hsp90 equal to full-length Hop suggesting that the rigid linker connecting TPR2A-2B is crucial for the function of Hop.<sup>207,214</sup> In combination with the acquired data showing that an additional interaction *via* Hop's TPR2B domain accounts for the stable Hsp90:Hop association (Figure 21 and Figure 25), the rigid linker connecting TPR2A-2B might be essential for proper TPR2B orientation. In addition, despite the preference towards the open conformation of Hsp90 (Figure 18), the observed interaction between Hop and the closed state of Hsp90 might further indicate that higher order Hsp90:substrate or



Hsp90:substrate:co-chaperone complexes exist, in which Hsp90 is closed and Hop still bound. As there was no evidence that Hop can open up Hsp90 (Figure 18), the co-chaperone as part of the higher-order complexes might not play an active role but may rather hold a stabilizing function.

#### 4.1.2 The Hsp70:Hop:Hsp90 complex

On the basis of the preassembled, V-shaped Hsp90<sub>2</sub>:Hop<sub>1</sub> complex, the interaction with Hsp70 was further investigated. Major difficulties occurred due to the high tendency of Hsp70 to form oligomers (see chapter 3.2.1). Hsp70 oligomerization has been reported *in vitro* and *in vivo* and is suggested to be related to chaperone function.<sup>347,348</sup> Along this line, the results of this work indicated that only Hsp70 monomers associate with the Hsp90<sub>2</sub>:Hop<sub>1</sub> complex (Figure 26), whereby Hsp70 oligomers might represent an inactive pool that could be accessed as needed. This observation coincides with earlier findings likewise describing the integration of monomeric Hsp70 into the Hsp70:Hop:Hsp90 complex.<sup>117,130,215</sup>

As concluded from affinity measurements (see chapter 4.1), Hop might adopt a distinct conformation when bound to Hsp90 depicting a high affinity interaction site for Hsp70 once the Hsp90:Hop complex is formed.<sup>137</sup> Indeed, the possibility that Hsp binding influences the structure of Hop what in turn affects the binding of the other Hsp has been previously proposed.<sup>369</sup> It has been shown that the interaction between Hop and the C-terminal peptide of Hsp70 involves the TPR1 and TPR2B domain of Hop, both able to individually interact with one Hsp70 molecule (Figure 53).<sup>137,207</sup> As described before (see chapter 4.1.1), the engagement of Hop's TPR2B domain however is pivotal for a stable Hsp90:Hop complex. Eventually, Hsp90 is likely to win the battle for TPR2B binding due to its higher affinity for Hop (Table 17). As part of the Hsp90<sub>2</sub>:Hop<sub>1</sub> complex, the TPR1 domain is thus the only available binding site for Hsp70 on Hop (Figure 53). In combination with the increased affinity of Hsp70 for Hop in presence of Hsp90 shown previously<sup>137</sup>, the binding of Hsp70 to Hsp90:Hop could be based on positive cooperativity, where the occupation of one binding site (TPR2B) makes the second one (TPR1) more attractive.

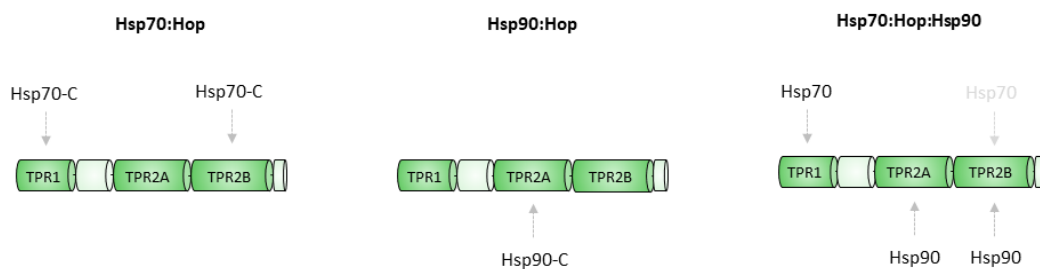


**Figure 53 Hsp70 and Hsp90 interaction with the TPR domains of Hop.**

With regard to the full-length proteins, the Hsp90:Hop interaction involves Hop's TPR2A-TPR2B domains leaving the TPR1 as the only remaining binding site for Hsp70.

## Discussion

Intriguingly, the addition of Hop and Hsp70 symmetrically affected the Hsp90 dimer. An additional binding site involving the NTD-MD interface of both Hsp90 arms revealed a direct interaction between Hsp70 and Hsp90 in presence of Hop (Figure 28). It has been shown that Hsp70 interacts *via* its C-terminal SBD with the TPR domains of Hop.<sup>192</sup> Thereby the N-terminally located Hsp70 NBD could readily associate with the NTD-MD region of Hsp90. The respective binding pockets were located at the outside of each Hsp90 arm. Due to spatial proportions, a single Hsp70 molecule is unlikely to be able to bind both outer sites of Hsp90 when simultaneously bound to Hop. Hence, a second Hsp70 monomer presumably occupies the opposite binding site on Hsp90. In this model, both Hsp70's would frame the Hsp90 dimer from the exterior (Figure 54). As it was proven that there is only one binding site for Hsp70 on Hop as part of the Hsp90<sub>2</sub>:Hop<sub>1</sub> complex (Figure 53), the second Hsp70 molecule would bind independent on Hop implicating a higher affinity conformation of Hsp90 as part of the Hsp90<sub>2</sub>:Hop<sub>1</sub> or Hsp70<sub>1</sub>:Hop<sub>1</sub>:Hsp90<sub>2</sub> complex. Yet, there is no experimental evidence that the binding of one Hsp70 to Hsp90:Hop triggers the binding of a second one. Hence, the Hop induced V-shape of Hsp90 (Figure 22) is likely to depict a high-affinity conformation for the NBDs of two Hsp70 monomers forming an Hsp70<sub>2</sub>:Hop<sub>1</sub>:Hsp90<sub>2</sub> complex. The stoichiometry of the Hsp70/Hsp90 chaperone machinery was further supported by molecular weight determination which is best in accordance with a 2:1:2 molar ratio for Hsp70:Hop:Hsp90 (Figure 41). Taken together, the results of this work support a model, where in presence of Hop one Hsp70 molecule is bound per NTD-MD region of Hsp90.

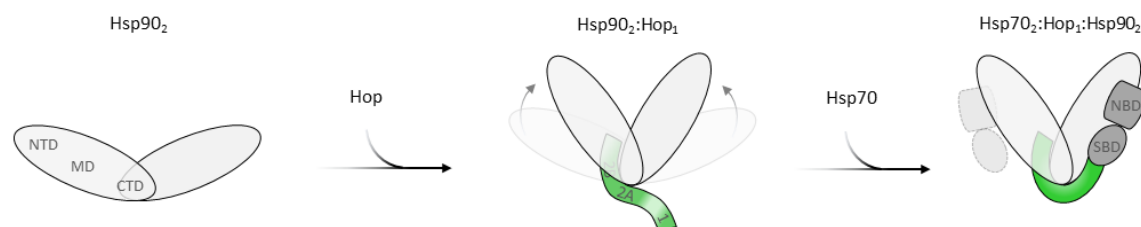


**Figure 54 The Hsp70:Hop:Hsp90 complex comprises two Hsp70 molecules.**

One Hsp70 monomer interacts *via* its C-terminal SBD with the TPR1 domain of Hop. The Hsp90<sub>2</sub>:Hop<sub>1</sub> complex with Hsp90's NTDs rotated inward (see chapter 4.1.1) presumably depicts a high affinity conformation for Hsp70-NBDs evoking the binding of the second, Hop-independently bound Hsp70.

Indeed, at the outset of this work there has been conflicting evidence regarding the amount of Hsp70 molecules bound to the Hsp90:Hop complex as well as their spatial orientation. Cryo-EM data reported low resolution structures of an Hsp70<sub>1</sub>:Hop<sub>1</sub>:Hsp90<sub>2</sub> complex, where a single Hsp70 was placed in between the Hsp90 dimer.<sup>117,130,215</sup> In contrast, data from mass spectrometry revealed an antiparallel Hsp70 dimer maintained in the Hsp70/Hsp90 chaperone machinery.<sup>235</sup> Noteworthy, in this model, one Hsp70 molecule interacts *via* Hop and Hsp90, similarly to the observations in this work, though directing the second Hsp70 to the same side due to dimerization. Most recently however, a 3.8 Å resolution structure obtained by cryo-EM demonstrated as suggested above two Hsp70 monomers each associated with the outer side of Hsp90, whereby only one Hsp70 was

bound *via* Hop.<sup>47</sup> Indeed, additional changes within the CTD of Hsp90 were observed in presence of Hop and Hsp70 compared to Hop only (Figure 27). In combination, these could be ascertained to the direct interaction of Hop with one Hsp70 molecule leading to small conformational changes within the Hsp90:Hop binding interface, so that Hsp70 can be simultaneously bound to the TPR1 domain of Hop *via* its SBD and the NTD-MD region of Hsp90 *via* the NBD (Figure 54).

Noteworthy, a direct though rather unspecific interaction between Hsp70 and Hsp90 could be observed by NMR in the absence of Hop (Figure 27). With regard to the bacterial and yeast homologues of Hsp70 and Hsp90<sup>93,133,134,370,371</sup>, which were shown to associate *in vitro* and *in vivo* independent of Hop, the direct interaction between the human chaperones was not entirely unexpected. The observed Hsp70 binding site in Hsp90's NTD-MD region in the presence of Hop (Figure 28) converged with the one predicted for the bacterial as well as yeast proteins in the absence of Hop<sup>134,370-373</sup> indicating a conserved Hsp70:Hsp90 interaction site. However, reported affinity values suggest a rather weak Hsp70:Hsp90 interaction even for bacteria and yeast ( $K_D(E. coli) = 13.4 \pm 3.3 \mu M^{370}$ ,  $K_D(S. cerevisiae) = 13.3 \pm 4.8 \mu M^{371}$ ). Hence, eukaryotic Hop, which has more than ten-times the affinity for both chaperones (Table 17), may compensate for the weak interaction indicating a distinct synergistic function of Hsp70 and Hsp90 within the Hsp70/Hsp90 chaperone machinery.

## 4.2 The Hsp70/Hsp90 chaperone machinery as a protective shell

Consistent with previous findings revealing a direct interaction between the intrinsically disordered protein Tau and the individual chaperones Hsp70 and Hsp90<sup>84,121,242,374</sup>, the results of this work demonstrated that Tau likewise acts as a substrate of the Hsp70/Hsp90 chaperone machinery. With regard to affinity measurements, it is suggested that Tau interacts with the Hsp70:Hop:Hsp90 complex more strongly when compared to Hsp70 or Hsp90 alone (Figure 31). Although Hsp70 contains a defined substrate-binding domain (SBD), yet there are no structural data demonstrating an Hsp70-SBD: Tau interaction. However, as the interaction with the SBD and the TPR1 domain of Hop is sustained by the C-terminal EEVD motif<sup>207</sup>, simultaneous substrate binding could be allocated to the SBD even within the Hsp70:Hop:Hsp90 complex. In addition, earlier studies revealed the Tau binding to a region within the NTD and MD of Hsp90 facing the dimer interface<sup>84</sup>, a region that is likewise accessible in the Hsp70:Hop:Hsp90 complex (Figure 28). Hence, the increased affinity of Tau for the Hsp70/Hsp90 chaperone machinery might be lead back to twice as much available interaction sites (Hsp70 and Hsp90), in turn suggesting that Tau is concurrently associated with both Hsp70 and Hsp90 within the Hsp70:Hop:Hsp90: Tau complex.

According to the determined molecular weight, each Hsp70/Hsp90 chaperone machinery monomer was attached to a single Tau molecule (Figure 41). The combination of NMR and

## Discussion

cross-link analysis (Figure 23 and Figure 44) was best in agreement with Tau placed central in between the Hsp90 arms stretched out from one side to the other, thereby contacting simultaneously the proposed binding site in Hsp90's NTD and MD<sup>84</sup>, both ends of Hop (TPR1 and TPR2B-DP2), as well as the SBD of Hsp70 (Figure 55). A dimeric assembly may allow additional contacts with the opposite Tau, giving rise to additional cross-links found in between the substrate and other regions of the Hsp70/Hsp90 chaperone machinery, which however were of lower confidence (Figure 44).

The combined data showed that a broad sequence of Tau including the repeat domains represents the major interaction site with each component of the Hsp70/Hsp90 chaperone machinery (Figure 39). Intriguingly, the same regions are involved in microtubule binding (see chapter 1.6.1).<sup>254</sup> The phenomenon of chaperones to bind sites in substrates that are in near proximity or involved in the ligand binding site has been previously described.<sup>375</sup> As this was suggested to protect labile regions against harmful interactions<sup>375</sup>, the dimeric Hsp70/Hsp90 chaperone machinery may similarly enclose the aggregation-prone regions of Tau.<sup>306,307</sup> In contrast, the N-terminal domains, which were not found in the core of Tau aggregates remained almost completely unbound (Figure 39), i.e. not in need of protection.

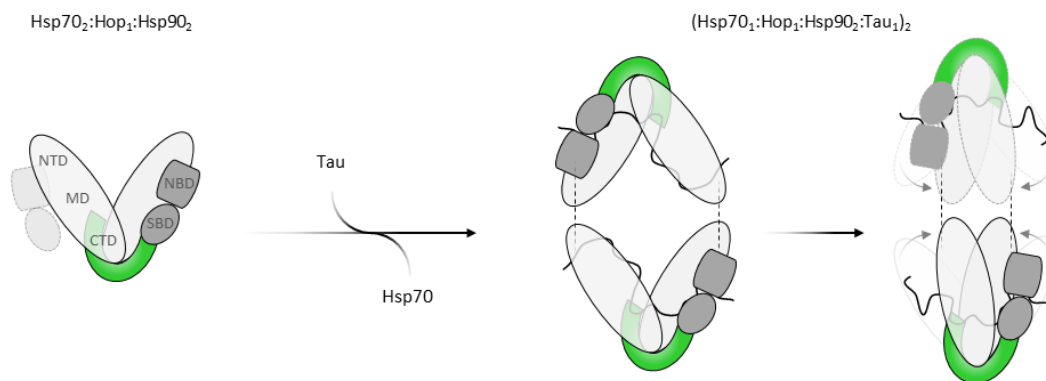


**Figure 55 Tau binding to the Hsp70/Hsp90 chaperone machinery induces its dimerization.**

Upon dimerization the Hop-independently bound Hsp70 molecule falls off due to the antiparallel orientation of the (Hsp70<sub>1</sub>:Hop<sub>1</sub>:Hsp90<sub>2</sub>:Tau<sub>1</sub>)<sub>2</sub> complex. Thereby, one Tau molecule per Hsp70/Hsp90 chaperone machinery gets shielded inside the dimer cavity.

Most strikingly, upon the addition of Tau the combined data were indicative for a dimerization of the Hsp70/Hsp90 chaperone machinery (see chapter 3.5.1 and 3.5.3). The accompanied release of the second Hop-independently bound Hsp70 molecule further suggested an antiparallel oriented (Hsp70<sub>1</sub>:Hop<sub>1</sub>:Hsp90<sub>2</sub>:Tau<sub>1</sub>)<sub>2</sub> dimer, where the Hop-bound Hsp70 molecule from the inversed monomer might occupy the second Hsp70 binding site on the opposite Hsp90 (Figure 55). In order to allow each remaining Hsp70 molecule to contact the outside of the opposing Hsp90, it is further suggested that Hsp90 adopts a more compact V-form in the

tetrameric state, i.e. within the Hsp70/Hsp90 chaperone machinery: Tau dimer, as compared to its dimeric state in complex with Hsp90:Hop or Hsp70:Hop:Hsp90 (Figure 55).

Though herewith the first evidence for a dimeric Hsp70/Hsp90 chaperone machinery is presented, a dimerized, tetrameric Hsp90 has been recently described for the mitochondrial paralogue TRAP1 (Figure 59).<sup>376,377</sup> Consistent with the dimerization of the Hsp70/Hsp90 chaperone machinery observed only in the presence of Tau (Figure 41), the formation of the tetrameric TRAP1 has been as well proposed to be related to substrate binding.<sup>377</sup> The Tau binding site on Hsp90 was described to be permanently accessible neither covered by a lid nor buried inside a cleft.<sup>84</sup> Beyond, it has been demonstrated that the repeat region, which represents the core of Tau aggregates<sup>306,307</sup>, is exposed when Tau is bound to Hsp90 conceivably facilitating Tau aggregation.<sup>378,379</sup> In a dimeric model of two antiparallel orientated Hsp70/Hsp90 chaperone machinery: Tau complexes however, each machinery could mutually cover the opposed substrate binding site (Figure 55). In this context the Hsp70/Hsp90 chaperone machinery might represent a protective shell, with subunit closure in the presence of Tau. Thereby, the bound substrate could be shielded from other Tau molecules in turn preventing Tau aggregation. Along this line, aggregation-prone Tau (PTau) might analogically be preserved soluble *via* the Hsp70/Hsp90 chaperone machinery dimer, as Hsp70/Hsp90 chaperone machinery:PTau complexes were formed to an equal extent as with wildtype Tau (Figure 50) (see chapter 4.8).

### 4.3 p23 serves for Tau binding

In contrast to earlier findings suggesting that Hop and p23 are mutually exclusive in one and the same complex<sup>130,167,238</sup>, p23 was found to associate with the Hsp70/Hsp90 chaperone machinery: Tau dimer generating a stable, likewise dimeric (Hsp70<sub>1</sub>:Hop<sub>1</sub>:Hsp90<sub>2</sub>:Tau<sub>1</sub>:p23<sub>1</sub>)<sub>2</sub> complex (Figure 35). In fact, the data indicated that along with Tau binding the Hsp70/Hsp90 chaperone machinery exists in a monomer-dimer equilibrium, which in presence of p23 is shifted towards the dimeric state (Figure 41). In the case of Tau as substrate, p23 thus appeared to take on a stabilizing role.

So far, p23 is believed to exclusively bind to the closed conformation of Hsp90<sup>122,222</sup>, which could indicate that within the (Hsp70<sub>1</sub>:Hop<sub>1</sub>:Hsp90<sub>2</sub>:Tau<sub>1</sub>:p23<sub>1</sub>)<sub>2</sub> complex, Hsp90 has continued towards a closed state. However, since high reliable cross-links between Hop's TPR2B domain and Hsp90's CTD-MD were present in the (Hsp70<sub>1</sub>:Hop<sub>1</sub>:Hsp90<sub>2</sub>:Tau<sub>1</sub>:p23<sub>1</sub>)<sub>2</sub> complex (Figure 44), the twisting of the two Hsp90 arms<sup>181</sup> suggesting to provoke Hop dislocation was yet excluded. Hence, in presence of the substrate Tau the data favor a model where Hsp90 is in a more open conformation. Altogether, Hsp90 is likely to retain a V-shape conformation even within the

## Discussion

(Hsp70<sub>1</sub>:Hop<sub>1</sub>:Hsp90<sub>2</sub>:Tau<sub>1</sub>:p23<sub>1</sub>)<sub>2</sub> complex, whereby the angular shape of the two Hsp90 arms remains to be specified.

Although it is known that p23 as a co-chaperone stabilizes the Hsp90:client interactions<sup>140</sup>, so far the addition of p23 was described to induce the substrate transfer from Hsp70 onto Hsp90 along with the release of Hsp70 and Hop.<sup>48,129,235</sup> However, in contrast to other Hsp90:substrate:p23 complexes, where the C-terminal tail of p23 interacts with the substrate via an  $\alpha$ -helical motif<sup>47,222,225,226</sup>, the C-terminal region of p23 seemed to be not involved in the Hsp70/Hsp90 chaperone machinery:Tau:p23 interaction (Figure 44), hence remaining freely accessible for additional binding partners. Instead, the  $\beta$ -sheet core of p23 was extensively cross-linked in particular with Tau (Figure 44). Consistent with its structural relationship to the crystalline subunit of sHsps (Figure 8), p23 thus might contribute against Tau aggregation by stabilizing the Hsp70/Hsp90 chaperone machinery:Tau interaction *via* its globular domain.<sup>232</sup> The discrimination of substrate holding over Hsp90 co-chaperone function of p23 might be based on affinity differences of p23 for the substrate and Hsp90, as well as the nature of p23:substrate interaction. Hence, if the p23:substrate interaction involves the p23 core, the substrate and Hsp90 compete for p23 binding, which, with regard to the results of this work, is clearly in favor of Tau.

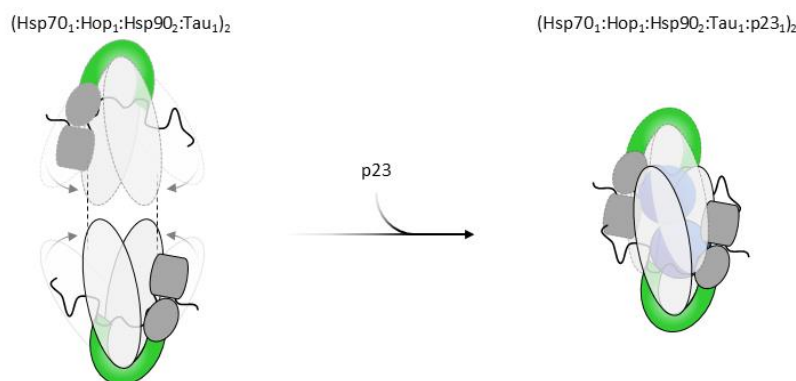


**Figure 56** The  $(\text{Hsp70}_1:\text{Hop}_1:\text{Hsp90}_2:\text{Tau}_1)_2$  dimer is stabilized by p23.

The p23:Tau interaction orientates the co-chaperone to the center of the Hsp70/Hsp90 chaperone machinery. Hsp90 as part of the  $(\text{Hsp70}_1:\text{Hop}_1:\text{Hsp90}_2:\text{Tau}_1)_2$  and  $(\text{Hsp70}_1:\text{Hop}_1:\text{Hsp90}_2:\text{Tau}_1:\text{p23}_1)_2$  complex most likely depicts a smaller angled V-shaped conformation compared to the Hsp90:Hop (Figure 52) and Hsp70:Hop:Hsp90 complex (Figure 54) to allow the Hsp70 molecules to reach the outer side of the opposing Hsp90.

Along this line, the majority of p23 cross-links were found with Tau, positioning the co-chaperone in between the two Hsp90 arms (Figure 44 and Figure 56). Consistent with this, abundant p23 cross-links with Hsp90's CTD were detected (Figure 44), opposite to the well-known interaction site in Hsp90's NTD-MD region.<sup>122,221,222</sup> Nevertheless, p23 was likewise found in close proximity to the N-terminal and middle domain of Hsp90 (Figure 44) supporting the presumed antiparallel orientation of the dimeric Hsp70/Hsp90 chaperone machinery with the opposite p23 molecule contacting the NTD-MD region of the reversed Hsp90 (Figure 56). Intriguingly, the

Hsp90:p23 interaction was described to be disturbed in the presence of ADP.<sup>220</sup> The observation that ADP did not dissociate p23 from the Hsp70/Hsp90 chaperone machinery: Tau complex (Figure 35) therefore supported the model in which the interaction of p23 with the Hsp70/Hsp90 chaperone machinery: Tau complex is not directed by Hsp90 binding (Figure 56).

#### 4.4 The alternation of Hop and CHIP controls the Hsp70/Hsp90 chaperone machinery: Tau interaction

The absent substrate transfer induced by p23 (see chapter 4.3) raised the possibility that the Hsp70/Hsp90 chaperone machinery might represent a deadlock creating an abnormal complex that can no longer be disbanded. Further experiments however rather refuted this hypothesis, as it has been demonstrated that CHIP, competing with Hop for the binding to Hsp70 and Hsp90<sup>57,207,355</sup>, was able to dissociate the Hsp70/Hsp90 chaperone machinery: Tau complex (see chapter 3.6, Figure 57). In fact, the same experiment supported the stabilizing role of p23, since higher amounts of CHIP were necessary to dissolve the Hsp70/Hsp90 chaperone machinery: Tau:p23 complex (Figure 47).

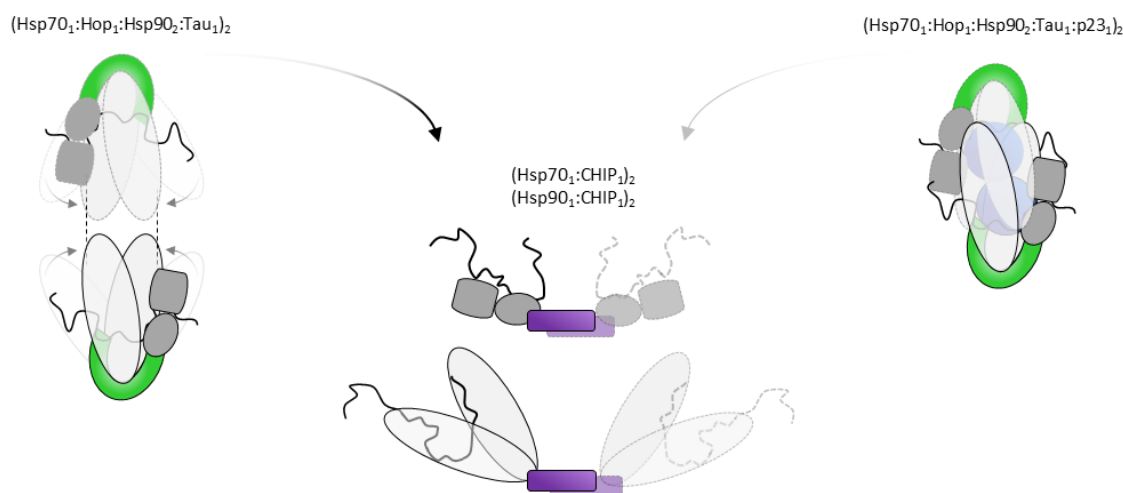


**Figure 57 The co-chaperones Hop and CHIP compete for the binding to Hsp70 and Hsp90.**

Hop and CHIP interact *via* their TPR-domains with the C-terminal regions of Hsp70 and Hsp90, thereby allowing the dynamic assembly and disassembly of the Hsp70/Hsp90 chaperone machinery. Hsp70:CHIP and Hsp90:CHIP complexes exist as dimers.<sup>57</sup> The CHIP-induced disintegration of the Hsp70/Hsp90 chaperone machinery: Tau complex was attenuated in the presence of p23 (Figure 47) indicated by the faint arrow.

Despite the roughly comparable affinities of Hop and CHIP for Hsp70 and Hsp90 (Table 17 and Table 18), with regard to the rather low intracellular concentrations of CHIP (0.0094  $\mu\text{M}$ ) compared to Hop (1.2  $\mu\text{M}$ ) (Table 18)<sup>57</sup>, it remains to be elucidated to which extent a dynamic interplay between Tau retention *via* Hop and Tau degradation *via* CHIP is maintained by Hsp70

## Discussion

and Hsp90 *in vivo*. Nonetheless, the combined data enclosing Tau-induced dimerization (see chapter 4.2), p23 stabilization (see chapter 4.3) and CHIP-mediated disintegration rather suggested that the Hsp70/Hsp90 chaperone machinery takes over an active protective rather than a passive harmful role.

**Table 18 Top: Reported affinity values of CHIP for Hsp70 and Hsp90. Bottom: Protein amounts of Hsp70, Hsp90, Hop and CHIP *in vivo*.**

Hsp70 - 70, Hsp90 – 90, C-terminal peptides - 70C and 90C). Affinity values were taken from literature determined by (1) ITC<sup>380</sup>, (2) fluorescence polarization assay<sup>363</sup>, (3) ITC<sup>57</sup> and (4) fluorescence polarization assay<sup>365</sup>.

Affinities	K <sub>D</sub> [μM]			K <sub>D</sub> (average) [μM]
CHIP:70	0.95±0.01 <sup>(1)</sup>			
CHIP:70C	0.51±0.03 <sup>(2)</sup>	1 <sup>(3)</sup>	1.9 <sup>(4)</sup>	<b>1.14±0.58</b>
CHIP:90	0.38±0.04 <sup>(1)</sup>			
CHIP:90C	1.32±0.11 <sup>(2)</sup>	4.5 <sup>(3)</sup>	4.9 <sup>(4)</sup>	<b>3.57±1.6</b>
Amounts	(1)		(3)	
Hsp70	0.94±0.001 %		8.8 μM	
Hsp90	0.60±0.01 %		3.8 μM	
Hop	0.20±0.01 %		1.2 μM	
CHIP	0.072±0.014 %		0.0094 μM	

### 4.5 The Hsp70/Hsp90 chaperone machinery: Tau interaction is independent on ATP hydrolysis

Numerous studies revealed the importance of distinct nucleotide bound states of Hsp70 and Hsp90 for the assembly of the Hsp70/Hsp90 chaperone machinery as well as for client binding. The nucleotide-free or ADP-bound form of Hsp70 favors the interaction with Hop<sup>167</sup>, substrates<sup>139,152,381</sup> as well as with Hsp90.<sup>139,370</sup> On the side of Hsp90, bulk experiments have demonstrated that Hsp90's ATP-bound form represents the high-affinity state for substrate binding<sup>382,383</sup>, though the affinity of Tau for Hsp90 was not enhanced in the presence of the ATP analog ATPγS.<sup>84</sup> The challenge to simultaneously stabilize the ADP-state of Hsp70 and the ATP-state of Hsp90 did not arise, as after all, any interaction that was investigated in this work could be observed in the absence of nucleotides. For both full-length Hop and the shorter Hop112a construct there was even a tendency to preferentially bind apo Hsp90 than the AMP-PNP-bound state (Figure 17 and Figure 24). Otherwise, only the direct interaction between Hsp70: Tau positively sensed the presence of AMP-PNP (Figure 30D), whereby the effect might be attributed to the dissociation of Hsp70 oligomers upon nucleotide binding, thereby increasing the amount of Hsp70 monomers, i.e. Tau interaction partners.<sup>384</sup>



For the formation of the (Hsp70<sub>1</sub>:Hop<sub>1</sub>:Hsp90<sub>2</sub>:Tau<sub>1</sub>:p23<sub>1</sub>)<sub>2</sub> complex no distinction was observed among the different nucleotide states (apo, AMP-PNP- or ADP-bound) (Figure 35D). This however posed the question, whether the ATP hydrolysis activity of both Hsp70 and Hsp90 plays any role for the chaperoning of Tau. It could very well be that for Tau as an IDP, the interaction with the Hsp70/Hsp90 chaperone machinery might be because of protein holding rather than protein folding, which in turn does not necessarily require energy. Hence, instead of the event of ATP hydrolysis that is reported to complete the Hsp90 action for other substrates<sup>181</sup>, additional co-chaperones such as Aha1 or PPIases<sup>344,385</sup> could, similarly to what has been shown with CHIP (see chapter 3.6), regulate the dynamic assembly and disassembly of the Hsp70/Hsp90 chaperone machinery: Tau complex.

#### 4.6 The role of Hsp40 for Tau binding to Hsp70

An advantageous effect of Hsp40 for the Hsp70:Hop, Hsp70:substrate and Hsp70:Hsp90 interaction is widely accepted due to its ability to convert the Hsp70-ATP state into the Hsp70-ADP form.<sup>110,114,137,139,173,386</sup> The ascribed catalytic activity was observed at already substoichiometric amounts of Hsp40 and is the highest in absence or at low concentrations of ATP, but is diminished at high amounts of nucleotide.<sup>137</sup> In this context previous studies working on the structural characterization of the Hsp70/Hsp90 chaperone machinery consistently included Hsp40 during protein incubation<sup>117,130,215,235</sup>, whereby Hsp40 was never present in the final complex (Table 15). However, regarding the intensity of complex formation observed in this work, the addition of Hsp40 had no effect on the amount of the Hsp70: Tau (Figure 30D) or (Hsp70<sub>1</sub>:Hop<sub>1</sub>:Hsp90<sub>2</sub>:Tau<sub>1</sub>)<sub>2</sub> complexes (Figure 30E). Notably, class A Hsp40 from yeast (Ydj1) was added during complex formation in previous studies<sup>47,130,137,215,235</sup>, whereas in the current work human class B Hsp40 (DnaJB4) was used.

Although possessing an additional EEVD-binding site for dual Hsp70 interaction, class B Hsp40s lack the zinc finger-like region.<sup>110,114,173</sup> It has been shown that Hsp40's can interact with unfolded substrates even in the absence of the zinc finger-like region.<sup>374</sup> But for yeast constructs it is reported that without this region substrate delivery to Hsp70 is abolished.<sup>386</sup> Hence, while the applied Hsp40 (DnaJB4) exhibited no impact on the Hsp70/Hsp90 chaperone machinery: Tau interaction, a class A paralogue could instead very well do. Since this is not yet fully verified, additional experiments are essential. Nonetheless, this may emphasize an essential role of Hsp40's zinc finger-like region potentially contributing to an increased stability of the machinery: Tau complex.

#### 4.7 Tau chaperoning by the Hsp70/Hsp90 chaperone machinery

Based on the combined data obtained in this work together with previous results a model for the chaperoning of Tau by the Hsp70/Hsp90 chaperone machinery was developed (Figure 58). Initially, the Hsp90 chaperone is stabilized in a V-shape conformation prior to Tau binding forming a stable Hsp70<sub>2</sub>:Hop<sub>1</sub>:Hsp90<sub>2</sub> complex (see chapter 4.1). Both the Hsp90 CTD-MD interaction *via* Hop's TPR2A-TPR2B domains and the Hsp70 SBD interaction *via* Hop's TPR1 domain were maintained within the (Hsp70<sub>1</sub>:Hop<sub>1</sub>:Hsp90<sub>2</sub>:Tau<sub>1</sub>:p23<sub>1</sub>)<sub>2</sub> complex (Figure 44). Besides, the interaction with Tau was presumed to induce the antiparallel dimerization of the Hsp70/Hsp90 chaperone machinery triggering the release of the second Hsp70 molecule (see chapter 4.2) as well as the association of the co-chaperone p23 (see chapter 4.3).

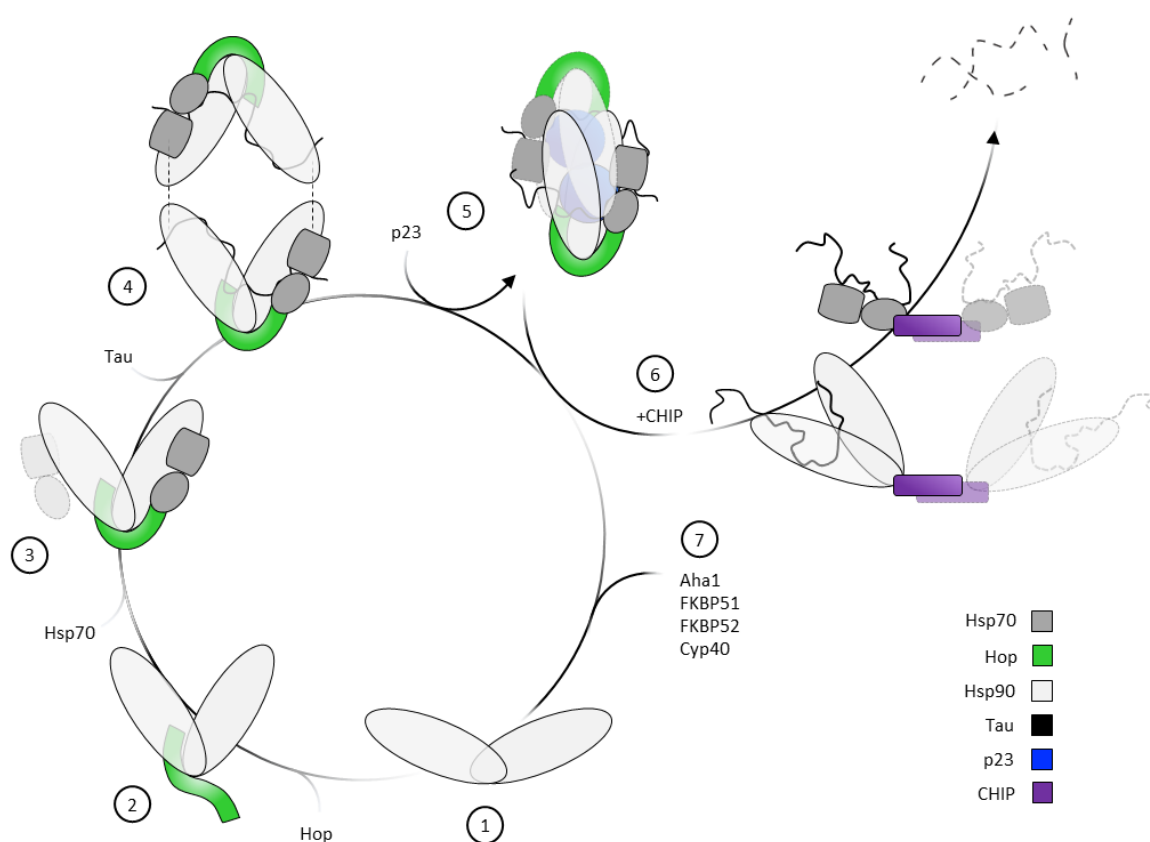


**Figure 58** Cartoon representation of the Hsp70/Hsp90 chaperone machinery-mediated Tau chaperoning.

(1) The Hsp90 dimer is predominantly present in its open conformation.<sup>118,179</sup> (2) A single Hop molecule stabilizes Hsp90 in a V-shaped conformation through direct interaction *via* its TPR2A-2B domains. (3) Two Hsp70 molecules can bind the Hsp90:Hop complex, whereby only one is bound by Hop's TPR1 domain. (4) Tau binding induces the formation of an antiparallel orientated Hsp70/Hsp90 chaperone machinery dimer among which the second, Hop-independently bound Hsp70 gets released. (5) The association of one p23 molecule per machinery monomer is directed by Tau. (6) The (Hsp70<sub>1</sub>:Hop<sub>1</sub>:Hsp90<sub>2</sub>:Tau<sub>1</sub>:p23<sub>1</sub>)<sub>2</sub> complex can be dissociated by CHIP directing Tau towards degradation pathways involving Hsp70:CHIP:Tau and Hsp90:CHIP:Tau complexes.<sup>57</sup> (7) The (Hsp70<sub>1</sub>:Hop<sub>1</sub>:Hsp90<sub>2</sub>:Tau<sub>1</sub>:p23<sub>1</sub>)<sub>2</sub> complex might be dissociated by additional co-chaperones (Aha1, FKBP51, FKBP52, Cyp40) allowing another round for Hsp70/Hsp90 chaperone machinery assembly.<sup>344,385</sup>

## Discussion

The antiparallel oriented Hsp90 within the Hsp70/Hsp90 chaperone machinery is proposed to have a protective function shielding Tau from the surrounding environment (see chapter 4.2). Consistent with this hypothesis two Hsp90 dimers of a V-shaped conformation would contact each other upside down forming two shears that interlock (Figure 59A). In contrast, tetrameric TRAP1 was demonstrated exclusively in its closed conformation with a substrate fragment trapped in between each dimer interface (Figure 59B, C).<sup>387</sup> In combination, both findings could be supplied by a model where the size of the substrate binding site on Hsp90 defines the chaperone's conformation: for smaller binding sites the closure of Hsp90 might be sufficient, more extended binding sites could require the formation of an inversed Hsp90 tetramer – in either way the conformational rearrangements are supposed to shelter the bound substrate (Figure 59A, B).

In agreement with this hypothesis, a substrate-bound closed conformation of Hsp90 was also presented recently in a monomeric Hsp70<sub>2</sub>:Hop1:Hsp90<sub>2</sub>:substrate complex.<sup>47</sup> Only a short region of the substrate was located within the Hsp90 dimer interface allowing Hsp90 closure, and therefore might not have required dimerization. Notable, a smaller binding site does not exclude an Hsp90 tetramer, as has been shown for TRAP1.<sup>377</sup> Moreover, since about four different configurations of the tetrameric TRAP1<sub>2</sub>:substrate<sub>2</sub> molecules were found (Figure 59C)<sup>377</sup>, it can be assumed that the propensity of Hsp90 to form tetramers can occur in many different ways, potentially engendering conformation specific functions.

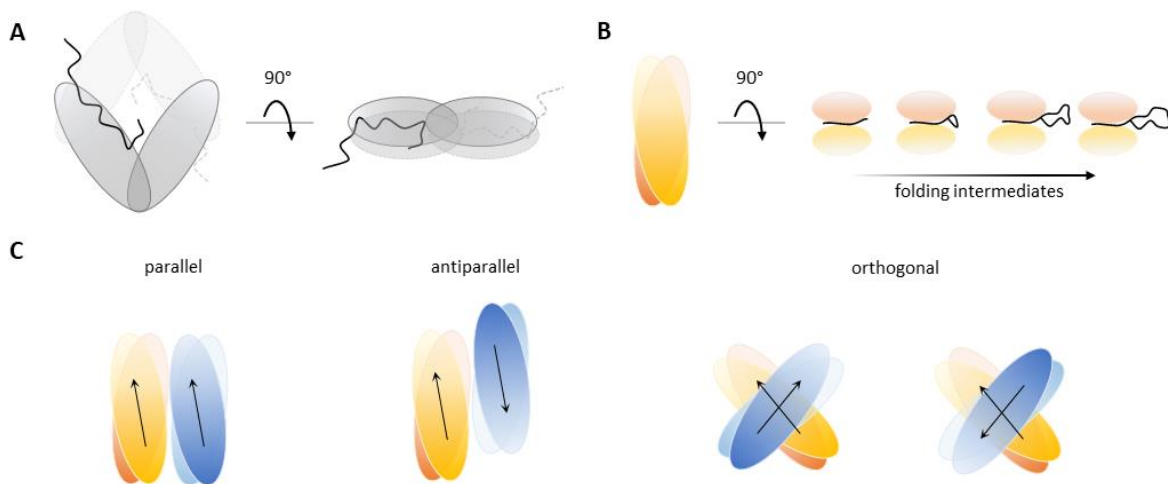


**Figure 59 Tetrameric states of Hsp90.**

**A** In the case of intrinsically disordered substrates such as Tau, a broad region of the substrate is bound (Figure 39)<sup>84</sup>, possibly impeding the closure of Hsp90 and thus involving a second Hsp90 dimer for substrate shielding. **B** In presence of foldable proteins only a small fragment of the substrate is bound to Hsp90 allowing the chaperone to adopt a closed conformation.<sup>47,387</sup> **C** Tetrameric states of human TRAP1 (mitochondrial Hsp90). In addition to its predominant dimeric nature, TRAP1 was found in multiple tetrameric states including a parallel, antiparallel and two orthogonal orientations.<sup>377</sup>

Remarkably, throughout the assembly of the Hsp70<sub>2</sub>:Hop<sub>1</sub>:Hsp90<sub>2</sub>, (Hsp70<sub>1</sub>:Hop<sub>1</sub>:Hsp90<sub>2</sub>:Tau<sub>1</sub>)<sub>2</sub> and (Hsp70<sub>1</sub>:Hop<sub>1</sub>:Hsp90<sub>2</sub>:Tau<sub>1</sub>:p23<sub>1</sub>)<sub>2</sub> complexes, the charged linker (cl) region of Hsp90 appeared highly flexible (see chapter 3.5.4). In the presence of Tau the NMR data indicated a distinct change in this region of Hsp90, which is in close proximity to the NTD (Figure 46). The Tau interaction site on Hsp90 did not involve Hsp90's cl<sup>84</sup> and beyond, cross-link analysis suggested that the cl remains unbound within the (Hsp70<sub>1</sub>:Hop<sub>1</sub>:Hsp90<sub>2</sub>:Tau<sub>1</sub>:p23<sub>1</sub>)<sub>2</sub> complex (Figure 44). Taken together, the observed change in the NMR spectrum (Figure 46) might suggest a conformational change within Hsp90's cl upon Tau binding. Admittedly, this observation represents solely a minor evidence for a relevance of Hsp90's N-terminal cl region for substrate binding. In fact, as few as one out of four isoleucines within the cl sensed the presence of Tau. However, a recent study investigated the conformations of Hsp90's cl in more detail and detected changes within the same regions of the cl related to substrate binding.<sup>187</sup> In combination, despite its unstructured character, the cl region might contribute to the binding of Tau to Hsp90, which however would need further experimental evidence.

#### 4.8 Pathologic Tau as substrate of the Hsp70/Hsp90 chaperone machinery

With regard to the many post-translational modifications with which Tau exists in eukaryotic cells (see chapter 1.6.1), it was further investigated whether these may have an effect on the binding of Tau to the Hsp70/Hsp90 chaperone machinery. Of particular interest were the binding properties of PTau<sup>Cdk2</sup> – the Tau protein being phosphorylated at sites similar to those found in Tau aggregates (Figure 49). The data showed that the pathologically modified Tau interacts with the Hsp70/Hsp90 chaperone machinery to the same extent as normal Tau, similarly including the association of p23 (Figure 50A-D). With this, the first indications suggesting that the Hsp70/Hsp90 chaperone machinery is likely to be involved in the physiological as well as the pathological chaperoning of Tau are presented.

Preceding studies have demonstrated that the inhibition of Hsp90 decreases PTau levels *in vivo*.<sup>295,388</sup> Intriguingly, though the interaction *via* Hsp70 persisted, PTau<sup>Cdk2</sup> showed no binding with Hsp90 as observed by native page (Figure 50E, F). Hence, the inhibitory effect of Hsp90 to reduce PTau levels is likely to target Hsp90 molecules as part of the Hsp70/Hsp90 chaperone machinery. Along this line, it was found that the extent of Hsp90 inhibition was the greatest in presence of all five components of the Hsp70/Hsp90 chaperone machinery suggesting that Hsp90 within the Hsp70/Hsp90 chaperone machinery occupies a distinct conformation with high affinity for the applied inhibitors.<sup>151</sup> In addition, it was demonstrated that the silencing of p23 gene expression evoked the reduction of PTau amounts.<sup>295</sup> Hence, in combination with the results of this work, it could be that the Hsp70/Hsp90 chaperone machinery: Tau complex – additionally stabilized by p23 – is fatally increasing PTau levels *in vivo*.

## Discussion

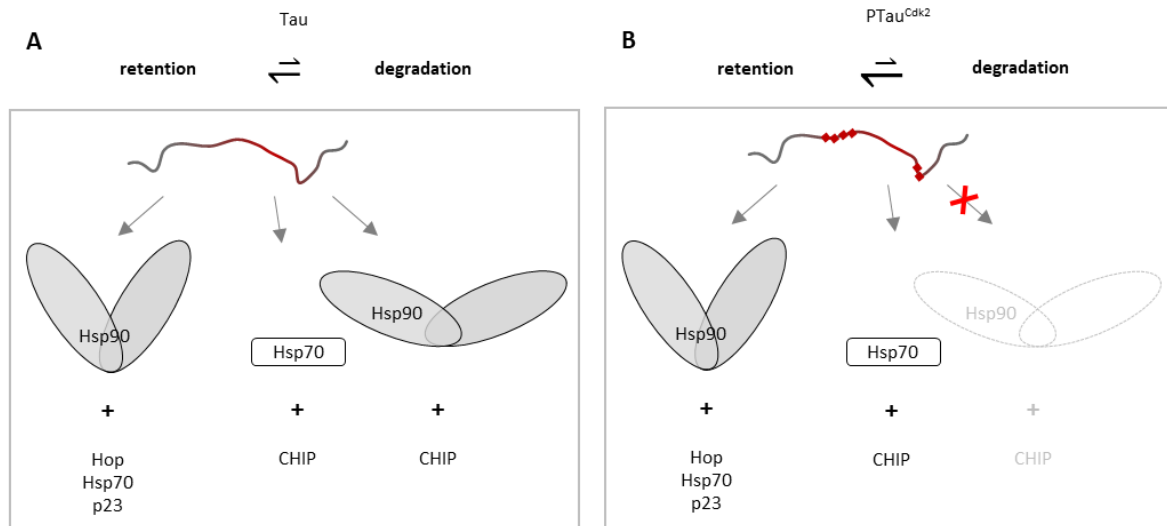


**Figure 60** Balance between protein retention and degradation of normal Tau and pathologic PTau<sup>Cdk2</sup>.

**A, B** Upon phosphorylation of Tau the interaction with Hsp90 alone is diminished shifting the balance towards protein retention *via* the Hsp70/Hsp90 chaperone machinery indicated by the unequal lengths of the equilibrium arrows.

Indeed, besides the suggested active protective role of the Hsp70/Hsp90 chaperone machinery to shield normal Tau molecules (see chapter 4.2), at the same time it was proposed to serve for protein retention.<sup>57</sup> A healthy cell might be able to maintain a vital proteostasis of Tau through a variety of chaperone interactions, directing Tau as needed. In contrast, for pathologically phosphorylated Tau (PTau) the interaction with Hsp90 is reduced or entirely lost (Figure 50E, F). Hence, the Hsp90 mediated degradation pathway *via* Hsp90:CHIP might be no longer available severely shifting the balance towards protein retention (Figure 60). But to what extent, if at all, the interaction between the Hsp70/Hsp90 chaperone machinery and PTau<sup>Cdk2</sup> is related to Tau aggregation yet remains to be shown.

## 5 Outlook

---

The results of this work present a biochemical and structural analysis of the interaction between the Hsp70/Hsp90 chaperone machinery and the intrinsically disordered protein Tau. Since only the interaction of Tau with the individual Hsp70 and Hsp90 has been investigated so far (see chapter 1.6.3), these are the first data that established the collaboration of both chaperone systems *via* Hop in relation to Tau binding. Herewith, the Hsp70/Hsp90 chaperone machinery initially appears conceivable to act as a central hub to maintain Tau proteostasis, revealing new perspectives in proteostasis research to combat Tau aggregation.

Providing the recipe of the minimal requirements necessary for the *in vitro* reconstitution of the Hsp70/Hsp90 chaperone machinery in complex with Tau (see chapter 2.4) may serve as fundamental basis for high-resolution structure determination. The clarification of the three-dimensional architectures of the intermediate Hsp70:Hop:Hsp90:Tau state and the Hsp70:Hop:Hsp90:Tau:p23 complex, as well as the subcomplexes Hsp70:CHIP:Tau and Hsp90:CHIP:Tau will be crucial for a detailed understanding of the pathway for Tau holding and Tau degradation, respectively. In specific, the detailed insights obtained about the binding sites and the spatial orientation of the proteins to one another may serve as template for future structure calculations. These include the detection of particularly highly flexible regions of Tau as well as of Hsp90, which may not be identifiable by e.g. cryo-EM.

Taken together, this work holds the template for prospective investigations to decipher the structure-function relationship of the Hsp70/Hsp90 chaperone machinery: Tau interaction. In this context, the established protocol can be used to analyze in great detail how small molecules affect the Hsp70:Hop:Hsp90:Tau:p23 complex and thus serves for target-oriented drug development focusing specifically on the activity of the Hsp70/Hsp90 chaperone machinery. In particular, the stimulation of pathways promoting the turnover of pathogenic Tau variants are of high interest to counteract and reduce the aggregation process.

Notably, direct interactions with Hsp70 and Hsp90 have been reported for other intrinsically disordered proteins as well.<sup>116,241,389</sup> Thus, possibly, the Hsp70/Hsp90 chaperone machinery mediated chaperoning of Tau described here may be brought to a broader sense. Future research directions including other IDPs such as  $\alpha$ -Synuclein will elucidate whether the interaction with the Hsp70/Hsp90 chaperone machinery is Tau specific, or that this in fact holds true for IDPs in general.

## 6 References

---

- 1 Jayaraj, G. G., Hipp, M. S. & Hartl, F. U. Functional Modules of the Proteostasis Network. *Cold Spring Harb Perspect Biol* 12, doi:10.1101/cshperspect.a033951 (2020).
- 2 Balch, W. E., Morimoto, R. I., Dillin, A. & Kelly, J. W. Adapting proteostasis for disease intervention. *Science* 319, 916-919, doi:10.1126/science.1141448 (2008).
- 3 Hipp, M. S., Park, S. H. & Hartl, F. U. Proteostasis impairment in protein-misfolding and -aggregation diseases. *Trends Cell Biol* 24, 506-514, doi:10.1016/j.tcb.2014.05.003 (2014).
- 4 Shamsi, T. N., Athar, T., Parveen, R. & Fatima, S. A review on protein misfolding, aggregation and strategies to prevent related ailments. *Int J Biol Macromol* 105, 993-1000, doi:10.1016/j.ijbiomac.2017.07.116 (2017).
- 5 Bossy-Wetzel, E., Schwarzenbacher, R. & Lipton, S. A. Molecular pathways to neurodegeneration. *Nat Med* 10 Suppl, S2-9, doi:10.1038/nm1067 (2004).
- 6 Koga, H., Kaushik, S. & Cuervo, A. M. Protein homeostasis and aging: The importance of exquisite quality control. *Ageing Res Rev* 10, 205-215, doi:10.1016/j.arr.2010.02.001 (2011).
- 7 Calamini, B. & Morimoto, R. I. Protein homeostasis as a therapeutic target for diseases of protein conformation. *Curr Top Med Chem* 12, 2623-2640, doi:10.2174/1568026611212220014 (2012).
- 8 Hipp, M. S., Kasturi, P. & Hartl, F. U. The proteostasis network and its decline in ageing. *Nat Rev Mol Cell Biol* 20, 421-435, doi:10.1038/s41580-019-0101-y (2019).
- 9 Klaipe, C. L., Jayaraj, G. G. & Hartl, F. U. Pathways of cellular proteostasis in aging and disease. *J Cell Biol* 217, 51-63, doi:10.1083/jcb.201709072 (2018).
- 10 Jungblut, P. R., Holzhutter, H. G., Apweiler, R. & Schluter, H. The speciation of the proteome. *Chem Cent J* 2, 16, doi:10.1186/1752-153X-2-16 (2008).
- 11 Hamilton, K. L. & Miller, B. F. Mitochondrial proteostasis as a shared characteristic of slowed aging: the importance of considering cell proliferation. *J Physiol* 595, 6401-6407, doi:10.1113/JP274335 (2017).
- 12 Spriggs, K. A., Bushell, M. & Willis, A. E. Translational regulation of gene expression during conditions of cell stress. *Mol Cell* 40, 228-237, doi:10.1016/j.molcel.2010.09.028 (2010).
- 13 Korovila, I. *et al.* Proteostasis, oxidative stress and aging. *Redox Biol* 13, 550-567, doi:10.1016/j.redox.2017.07.008 (2017).
- 14 Aviner, R. & Frydman, J. Proteostasis in Viral Infection: Unfolding the Complex Virus-Chaperone Interplay. *Cold Spring Harb Perspect Biol* 12, doi:10.1101/cshperspect.a034090 (2020).
- 15 de Graff, A. M., Mosedale, D. E., Sharp, T., Dill, K. A. & Grainger, D. J. Proteostasis is adaptive: Balancing chaperone holdases against foldases. *PLoS Comput Biol* 16, e1008460, doi:10.1371/journal.pcbi.1008460 (2020).
- 16 Morimoto, R. I. & Cuervo, A. M. Proteostasis and the aging proteome in health and disease. *J Gerontol A Biol Sci Med Sci* 69 Suppl 1, S33-38, doi:10.1093/gerona/glu049 (2014).

## References

- 17 Zhang, J. Protein-length distributions for the three domains of life. *Trends Genet* 16, 107-109, doi:10.1016/s0168-9525(99)01922-8 (2000).
- 18 Kaeberlein, M. & Kennedy, B. K. Protein translation, 2007. *Aging Cell* 6, 731-734, doi:10.1111/j.1474-9726.2007.00341.x (2007).
- 19 Opron, K. & Burton, Z. F. Ribosome Structure, Function, and Early Evolution. *Int J Mol Sci* 20, doi:10.3390/ijms20010040 (2018).
- 20 Lomakin, I. B. *et al.* Crystal Structure of the Human Ribosome in Complex with DENR-MCT-1. *Cell Rep* 20, 521-528, doi:10.1016/j.celrep.2017.06.025 (2017).
- 21 Yang, J., Gao, M., Xiong, J., Su, Z. & Huang, Y. Features of molecular recognition of intrinsically disordered proteins via coupled folding and binding. *Protein Sci* 28, 1952-1965, doi:10.1002/pro.3718 (2019).
- 22 Hartl, F. U., Bracher, A. & Hayer-Hartl, M. Molecular chaperones in protein folding and proteostasis. *Nature* 475, 324-332, doi:10.1038/nature10317 (2011).
- 23 Kramer, G., Boehringer, D., Ban, N. & Bukau, B. The ribosome as a platform for co-translational processing, folding and targeting of newly synthesized proteins. *Nat Struct Mol Biol* 16, 589-597, doi:10.1038/nsmb.1614 (2009).
- 24 Mannini, B. & Chiti, F. Chaperones as Suppressors of Protein Misfolded Oligomer Toxicity. *Front Mol Neurosci* 10, 98, doi:10.3389/fnmol.2017.00098 (2017).
- 25 Wickner, W. & Schekman, R. Protein translocation across biological membranes. *Science* 310, 1452-1456, doi:10.1126/science.1113752 (2005).
- 26 Kaushik, S. & Cuervo, A. M. Chaperone-mediated autophagy: a unique way to enter the lysosome world. *Trends Cell Biol* 22, 407-417, doi:10.1016/j.tcb.2012.05.006 (2012).
- 27 Wolf, D. H. & Hilt, W. The proteasome: a proteolytic nanomachine of cell regulation and waste disposal. *Biochim Biophys Acta* 1695, 19-31, doi:10.1016/j.bbamcr.2004.10.007 (2004).
- 28 Frydman, J. Folding of newly translated proteins in vivo: the role of molecular chaperones. *Annu Rev Biochem* 70, 603-647, doi:10.1146/annurev.biochem.70.1.603 (2001).
- 29 Balchin, D., Hayer-Hartl, M. & Hartl, F. U. In vivo aspects of protein folding and quality control. *Science* 353, aac4354, doi:10.1126/science.aac4354 (2016).
- 30 Dobson, C. M. Principles of protein folding, misfolding and aggregation. *Semin Cell Dev Biol* 15, 3-16, doi:10.1016/j.semcdb.2003.12.008 (2004).
- 31 Wang, W., Nema, S. & Teagarden, D. Protein aggregation--pathways and influencing factors. *Int J Pharm* 390, 89-99, doi:10.1016/j.ijpharm.2010.02.025 (2010).
- 32 Frieden, C. Protein aggregation processes: In search of the mechanism. *Protein Sci* 16, 2334-2344, doi:10.1110/ps.073164107 (2007).
- 33 Dinner, A. R., Sali, A., Smith, L. J., Dobson, C. M. & Karplus, M. Understanding protein folding via free-energy surfaces from theory and experiment. *Trends Biochem Sci* 25, 331-339, doi:10.1016/s0968-0004(00)01610-8 (2000).
- 34 Finkelstein, A. V. 50+ Years of Protein Folding. *Biochemistry (Mosc)* 83, S3-S18, doi:10.1134/S000629791814002X (2018).



## References

- 35 Clark, P. L. Protein folding in the cell: reshaping the folding funnel. *Trends Biochem Sci* 29, 527-534, doi:10.1016/j.tibs.2004.08.008 (2004).
- 36 Hartl, F. U. Molecular chaperones in cellular protein folding. *Nature* 381, 571-579, doi:10.1038/381571a0 (1996).
- 37 Hartl, F. U. & Hayer-Hartl, M. Molecular chaperones in the cytosol: from nascent chain to folded protein. *Science* 295, 1852-1858, doi:10.1126/science.1068408 (2002).
- 38 Hartl, F. U. & Hayer-Hartl, M. Converging concepts of protein folding in vitro and in vivo. *Nat Struct Mol Biol* 16, 574-581, doi:10.1038/nsmb.1591 (2009).
- 39 Faller, P., Hureau, C. & La Penna, G. Metal ions and intrinsically disordered proteins and peptides: from Cu/Zn amyloid-beta to general principles. *Acc Chem Res* 47, 2252-2259, doi:10.1021/ar400293h (2014).
- 40 Tompa, P. Intrinsically disordered proteins: a 10-year recap. *Trends Biochem Sci* 37, 509-516, doi:10.1016/j.tibs.2012.08.004 (2012).
- 41 Uversky, V. N. Unusual biophysics of intrinsically disordered proteins. *Biochim Biophys Acta* 1834, 932-951, doi:10.1016/j.bbapap.2012.12.008 (2013).
- 42 Eliezer, D. Biophysical characterization of intrinsically disordered proteins. *Curr Opin Struct Biol* 19, 23-30, doi:10.1016/j.sbi.2008.12.004 (2009).
- 43 Nooren, I. M. & Thornton, J. M. Diversity of protein-protein interactions. *EMBO J* 22, 3486-3492, doi:10.1093/emboj/cdg359 (2003).
- 44 Mulgrew-Nesbitt, A. *et al.* The role of electrostatics in protein-membrane interactions. *Biochim Biophys Acta* 1761, 812-826, doi:10.1016/j.bbalip.2006.07.002 (2006).
- 45 Das, T. & Eliezer, D. Membrane interactions of intrinsically disordered proteins: The example of alpha-synuclein. *Biochim Biophys Acta Proteins Proteom* 1867, 879-889, doi:10.1016/j.bbapap.2019.05.001 (2019).
- 46 Finkelstein, J. Metalloproteins. *Nature* 460, 813, doi:10.1038/460813a (2009).
- 47 Wang, R. Y.-R. *et al.* GR chaperone cycle mechanism revealed by cryo-EM: inactivation of GR by GR:Hsp90:Hsp70:Hsp client-loading complex. *bioRxiv*, 2020.2011.2005.370247, doi:10.1101/2020.11.05.370247 (2020).
- 48 Noddings, C. M., Wang, R. Y.-R. & Agard, D. A. GR chaperone cycle mechanism revealed by cryo-EM: reactivation of GR by the GR:Hsp90:p23 client-maturation complex. *bioRxiv*, 2020.2009.2012.294975, doi:10.1101/2020.09.12.294975 (2020).
- 49 Ben-Zvi, A. P. & Goloubinoff, P. Review: mechanisms of disaggregation and refolding of stable protein aggregates by molecular chaperones. *J Struct Biol* 135, 84-93, doi:10.1006/jsbi.2001.4352 (2001).
- 50 Liberek, K., Lewandowska, A. & Zietkiewicz, S. Chaperones in control of protein disaggregation. *EMBO J* 27, 328-335, doi:10.1038/sj.emboj.7601970 (2008).
- 51 Ketterer, N., Dreiseidler, M., Tawo, R. & Hohfeld, J. Chaperone-assisted degradation: multiple paths to destruction. *Biol Chem* 391, 481-489, doi:10.1515/BC.2010.058 (2010).

## References

- 52 Ding, W. X. & Yin, X. M. Sorting, recognition and activation of the misfolded protein degradation pathways through macroautophagy and the proteasome. *Autophagy* 4, 141-150, doi:10.4161/auto.5190 (2008).
- 53 Kaganovich, D., Kopito, R. & Frydman, J. Misfolded proteins partition between two distinct quality control compartments. *Nature* 454, 1088-1095, doi:10.1038/nature07195 (2008).
- 54 Goldberg, A. L. Protein degradation and protection against misfolded or damaged proteins. *Nature* 426, 895-899, doi:10.1038/nature02263 (2003).
- 55 Groll, M., Bochtler, M., Brandstetter, H., Clausen, T. & Huber, R. Molecular machines for protein degradation. *ChemBiochem* 6, 222-256, doi:10.1002/cbic.200400313 (2005).
- 56 Dikic, I. Proteasomal and Autophagic Degradation Systems. *Annu Rev Biochem* 86, 193-224, doi:10.1146/annurev-biochem-061516-044908 (2017).
- 57 Kundrat, L. & Regan, L. Balance between folding and degradation for Hsp90-dependent client proteins: a key role for CHIP. *Biochemistry* 49, 7428-7438, doi:10.1021/bi100386w (2010).
- 58 Glickman, M. H. & Ciechanover, A. The ubiquitin-proteasome proteolytic pathway: destruction for the sake of construction. *Physiol Rev* 82, 373-428, doi:10.1152/physrev.00027.2001 (2002).
- 59 Schrader, E. K., Harstad, K. G. & Matouschek, A. Targeting proteins for degradation. *Nat Chem Biol* 5, 815-822, doi:10.1038/nchembio.250 (2009).
- 60 Dice, J. F. Chaperone-mediated autophagy. *Autophagy* 3, 295-299, doi:10.4161/auto.4144 (2007).
- 61 Majeski, A. E. & Dice, J. F. Mechanisms of chaperone-mediated autophagy. *Int J Biochem Cell Biol* 36, 2435-2444, doi:10.1016/j.biocel.2004.02.013 (2004).
- 62 Bukau, B., Weissman, J. & Horwich, A. Molecular chaperones and protein quality control. *Cell* 125, 443-451, doi:10.1016/j.cell.2006.04.014 (2006).
- 63 Kim, Y. E., Hipp, M. S., Bracher, A., Hayer-Hartl, M. & Hartl, F. U. Molecular chaperone functions in protein folding and proteostasis. *Annu Rev Biochem* 82, 323-355, doi:10.1146/annurev-biochem-060208-092442 (2013).
- 64 Lee, S. & Tsai, F. T. Molecular chaperones in protein quality control. *J Biochem Mol Biol* 38, 259-265, doi:10.5483/bmbrep.2005.38.3.259 (2005).
- 65 Walter, S. & Buchner, J. Molecular chaperones--cellular machines for protein folding. *Angew Chem Int Ed Engl* 41, 1098-1113, doi:10.1002/1521-3773(20020402)41:7<1098::aid-anie1098>3.0.co;2-9 (2002).
- 66 Kumar, C. M., Mande, S. C. & Mahajan, G. Multiple chaperonins in bacteria--novel functions and non-canonical behaviors. *Cell Stress Chaperones* 20, 555-574, doi:10.1007/s12192-015-0598-8 (2015).
- 67 Slavotinek, A. M. & Biesecker, L. G. Unfolding the role of chaperones and chaperonins in human disease. *Trends Genet* 17, 528-535, doi:10.1016/s0168-9525(01)02413-1 (2001).

## References

- 68 Leitner, A. *et al.* The molecular architecture of the eukaryotic chaperonin TRiC/CCT. *Structure* 20, 814-825, doi:10.1016/j.str.2012.03.007 (2012).
- 69 Zeilstra-Ryalls, J., Fayet, O. & Georgopoulos, C. The universally conserved GroE (Hsp60) chaperonins. *Annu Rev Microbiol* 45, 301-325, doi:10.1146/annurev.mi.45.100191.001505 (1991).
- 70 Chen, D. H. *et al.* Visualizing GroEL/ES in the act of encapsulating a folding protein. *Cell* 153, 1354-1365, doi:10.1016/j.cell.2013.04.052 (2013).
- 71 Horwich, A. L., Fenton, W. A., Chapman, E. & Farr, G. W. Two families of chaperonin: physiology and mechanism. *Annu Rev Cell Dev Biol* 23, 115-145, doi:10.1146/annurev.cellbio.23.090506.123555 (2007).
- 72 Liou, A. K. & Willison, K. R. Elucidation of the subunit orientation in CCT (chaperonin containing TCP1) from the subunit composition of CCT micro-complexes. *EMBO J* 16, 4311-4316, doi:10.1093/emboj/16.14.4311 (1997).
- 73 Zhang, J. *et al.* Cryo-EM structure of a group II chaperonin in the prehydrolysis ATP-bound state leading to lid closure. *Structure* 19, 633-639, doi:10.1016/j.str.2011.03.005 (2011).
- 74 Saibil, H. R., Fenton, W. A., Clare, D. K. & Horwich, A. L. Structure and allostery of the chaperonin GroEL. *J Mol Biol* 425, 1476-1487, doi:10.1016/j.jmb.2012.11.028 (2013).
- 75 Ryabova, N. A., Marchenkov, V. V., Marchenkova, S. Y., Kotova, N. V. & Semisotnov, G. V. Molecular chaperone GroEL/ES: unfolding and refolding processes. *Biochemistry (Mosc)* 78, 1405-1414, doi:10.1134/S0006297913130038 (2013).
- 76 Xu, Z., Horwich, A. L. & Sigler, P. B. The crystal structure of the asymmetric GroEL-GroES-(ADP)<sub>7</sub> chaperonin complex. *Nature* 388, 741-750, doi:10.1038/41944 (1997).
- 77 Morán Luengo, T., Kityk, R., Mayer, M. P. & Rüdiger, S. G. D. Hsp90 Breaks the Deadlock of the Hsp70 Chaperone System. *Molecular Cell* 70, 545-552.e549, doi:https://doi.org/10.1016/j.molcel.2018.03.028 (2018).
- 78 Zhang, J. *et al.* Mechanism of folding chamber closure in a group II chaperonin. *Nature* 463, 379-383, doi:10.1038/nature08701 (2010).
- 79 Booth, C. R. *et al.* Mechanism of lid closure in the eukaryotic chaperonin TRiC/CCT. *Nature Structural & Molecular Biology* 15, 746-753, doi:10.1038/nsmb.1436 (2008).
- 80 Spiess, C., Meyer, A. S., Reissmann, S. & Frydman, J. Mechanism of the eukaryotic chaperonin: protein folding in the chamber of secrets. *Trends in Cell Biology* 14, 598-604, doi:https://doi.org/10.1016/j.tcb.2004.09.015 (2004).
- 81 Wang, D. Y., Kamuda, K., Montoya, G. & Mesa, P. The TRiC/CCT Chaperonin and Its Role in Uncontrolled Proliferation. *Adv Exp Med Biol* 1243, 21-40, doi:10.1007/978-3-030-40204-4\_2 (2020).
- 82 Freilich, R. *et al.* Competing protein-protein interactions regulate binding of Hsp27 to its client protein tau. *Nat Commun* 9, 4563, doi:10.1038/s41467-018-07012-4 (2018).
- 83 Young, Z. T. *et al.* Stabilizing the Hsp70-Tau Complex Promotes Turnover in Models of Tauopathy. *Cell Chem Biol* 23, 992-1001, doi:10.1016/j.chembiol.2016.04.014 (2016).

## References

- 84 Karagoz, G. E. *et al.* Hsp90-Tau complex reveals molecular basis for specificity in chaperone action. *Cell* 156, 963-974, doi:10.1016/j.cell.2014.01.037 (2014).
- 85 Jee, H. Size dependent classification of heat shock proteins: a mini-review. *J Exerc Rehabil* 12, 255-259, doi:10.12965/jer.1632642.321 (2016).
- 86 Whitley, D., Goldberg, S. P. & Jordan, W. D. Heat shock proteins: a review of the molecular chaperones. *J Vasc Surg* 29, 748-751, doi:10.1016/s0741-5214(99)70329-0 (1999).
- 87 Kampinga, H. H. *et al.* Guidelines for the nomenclature of the human heat shock proteins. *Cell Stress Chaperones* 14, 105-111, doi:10.1007/s12192-008-0068-7 (2009).
- 88 Zolkiewski, M., Zhang, T. & Nagy, M. Aggregate reactivation mediated by the Hsp100 chaperones. *Arch Biochem Biophys* 520, 1-6, doi:10.1016/j.abb.2012.01.012 (2012).
- 89 Parsell, D. A., Kowal, A. S., Singer, M. A. & Lindquist, S. Protein disaggregation mediated by heat-shock protein Hsp104. *Nature* 372, 475-478, doi:10.1038/372475a0 (1994).
- 90 Richter, K., Haslbeck, M. & Buchner, J. The heat shock response: life on the verge of death. *Mol Cell* 40, 253-266, doi:10.1016/j.molcel.2010.10.006 (2010).
- 91 Hoter, A., El-Sabban, M. E. & Naim, H. Y. The HSP90 Family: Structure, Regulation, Function, and Implications in Health and Disease. *Int J Mol Sci* 19, doi:10.3390/ijms19092560 (2018).
- 92 Zuiderweg, E. R., Hightower, L. E. & Gestwicki, J. E. The remarkable multivalency of the Hsp70 chaperones. *Cell Stress Chaperones* 22, 173-189, doi:10.1007/s12192-017-0776-y (2017).
- 93 Genest, O., Wickner, S. & Doyle, S. M. Hsp90 and Hsp70 chaperones: Collaborators in protein remodeling. *J Biol Chem* 294, 2109-2120, doi:10.1074/jbc.REV118.002806 (2019).
- 94 Morán Luengo, T., Mayer, M. P. & Rüdiger, S. G. D. The Hsp70–Hsp90 Chaperone Cascade in Protein Folding. *Trends in Cell Biology* 29, 164-177, doi:https://doi.org/10.1016/j.tcb.2018.10.004 (2019).
- 95 Ernst, K. *et al.* Hsp70 facilitates trans-membrane transport of bacterial ADP-ribosylating toxins into the cytosol of mammalian cells. *Sci Rep* 7, 2724, doi:10.1038/s41598-017-02882-y (2017).
- 96 Quintana-Gallardo, L. *et al.* The cochaperone CHIP marks Hsp70- and Hsp90-bound substrates for degradation through a very flexible mechanism. *Sci Rep* 9, 5102, doi:10.1038/s41598-019-41060-0 (2019).
- 97 Nillegoda, N. B., Wentink, A. S. & Bukau, B. Protein Disaggregation in Multicellular Organisms. *Trends Biochem Sci* 43, 285-300, doi:10.1016/j.tibs.2018.02.003 (2018).
- 98 Mogk, A. & Bukau, B. Role of sHsps in organizing cytosolic protein aggregation and disaggregation. *Cell Stress Chaperones* 22, 493-502, doi:10.1007/s12192-017-0762-4 (2017).
- 99 Webster, J. M., Darling, A. L., Uversky, V. N. & Blair, L. J. Small Heat Shock Proteins, Big Impact on Protein Aggregation in Neurodegenerative Disease. *Front Pharmacol* 10, 1047, doi:10.3389/fphar.2019.01047 (2019).
- 100 Morimoto, R. I. Cells in stress: transcriptional activation of heat shock genes. *Science* 259, 1409-1410, doi:10.1126/science.8451637 (1993).

## References

- 101 Dayalan Naidu, S. & Dinkova-Kostova, A. T. Regulation of the mammalian heat shock factor 1. *The FEBS Journal* 284, 1606-1627, doi:<https://doi.org/10.1111/febs.13999> (2017).
- 102 Morimoto, R. I. Regulation of the heat shock transcriptional response: cross talk between a family of heat shock factors, molecular chaperones, and negative regulators. *Genes Dev* 12, 3788-3796, doi:10.1101/gad.12.24.3788 (1998).
- 103 Shi, Y., Mosser, D. D. & Morimoto, R. I. Molecular chaperones as HSF1-specific transcriptional repressors. *Genes & Development* 12, 654-666 (1998).
- 104 Ali, A., Bharadwaj, S., O'Carroll, R. & Ovsenek, N. HSP90 interacts with and regulates the activity of heat shock factor 1 in *Xenopus* oocytes. *Mol Cell Biol* 18, 4949-4960, doi:10.1128/mcb.18.9.4949 (1998).
- 105 Neef, D. W. *et al.* A direct regulatory interaction between chaperonin TRiC and stress-responsive transcription factor HSF1. *Cell Rep* 9, 955-966, doi:10.1016/j.celrep.2014.09.056 (2014).
- 106 Zou, J., Guo, Y., Guettouche, T., Smith, D. F. & Voellmy, R. Repression of heat shock transcription factor HSF1 activation by HSP90 (HSP90 complex) that forms a stress-sensitive complex with HSF1. *Cell* 94, 471-480, doi:10.1016/s0092-8674(00)81588-3 (1998).
- 107 Vihervaara, A. & Sistonen, L. HSF1 at a glance. *J Cell Sci* 127, 261-266, doi:10.1242/jcs.132605 (2014).
- 108 Satyal, S. H., Chen, D., Fox, S. G., Kramer, J. M. & Morimoto, R. I. Negative regulation of the heat shock transcriptional response by HSBP1. *Genes Dev* 12, 1962-1974, doi:10.1101/gad.12.13.1962 (1998).
- 109 Qian, S. B., McDonough, H., Boellmann, F., Cyr, D. M. & Patterson, C. CHIP-mediated stress recovery by sequential ubiquitination of substrates and Hsp70. *Nature* 440, 551-555, doi:10.1038/nature04600 (2006).
- 110 Liu, Q., Liang, C. & Zhou, L. Structural and functional analysis of the Hsp70/Hsp40 chaperone system. *Protein Sci* 29, 378-390, doi:10.1002/pro.3725 (2020).
- 111 Li, J. & Buchner, J. Structure, function and regulation of the hsp90 machinery. *Biomed J* 36, 106-117, doi:10.4103/2319-4170.113230 (2013).
- 112 Serlidaki, D. *et al.* Functional diversity between HSP70 paralogs caused by variable interactions with specific co-chaperones. *Journal of Biological Chemistry* 295, 7301-7316, doi:<https://doi.org/10.1074/jbc.RA119.012449> (2020).
- 113 Radli, M. & Rudiger, S. G. D. Dancing with the Diva: Hsp90-Client Interactions. *J Mol Biol* 430, 3029-3040, doi:10.1016/j.jmb.2018.05.026 (2018).
- 114 Faust, O. *et al.* HSP40 proteins use class-specific regulation to drive HSP70 functional diversity. *Nature* 587, 489-494, doi:10.1038/s41586-020-2906-4 (2020).
- 115 Sahasrabudhe, P., Rohrberg, J., Biebl, M. M., Rutz, D. A. & Buchner, J. The Plasticity of the Hsp90 Co-chaperone System. *Mol Cell* 67, 947-961 e945, doi:10.1016/j.molcel.2017.08.004 (2017).

## References

- 116 Wentink, A. S. *et al.* Molecular dissection of amyloid disaggregation by human HSP70. *Nature* 587, 483-488, doi:10.1038/s41586-020-2904-6 (2020).
- 117 Alvira, S. *et al.* Structural characterization of the substrate transfer mechanism in Hsp70/Hsp90 folding machinery mediated by Hop. *Nat Commun* 5, 5484, doi:10.1038/ncomms6484 (2014).
- 118 Wortmann, P., Gotz, M. & Hugel, T. Cooperative Nucleotide Binding in Hsp90 and Its Regulation by Aha1. *Biophys J* 113, 1711-1718, doi:10.1016/j.bpj.2017.08.032 (2017).
- 119 Verba, K. A. *et al.* Atomic structure of Hsp90-Cdc37-Cdk4 reveals that Hsp90 traps and stabilizes an unfolded kinase. *Science* 352, 1542-1547, doi:10.1126/science.aaf5023 (2016).
- 120 Dean, M. E. & Johnson, J. L. Human Hsp90 cochaperones: perspectives on tissue-specific expression and identification of cochaperones with similar in vivo functions. *Cell Stress Chaperones* 26, 3-13, doi:10.1007/s12192-020-01167-0 (2021).
- 121 Oroz, J. *et al.* Structure and pro-toxic mechanism of the human Hsp90/PPIase/Tau complex. *Nat Commun* 9, 4532, doi:10.1038/s41467-018-06880-0 (2018).
- 122 Ali, M. M. *et al.* Crystal structure of an Hsp90-nucleotide-p23/Sba1 closed chaperone complex. *Nature* 440, 1013-1017, doi:10.1038/nature04716 (2006).
- 123 Hohfeld, J., Cyr, D. M. & Patterson, C. From the cradle to the grave: molecular chaperones that may choose between folding and degradation. *EMBO Rep* 2, 885-890, doi:10.1093/embo-reports/kve206 (2001).
- 124 Shorter, J. The mammalian disaggregase machinery: Hsp110 synergizes with Hsp70 and Hsp40 to catalyze protein disaggregation and reactivation in a cell-free system. *PLoS One* 6, e26319, doi:10.1371/journal.pone.0026319 (2011).
- 125 Hanna, J., Guerra-Moreno, A., Ang, J. & Micoogullari, Y. Protein Degradation and the Pathologic Basis of Disease. *Am J Pathol* 189, 94-103, doi:10.1016/j.ajpath.2018.09.004 (2019).
- 126 Johnston, H. E. & Samant, R. S. Alternative systems for misfolded protein clearance: life beyond the proteasome. *FEBS J*, doi:10.1111/febs.15617 (2020).
- 127 Ross, C. A. & Poirier, M. A. Protein aggregation and neurodegenerative disease. *Nat Med* 10 Suppl, S10-17, doi:10.1038/nm1066 (2004).
- 128 Dobson, C. M. Protein aggregation and its consequences for human disease. *Protein Pept Lett* 13, 219-227, doi:10.2174/092986606775338362 (2006).
- 129 Wegele, H., Wandinger, S. K., Schmid, A. B., Reinstein, J. & Buchner, J. Substrate transfer from the chaperone Hsp70 to Hsp90. *J Mol Biol* 356, 802-811, doi:10.1016/j.jmb.2005.12.008 (2006).
- 130 Kirschke, E., Goswami, D., Southworth, D., Griffin, P. R. & Agard, D. A. Glucocorticoid receptor function regulated by coordinated action of the Hsp90 and Hsp70 chaperone cycles. *Cell* 157, 1685-1697, doi:10.1016/j.cell.2014.04.038 (2014).
- 131 Kohler, V. & Andreasson, C. Hsp70-mediated quality control: should I stay or should I go? *Biol Chem* 401, 1233-1248, doi:10.1515/hsz-2020-0187 (2020).

## References

- 132 Clerico, E. M., Tilitky, J. M., Meng, W. & Gierasch, L. M. How hsp70 molecular machines interact with their substrates to mediate diverse physiological functions. *J Mol Biol* 427, 1575-1588, doi:10.1016/j.jmb.2015.02.004 (2015).
- 133 Genest, O., Hoskins, J. R., Camberg, J. L., Doyle, S. M. & Wickner, S. Heat shock protein 90 from *Escherichia coli* collaborates with the DnaK chaperone system in client protein remodeling. *Proc Natl Acad Sci U S A* 108, 8206-8211, doi:10.1073/pnas.1104703108 (2011).
- 134 Genest, O., Hoskins, J. R., Kravats, A. N., Doyle, S. M. & Wickner, S. Hsp70 and Hsp90 of *E. coli* Directly Interact for Collaboration in Protein Remodeling. *J Mol Biol* 427, 3877-3889, doi:10.1016/j.jmb.2015.10.010 (2015).
- 135 Dittmar, K. D., Banach, M., Galigniana, M. D. & Pratt, W. B. The role of DnaJ-like proteins in glucocorticoid receptor.hsp90 heterocomplex assembly by the reconstituted hsp90.p60.hsp70 foldosome complex. *J Biol Chem* 273, 7358-7366, doi:10.1074/jbc.273.13.7358 (1998).
- 136 Lackie, R. E. *et al.* The Hsp70/Hsp90 Chaperone Machinery in Neurodegenerative Diseases. *Front Neurosci* 11, 254, doi:10.3389/fnins.2017.00254 (2017).
- 137 Hernandez, M. P., Sullivan, W. P. & Toft, D. O. The assembly and intermolecular properties of the hsp70-Hop-hsp90 molecular chaperone complex. *J Biol Chem* 277, 38294-38304, doi:10.1074/jbc.M206566200 (2002).
- 138 Kosano, H., Stensgard, B., Charlesworth, M. C., McMahon, N. & Toft, D. The assembly of progesterone receptor-hsp90 complexes using purified proteins. *J Biol Chem* 273, 32973-32979, doi:10.1074/jbc.273.49.32973 (1998).
- 139 Morishima, Y. *et al.* The Hsp organizer protein hop enhances the rate of but is not essential for glucocorticoid receptor folding by the multiprotein Hsp90-based chaperone system. *J Biol Chem* 275, 6894-6900, doi:10.1074/jbc.275.10.6894 (2000).
- 140 Dittmar, K. D., Demady, D. R., Stancato, L. F., Krishna, P. & Pratt, W. B. Folding of the glucocorticoid receptor by the heat shock protein (hsp) 90-based chaperone machinery. The role of p23 is to stabilize receptor.hsp90 heterocomplexes formed by hsp90.p60.hsp70. *J Biol Chem* 272, 21213-21220, doi:10.1074/jbc.272.34.21213 (1997).
- 141 Dittmar, K. D. & Pratt, W. B. Folding of the glucocorticoid receptor by the reconstituted Hsp90-based chaperone machinery. The initial hsp90.p60.hsp70-dependent step is sufficient for creating the steroid binding conformation. *J Biol Chem* 272, 13047-13054, doi:10.1074/jbc.272.20.13047 (1997).
- 142 Hutchison, K. A., Dittmar, K. D., Czar, M. J. & Pratt, W. B. Proof that hsp70 is required for assembly of the glucocorticoid receptor into a heterocomplex with hsp90. *Journal of Biological Chemistry* 269, 5043-5049, doi:https://doi.org/10.1016/S0021-9258(17)37651-2 (1994).
- 143 Schumacher, R. J. *et al.* ATP-dependent chaperoning activity of reticulocyte lysate. *J Biol Chem* 269, 9493-9499 (1994).

## References

- 144 Hutchison, K. A. *et al.* The 23-kDa acidic protein in reticulocyte lysate is the weakly bound component of the hsp foldosome that is required for assembly of the glucocorticoid receptor into a functional heterocomplex with hsp90. *J Biol Chem* 270, 18841-18847, doi:10.1074/jbc.270.32.18841 (1995).
- 145 Johnson, J. L. & Toft, D. O. A novel chaperone complex for steroid receptors involving heat shock proteins, immunophilins, and p23. *J Biol Chem* 269, 24989-24993 (1994).
- 146 Pratt, W. B. & Dittmar, K. D. Studies with Purified Chaperones Advance the Understanding of the Mechanism of Glucocorticoid Receptor-hsp90 Heterocomplex Assembly. *Trends Endocrinol Metab* 9, 244-252, doi:10.1016/s1043-2760(98)00059-9 (1998).
- 147 Pratt, W. B. & Toft, D. O. Regulation of signaling protein function and trafficking by the hsp90/hsp70-based chaperone machinery. *Exp Biol Med (Maywood)* 228, 111-133, doi:10.1177/153537020322800201 (2003).
- 148 Naruse, K., Matsuura-Suzuki, E., Watanabe, M., Iwasaki, S. & Tomari, Y. In vitro reconstitution of chaperone-mediated human RISC assembly. *RNA* 24, 6-11, doi:10.1261/rna.063891.117 (2018).
- 149 Dahiya, V. *et al.* Coordinated Conformational Processing of the Tumor Suppressor Protein p53 by the Hsp70 and Hsp90 Chaperone Machineries. *Mol Cell* 74, 816-830 e817, doi:10.1016/j.molcel.2019.03.026 (2019).
- 150 Hu, J., Toft, D., Anselmo, D. & Wang, X. In Vitro Reconstitution of Functional Hepadnavirus Reverse Transcriptase with Cellular Chaperone Proteins. *Journal of Virology* 76, 269-279, doi:10.1128/jvi.76.1.269-279.2002 (2002).
- 151 Kamal, A. *et al.* A high-affinity conformation of Hsp90 confers tumour selectivity on Hsp90 inhibitors. *Nature* 425, 407-410, doi:10.1038/nature01913 (2003).
- 152 Rosenzweig, R., Nillegoda, N. B., Mayer, M. P. & Bukau, B. The Hsp70 chaperone network. *Nat Rev Mol Cell Biol* 20, 665-680, doi:10.1038/s41580-019-0133-3 (2019).
- 153 Radons, J. The human HSP70 family of chaperones: where do we stand? *Cell Stress Chaperones* 21, 379-404, doi:10.1007/s12192-016-0676-6 (2016).
- 154 Fernandez-Fernandez, M. R. & Valpuesta, J. M. Hsp70 chaperone: a master player in protein homeostasis. *F1000Res* 7, doi:10.12688/f1000research.15528.1 (2018).
- 155 Flaherty, K. M., McKay, D. B., Kabsch, W. & Holmes, K. C. Similarity of the three-dimensional structures of actin and the ATPase fragment of a 70-kDa heat shock cognate protein. *Proc Natl Acad Sci U S A* 88, 5041-5045, doi:10.1073/pnas.88.11.5041 (1991).
- 156 Mayer, M. P. *et al.* Multistep mechanism of substrate binding determines chaperone activity of Hsp70. *Nat Struct Biol* 7, 586-593, doi:10.1038/76819 (2000).
- 157 Arakawa, A., Handa, N., Shirouzu, M. & Yokoyama, S. Biochemical and structural studies on the high affinity of Hsp70 for ADP. *Protein Sci* 20, 1367-1379, doi:10.1002/pro.663 (2011).
- 158 Zhang, P., Leu, J. I., Murphy, M. E., George, D. L. & Marmorstein, R. Crystal structure of the stress-inducible human heat shock protein 70 substrate-binding domain in complex with peptide substrate. *PLoS One* 9, e103518, doi:10.1371/journal.pone.0103518 (2014).



## References

- 159 Kityk, R., Kopp, J. & Mayer, M. P. Molecular Mechanism of J-Domain-Triggered ATP Hydrolysis by Hsp70 Chaperones. *Mol Cell* 69, 227-237 e224, doi:10.1016/j.molcel.2017.12.003 (2018).
- 160 Qi, R. *et al.* Allosteric opening of the polypeptide-binding site when an Hsp70 binds ATP. *Nat Struct Mol Biol* 20, 900-907, doi:10.1038/nsmb.2583 (2013).
- 161 Wittung-Stafshede, P., Guidry, J., Horne, B. E. & Landry, S. J. The J-domain of Hsp40 couples ATP hydrolysis to substrate capture in Hsp70. *Biochemistry* 42, 4937-4944, doi:10.1021/bi027333o (2003).
- 162 Perales-Calvo, J., Giganti, D., Stirnemann, G. & Garcia-Manyes, S. The force-dependent mechanism of DnaK-mediated mechanical folding. *Sci Adv* 4, eaaq0243, doi:10.1126/sciadv.aaq0243 (2018).
- 163 Sousa, R. & Lafer, E. M. The Physics of Entropic Pulling: A Novel Model for the Hsp70 Motor Mechanism. *Int J Mol Sci* 20, doi:10.3390/ijms20092334 (2019).
- 164 Bracher, A. & Verghese, J. The nucleotide exchange factors of Hsp70 molecular chaperones. *Front Mol Biosci* 2, 10, doi:10.3389/fmolb.2015.00010 (2015).
- 165 Szabo, A. *et al.* The ATP hydrolysis-dependent reaction cycle of the Escherichia coli Hsp70 system DnaK, DnaJ, and GrpE. *Proc Natl Acad Sci U S A* 91, 10345-10349, doi:10.1073/pnas.91.22.10345 (1994).
- 166 Rudiger, S., Buchberger, A. & Bukau, B. Interaction of Hsp70 chaperones with substrates. *Nat Struct Biol* 4, 342-349, doi:10.1038/nsb0597-342 (1997).
- 167 Johnson, B. D., Schumacher, R. J., Ross, E. D. & Toft, D. O. Hop modulates Hsp70/Hsp90 interactions in protein folding. *J Biol Chem* 273, 3679-3686, doi:10.1074/jbc.273.6.3679 (1998).
- 168 Kelley, W. L. The J-domain family and the recruitment of chaperone power. *Trends Biochem Sci* 23, 222-227, doi:10.1016/s0968-0004(98)01215-8 (1998).
- 169 Qian, Y. Q., Patel, D., Hartl, F. U. & McColl, D. J. Nuclear magnetic resonance solution structure of the human Hsp40 (HDJ-1) J-domain. *J Mol Biol* 260, 224-235, doi:10.1006/jmbi.1996.0394 (1996).
- 170 Kampinga, H. H. & Craig, E. A. The HSP70 chaperone machinery: J proteins as drivers of functional specificity. *Nat Rev Mol Cell Biol* 11, 579-592, doi:10.1038/nrm2941 (2010).
- 171 Cyr, D. M., Langer, T. & Douglas, M. G. DnaJ-like proteins: molecular chaperones and specific regulators of Hsp70. *Trends Biochem Sci* 19, 176-181, doi:10.1016/0968-0004(94)90281-x (1994).
- 172 Suzuki, H. *et al.* Peptide-binding sites as revealed by the crystal structures of the human Hsp40 Hdj1 C-terminal domain in complex with the octapeptide from human Hsp70. *Biochemistry* 49, 8577-8584, doi:10.1021/bi100876n (2010).
- 173 Yu, H. Y., Ziegelhoffer, T. & Craig, E. A. Functionality of Class A and Class B J-protein co-chaperones with Hsp70. *FEBS Lett* 589, 2825-2830, doi:10.1016/j.febslet.2015.07.040 (2015).

## References

- 174 Fan, C. Y., Lee, S. & Cyr, D. M. Mechanisms for regulation of Hsp70 function by Hsp40. *Cell Stress Chaperones* 8, 309-316, doi:10.1379/1466-1268(2003)008<0309:mfrohf>2.0.co;2 (2003).
- 175 Summers, D. W., Douglas, P. M., Ramos, C. H. & Cyr, D. M. Polypeptide transfer from Hsp40 to Hsp70 molecular chaperones. *Trends Biochem Sci* 34, 230-233, doi:10.1016/j.tibs.2008.12.009 (2009).
- 176 Jiang, Y., Rossi, P. & Kalodimos, C. G. Structural basis for client recognition and activity of Hsp40 chaperones. *Science* 365, 1313-1319, doi:10.1126/science.aax1280 (2019).
- 177 Li, J., Qian, X. & Sha, B. The crystal structure of the yeast Hsp40 Ydj1 complexed with its peptide substrate. *Structure* 11, 1475-1483, doi:10.1016/j.str.2003.10.012 (2003).
- 178 Han, W. & Christen, P. Mechanism of the targeting action of DnaJ in the DnaK molecular chaperone system. *J Biol Chem* 278, 19038-19043, doi:10.1074/jbc.M300756200 (2003).
- 179 Krukenberg, K. A., Street, T. O., Lavery, L. A. & Agard, D. A. Conformational dynamics of the molecular chaperone Hsp90. *Q Rev Biophys* 44, 229-255, doi:10.1017/S0033583510000314 (2011).
- 180 Biebl, M. M. & Buchner, J. Structure, Function, and Regulation of the Hsp90 Machinery. *Cold Spring Harb Perspect Biol* 11, doi:10.1101/cshperspect.a034017 (2019).
- 181 Schopf, F. H., Biebl, M. M. & Buchner, J. The HSP90 chaperone machinery. *Nat Rev Mol Cell Biol* 18, 345-360, doi:10.1038/nrm.2017.20 (2017).
- 182 Dutta, R. & Inouye, M. GHKL, an emergent ATPase/kinase superfamily. *Trends Biochem Sci* 25, 24-28, doi:10.1016/s0968-0004(99)01503-0 (2000).
- 183 Richter, K., Muschler, P., Hainzl, O. & Buchner, J. Coordinated ATP hydrolysis by the Hsp90 dimer. *J Biol Chem* 276, 33689-33696, doi:10.1074/jbc.M103832200 (2001).
- 184 Verma, S., Goyal, S., Jamal, S., Singh, A. & Grover, A. Hsp90: Friends, clients and natural foes. *Biochimie* 127, 227-240, doi:10.1016/j.biochi.2016.05.018 (2016).
- 185 Hainzl, O., Lapina, M. C., Buchner, J. & Richter, K. The charged linker region is an important regulator of Hsp90 function. *J Biol Chem* 284, 22559-22567, doi:10.1074/jbc.M109.031658 (2009).
- 186 Jahn, M. *et al.* The charged linker of the molecular chaperone Hsp90 modulates domain contacts and biological function. *Proc Natl Acad Sci U S A* 111, 17881-17886, doi:10.1073/pnas.1414073111 (2014).
- 187 Lopez, A., Elimelech, A. R., Klimm, K. & Sattler, M. The Charged Linker Modulates the Conformations and Molecular Interactions of Hsp90. *Chembiochem*, doi:10.1002/cbic.202000699 (2020).
- 188 Scheibel, T. *et al.* The charged region of Hsp90 modulates the function of the N-terminal domain. *Proc Natl Acad Sci U S A* 96, 1297-1302, doi:10.1073/pnas.96.4.1297 (1999).
- 189 Tsutsumi, S. *et al.* Charged linker sequence modulates eukaryotic heat shock protein 90 (Hsp90) chaperone activity. *Proc Natl Acad Sci U S A* 109, 2937-2942, doi:10.1073/pnas.1114414109 (2012).

## References

- 190 Cunningham, C. N., Southworth, D. R., Krukenberg, K. A. & Agard, D. A. The conserved arginine 380 of Hsp90 is not a catalytic residue, but stabilizes the closed conformation required for ATP hydrolysis. *Protein Sci* 21, 1162-1171, doi:10.1002/pro.2103 (2012).
- 191 Meyer, P. *et al.* Structural and functional analysis of the middle segment of hsp90: implications for ATP hydrolysis and client protein and cochaperone interactions. *Mol Cell* 11, 647-658, doi:10.1016/s1097-2765(03)00065-0 (2003).
- 192 Brinker, A. *et al.* Ligand discrimination by TPR domains. Relevance and selectivity of EEVD-recognition in Hsp70 x Hop x Hsp90 complexes. *J Biol Chem* 277, 19265-19275, doi:10.1074/jbc.M109002200 (2002).
- 193 Scheufler, C. *et al.* Structure of TPR domain-peptide complexes: critical elements in the assembly of the Hsp70-Hsp90 multichaperone machine. *Cell* 101, 199-210, doi:10.1016/S0092-8674(00)80830-2 (2000).
- 194 Wandinger, S. K., Richter, K. & Buchner, J. The Hsp90 chaperone machinery. *J Biol Chem* 283, 18473-18477, doi:10.1074/jbc.R800007200 (2008).
- 195 Karagoz, G. E. & Rudiger, S. G. Hsp90 interaction with clients. *Trends Biochem Sci* 40, 117-125, doi:10.1016/j.tibs.2014.12.002 (2015).
- 196 Chen, B., Piel, W. H., Gui, L., Bruford, E. & Monteiro, A. The HSP90 family of genes in the human genome: insights into their divergence and evolution. *Genomics* 86, 627-637, doi:10.1016/j.ygeno.2005.08.012 (2005).
- 197 Lee, B. L. *et al.* The Hsp90 Chaperone: (1)H and (19)F Dynamic Nuclear Magnetic Resonance Spectroscopy Reveals a Perfect Enzyme. *Biochemistry* 58, 1869-1877, doi:10.1021/acs.biochem.9b00144 (2019).
- 198 Southworth, D. R. & Agard, D. A. Species-dependent ensembles of conserved conformational states define the Hsp90 chaperone ATPase cycle. *Mol Cell* 32, 631-640, doi:10.1016/j.molcel.2008.10.024 (2008).
- 199 Soti, C., Racz, A. & Csermely, P. A Nucleotide-dependent molecular switch controls ATP binding at the C-terminal domain of Hsp90. N-terminal nucleotide binding unmask a C-terminal binding pocket. *J Biol Chem* 277, 7066-7075, doi:10.1074/jbc.M105568200 (2002).
- 200 Soti, C., Radics, L., Yahara, I. & Csermely, P. Interaction of vanadate oligomers and permolybdate with the 90-kDa heat-shock protein, Hsp90. *Eur J Biochem* 255, 611-617, doi:10.1046/j.1432-1327.1998.2550611.x (1998).
- 201 Panaretou, B. *et al.* Activation of the ATPase activity of hsp90 by the stress-regulated cochaperone aha1. *Mol Cell* 10, 1307-1318, doi:10.1016/s1097-2765(02)00785-2 (2002).
- 202 Richter, K. *et al.* Conserved conformational changes in the ATPase cycle of human Hsp90. *J Biol Chem* 283, 17757-17765, doi:10.1074/jbc.M800540200 (2008).
- 203 Siligardi, G. *et al.* Co-chaperone regulation of conformational switching in the Hsp90 ATPase cycle. *J Biol Chem* 279, 51989-51998, doi:10.1074/jbc.M410562200 (2004).
- 204 Wolmarans, A., Lee, B., Spyrapoulos, L. & LaPointe, P. The Mechanism of Hsp90 ATPase Stimulation by Aha1. *Sci Rep* 6, 33179, doi:10.1038/srep33179 (2016).

## References

- 205 McLaughlin, S. H. *et al.* The co-chaperone p23 arrests the Hsp90 ATPase cycle to trap client  
proteins. *J Mol Biol* 356, 746-758, doi:10.1016/j.jmb.2005.11.085 (2006).
- 206 Richter, K., Muschler, P., Hainzl, O., Reinstein, J. & Buchner, J. Sti1 is a non-competitive  
inhibitor of the Hsp90 ATPase. Binding prevents the N-terminal dimerization reaction  
during the atpase cycle. *J Biol Chem* 278, 10328-10333, doi:10.1074/jbc.M213094200 (2003).
- 207 Schmid, A. B. *et al.* The architecture of functional modules in the Hsp90 co-chaperone  
Sti1/Hop. *EMBO J* 31, 1506-1517, doi:10.1038/emboj.2011.472 (2012).
- 208 Young, J. C., Moarefi, I. & Hartl, F. U. Hsp90: a specialized but essential protein-folding  
tool. *J Cell Biol* 154, 267-273, doi:10.1083/jcb.200104079 (2001).
- 209 Bukau, B. & Horwich, A. L. The Hsp70 and Hsp60 chaperone machines. *Cell* 92, 351-366,  
doi:10.1016/s0092-8674(00)80928-9 (1998).
- 210 Daturpalli, S., Waudby, C. A., Meehan, S. & Jackson, S. E. Hsp90 inhibits alpha-synuclein  
aggregation by interacting with soluble oligomers. *J Mol Biol* 425, 4614-4628,  
doi:10.1016/j.jmb.2013.08.006 (2013).
- 211 Chen, S. & Smith, D. F. Hop as an adaptor in the heat shock protein 70 (Hsp70) and hsp90  
chaperone machinery. *J Biol Chem* 273, 35194-35200, doi:10.1074/jbc.273.52.35194 (1998).
- 212 Perez-Riba, A. & Itzhaki, L. S. The tetratricopeptide-repeat motif is a versatile platform  
that enables diverse modes of molecular recognition. *Curr Opin Struct Biol* 54, 43-49,  
doi:10.1016/j.sbi.2018.12.004 (2019).
- 213 Blatch, G. L. & Lassle, M. The tetratricopeptide repeat: a structural motif mediating  
protein-protein interactions. *Bioessays* 21, 932-939, doi:10.1002/(SICI)1521-  
1878(199911)21:11<932::AID-BIES5>3.0.CO;2-N (1999).
- 214 Rohl, A. *et al.* Hsp90 regulates the dynamics of its cochaperone Sti1 and the transfer of  
Hsp70 between modules. *Nat Commun* 6, 6655, doi:10.1038/ncomms7655 (2015).
- 215 Southworth, D. R. & Agard, D. A. Client-loading conformation of the Hsp90 molecular  
chaperone revealed in the cryo-EM structure of the human Hsp90:Hop complex. *Mol Cell*  
42, 771-781, doi:10.1016/j.molcel.2011.04.023 (2011).
- 216 Onuoha, S. C., Coulstock, E. T., Grossmann, J. G. & Jackson, S. E. Structural studies on  
the co-chaperone Hop and its complexes with Hsp90. *J Mol Biol* 379, 732-744,  
doi:10.1016/j.jmb.2008.02.013 (2008).
- 217 Felts, S. J. & Toft, D. O. p23, a simple protein with complex activities. *Cell Stress Chaperones*  
8, 108-113, doi:10.1379/1466-1268(2003)008<0108:paspwc>2.0.co;2 (2003).
- 218 Rehn, A. B. & Buchner, J. p23 and Aha1. *Subcell Biochem* 78, 113-131, doi:10.1007/978-3-  
319-11731-7\_6 (2015).
- 219 Johnson, J. L. & Toft, D. O. Binding of p23 and hsp90 during assembly with the  
progesterone receptor. *Mol Endocrinol* 9, 670-678, doi:10.1210/mend.9.6.8592513 (1995).
- 220 Sullivan, W. *et al.* Nucleotides and two functional states of hsp90. *J Biol Chem* 272, 8007-  
8012, doi:10.1074/jbc.272.12.8007 (1997).

## References

- 221 Karagoz, G. E. *et al.* N-terminal domain of human Hsp90 triggers binding to the cochaperone p23. *Proc Natl Acad Sci U S A* 108, 580-585, doi:10.1073/pnas.1011867108 (2011).
- 222 Martinez-Yamout, M. A. *et al.* Localization of sites of interaction between p23 and Hsp90 in solution. *J Biol Chem* 281, 14457-14464, doi:10.1074/jbc.M601759200 (2006).
- 223 Weaver, A. J., Sullivan, W. P., Felts, S. J., Owen, B. A. & Toft, D. O. Crystal structure and activity of human p23, a heat shock protein 90 co-chaperone. *J Biol Chem* 275, 23045-23052, doi:10.1074/jbc.M003410200 (2000).
- 224 Weikl, T., Abelmann, K. & Buchner, J. An unstructured C-terminal region of the Hsp90 co-chaperone p23 is important for its chaperone function. *J Mol Biol* 293, 685-691, doi:10.1006/jmbi.1999.3172 (1999).
- 225 Seraphim, T. V. *et al.* The C-terminal region of the human p23 chaperone modulates its structure and function. *Arch Biochem Biophys* 565, 57-67, doi:10.1016/j.abb.2014.10.015 (2015).
- 226 Biebl, M. M. *et al.* Structural elements in the flexible tail of the co-chaperone p23 coordinate client binding and progression of the Hsp90 chaperone cycle. *Nat Commun* 12, 828, doi:10.1038/s41467-021-21063-0 (2021).
- 227 Bagneris, C. *et al.* Crystal structures of alpha-crystallin domain dimers of alphaB-crystallin and Hsp20. *J Mol Biol* 392, 1242-1252, doi:10.1016/j.jmb.2009.07.069 (2009).
- 228 Sullivan, W. P., Owen, B. A. & Toft, D. O. The influence of ATP and p23 on the conformation of hsp90. *J Biol Chem* 277, 45942-45948, doi:10.1074/jbc.M207754200 (2002).
- 229 Bose, S., Weikl, T., Bugl, H. & Buchner, J. Chaperone function of Hsp90-associated proteins. *Science* 274, 1715-1717, doi:10.1126/science.274.5293.1715 (1996).
- 230 Forafonov, F. *et al.* p23/Sba1p protects against Hsp90 inhibitors independently of its intrinsic chaperone activity. *Mol Cell Biol* 28, 3446-3456, doi:10.1128/MCB.02246-07 (2008).
- 231 Freeman, B. C., Toft, D. O. & Morimoto, R. I. Molecular chaperone machines: chaperone activities of the cyclophilin Cyp-40 and the steroid aporeceptor-associated protein p23. *Science* 274, 1718-1720, doi:10.1126/science.274.5293.1718 (1996).
- 232 Garcia-Ranea, J. A., Mirey, G., Camonis, J. & Valencia, A. p23 and HSP20/alpha-crystallin proteins define a conserved sequence domain present in other eukaryotic protein families. *FEBS Lett* 529, 162-167, doi:10.1016/s0014-5793(02)03321-5 (2002).
- 233 Carra, S. *et al.* The growing world of small heat shock proteins: from structure to functions. *Cell Stress Chaperones* 22, 601-611, doi:10.1007/s12192-017-0787-8 (2017).
- 234 Wu, H., Hyun, J., Martinez-Yamout, M. A., Park, S. J. & Dyson, H. J. Characterization of an Hsp90-Independent Interaction between Co-Chaperone p23 and Transcription Factor p53. *Biochemistry* 57, 935-944, doi:10.1021/acs.biochem.7b01076 (2018).

## References

- 235 Morgner, N. *et al.* Hsp70 forms antiparallel dimers stabilized by post-translational modifications to position clients for transfer to Hsp90. *Cell Rep* 11, 759-769, doi:10.1016/j.celrep.2015.03.063 (2015).
- 236 Morishima, Y. *et al.* The hsp90 cochaperone p23 is the limiting component of the multiprotein hsp90/hsp70-based chaperone system in vivo where it acts to stabilize the client protein: hsp90 complex. *J Biol Chem* 278, 48754-48763, doi:10.1074/jbc.M309814200 (2003).
- 237 Picard, D. Intracellular dynamics of the Hsp90 co-chaperone p23 is dictated by Hsp90. *Exp Cell Res* 312, 198-204, doi:10.1016/j.yexcr.2005.10.009 (2006).
- 238 Richter, K., Walter, S. & Buchner, J. The Co-chaperone Sba1 connects the ATPase reaction of Hsp90 to the progression of the chaperone cycle. *J Mol Biol* 342, 1403-1413, doi:10.1016/j.jmb.2004.07.064 (2004).
- 239 Birol, M. & Melo, A. M. Untangling the Conformational Polymorphism of Disordered Proteins Associated With Neurodegeneration at the Single-Molecule Level. *Front Mol Neurosci* 12, 309, doi:10.3389/fnmol.2019.00309 (2019).
- 240 Martinelli, A. H. S., Lopes, F. C., John, E. B. O., Carlini, C. R. & Ligabue-Braun, R. Modulation of Disordered Proteins with a Focus on Neurodegenerative Diseases and Other Pathologies. *Int J Mol Sci* 20, doi:10.3390/ijms20061322 (2019).
- 241 Burmann, B. M. *et al.* Regulation of alpha-synuclein by chaperones in mammalian cells. *Nature* 577, 127-132, doi:10.1038/s41586-019-1808-9 (2020).
- 242 Jinwal, U. K. *et al.* Imbalance of Hsp70 family variants fosters tau accumulation. *FASEB J* 27, 1450-1459, doi:10.1096/fj.12-220889 (2013).
- 243 Vymetal, J., Vondrasek, J. & Hlouchova, K. Sequence Versus Composition: What Prescribes IDP Biophysical Properties? *Entropy (Basel)* 21, doi:10.3390/e21070654 (2019).
- 244 Dunker, A. K. *et al.* Intrinsically disordered protein. *J Mol Graph Model* 19, 26-59, doi:10.1016/s1093-3263(00)00138-8 (2001).
- 245 Oldfield, C. J. & Dunker, A. K. Intrinsically disordered proteins and intrinsically disordered protein regions. *Annu Rev Biochem* 83, 553-584, doi:10.1146/annurev-biochem-072711-164947 (2014).
- 246 Fung, H. Y. J., Birol, M. & Rhoades, E. IDPs in macromolecular complexes: the roles of multivalent interactions in diverse assemblies. *Curr Opin Struct Biol* 49, 36-43, doi:10.1016/j.sbi.2017.12.007 (2018).
- 247 Balendiran, G. K. *et al.* Crystal structure and thermodynamic analysis of human brain fatty acid-binding protein. *J Biol Chem* 275, 27045-27054, doi:10.1074/jbc.M003001200 (2000).
- 248 Leach, B. I. *et al.* Leukemia fusion target AF9 is an intrinsically disordered transcriptional regulator that recruits multiple partners via coupled folding and binding. *Structure* 21, 176-183, doi:10.1016/j.str.2012.11.011 (2013).
- 249 Nordyke, C. T., Ahmed, Y. M., Puterbaugh, R. Z., Bowman, G. R. & Varga, K. Intrinsically Disordered Bacterial Polar Organizing Protein Z, PopZ, Interacts with Protein Binding

## References

- Partners Through an N-terminal Molecular Recognition Feature. *J Mol Biol* 432, 6092-6107, doi:10.1016/j.jmb.2020.09.020 (2020).
- 250 Sturlese, M. *et al.* The lineage-specific, intrinsically disordered N-terminal extension of monothiol glutaredoxin 1 from trypanosomes contains a regulatory region. *Sci Rep* 8, 13716, doi:10.1038/s41598-018-31817-4 (2018).
- 251 Junod, S. L., Kelich, J. M., Ma, J. & Yang, W. Nucleocytoplasmic transport of intrinsically disordered proteins studied by high-speed super-resolution microscopy. *Protein Sci* 29, 1459-1472, doi:10.1002/pro.3845 (2020).
- 252 Rezaei-Ghaleh, N. *et al.* Local and Global Dynamics in Intrinsically Disordered Synuclein. *Angew Chem Int Ed Engl* 57, 15262-15266, doi:10.1002/anie.201808172 (2018).
- 253 van der Lee, R. *et al.* Classification of intrinsically disordered regions and proteins. *Chem Rev* 114, 6589-6631, doi:10.1021/cr400525m (2014).
- 254 Wang, Y. & Mandelkow, E. Tau in physiology and pathology. *Nat Rev Neurosci* 17, 5-21, doi:10.1038/nrn.2015.1 (2016).
- 255 Wright, P. E. & Dyson, H. J. Intrinsically disordered proteins in cellular signalling and regulation. *Nat Rev Mol Cell Biol* 16, 18-29, doi:10.1038/nrm3920 (2015).
- 256 Babu, M. M., van der Lee, R., de Groot, N. S. & Gsponer, J. Intrinsically disordered proteins: regulation and disease. *Curr Opin Struct Biol* 21, 432-440, doi:10.1016/j.sbi.2011.03.011 (2011).
- 257 Mukrasch, M. D. *et al.* Structural polymorphism of 441-residue tau at single residue resolution. *PLoS Biol* 7, e34, doi:10.1371/journal.pbio.1000034 (2009).
- 258 Uversky, V. N. Intrinsically disordered proteins and their environment: effects of strong denaturants, temperature, pH, counter ions, membranes, binding partners, osmolytes, and macromolecular crowding. *Protein J* 28, 305-325, doi:10.1007/s10930-009-9201-4 (2009).
- 259 Fuxreiter, M. Fuzziness: linking regulation to protein dynamics. *Mol Biosyst* 8, 168-177, doi:10.1039/c1mb05234a (2012).
- 260 Linding, R., Schymkowitz, J., Rousseau, F., Diella, F. & Serrano, L. A comparative study of the relationship between protein structure and beta-aggregation in globular and intrinsically disordered proteins. *J Mol Biol* 342, 345-353, doi:10.1016/j.jmb.2004.06.088 (2004).
- 261 Marsh, A. P. Molecular mechanisms of proteinopathies across neurodegenerative disease: a review. *Neurol Res Pract* 1, 35, doi:10.1186/s42466-019-0039-8 (2019).
- 262 Morris, A. M., Watzky, M. A. & Finke, R. G. Protein aggregation kinetics, mechanism, and curve-fitting: a review of the literature. *Biochim Biophys Acta* 1794, 375-397, doi:10.1016/j.bbapap.2008.10.016 (2009).
- 263 von Bergen, M., Barghorn, S., Biernat, J., Mandelkow, E.-M. & Mandelkow, E. Tau aggregation is driven by a transition from random coil to beta sheet structure. *Biochimica et Biophysica Acta (BBA) - Molecular Basis of Disease* 1739, 158-166, doi:https://doi.org/10.1016/j.bbadis.2004.09.010 (2005).

## References

- 264 Bayer, T. A. Proteinopathies, a core concept for understanding and ultimately treating degenerative disorders? *Eur Neuropsychopharmacol* 25, 713-724, doi:10.1016/j.euroneuro.2013.03.007 (2015).
- 265 Lanson, N. A., Jr. & Pandey, U. B. FUS-related proteinopathies: lessons from animal models. *Brain Res* 1462, 44-60, doi:10.1016/j.brainres.2012.01.039 (2012).
- 266 Lee, V. M., Goedert, M. & Trojanowski, J. Q. Neurodegenerative tauopathies. *Annu Rev Neurosci* 24, 1121-1159, doi:10.1146/annurev.neuro.24.1.1121 (2001).
- 267 Arendt, T., Stieler, J. T. & Holzer, M. Tau and tauopathies. *Brain Res Bull* 126, 238-292, doi:10.1016/j.brainresbull.2016.08.018 (2016).
- 268 Mamun, A. A., Uddin, M. S., Mathew, B. & Ashraf, G. M. Toxic tau: structural origins of tau aggregation in Alzheimer's disease. *Neural Regen Res* 15, 1417-1420, doi:10.4103/1673-5374.274329 (2020).
- 269 Kadavath, H. *et al.* Tau stabilizes microtubules by binding at the interface between tubulin heterodimers. *Proc Natl Acad Sci U S A* 112, 7501-7506, doi:10.1073/pnas.1504081112 (2015).
- 270 Hernandez, F. *et al.* New Beginnings in Alzheimer's Disease: The Most Prevalent Tauopathy. *J Alzheimers Dis* 64, S529-S534, doi:10.3233/JAD-179916 (2018).
- 271 Du, X., Wang, X. & Geng, M. Alzheimer's disease hypothesis and related therapies. *Transl Neurodegener* 7, 2, doi:10.1186/s40035-018-0107-y (2018).
- 272 Lyketsos, C. G. Treatment Development for Alzheimer's Disease: How Are We Doing? *Adv Exp Med Biol* 1195, 19, doi:10.1007/978-3-030-32633-3\_3 (2020).
- 273 Atri, A. The Alzheimer's Disease Clinical Spectrum: Diagnosis and Management. *Med Clin North Am* 103, 263-293, doi:10.1016/j.mcna.2018.10.009 (2019).
- 274 Association, A. s. 2019 Alzheimer's disease facts and figures. *Alzheimer's & Dementia* 15, 321-387, doi:https://doi.org/10.1016/j.jalz.2019.01.010 (2019).
- 275 Jeganathan, S., von Bergen, M., Mandelkow, E. M. & Mandelkow, E. The natively unfolded character of tau and its aggregation to Alzheimer-like paired helical filaments. *Biochemistry* 47, 10526-10539, doi:10.1021/bi800783d (2008).
- 276 Mandelkow, E., von Bergen, M., Biernat, J. & Mandelkow, E. M. Structural principles of tau and the paired helical filaments of Alzheimer's disease. *Brain Pathol* 17, 83-90, doi:10.1111/j.1750-3639.2007.00053.x (2007).
- 277 Goedert, M., Spillantini, M. G., Jakes, R., Rutherford, D. & Crowther, R. A. Multiple isoforms of human microtubule-associated protein tau: sequences and localization in neurofibrillary tangles of Alzheimer's disease. *Neuron* 3, 519-526, doi:10.1016/0896-6273(89)90210-9 (1989).
- 278 Gustke, N., Trinczek, B., Biernat, J., Mandelkow, E. M. & Mandelkow, E. Domains of tau protein and interactions with microtubules. *Biochemistry* 33, 9511-9522, doi:10.1021/bi00198a017 (1994).
- 279 Santarella, R. A. *et al.* Surface-decoration of microtubules by human tau. *J Mol Biol* 339, 539-553, doi:10.1016/j.jmb.2004.04.008 (2004).



## References

- 280 Brouhard, G. J. & Rice, L. M. Microtubule dynamics: an interplay of biochemistry and  
mechanics. *Nat Rev Mol Cell Biol* 19, 451-463, doi:10.1038/s41580-018-0009-y (2018).
- 281 Chen, J., Kanai, Y., Cowan, N. J. & Hirokawa, N. Projection domains of MAP2 and tau  
determine spacings between microtubules in dendrites and axons. *Nature* 360, 674-677,  
doi:10.1038/360674a0 (1992).
- 282 Melkova, K. *et al.* Structure and Functions of Microtubule Associated Proteins Tau and  
MAP2c: Similarities and Differences. *Biomolecules* 9, doi:10.3390/biom9030105 (2019).
- 283 Tracy, T. E. & Gan, L. Tau-mediated synaptic and neuronal dysfunction in  
neurodegenerative disease. *Curr Opin Neurobiol* 51, 134-138,  
doi:10.1016/j.conb.2018.04.027 (2018).
- 284 Goedert, M. & Jakes, R. Expression of separate isoforms of human tau protein: correlation  
with the tau pattern in brain and effects on tubulin polymerization. *EMBO J* 9, 4225-4230  
(1990).
- 285 Combs, B., Mueller, R. L., Morfini, G., Brady, S. T. & Kanaan, N. M. Tau and Axonal  
Transport Misregulation in Tauopathies. *Adv Exp Med Biol* 1184, 81-95, doi:10.1007/978-  
981-32-9358-8\_7 (2019).
- 286 Biundo, F., Del Prete, D., Zhang, H., Arancio, O. & D'Adamio, L. A role for tau in learning,  
memory and synaptic plasticity. *Sci Rep* 8, 3184, doi:10.1038/s41598-018-21596-3 (2018).
- 287 Kellogg, E. H. *et al.* Near-atomic model of microtubule-tau interactions. *Science* 360, 1242-  
1246, doi:10.1126/science.aat1780 (2018).
- 288 Johnson, G. V. & Stoothoff, W. H. Tau phosphorylation in neuronal cell function and  
dysfunction. *J Cell Sci* 117, 5721-5729, doi:10.1242/jcs.01558 (2004).
- 289 Morris, M. *et al.* Tau post-translational modifications in wild-type and human amyloid  
precursor protein transgenic mice. *Nat Neurosci* 18, 1183-1189, doi:10.1038/nn.4067 (2015).
- 290 Trushina, N. I., Bakota, L., Mulikdjanian, A. Y. & Brandt, R. The Evolution of Tau  
Phosphorylation and Interactions. *Front Aging Neurosci* 11, 256,  
doi:10.3389/fnagi.2019.00256 (2019).
- 291 Alonso, A., Zaidi, T., Novak, M., Grundke-Iqbal, I. & Iqbal, K. Hyperphosphorylation  
induces self-assembly of tau into tangles of paired helical filaments/straight filaments. *Proc  
Natl Acad Sci U S A* 98, 6923-6928, doi:10.1073/pnas.121119298 (2001).
- 292 Barghorn, S., Davies, P. & Mandelkow, E. Tau paired helical filaments from Alzheimer's  
disease brain and assembled in vitro are based on beta-structure in the core domain.  
*Biochemistry* 43, 1694-1703, doi:10.1021/bi0357006 (2004).
- 293 Hanger, D. P., Anderton, B. H. & Noble, W. Tau phosphorylation: the therapeutic  
challenge for neurodegenerative disease. *Trends Mol Med* 15, 112-119,  
doi:10.1016/j.molmed.2009.01.003 (2009).
- 294 Thies, E. & Mandelkow, E. M. Missorting of tau in neurons causes degeneration of  
synapses that can be rescued by the kinase MARK2/Par-1. *J Neurosci* 27, 2896-2907,  
doi:10.1523/JNEUROSCI.4674-06.2007 (2007).

## References

- 295 Dickey, C. A. *et al.* The high-affinity HSP90-CHIP complex recognizes and selectively degrades phosphorylated tau client proteins. *J Clin Invest* 117, 648-658, doi:10.1172/JCI29715 (2007).
- 296 Grundke-Iqbal, I. *et al.* Microtubule-associated protein tau. A component of Alzheimer paired helical filaments. *J Biol Chem* 261, 6084-6089 (1986).
- 297 Cohen, T. J. *et al.* The acetylation of tau inhibits its function and promotes pathological tau aggregation. *Nat Commun* 2, 252, doi:10.1038/ncomms1255 (2011).
- 298 Cook, C. *et al.* Acetylation of the KXGS motifs in tau is a critical determinant in modulation of tau aggregation and clearance. *Hum Mol Genet* 23, 104-116, doi:10.1093/hmg/ddt402 (2014).
- 299 Min, S. W. *et al.* Acetylation of tau inhibits its degradation and contributes to tauopathy. *Neuron* 67, 953-966, doi:10.1016/j.neuron.2010.08.044 (2010).
- 300 Liu, F. *et al.* Role of glycosylation in hyperphosphorylation of tau in Alzheimer's disease. *FEBS Lett* 512, 101-106, doi:10.1016/s0014-5793(02)02228-7 (2002).
- 301 Wang, J. Z., Grundke-Iqbal, I. & Iqbal, K. Glycosylation of microtubule-associated protein tau: an abnormal posttranslational modification in Alzheimer's disease. *Nat Med* 2, 871-875, doi:10.1038/nm0896-871 (1996).
- 302 Meraz-Rios, M. A., Lira-De Leon, K. I., Campos-Pena, V., De Anda-Hernandez, M. A. & Mena-Lopez, R. Tau oligomers and aggregation in Alzheimer's disease. *J Neurochem* 112, 1353-1367, doi:10.1111/j.1471-4159.2009.06511.x (2010).
- 303 Pavlova, A. *et al.* Protein structural and surface water rearrangement constitute major events in the earliest aggregation stages of tau. *Proc Natl Acad Sci U S A* 113, E127-136, doi:10.1073/pnas.1504415113 (2016).
- 304 Lasagna-Reeves, C. A. *et al.* Identification of oligomers at early stages of tau aggregation in Alzheimer's disease. *FASEB J* 26, 1946-1959, doi:10.1096/fj.11-199851 (2012).
- 305 Scheres, S. H., Zhang, W., Falcon, B. & Goedert, M. Cryo-EM structures of tau filaments. *Curr Opin Struct Biol* 64, 17-25, doi:10.1016/j.sbi.2020.05.011 (2020).
- 306 Falcon, B. *et al.* Structures of filaments from Pick's disease reveal a novel tau protein fold. *Nature* 561, 137-140, doi:10.1038/s41586-018-0454-y (2018).
- 307 Fitzpatrick, A. W. P. *et al.* Cryo-EM structures of tau filaments from Alzheimer's disease. *Nature* 547, 185-190, doi:10.1038/nature23002 (2017).
- 308 Goedert, M., Falcon, B., Zhang, W., Ghetti, B. & Scheres, S. H. W. Distinct Conformers of Assembled Tau in Alzheimer's and Pick's Diseases. *Cold Spring Harb Symp Quant Biol* 83, 163-171, doi:10.1101/sqb.2018.83.037580 (2018).
- 309 Dregni, A. J. *et al.* In vitro 0N4R tau fibrils contain a monomorphic beta-sheet core enclosed by dynamically heterogeneous fuzzy coat segments. *Proc Natl Acad Sci U S A* 116, 16357-16366, doi:10.1073/pnas.1906839116 (2019).
- 310 Wegmann, S., Medalsy, I. D., Mandelkow, E. & Muller, D. J. The fuzzy coat of pathological human Tau fibrils is a two-layered polyelectrolyte brush. *Proc Natl Acad Sci U S A* 110, E313-321, doi:10.1073/pnas.1212100110 (2013).

## References

- 311 Zhukareva, V. *et al.* Loss of brain tau defines novel sporadic and familial tauopathies with frontotemporal dementia. *Ann Neurol* 49, 165-175, doi:10.1002/1531-8249(20010201)49:2<165::aid-ana36>3.0.co;2-3 (2001).
- 312 Lasagna-Reeves, C. A. *et al.* Alzheimer brain-derived tau oligomers propagate pathology from endogenous tau. *Sci Rep* 2, 700, doi:10.1038/srep00700 (2012).
- 313 Maeda, S. *et al.* Granular tau oligomers as intermediates of tau filaments. *Biochemistry* 46, 3856-3861, doi:10.1021/bi061359o (2007).
- 314 Ballatore, C., Lee, V. M. & Trojanowski, J. Q. Tau-mediated neurodegeneration in Alzheimer's disease and related disorders. *Nat Rev Neurosci* 8, 663-672, doi:10.1038/nrn2194 (2007).
- 315 LaFerla, F. M. & Oddo, S. Alzheimer's disease: Abeta, tau and synaptic dysfunction. *Trends Mol Med* 11, 170-176, doi:10.1016/j.molmed.2005.02.009 (2005).
- 316 Sato, C. *et al.* Tau Kinetics in Neurons and the Human Central Nervous System. *Neuron* 97, 1284-1298 e1287, doi:10.1016/j.neuron.2018.02.015 (2018).
- 317 Clavaguera, F., Grueninger, F. & Tolnay, M. Intercellular transfer of tau aggregates and spreading of tau pathology: Implications for therapeutic strategies. *Neuropharmacology* 76 Pt A, 9-15, doi:10.1016/j.neuropharm.2013.08.037 (2014).
- 318 Nizynski, B., Dzwolak, W. & Nieznanski, K. Amyloidogenesis of Tau protein. *Protein Sci* 26, 2126-2150, doi:10.1002/pro.3275 (2017).
- 319 Frost, B., Gotz, J. & Feany, M. B. Connecting the dots between tau dysfunction and neurodegeneration. *Trends Cell Biol* 25, 46-53, doi:10.1016/j.tcb.2014.07.005 (2015).
- 320 Hervas, R. & Oroz, J. Mechanistic Insights into the Role of Molecular Chaperones in Protein Misfolding Diseases: From Molecular Recognition to Amyloid Disassembly. *Int J Mol Sci* 21, doi:10.3390/ijms21239186 (2020).
- 321 Thompson, A. D. *et al.* Analysis of the tau-associated proteome reveals that exchange of Hsp70 for Hsp90 is involved in tau degradation. *ACS Chem Biol* 7, 1677-1686, doi:10.1021/cb3002599 (2012).
- 322 Blair, L. J. *et al.* Accelerated neurodegeneration through chaperone-mediated oligomerization of tau. *J Clin Invest* 123, 4158-4169, doi:10.1172/JCI69003 (2013).
- 323 Petrucelli, L. *et al.* CHIP and Hsp70 regulate tau ubiquitination, degradation and aggregation. *Hum Mol Genet* 13, 703-714, doi:10.1093/hmg/ddh083 (2004).
- 324 Dou, F. *et al.* Chaperones increase association of tau protein with microtubules. *Proc Natl Acad Sci U S A* 100, 721-726, doi:10.1073/pnas.242720499 (2003).
- 325 Nachman, E. *et al.* Disassembly of Tau fibrils by the human Hsp70 disaggregation machinery generates small seeding-competent species. *J Biol Chem* 295, 9676-9690, doi:10.1074/jbc.RA120.013478 (2020).
- 326 Paholikova, K. *et al.* N-terminal truncation of microtubule associated protein tau dysregulates its cellular localization. *J Alzheimers Dis* 43, 915-926, doi:10.3233/JAD-140996 (2015).

## References

- 327 Gasteiger, E. *et al.* ExPASy: The proteomics server for in-depth protein knowledge and analysis. *Nucleic Acids Res* 31, 3784-3788, doi:10.1093/nar/gkg563 (2003).
- 328 Madeira, F. *et al.* The EMBL-EBI search and sequence analysis tools APIs in 2019. *Nucleic Acids Res* 47, W636-W641, doi:10.1093/nar/gkz268 (2019).
- 329 Tugarinov, V., Kanelis, V. & Kay, L. E. Isotope labeling strategies for the study of high-molecular-weight proteins by solution NMR spectroscopy. *Nat Protoc* 1, 749-754, doi:10.1038/nprot.2006.101 (2006).
- 330 Pollard, T. D. A guide to simple and informative binding assays. *Mol Biol Cell* 21, 4061-4067, doi:10.1091/mbc.E10-08-0683 (2010).
- 331 Wiseman, T., Williston, S., Brandts, J. F. & Lin, L. N. Rapid measurement of binding constants and heats of binding using a new titration calorimeter. *Anal Biochem* 179, 131-137, doi:10.1016/0003-2697(89)90213-3 (1989).
- 332 Varese, M., Guardiola, S., Garcia, J. & Giralt, E. Enthalpy- versus Entropy-Driven Molecular Recognition in the Era of Biologics. *Chembiochem* 20, 2981-2986, doi:10.1002/cbic.201900270 (2019).
- 333 Bodenhausen, G. & Ruben, D. J. Natural abundance nitrogen-15 NMR by enhanced heteronuclear spectroscopy. *Chemical Physics Letters* 69, 185-189, doi:https://doi.org/10.1016/0009-2614(80)80041-8 (1980).
- 334 Schutz, S. & Sprangers, R. Methyl TROSY spectroscopy: A versatile NMR approach to study challenging biological systems. *Prog Nucl Magn Reson Spectrosc* 116, 56-84, doi:10.1016/j.pnmrs.2019.09.004 (2020).
- 335 Tugarinov, V., Hwang, P. M., Ollerenshaw, J. E. & Kay, L. E. Cross-correlated relaxation enhanced  $^1\text{H}$ [bond] $^{13}\text{C}$  NMR spectroscopy of methyl groups in very high molecular weight proteins and protein complexes. *J Am Chem Soc* 125, 10420-10428, doi:10.1021/ja030153x (2003).
- 336 Lee, W., Tonelli, M. & Markley, J. L. NMRFAM-SPARKY: enhanced software for biomolecular NMR spectroscopy. *Bioinformatics* 31, 1325-1327, doi:10.1093/bioinformatics/btu830 (2015).
- 337 Williamson, M. P. Using chemical shift perturbation to characterise ligand binding. *Progress in Nuclear Magnetic Resonance Spectroscopy* 73, 1-16, doi:https://doi.org/10.1016/j.pnmrs.2013.02.001 (2013).
- 338 Schrodinger, LLC. *The PyMOL Molecular Graphics System, Version 2.0.4* (2015).
- 339 Stetefeld, J., McKenna, S. A. & Patel, T. R. Dynamic light scattering: a practical guide and applications in biomedical sciences. *Biophys Rev* 8, 409-427, doi:10.1007/s12551-016-0218-6 (2016).
- 340 Cox, J. & Mann, M. MaxQuant enables high peptide identification rates, individualized p.p.b.-range mass accuracies and proteome-wide protein quantification. *Nat Biotechnol* 26, 1367-1372, doi:10.1038/nbt.1511 (2008).

## References

- 341 Chen, Z. L. *et al.* A high-speed search engine pLink 2 with systematic evaluation for proteome-scale identification of cross-linked peptides. *Nat Commun* 10, 3404, doi:10.1038/s41467-019-11337-z (2019).
- 342 Cheeseman, M. D. *et al.* Exploiting Protein Conformational Change to Optimize Adenosine-Derived Inhibitors of HSP70. *J Med Chem* 59, 4625-4636, doi:10.1021/acs.jmedchem.5b02001 (2016).
- 343 Grimm, M., Zimniak, T., Kahraman, A. & Herzog, F. xVis: a web server for the schematic visualization and interpretation of crosslink-derived spatial restraints. *Nucleic Acids Res* 43, W362-369, doi:10.1093/nar/gkv463 (2015).
- 344 Li, J., Richter, K. & Buchner, J. Mixed Hsp90-cochaperone complexes are important for the progression of the reaction cycle. *Nat Struct Mol Biol* 18, 61-66, doi:10.1038/nsmb.1965 (2011).
- 345 Prodromou, C. *et al.* Regulation of Hsp90 ATPase activity by tetratricopeptide repeat (TPR)-domain co-chaperones. *EMBO J* 18, 754-762, doi:10.1093/emboj/18.3.754 (1999).
- 346 Oroz, J., Blair, L. J. & Zweckstetter, M. Dynamic Aha1 co-chaperone binding to human Hsp90. *Protein Sci* 28, 1545-1551, doi:10.1002/pro.3678 (2019).
- 347 Angelidis, C. E., Lazaridis, I. & Pagoulatos, G. N. Aggregation of hsp70 and hsc70 in vivo is distinct and temperature-dependent and their chaperone function is directly related to non-aggregated forms. *Eur J Biochem* 259, 505-512, doi:10.1046/j.1432-1327.1999.00078.x (1999).
- 348 Aprile, F. A. *et al.* Hsp70 oligomerization is mediated by an interaction between the interdomain linker and the substrate-binding domain. *PLoS One* 8, e67961, doi:10.1371/journal.pone.0067961 (2013).
- 349 Nemoto, T. K., Fukuma, Y., Itoh, H., Takagi, T. & Ono, T. A disulfide bridge mediated by cysteine 574 is formed in the dimer of the 70-kDa heat shock protein. *J Biochem* 139, 677-687, doi:10.1093/jb/mvj071 (2006).
- 350 Sillen, A. *et al.* NMR investigation of the interaction between the neuronal protein tau and the microtubules. *Biochemistry* 46, 3055-3064, doi:10.1021/bi061920i (2007).
- 351 Trinczek, B., Biernat, J., Baumann, K., Mandelkow, E. M. & Mandelkow, E. Domains of tau protein, differential phosphorylation, and dynamic instability of microtubules. *Mol Biol Cell* 6, 1887-1902, doi:10.1091/mbc.6.12.1887 (1995).
- 352 Shi, Y. *et al.* Structural characterization by cross-linking reveals the detailed architecture of a coatomer-related heptameric module from the nuclear pore complex. *Mol Cell Proteomics* 13, 2927-2943, doi:10.1074/mcp.M114.041673 (2014).
- 353 Augusteyn, R. C. alpha-crystallin: a review of its structure and function. *Clin Exp Optom* 87, 356-366, doi:10.1111/j.1444-0938.2004.tb03095.x (2004).
- 354 Fernandez-Fernandez, M. R., Gragera, M., Ochoa-Ibarrola, L., Quintana-Gallardo, L. & Valpuesta, J. M. Hsp70 - a master regulator in protein degradation. *FEBS Lett* 591, 2648-2660, doi:10.1002/1873-3468.12751 (2017).

## References

- 355 Paul, I. & Ghosh, M. K. The E3 ligase CHIP: insights into its structure and regulation. *Biomed Res Int* 2014, 918183, doi:10.1155/2014/918183 (2014).
- 356 Ihara, Y., Nukina, N., Miura, R. & Ogawara, M. Phosphorylated tau protein is integrated into paired helical filaments in Alzheimer's disease. *J Biochem* 99, 1807-1810, doi:10.1093/oxfordjournals.jbchem.a135662 (1986).
- 357 Schwalbe, M. *et al.* Phosphorylation of human Tau protein by microtubule affinity-regulating kinase 2. *Biochemistry* 52, 9068-9079, doi:10.1021/bi401266n (2013).
- 358 Simic, G. *et al.* Tau Protein Hyperphosphorylation and Aggregation in Alzheimer's Disease and Other Tauopathies, and Possible Neuroprotective Strategies. *Biomolecules* 6, 6, doi:10.3390/biom6010006 (2016).
- 359 Bibow, S. *et al.* Structural impact of proline-directed pseudophosphorylation at AT8, AT100, and PHF1 epitopes on 441-residue tau. *J Am Chem Soc* 133, 15842-15845, doi:10.1021/ja205836j (2011).
- 360 Amniai, L. *et al.* Alzheimer disease specific phosphoepitopes of Tau interfere with assembly of tubulin but not binding to microtubules. *FASEB J* 23, 1146-1152, doi:10.1096/fj.08-121590 (2009).
- 361 Baumann, K., Mandelkow, E. M., Biernat, J., Piwnica-Worms, H. & Mandelkow, E. Abnormal Alzheimer-like phosphorylation of tau-protein by cyclin-dependent kinases cdk2 and cdk5. *FEBS Lett* 336, 417-424, doi:10.1016/0014-5793(93)80849-p (1993).
- 362 Gotz, J., Chen, F., van Dorpe, J. & Nitsch, R. M. Formation of neurofibrillary tangles in P3011 tau transgenic mice induced by Abeta 42 fibrils. *Science* 293, 1491-1495, doi:10.1126/science.1062097 (2001).
- 363 Assimon, V. A., Southworth, D. R. & Gestwicki, J. E. Specific Binding of Tetratricopeptide Repeat Proteins to Heat Shock Protein 70 (Hsp70) and Heat Shock Protein 90 (Hsp90) Is Regulated by Affinity and Phosphorylation. *Biochemistry* 54, 7120-7131, doi:10.1021/acs.biochem.5b00801 (2015).
- 364 Lott, A., Oroz, J. & Zweckstetter, M. Molecular basis of the interaction of Hsp90 with its co-chaperone Hop. *Protein Sci* 29, 2422-2432, doi:10.1002/pro.3969 (2020).
- 365 Muller, P. *et al.* C-terminal phosphorylation of Hsp70 and Hsp90 regulates alternate binding to co-chaperones CHIP and HOP to determine cellular protein folding/degradation balances. *Oncogene* 32, 3101-3110, doi:10.1038/onc.2012.314 (2013).
- 366 Carrigan, P. E. *et al.* Multiple domains of the co-chaperone Hop are important for Hsp70 binding. *J Biol Chem* 279, 16185-16193, doi:10.1074/jbc.M314130200 (2004).
- 367 Yi, F., Doudevski, I. & Regan, L. HOP is a monomer: investigation of the oligomeric state of the co-chaperone HOP. *Protein Sci* 19, 19-25, doi:10.1002/pro.278 (2010).
- 368 Morra, G., Verkhivker, G. & Colombo, G. Modeling signal propagation mechanisms and ligand-based conformational dynamics of the Hsp90 molecular chaperone full-length dimer. *PLoS Comput Biol* 5, e1000323, doi:10.1371/journal.pcbi.1000323 (2009).

## References

- 369 Carrigan, P. E., Sikkink, L. A., Smith, D. F. & Ramirez-Alvarado, M. Domain:domain interactions within Hop, the Hsp70/Hsp90 organizing protein, are required for protein stability and structure. *Protein Sci* 15, 522-532, doi:10.1110/ps.051810106 (2006).
- 370 Kravats, A. N. *et al.* Interaction of E. coli Hsp90 with DnaK Involves the DnaJ Binding Region of DnaK. *J Mol Biol* 429, 858-872, doi:10.1016/j.jmb.2016.12.014 (2017).
- 371 Kravats, A. N. *et al.* Functional and physical interaction between yeast Hsp90 and Hsp70. *Proc Natl Acad Sci U S A* 115, E2210-E2219, doi:10.1073/pnas.1719969115 (2018).
- 372 Doyle, S. M. *et al.* Intermolecular Interactions between Hsp90 and Hsp70. *J Mol Biol* 431, 2729-2746, doi:10.1016/j.jmb.2019.05.026 (2019).
- 373 Reidy, M., Kumar, S., Anderson, D. E. & Masison, D. C. Dual Roles for Yeast Sti1/Hop in Regulating the Hsp90 Chaperone Cycle. *Genetics* 209, 1139-1154, doi:10.1534/genetics.118.301178 (2018).
- 374 Mok, S. A. *et al.* Mapping interactions with the chaperone network reveals factors that protect against tau aggregation. *Nat Struct Mol Biol* 25, 384-393, doi:10.1038/s41594-018-0057-1 (2018).
- 375 Rohl, A., Rohrberg, J. & Buchner, J. The chaperone Hsp90: changing partners for demanding clients. *Trends Biochem Sci* 38, 253-262, doi:10.1016/j.tibs.2013.02.003 (2013).
- 376 Joshi, A. *et al.* The mitochondrial HSP90 paralog TRAP1 forms an OXPHOS-regulated tetramer and is involved in mitochondrial metabolic homeostasis. *BMC Biol* 18, 10, doi:10.1186/s12915-020-0740-7 (2020).
- 377 Liu, Y., Sun, M., Elnatan, D., Larson, A. G. & Agard, D. A. Cryo-EM analysis of human mitochondrial Hsp90 in multiple tetrameric states. *bioRxiv*, 2020.2011.2004.368837, doi:10.1101/2020.11.04.368837 (2020).
- 378 Tortosa, E. *et al.* Binding of Hsp90 to tau promotes a conformational change and aggregation of tau protein. *J Alzheimers Dis* 17, 319-325, doi:10.3233/JAD-2009-1049 (2009).
- 379 Weickert, S., Wawrzyniuk, M., John, L. H., Rudiger, S. G. D. & Drescher, M. The mechanism of Hsp90-induced oligomerization of Tau. *Sci Adv* 6, eaax6999, doi:10.1126/sciadv.aax6999 (2020).
- 380 Stankiewicz, M., Nikolay, R., Rybin, V. & Mayer, M. P. CHIP participates in protein triage decisions by preferentially ubiquitinating Hsp70-bound substrates. *FEBS J* 277, 3353-3367, doi:10.1111/j.1742-4658.2010.07737.x (2010).
- 381 Vogel, M., Mayer, M. P. & Bukau, B. Allosteric regulation of Hsp70 chaperones involves a conserved interdomain linker. *J Biol Chem* 281, 38705-38711, doi:10.1074/jbc.M609020200 (2006).
- 382 Grenert, J. P., Johnson, B. D. & Toft, D. O. The importance of ATP binding and hydrolysis by hsp90 in formation and function of protein heterocomplexes. *J Biol Chem* 274, 17525-17533, doi:10.1074/jbc.274.25.17525 (1999).

## References

- 383 McLaughlin, S. H., Ventouras, L. A., Lobbezoo, B. & Jackson, S. E. Independent ATPase activity of Hsp90 subunits creates a flexible assembly platform. *J Mol Biol* 344, 813-826, doi:10.1016/j.jmb.2004.09.055 (2004).
- 384 Benaroudj, N., Triniolles, F. & Ladjimi, M. M. Effect of nucleotides, peptides, and unfolded proteins on the self-association of the molecular chaperone HSC70. *J Biol Chem* 271, 18471-18476, doi:10.1074/jbc.271.31.18471 (1996).
- 385 Lorenz, O. R. *et al.* Modulation of the Hsp90 chaperone cycle by a stringent client protein. *Mol Cell* 53, 941-953, doi:10.1016/j.molcel.2014.02.003 (2014).
- 386 Fan, C. Y., Ren, H. Y., Lee, P., Caplan, A. J. & Cyr, D. M. The type I Hsp40 zinc finger-like region is required for Hsp70 to capture non-native polypeptides from Ydj1. *J Biol Chem* 280, 695-702, doi:10.1074/jbc.M410645200 (2005).
- 387 Liu, Y., Elnatan, D., Sun, M., Myasnikov, A. G. & Agard, D. A. Cryo-EM reveals the dynamic interplay between mitochondrial Hsp90 and SdhB folding intermediates. *bioRxiv*, 2020.2010.2006.327627, doi:10.1101/2020.10.06.327627 (2020).
- 388 Dickey, C. A. *et al.* HSP induction mediates selective clearance of tau phosphorylated at proline-directed Ser/Thr sites but not KXGS (MARK) sites. *FASEB J* 20, 753-755, doi:10.1096/fj.05-5343fje (2006).
- 389 Bohush, A., Bieganowski, P. & Filipek, A. Hsp90 and Its Co-Chaperones in Neurodegenerative Diseases. *Int J Mol Sci* 20, doi:10.3390/ijms20204976 (2019).



## 7 Appendix

### 7.1 List of published items

A detailed list of the figures adopted from my first author publication is presented below. Respective author contributions can be found on page VIII.

Figure in this thesis	→	Figure in doi: <a href="https://doi.org/10.1002/pro.3969">10.1002/pro.3969</a>
Figure 17 corresponds to	→	Figure S1A, B
Figure 18 corresponds to	→	Figure S1C, D, E
Figure 19 corresponds to	→	Figure 1A, B
Figure 21 corresponds to	→	Figure 2A, B
Figure 22 corresponds to	→	Figure 2C
Figure 23 corresponds to	→	Figure S2
Figure 24B corresponds to	→	Figure S3A
Figure 24C, D corresponds to	→	Figure 3B, C
Figure 25A, B corresponds to	→	Figure 3D, E
Figure 25C corresponds to	→	Figure S3B

### 7.2 Supplementary Information

This section lists additional information relevant to the Methods (see chapter 2.3) and Results (see chapter 3.5.2), which were not included in the respective chapters for space saving.

#### *Sequences and plasmid maps*

**Table A 1 Gene sequences of the proteins used in this work.**

Gene sequences (3' to 5') and cloning specifications of human CHIP, Hop, the Hop construct Hop112a, Hsp40, Hsp70, Hsp90 $\beta$ , p23 and Tau- in alphabetical order; gene denotation in capital letters – respective protein terms are indicated in brackets.

Gene	Sequence 3' → 5'	Cloning vector Restriction Sites
STUB1 (CHIP)	ATGAAGGGCAAGGAGGAGAAGGAGGGCGGCGCACGGCTGGGCGCTGGCGGCGGAA GCCCCGAGAAGAGCCGAGCGCGCAGGAGCTCAAGGAGCAGGGCAATCGTCTGTT CGTGGGCCGAAAAGTACCCGGAGGCAGCGGCTGTACGGCCGCGCGATCACCCGG AACCGCTGGTGGCCGTGTATTACACCAACGGGCTTGTGCTACCTGAAGATGC AGCAGCACGAGCAGGCCCTGGCCGACTGCCGGCGGCCCTGGAGCTGGACGGGCA GTCTGTGAAGGCGCACTTCTCCTGGGCGAGTCCAGCTGGAGATGGAGAGCTAT GATGAGGCCATCGCCAATCTGCAGCGAGCTTACAGCCTGGCCAAGGAGCAGCGGC TGAACCTCGGGGACGACATCCCAGCGCTTTCGAATCGCGAAGAAGAAGCGCTG GAACAGCATTGAGGAGCGGCGCATCCACCAGGAGAGCGAGCTGCACTCCTACCTC TCCAGGCTCATTGCCGCGGAGCGTGAGAGGGAGCTGGAAGAGTGCCAGCGAAACC ACGAGGGTGATGAGGACGACAGCCAGCTCCGGGCCAGCAGGCCTGCATTGAGGC	pET28a BamHI - EcoRI

Appendix

	<p>CAAGCACGACAAGTACATGGCGGACATGGACGAGCTTTTTCTCAGGTGGATGAG AAGAGGAAGAAGCGAGACATCCCCGACTACCTGTGTGGCAAGATCAGCTTTGAGC TGATCGGGAGCCGTGCATCACGCCAGTGGCATACCTACGACCGCAAGGACAT CGAGGAGCACCTGCAGCGTGTGGTCAATTTGACCCCGTGACCCGGAGCCCCCTG ACCCAGGAACAGCTCATCCCAACTTGGCTATGAAGGAGGTTATTGACGCATTCA TCTCTGAGAATGGCTGGGTGGAGGACTACTGA</p>	
<p>STP1 (Hop)</p>	<p>ATGGAGCAGGTCAATGAGCTGAAGGAGAAAGGCAACAAGGCCCTGAGCGTGGGTA ACATCGATGATGCCTTACAGTGTACTCCGAAGCTATTAAGCTGGATCCCCACAA CCACGTGCTGTACAGCAACCGTTCTGTGCTATGCCAAGAAAGGAGACTACCAG AAGGCTTATGAGGATGGCTGCAAGACTGTGACCTAAAGCCTGACTGGGGCAAGG GCTATTCACGAAAAGCAGCAGCTCTAGAGTCTTAAACCGCTTTGAAGAAGCCAA GCGAACCTATGAGGAGGGCTTAAAACACGAGGCAATAAACCCTCAACTGAAAGAG GGTTTACAGAATATGGAGGCCAGGTTGGCAGAGAGAAAATTCATGAACCCTTTCA ACATGCCTAATCTGTATCAGAAGTTGGAGAGTGATCCAGGACAAGGACACTACT CAGTGATCCTACCTACCGGAGCTGATAGAGCAGCTACGAAACAAGCCTTCTGAC CTGGGCACGAAACTACAAGATCCCGGATCATGACCACTCTCAGCGTCTCCTCTG GGTTCGATCTGGGCAGTATGGATGAGGAGGAAGAGATTGCAACACCTCCACCACC ACCCCTCCCAAAAAGGAGACCAAGCCAGAGCCAATGGAAGAAGATCTTCCAGAG AATAAGAAGCAGGCACTGAAAGAAAAGAGCTGGGGAACGATGCCTACAAGAAGA AAGACTTTGACACAGCCTTGAAGCATTACGACAAAAGCCAAAGGAGCTGGACCCAC TAACATGACTTACATTACCAATCAAGCAGCGGTATACTTTGAAAAGGGCGACTAC AATAAGTGCCGGGAGCTTTGTGAGAAGGCCATTGAAGTGGGGAGAGAAAACCGAG AAGACTATCGACAGATTGCCAAAGCATATGCTCGAATTGGCAACTCCTACTTCAA AGAAGAAAAGTACAAGGATGCCATCCATTTCTATAACAAGTCTCTGGCAGAGCAC CGAACCCAGATGTGCTCAAGAAAATGCCAGCAGGCAGAGAAAATCCTGAAGGAGC AAGAGCGGCTGGCCTACATAAAACCCGACCTGGCTTTGGAGGAGAGAACAAGG CAACGAGTGTTCAGAAAAGGGGACTATCCCAGGCCATGAAGCATTATACAGAA GCCATCAAAAGGAACCCGAAAGATGCCAAATTATACAGCAATCGAGCTGCCTGT ACACCAAACCTCTGGAGTCCAGCTGGCACTCAAGGACTGTGAGGAATGTATCCA CTGGAGCCGACCTTCATCAAGGGTTATACACGGAAGCCGCTGCGCTGGGAAGCG ATGAAGGACTACACCAAGCCATGGATGTGTACCAGAAGGCGCTAGACCTGGACT CCAGCTGTAAAGAGCGGCAGAGCGCTACCAGCGCTGTATGATGGCGCAGTACAA CCGGCAGCAGCCCCGAAGATGTGAAGCAGCAGCCATGGCCGACCTGAGGTG CAGCAGATCATGAGTGACCCAGCCATGCGCTTATCTTGAACAGATGCGAAGG ACCCCGAGGCACTCAGCGAACACTTAAAGAATCCTGTAATAGCACAGAAGATCCA GAAGCTGATGGATGTGGGTCTGATTGCAATTCGGTAG</p>	<p>pET28a NheI - XhoI</p>
<p>(Hop112a)</p>	<p>ATGGAGCAGGTCAATGAGCTGAAGGAGAAAGGCAACAAGGCCCTGAGCGTGGGTA ACATCGATGATGCCTTACAGTGTACTCCGAAGCTATTAAGCTGGATCCCCACAA CCACGTGCTGTACAGCAACCGTTCTGTGCTATGCCAAGAAAGGAGACTACCAG AAGGCTTATGAGGATGGCTGCAAGACTGTGACCTAAAGCCTGACTGGGGCAAGG GCTATTCACGAAAAGCAGCAGCTCTAGAGTCTTAAACCGCTTTGAAGAAGCCAA GCGAACCTATGAGGAGGGCTTAAAACACGAGGCAATAAACCCTCAACTGAAAGAG GGTTTACAGAATATGGAGGCCAGGTTGGCAGAGAGAAAATTCATGAACCCTTTCA ACATGCCTAATCTGTATCAGAAGTTGGAGAGTGATCCAGGACAAGGACACTACT CAGTGATCCTACCTACCGGAGCTGATAGAGCAGCTACGAAACAAGCCTTCTGAC CTGGGCACGAAACTACAAGATCCCGGATCATGACCACTCTCAGCGTCTCCTCTG GGTTCGATCTGGGCAGTATGGATGAGGAGGAAGAGATTGCAACACCTCCACCACC ACCCCTCCCAAAAAGGAGACCAAGCCAGAGCCAATGGAAGAAGATCTTCCAGAG AATAAGAAGCAGGCACTGAAAGAAAAGAGCTGGGGAACGATGCCTACAAGAAGA AAGACTTTGACACAGCCTTGAAGCATTACGACAAAAGCCAAAGGAGCTGGACCCAC TAACATGACTTACATTACCAATCAAGCAGCGGTATACTTTGAAAAGGGCGACTAC AATAAGTGCCGGGAGCTTTGTGAGAAGGCCATTGAAGTGGGGAGAGAAAACCGAG AAGACTATCGACAGATTGCCAAAGCATATGCTCGAATTGGCAACTCCTACTTCAA AGAAGAAAAGTACAAGGATGCCATCCATTTCTATAACAAGTCTCTGGCAGAGCAC CGAACCCAGATGTGCTCAAGAAAATGCCAGCAGGCAGAGAAAATCCTGAAGGAGC AAGAGCGGCTGTAG</p>	
<p>DNAJB4 (Hsp40)</p>	<p>ATGGGAAAAGACTATTATTGCATTTTGGGAATTGAGAAAAGGAGCTTCAGATGAAG ATATTAAAAGGCTTACCGAAAACAAGCCCTCAAATTTTCATCCGGACAAGAACA ATCTCCTCAGGCAGAGGAAAATTTAAAGAGGTCGCAGAAGCTTATGAAGTATTG AGTGATCCTAAAAGAGAGAAAATATATGATCAGTTTGGGGAGGAAGGTTGAAAG GAGGAGCAGGAGGTAAGTATGACAAAGGAGGTACCTTCCGGTACACCTTTTCATGG CGATCCTCATGCTACATTTGCTGCATTTTTCGGAGGTCACACCCCTTTGAAATT TTCTTTGGAAGACGAATGGGTGGTGGTAGAGATTCTGAAGAAATGGAATGATG GTGATCCTTTTGTAGTGCCTTTGGTTTCAGCATGAATGGATATCCAAGAGACAGGAA TTCTGTGGGGCCATCCCGCTCAAACAAGATCCTCCAGTTATTTCATGAACCTTAGA GTATCACTTGAAGAGATATATAGTGGTGTACCAACCGGATGAAGATTTCTCGAA AAAGGCTAAACGCTGATGGAAGGAGTTACAGATCTGAGGACAAAATTTCTTACCAT TGAGATTAAGGAGGTTGGAAAGAGGCACCAAAATTAATTTTCCAAGAGAGGGA GATGAAACACCAATAGTATTCAGCAGACATTGTTTTTATCATTAAAGACAAG ATCATCCAAAATTTAAAGGGATGGATCAAATATAATTTTACTGCTAAAATTAG TTTTACGAGGCGCATGTGTGGCTGCTCAATTAATGTACCAACACTGGATGGAAAG AACATACCTATGTCAGTAAATGATATTGTGAAACCCGGAATGAGGAGAAGAAATTA</p>	<p>pET28a NheI - XhoI</p>

Appendix

	<p>TTGGATATGGGCTGCCATTTCCAAAAAATCCTGACCAACGTGGTGACCTTCTAAT          AGAATTTGAGGTGTCTTCCAGATACTATATCTTCTTCATCCAAAGAAGTACTT          AGGAAACATCTTCTGCCTCATAG</p>	
<p>HSPA1A (Hsp70)</p>	<p>ATGGGCAGCAGCCATCATCATCATCATCACAGCAGCGGCCTGGTGCCGCGCGGC          AGCCATATGGCTAGCATGACTGGTGACAGCAAATGGGTGCGGGATCCGAATTC          ACCGGCATGGCCAAAGCCGCGGGATCGGCATCGACCTGGGCACCACCTACTCC          TGCGTGGGGGTGTTCCAACACGGCAAGGTGGAGATCATCGCCAACGACCAGGGC          AACCCGACCACCCAGCTACGTGGCCTTACGGACACCGAGCGGCTCATCGGG          GATGCGGCCAAGAACCAGGTGGCGCTGAACCCGCAAGAACCCGTGTTGAGCGG          AAGCGGTGATCGGCGCAAGTTCGGCGACCCGGTGGTGCAGTCCGACATGAAG          CACTGGCCTTTCAGGTGATCAACGACGGAGACAAGCCCAAGGTGCAGGTGAGC          TACAAGGGGGAGACCAAGGCATTTACCCCGAGGAGATCTCGTCCATGGTGTG          ACCAAGATGAAGGAGATCGCGAGGCGTACTGGGCTACCCGGTGACCAAGCGG          GTGATCACCGTGCCGGCCTACTTCAACGACTCGCAGCGCCAGGCCACCAAGGAT          GCGGGTGTGATCGCGGGGCTCAACGTGCTGCGGATCATCAACGAGCCACGGCC          GCCGCCATCGCCTACGGCCTGGACAGAACGGGCAAGGGGGAGCGCAACGTGCTC          ATCTTTGACCTGGGCGGGGCACCTTCGACGTGTCCATCTGACGATCGACGAC          GGCATCTTTCAGGTGAAGGCCACGGCCGGGGACACCCACCTGGGTGGGGAGGAC          TTTGACAACAGGCTGGTGAACCCTTCGTGGAGGAGTTCAAGAGAAAACACAAG          AAGGACATCAGCCAGAACAAGCGAGCCGTGAGGGCGCTGCGCACCCGCTGCGAG          AGGGCCAAGAGGACCCTGTCTCCAGCACCAGGCCAGCCTGGAGATCGACTCC          CTGTTTGGGGCATCGACTTCTACAGTCCATCACAGGGCGAGGTTTCGAGGAG          CTGTGTTCCGACCTGTTCCGAAGCACCTGGAGCCGTGGAGAAGGCTCTGCGC          GACGCCAAGCTGGACAAGGCCAGATTCACGACCTGGTCTGGTGGGGGGTCC          ACCCGCATCCCCAAGGTGCAAGTGTCTGACGACTTCTTCAACGGGCGCGAC          CTGAACAAGAGCATCAACCCGACGAGGCTGTGGCTACCGGGCGGGCGTGCAG          GCGGCCATCTGATGGGGACAAGTCCGAGAACGTGCAGGACCTGTCTGTCTG          GACGTGGCTCCCCTGTCTGGGGTGGAGACGGCCGGAGGCGTGTGACTGCC          CTGATCAAGCGCAACTCCACCATCCCCACCAAGCAGACGAGATCTTACCACC          TACTCCGACAACCAACCCGGGGTGTGATCCAGGTGTACGAGGGCGAGAGGGCC          ATGACGAAAGACAACAATCTGTTGGGGCGCTTCGAGCTGAGCGGCATCCCTCCG          GCCCCAGGGGGCTGCCAGATCGAGGTGACCTTCGACATCGATGCCAACGGC          ATCTGAACGTACGGCCACGGACAAGAGCACGGCAAGGCCAACCAAGATCAC          ATCAACAAGGACAAGGGCCCTGAGCAAGGAGGAGATCGAGCGCATGGTGCAG          GAGGCGGAGAAGTACAAGCGGAGGACGAGGTGCAGCGGAGAGGGTGTGAGCC          AAGAAGCCCTGGAGTCTACGCCCTCAACATGAAGAGCGCCGTGGAGGATGAG          GGGCTCAAGGGCAAGATCAGCGAGGCGGACAAGAAGAAGGTGCTGGACAAGTGT          CAAGAGTCTATCTGTGGCTGGACGCCAACACCTTGGCCGAGAAGGACGAGTTT          GAGCACAAGAGGAAGGAGCTGGAGCAGGTGTGTAACCCATCATCAGCGGACTG          TACCAGGGTGCCTGGTCCCGGGCTGGGGCTTCGGGGCTCAGGGTCCCAAG          GGAGGGTCTGGGTGAGGCCACCATTGAGGAGGTAGATTAG</p>	<p>pET28a NdeI - HindIII</p>
<p>HSP90AB1 (Hsp90β)</p>	<p>ATGCCTGAGGAAGTGCACCATGGAGAGGAGGAGGTGGAGACTTTTGCCTTTCAGG          CAGAAATGGCCAACTCATGTCCCTCATCATCAATACCTTCTATTTCCAACAAGGA          GATTTCCCTTCGGGAGTTGATCTCTAATGCTTCTGATGCCTTGGACAAGATTCGC          TATGAGAGCCTGACAGACCCTTCGAAGTTGGACAGTGGTAAAGAGCTGAAAATTG          ACATCATCCCAACCTCAGGAACGTACCTGACTTTGGTAGACACAGGCATTGG          CATGACCAAAAGTGTATCTATAAATAATTTGGGAACCATTGCCAAGTCTGGTACT          AAAGCATTATGAGGCTCTTCAGGCTGGTGCAGACATCTCCATGATTGGGCAGT          TTGGTGTGGCTTTTATTCTGCCTACTTGGTGGCAGAGAAAGTGGTGTGATCAC          AAAGCACAACGATGATGAACAGTATGCTTGGGAGTCTTCTGCTGGAGTTCTTCC          ACTGTGCGTGTGACCATGGTGGAGCCATTGGCAGGGGTACCAAAGTGTCTCTCC          ATCTTAAAGAAGATCAGACAGAGTACCTAGAAGAGAGGGCGGTCAAAGAAGTAGT          GAAGAAGCATTTCTCAGTTTATAGGCTATCCCATCACCCCTTTATTTGGAGAAGGAA          CGAGAGAAGGAAATTAGTGATGATGAGGCAGAGGAAGAGAAAGGTGAGAAAGAAG          AGGAAGATAAAGATGATGAAGAAAAGCCCAAGATCGAAGATGTGGGTTTCAGATGA          GGAGGATGACAGCGGTAAGGATAAGAAGAAGAAAACCTAAGAAGATCAAAGAAGAAA          TACATTGATCAGGAAGAATAAACAAGACCAAGCCTATTTGGACCAGAAACCCTG          ATGACATCACCAAGAGGAGTATGGAGAATTCTACAAGAGCCTCACTAATGACTG          GGAAGACCACTTGGCAGTCAAGCACTTTTCTGTAGAAGGTGAGTTGGAATTCAGG          GCATGTCTATTTATTCCTCGTCCGGCTCCCTTTGACCTTTTGGACAAGAAGA          AAAAGAACAACATCAAACCTATGTCCGCCGTGTGTTTATCATGACAGCTGTGGA          TGAGTTGATACCAGAGTATCTCAATTTTATCCGTGGTGTGGTTGACTCTGAGGAT          CTGCCCTGAACATCTCCCGAGAAATGCTCCAGCAGAGCAAAATCTTGAAGTCA          TTCCGAAAACAGATGTTAAGAAGTGCCTTGAGCTTCTCTGAGCTGGCAGGAA          CAAGGAGAATTACAAGAAATCTATGAGGCATTCTTAAAAATCTCAAGCTTGGGA          ATCCACGAAGACTCCACTAACCGCCGCGCCTGTCTGAGCTGCTGCGCTATCATA          CCTCCAGTCTGGAGATGAGATGACATCTCTGTGACAGTATGTTTCTCGCATGAA          GGAGACACAGAAGTCCATCTATTACATCACTGGTGAGAGCAAGAGCAGGTGGCC          AACTCAGCTTTTGTGGAGCGAGTGCAGAAACGGGGCTTCGAGGTGGTATATATGA          CCGAGCCCATTTGACGAGTACTGTGTGACGAGCTCAAGGAATTTGATGGGAGAG          CCTGGTCTCAGTTACCAAGGAGGGTCTGGAGCTGCCTGAGGATGAGGAGGAGAAG          AAGAAGATGGAAGAGAGCAAGGCAAGTTTGAGAACCCTCTGCAAGCTCATGAAAG          AAATCTTAGATAAGAGGTTGAGAAGGTGACAATCTCCAATAGACTTGTGTCTT          ACCTGTCTGATTGTGACCAGCACCTACGGCTGGACAGCCAATATGGAGCGGATC</p>	<p>pET28a NheI - NotI</p>

## Appendix

	<p>ATGAAAGCCAGGCACTTCGGGACAACCTCCACCATGGGCTATATGATGGCCAAAA  AGCACCTGGAGATCAACCCTGACCACCCCATTTGTGGAGACGCTGCGGCAGAAGGC  TGAGGCCGACAAGAATGATAAGGCAGTTAAGGACCTGGTGGTGTCTGCTGTTGAA  ACCGCCCTGCTATCTTCTGGCTTTTCCCTTGAGGATCCCCAGACCCACTCCAACC  GCATCTATCGCATGATCAAGCTAGGTCTAGGTATTGATGAAGATGAAGTGGCAGC  AGAGGAACCCAATGCTGCAGTTCCTGATGAGATCCCCCTCTCGAGGGCGATGAG  GATGCGTCTCGCATGGAAGAAGTCGATTAG</p>	
<p style="text-align: center;">PTGES3 (p23)</p>	<p>ATGCAGCCTGCTTCTGCAAAGTGGTACGATCGAAGGGACTATGTCTTCATTGAAT  TTTGTGTTGAAGACAGTAAGGATGTTAATGTAAATTTTGAAAAATCCAAACTTAC  ATTGAGTTGCTCTCGGAGGAAGTGATAATTTAAGCATTAAATGAAATTGATCTT  TTTCACTGTATTGATCCAAATGATTCCAAGCATAAAAGAACGGACAGATCAATTT  TATGTTGTTTACGAAAAGGAGAATCTGGCCAGTCAATGGCCAAGGTTAACAAAAGA  AAGGGCAAAGCTTAATTGGCTTAGTGTGACTTCAATAATTGGAAGACTGGGAA  GATGATTCAGATGAAGACATGTCTAATTTTGATCGTTTCTCTGAGATGATGAACA  ACATGGGTGGTATGAGGATGTAGATTTACCAGAAGTAGATGGAGCAGATGATGA  TTCACAAGACAGTATGATGAAAAAATGCCAGATCTGGAGTAG</p>	<p style="text-align: center;">pET28a NheI - XhoI</p>
<p style="text-align: center;">MAPT (Tau)</p>	<p>ATGGCTGAGCCCCGCCAGGAGTTCGAAGTATGGAAGATCAGCTGGGACGTACG  GGTTGGGGGACAGGAAAGATCAGGGGGGCTACCCATGCACCAAGACCAAGAGGG  TGACACGGACGCTGGCCTGAAAGAATCTCCCTGCAGACCCCACTGAGGACGGA  TCTGAGGAACCGGGCTCTGAAACCTCTGATGCTAAGAGCACTCCAACAGCGGAAG  ATGTGACAGCACCTTAGTGGATGAGGGAGCTCCCGGCAAGCAGGCTGCCCGCA  GCCCCACACGGAGATCCCAGAAGGAACCACAGCTGAAGAAGCAGGCAATTGGAGAC  ACCCCCAGCTGGAAGACGAAGCTGCTGGTACGTGACCCAAGCTCGCATGGTCA  GTAAAAGCAAAGACGGGACTGGAAGCGATGACAAAAAGCCAAGGGGGCTGATGG  TAAAACGAAGATCGCCACACCGGGGAGCAGCCCTCCAGGCCAGAAGGGCCAG  GCCAACGCCACCAGGATCCAGCAAAAACCCCGCCGCTCCAAGACACCACCCA  GCTCTGGTGAACCTCCAAAATCAGGGGATCGCAGCGGCTACAGCAGCCCCGGCTC  CCCAGGCACTCCCGGCAGCCGCTCCCGCACCCCCGTCCTTCCAACCCACCCACC  CGGGAGCCCAAGAAGGTGGCAGTGGTCCGTACTIONCACCAAGTCGCCGCTTCCG  CCAAGAGCCGCTGCAGACAGCCCCGTGCCATGCCAGACCTGAAGAATGTCAA  GTCCAAGATCGGCTCCACTGAGAACCTGAAGCACCAGCCGGGAGGCGGGAAGGTG  CAGATAATTAATAAGAAGCTGGATCTTAGCAACGTCCAGTCCAAGTGTGGTCAA  AGGATAATATCAAACACGTCCCGGGAGGCGGCAGTGTGCAAATAGTCTACAAACC  AGTTGACCTGAGCAAGGTGACCTCCAAGTGTGGCTCATTAGGCAACATCCATCAT  AAACCAGGAGGTGGCCAGGTGGAAGTAAATCTGAGAAGCTTGACTTCAAGGACA  GATCCAGTCGAAGATTGGGTCCCTGGACAATATACCCACGTCCCTGGCGGAGG  AAATAAAAAGATTGAAACCCACAAGCTGACCTTCCGCGAGAACGCCAAAGCCAAG  ACAGACCACGGGGCGGAGATCGTGTACAAGTCGCCAGTGGTGTCTGGGGACAGT  CTCCACGGCATCTCAGCAATGTCTCTCCACCGGCAGCATCGACATGGTAGACTC  GCCCCAGCTCGCCACGCTAGCTGACGAGGTGTCTGCCTCCCTGGCCAAGCAGGGT  TTG</p>	<p style="text-align: center;">pNG2 NdeI - BamHI</p>

## Appendix

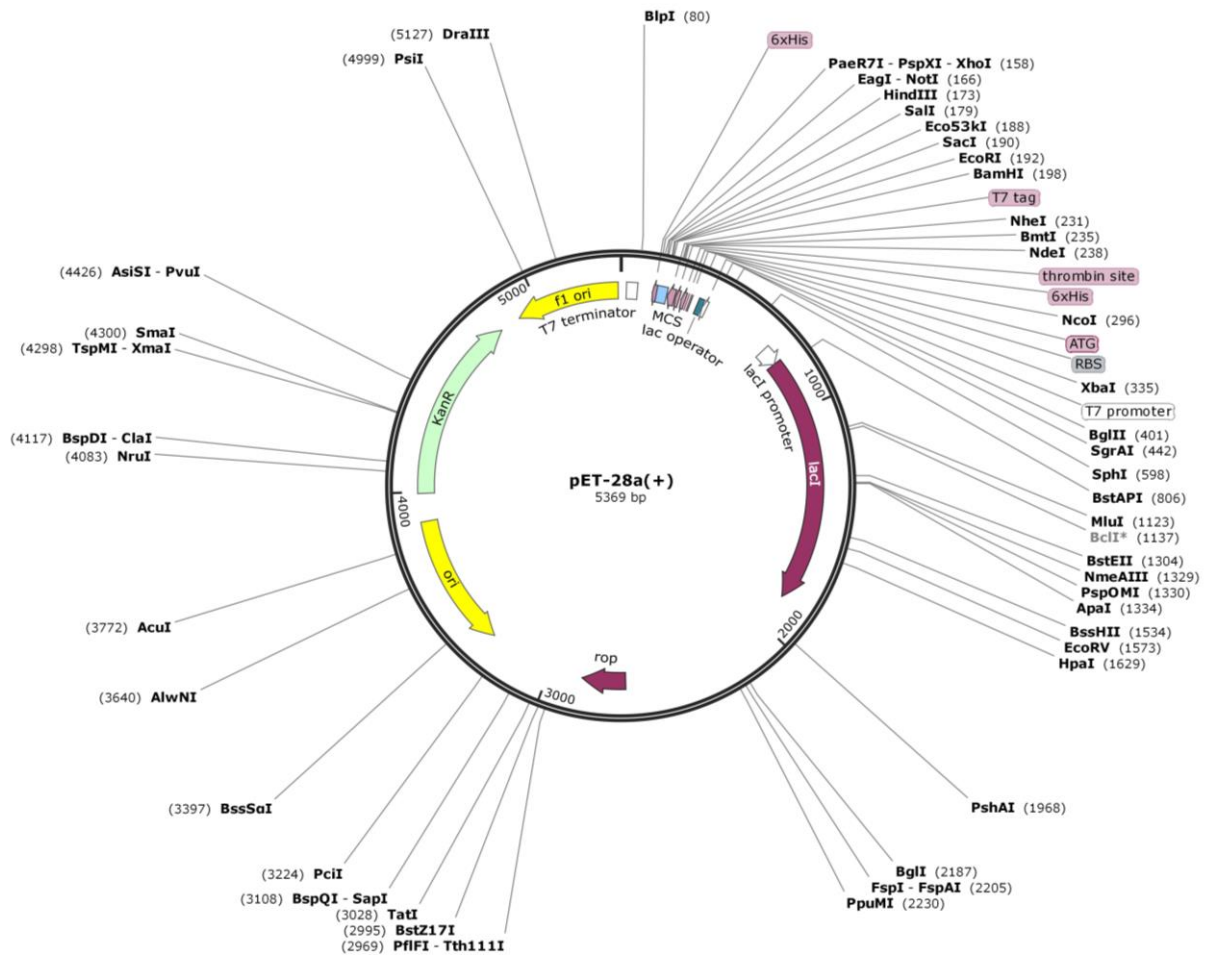


**Figure A 1** The pET28a cloning vector.

The gene of interest was cloned into the multiple cloning site (MCS) using the restriction sites specified in Table A 1. Gene expression is under the control of the T7-expression system, in turn regulated by the lacI repressor. pET28a encodes for kanamycin resistance (KanR) and the repressor of primer (rop) for the regulation of plasmid replication with 'ori' as the origin of replication. f1 ori – origin of replication to produce single stranded DNA; 6xHis – histidine tag; RBS – ribosomal binding site. Restriction sites with unique 6+ cutters are shown in black. The vector map was created with SnapGene.

## Appendix

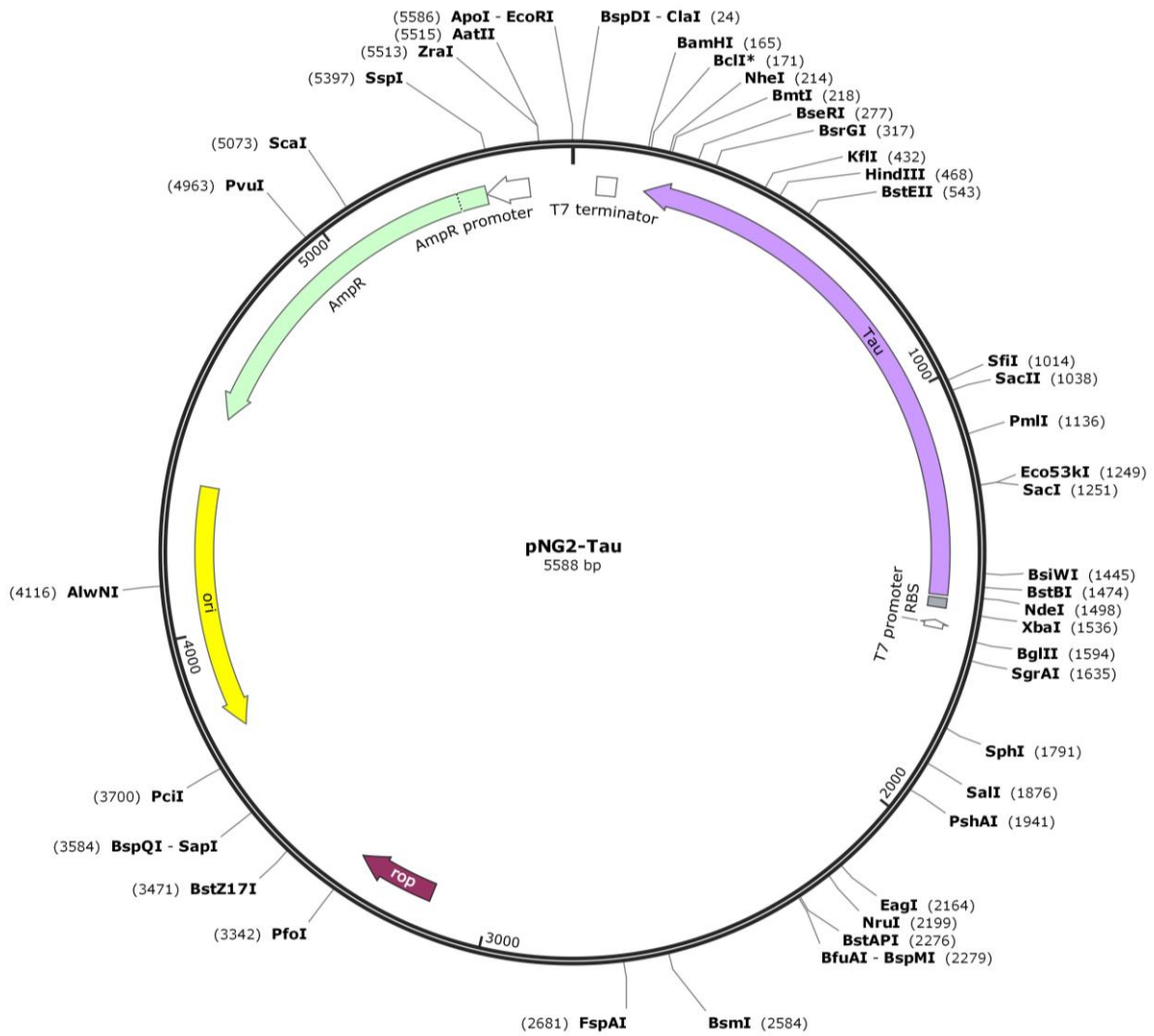


**Figure A 2** The pNG2 cloning vector encoding the protein Tau.

The vector was thankfully received from the lab of Eckhard Mandelkow at the DZNE Bonn with the Tau sequence cloned into the pNG2 vector using the restriction sites NdeI and BamHI. Gene expression is controlled by the T7-expression system; RBS – ribosomal binding site. The regulation of gene expression is ensured in *E. coli* BL21(DE3), whose genomic DNA encodes for the T7 polymerase, which in turn is under the control of the lac operon. pNG2 encodes for ampicillin resistance (AmpR) and the repressor of primer (rop) for the regulation of plasmid replication with 'ori' as the origin of replication. Restriction sites with unique 6+ cutters are shown in black. The vector map was created with SnapGene.

## Appendix

**Table A 2 Protein sequences of the proteins used in this work.**

Protein sequences (N- to C-terminus) of recombinantly expressed human CHIP, Hop, the Hop construct Hop112a, Hsp40, Hsp70, Hsp90 $\beta$ , p23, Tau and the Tau constructs K18 and K32– in alphabetical order; N-terminal tags including the His<sub>6</sub>-sequence are colored in grey. | marks the tag cleavage site – in the case of full-length Hop and Hsp90 the tag was not removed; Tau was expressed without tag.

Protein	Sequence N → C
CHIP	MGSSHHHHHSSGLVPR   GSHMASMTGGQQMGRGSEFMKGKKEKEGGARLGAGGGSPEKSPSAQELKEQGNRLF VGRKYPEAAACYGRAI TRNPLVAVYYNTRALCYLKMQQHEQALADCRRALELDGQSVKAHFFLGGCCQLEMESYD EAIANLQRAYSLAKEQRLNFGDDIPALRIAKKKRWNSEIERRIHQESSELHSYLSRLIAAERERELEECQRNHE GDEDDSHVRAQQACIEAKHDKYAMDDELFSQVDEKRRKRDIPDYLCGKISFELMREPCITPPSGITYDRKDIEE HLQRVGHFDPVTRSPLTQEQLIPNLAMKEVIDAFISENGWVEDY
Hop	MGSSHHHHHSSGLVPRGSHMASMEQVNELKEKGNKALSVGNIDDALQCYSEAIKLDPHNHVLYSNRSAAAYAKK GDYQKAYEDGCKTVDLKPDWKGKYSRKAALAEFLNRFEEAKRTYEEGLKHEANNPQLKEGLQNMEARLAERKFM NPFNMPNLYQKLESDPRTRTLSDPTYRELIEQLRNKPSDLGTLKQDPRIMTTLVLLGVLDLGSMDDEEEIATP PPPPPPKKETKPEPMEEDLPENKKQALKEKELGNDAYKKKDFDTALKHYDKAKELDPTNMTYITNQAAVYFEKG DYNKRELCEKAEVGRENRREDYRQIAKAYARIGNSYFKKEEKYKDAIHFYNKSLAEHRTPDVLKCCQQAELILK EQERLAYINPDALALEKNKGNCFQKGDYQAMKHYTEAIKRNPKDAKLYSNRAACYTKLLEFQLALKDCEECI QLEPTFIKGYTRKAAALEAMKDYTKAMDVYQKALDLDSSCKEADGYQRCMMAQYNRHSDPEVVKRRAMADPEV QQIMSDPAMRLILEQMOKDPQALSEHLKPNVIAQKIQLKMDVGLIATR
Hop112a	MGSSHHHHHSSGLVPR   GSHMASMEQVNELKEKGNKALSVGNIDDALQCYSEAIKLDPHNHVLYSNRSAAAYAKK RGDYQKAYEDGCKTVDLKPDWKGKYSRKAALAEFLNRFEEAKRTYEEGLKHEANNPQLKEGLQNMEARLAERKFM NPFNMPNLYQKLESDPRTRTLSDPTYRELIEQLRNKPSDLGTLKQDPRIMTTLVLLGVLDLGSMDDEEEIATP PPPPPPKKETKPEPMEEDLPENKKQALKEKELGNDAYKKKDFDTALKHYDKAKELDPTNMTYITNQAAVYFEK GDYNKRELCEKAEVGRENRREDYRQIAKAYARIGNSYFKKEEKYKDAIHFYNKSLAEHRTPDVLKCCQQAELIL KEQERL
Hsp40	MGSSHHHHHSSGLVPR   GSHMASMGKDYICILGIEKGSDEDIKKAYRKQALKFHPDNKNSPQAEKFKVEAE AYEVLSDPKKREIYDQFGEGLKGGAGGTGGGGTFRYTFHGDPHATFAAFFGGSNPFIFFGRRMGGGRDSE MEIDGDPFSAFGFSMNGYPRDRNSVGSRLKQDPPVIELHRSVLEEIYSGCTKRMKISRKRLNADGRSRYSEDK ILTIIEIKKGWKEGTKITFPREGDETPNSIPADIVFIKDKDHPKFKRDGNSNIYTAKISLREALCGCSINVP TL DGRNIPMSVNDIVKPGMRRIIGYGLPFPKPNPQDGLLIEFEVSPDITSSSSKEVLRKHLPS
Hsp70	MGSSHHHHHSSGLVPR   GSHMASMTGGQQMGRGSEFTGMAKAAAIGIDLGTYSVGVFQHGKVEIANDQGN RTTPSYVAFTDTERLIGDAAKNQVALNPQNTVFDKRLIGRKFQDPVQSDMKHWPVQVINDGDKPKVQVSYKG ETKAFYPEEIISSMVLTKMKEIAEAYLGYPVNTAVITVPAYFNDSQRQATKDAGVIAGLNVLRINEPTAAAIAY GLDRTGKGERNVLIFDLGGGTFDVSIITIDDDGIFEVKATAGDTHLGGEDFDNRLVNHFEVEFKRKHKKDISQNK RAVRLRTACERAKRFLSSSTQASLEIDSLFEGIDFYTSITRARFEELCSDLFRSTLEPVEKALRDAKLDKAI HDLVLVGGSTRIPKVQKLLQDFNDRDLNKSINPDEAVAYGAAVQAAILMGDKSENVQDLLLLDVAPLSLGL ETAGGVMTALIKRNSTIPKQQTIFTTYSDNQPGVLIQVYEGERAMTKDNNLLGRFELSGIPAPRGVQIEVTFD IDANGILNVTATDKSTGKANKITITNDKGRLSKEEIERMVQEAKEYKADEVQREVSAKNALESYAFNMKSAV EDEGLKGI SEADKKVLDKCEQEVISWLDANTLAEKDEFEHKRKELEQVCNPIISGLYQAGGPGGPGGAQGP KGGSGSGPTIEEVD
Hsp90 $\beta$	MGSSHHHHHSSGLVPRGSHMASMPEEVHGGEEVEVTFQAEIAQLMSLIINTFYNSKEIFLRELI SNASDAL DKIRYESLTDPSKLDGKELKIDIPNPQERTLTLVDTGIGMTKADLNNLGTIAKSGTKAFMEALQAGADISM IGQFVGVGFYSAYLVAEKVVVITKHNDDEQYAWESSAGGSFTVRADHGEPVIGRGTKVIHLHLEDQTEYLEERRVK EVVKKHSQFYGYPITLYLEKEKEKEISDDEAEKEEKEEEDKDEEKPKEIEDVGSDEEDDSGDKKKKTKKIK EKYIDQEEELNKTPIWTRNPDDITQEEYGEFYKSLTNDWEDHLAVKHFSVEGQLEFRALLFIPRAPPDLFENK RKKNNIKLYVRRVIFMDSCEDELIPEYLNFRVVDSEDLPLNISREMLQQSKILKVIKRNIVKCKLELSELA E DKENYKFFYEAFSKNLKLGIHEDSTNRRRSELLRYHTSQSGDEMTSLSEYVSRMKTQKSIYYITGESKEQVA NSAFVERVRKRGFVYVYMTPEIDEYCVQQLKEFDGKSLVSVTKEGLELPEDEEKKKMEESKAKFENLCKLMKE ILDKKVEKVTISNRLVSSPCCIVTSTYGWANMERIMKAQALRDNSTMGYMAKHHLEINPDHPIVEVTLRQKAE ADKNDKAVKDLVVLLFETALLSSGFSLEDPPQTHSNRIYRMIKLGLGIDEVVAEEEPNAAVPEIIPPELGDEDA SRMEEVD
p23	MGSSHHHHHSSGLVPR   GSHMASMPASAKWYDRRDYVFIIEFCVEDSKDVNVNFEKSKLTFSCLGSDNFKHL NEIDLPHCIDPNDKSKHRTDRSILCCLRKGSQSWPRLTKERAKLNWLSVDFNNWWDWEDSDSDMSNDFRFS EMMNNMGDEDVDLPEVDGADDDSDSDEKMPDLE
Tau (Isoform F)	MAEPRQEFVEMEDHAGTYGLGRDKDQGGYTMHQDQEGDTDAGLKE SPLQTPTEGDGSEEPGSETSDAKSTPTAED VTAPLVDEGAPGKQAAQPHTEIPEGTTAAEEAGIGDTPSLEDEAAGHVTQARMVSKSKDGTGSDDKKAKGADGK TKIATPRGAAPPQKQANATRIPAKTPAPKTPSSGEPKPSGDRSGYSSPGSPGTPGSRSRTPSLPTPPTRE PKKVAVVRTPPKSPSSAKSRLQTAPEVMPDLDKNNVSKIGSTENLKHQPGGGKVIINKKLDLSDNVQSKCGSKDN IKHVPGGGSVQIVYKPVVLSKVTSCKSLGNIHHKPGGGQVEVKSEKLDKDRVQSKIGSLDNI THVPGGGNKK IETHKLTFRENAKAKTDHGAIEVYKSPVVSVDTSRHLSDNVSTGSDIMVDSPLATLADEVASLAKQGL

## Appendix

K18	MQTAPVPMFDLKNVSKIGSTENLKHQPGGGKVQI INKKLDLSNVQSKCGSKDNIKHVPGGGSVQIVYKPV DLS KVTSKCGSLGNIH HKPGGGQVEVKSEKLD FKDRVQSKIGSLDNI THVPGGGNKKIE
K32	MSSPGSPGTPGSRSRTPSLPTPPTREPKKVA VVRTPPKSPSSAKSRLQTAPVPMFDLKNVSKIGSTENLKHQ P GGGKVQI INKKLDLSNVQSKCGSKDNIKHVPGGGSVQIVYKPV DLSKVTSKCGSLGNIH HKPGGGQVEVKSEK L DFKDRVQSKIGSLDNI THVPGGGNKKIETHKLT FRENAAKAKTDHGAEIVY

### Purification examples

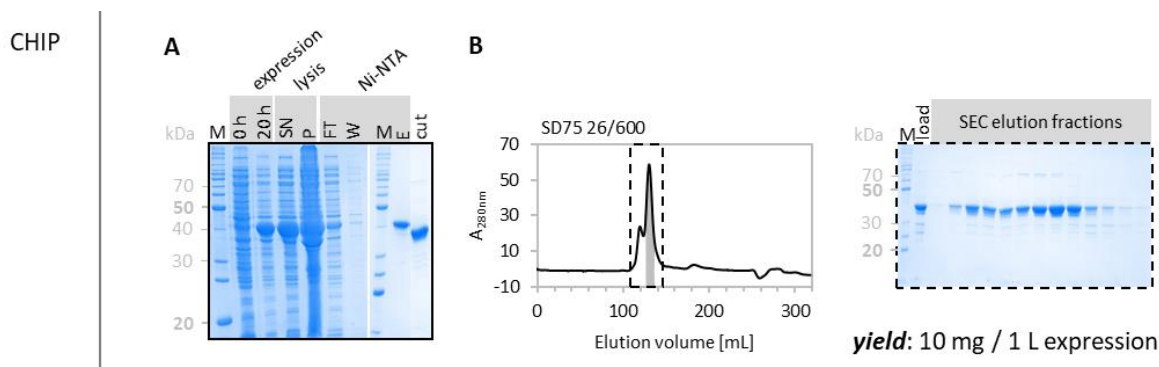


**Figure A 3 Purification of the CHIP protein (tagged: 38.68 kDa; cut: 36.79 kDa) via IMAC (Ni-NTA) and SEC.**

**A** SDS page analysis (12 % gel) of CHIP protein production and purification. 0 h – time point of IPTG induction; 20 h – time point of cell harvesting; SN – supernatant after lysis by sonication; FT / W / E – flow through / wash / elution of IMAC; cut – CHIP protein after o/n incubation with thrombin protease. **B** Size exclusion chromatogram of CHIP using an SD75 26/600 column (1 mL/min). The dashed box marks the elution fractions analyzed by SDS page (12 % gel) on the right. Fractions of interest are shaded in grey and were used for further experiments. The purification protocol is described in 2.3.4.1.

### Hop

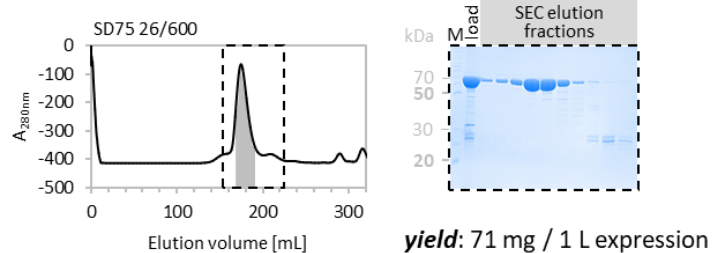


**Figure A 4 Purification of the Hop protein (65.09 kDa) via IMAC (Ni-NTA) and SEC.**

Size exclusion chromatogram of Hop using an SD75 26/600 column (2 mL/min). The dashed box marks the elution fractions analyzed by SDS page (12 % gel) on the right. Fractions of interest are shaded in grey and were used for further experiments. The purification protocol is described in 2.3.4.2.



Hop112a

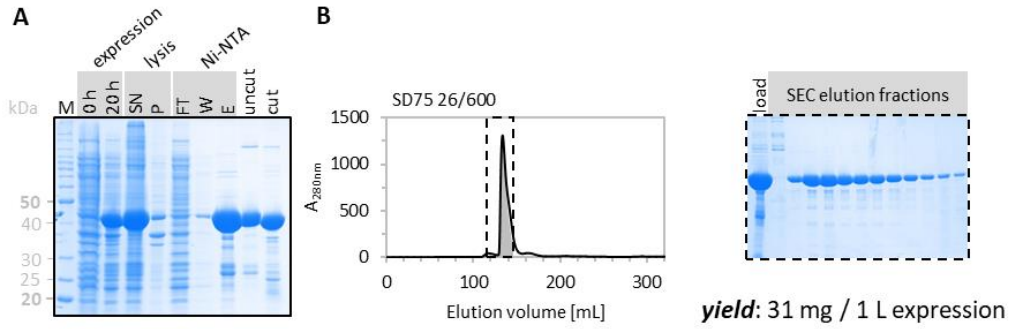


**Figure A 5 Purification of the Hop112a protein (tagged: 43.21 kDa; cut: 41.33 kDa) via IMAC (Ni-NTA) and SEC.**

**A** SDS page analysis (12 % gel) of Hop112a protein production and purification. 0 h – time point of IPTG induction; 20 h – time point of cell harvesting; SN – supernatant after lysis by sonication; P – pellet after cell lysis; FT / W / E – flow through / wash / elution of IMAC; cut – Hop112a protein after 3 h incubation with thrombin protease. **B** Size exclusion chromatogram of Hop112a using an SD75 26/600 column (2 mL/min). The dashed box marks the elution fractions analyzed by SDS page (12 % gel) on the right. Fractions of interest are shaded in grey. The purification protocol is described in 2.3.4.3.

Hsp40

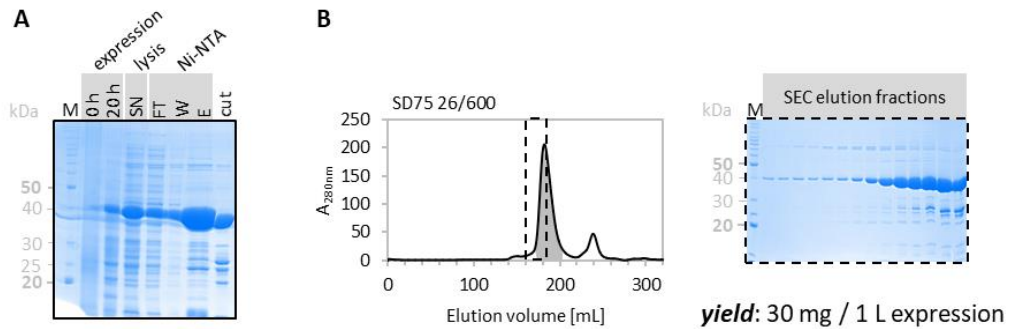


**Figure A 6 Purification of the Hsp40 protein (tagged: 40.26 kDa; cut: 38.38 kDa) via IMAC (Ni-NTA) and SEC.**

**A** SDS page analysis (12 % gel) of Hsp40 protein production and purification. 0 h – time point of IPTG induction; 20 h – time point of cell harvesting; SN – supernatant after lysis by sonication; FT / W / E – flow through / wash / elution of IMAC; cut – Hsp40 protein after o/n incubation with thrombin protease. **B** Size exclusion chromatogram of Hsp40 using an SD75 26/600 column (1.8 mL/min). The dashed box marks the elution fractions analyzed by SDS page (12 % gel) on the right. Fractions of interest are shaded in grey and were used for further experiments. The purification protocol is described in 2.3.4.4.

Hsp70

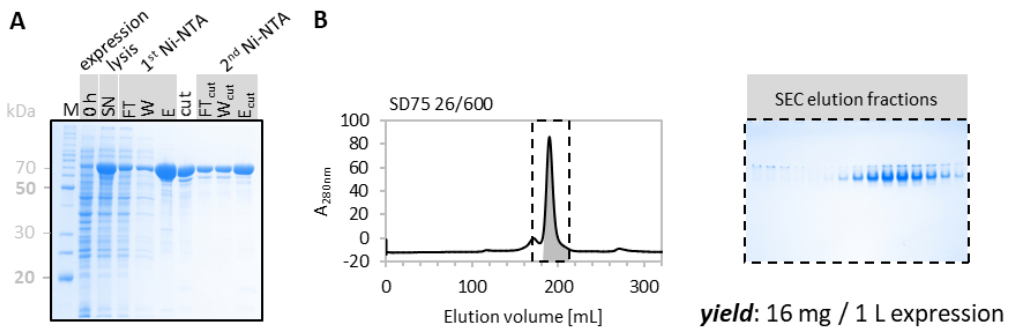


**Figure A 7 Purification of the Hsp70 protein (tagged: 74.03 kDa; cut: 72.15 kDa) via IMAC (Ni-NTA) followed by tag cleavage, a second IMAC (Ni-NTA) and SEC.**

**A** SDS page analysis (12 % gel) of Hsp70 protein production and purification. 0 h – time point of IPTG induction; SN – supernatant after lysis by sonication; FT / W / E – flow through / wash / elution of first IMAC; cut – Hsp70 protein after o/n incubation with thrombin protease; FT<sub>cut</sub> / W<sub>cut</sub> / E<sub>cut</sub> – flow through / wash / elution of second IMAC. **B** Size exclusion chromatogram of Hsp70 using an SD75 26/600 column (0.75 mL/min). The dashed box marks the elution fractions analyzed by native page (7.5 % gel) on the right. Fractions of interest are shaded in grey and were used for further experiments. The purification protocol is described in 2.3.4.5.

## Appendix

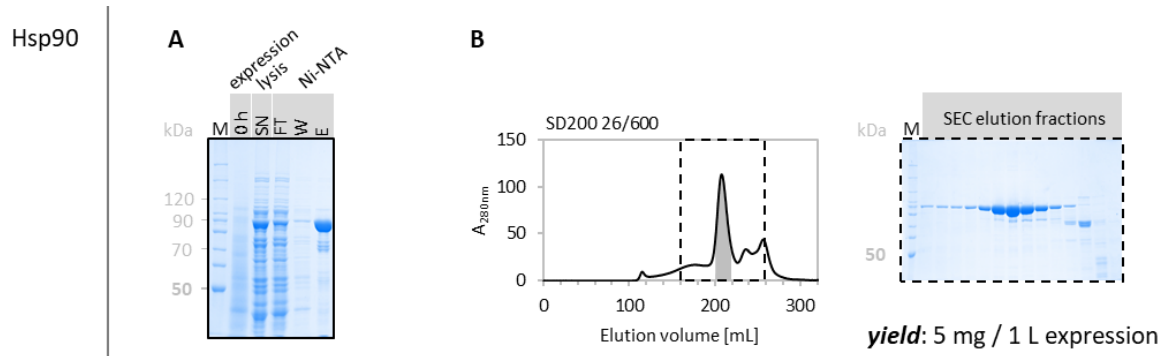


**Figure A 8 Purification of the Hsp90 protein (85.72 kDa) via IMAC (Ni-NTA) and SEC.**

**A** SDS page analysis (8 % gel) of Hsp90 protein production and purification. 0 h – time point of IPTG induction; SN – supernatant after lysis by sonication; FT / W / E – flow through / wash / elution of IMAC. **B** Size exclusion chromatogram of Hsp90 using an SD200 26/600 column (2 mL/min). The dashed box marks the elution fractions analyzed by SDS page (8 % gel) on the right. Fractions of interest are shaded in grey and were used for further experiments. The purification protocol is described in 2.3.4.6.

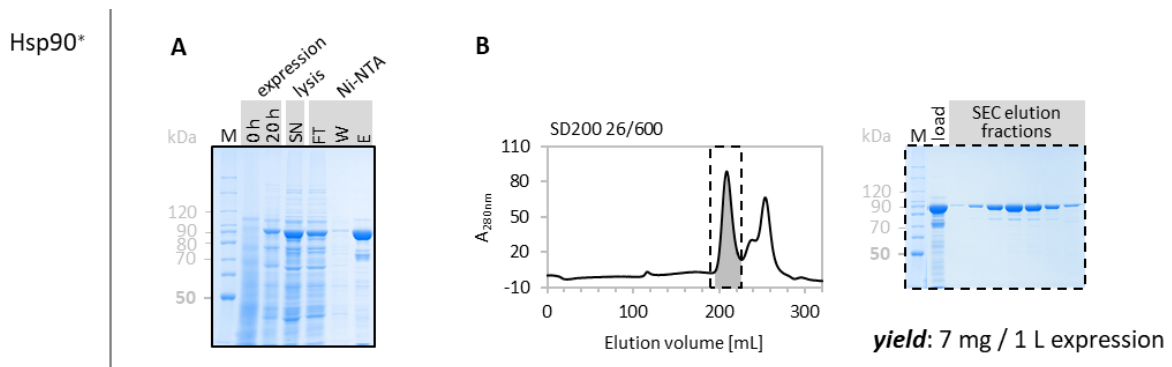


**Figure A 9 Purification of the Hsp90\* protein (96.55 kDa) via IMAC (Ni-NTA) and SEC.**

**A** SDS page analysis (8 % gel) of Hsp90\* protein production and purification. 0 h – time point of IPTG induction; 20 h – time point of cell harvesting; SN – supernatant after lysis by sonication; FT / W / E – flow through / wash / elution of IMAC. **B** Size exclusion chromatogram of Hsp90\* using an SD200 26/600 column (2 mL/min). The dashed box marks the elution fractions analyzed by SDS page (8 % gel) on the right. Fractions of interest are shaded in grey and were used for further experiments.

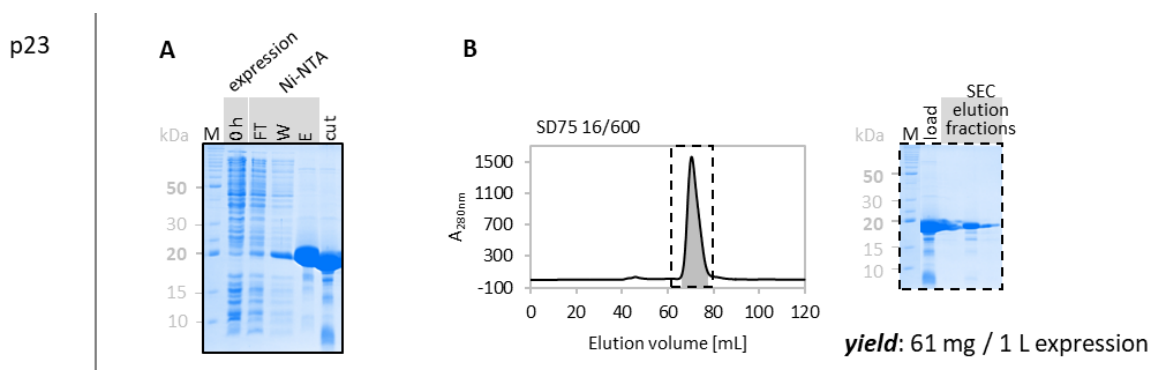


**Figure A 10 Purification of the p23 protein (tagged: 21.15 kDa; cut: 19.27 kDa) via IMAC (Ni-NTA) and SEC.**

**A** SDS page analysis (15 % gel) of p23 protein production and purification. 0 h – time point of IPTG induction; FT / W / E – flow through / wash / elution of IMAC; cut – p23 protein after o/n incubation with thrombin protease. **B** Size exclusion chromatogram of p23 using an SD75 16/600 column (1.8 mL/min). The dashed box marks the elution fractions analyzed by SDS page (15 % gel) on the right. Fractions of interest are shaded in grey and were used for further experiments. The purification protocol is described in 2.3.4.8.

## Appendix

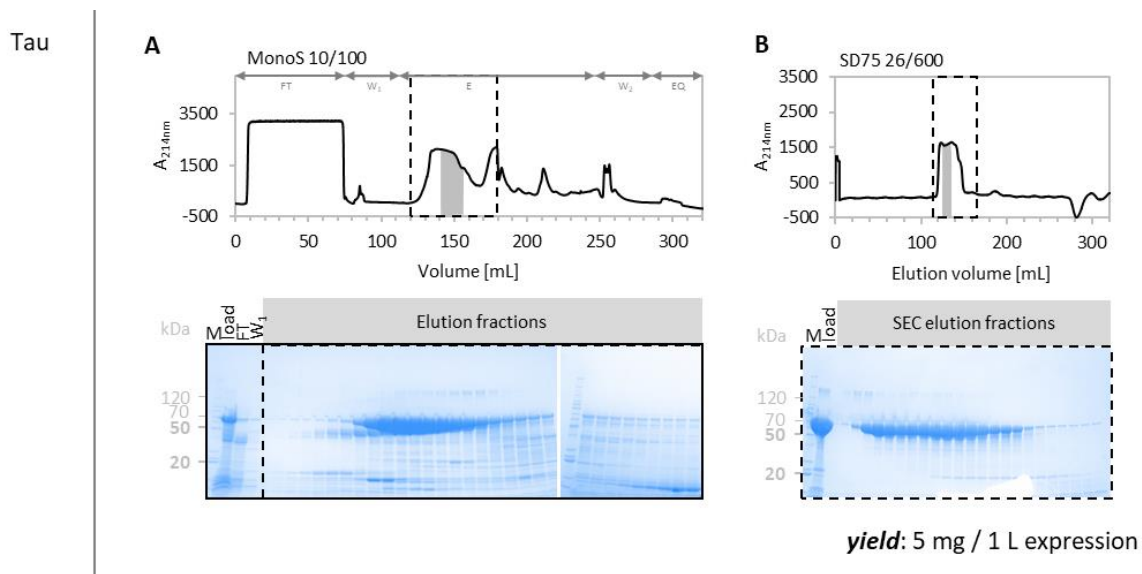


**Figure A 11 Purification of the Tau protein (45.85 kDa) via IEX and SEC.**

**A** Cation exchange chromatogram of the Tau protein using a Mono S 10/100 column (2 mL/min) (top) and the corresponding SDS page analysis (4-20 % gradient gel) of selected fractions (bottom). FT – flow through during sample application in buffer A;  $W_1$  – wash with buffer A; E – linear elution (0-60 % buffer B);  $W_2$  – wash with buffer B; EQ – column equilibration back to buffer A. **B** Size exclusion chromatogram of the Tau protein using an SD75 26/600 column (2 mL/min). The dashed box marks the elution fractions analyzed by SDS page (4-15 % gradient gel) shown below. Fractions of interest are shaded in grey and were used for further experiments. The purification protocol is described in 2.3.4.9.

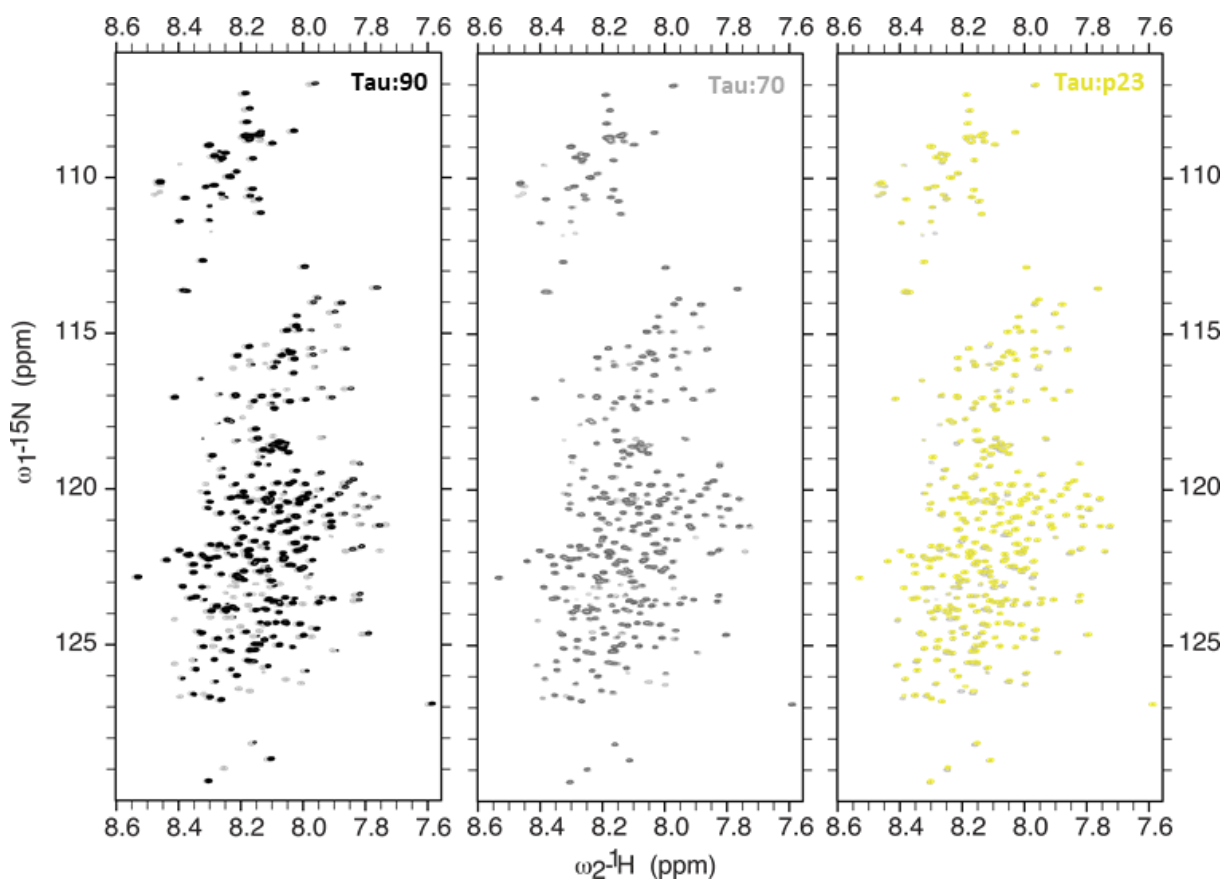


**Figure A 12 Tau NMR spectra in presence of Hsp90, Hsp70 and p23.**

$^{15}\text{N}$ - $^1\text{H}$  HSQC spectra of Tau alone (grey) and in the presence of the Hsp90 (black; 1:4), Hsp70 (dark grey; 1:4) and p23 (yellow; 1:10).

## Appendix

### *Selected cross-links*

**Table A 3 Selected intra- and intermolecular cross-links within the Hsp70:Hsp90:Tau:p23 complex cross-linked with disuccinimidyl suberate (DSS).**

Threshold: minimum of 3 hits and 5% of the maximum score ( $\geq 1.1125$ ).

Protein1	Protein2	Pos1	Pos2	Hits	Score
Hop	Hop	31	96	44	6.56
Hop	Hop	36	73	13	1.66
Hop	Hop	36	101	3	4.53
Hop	Hop	55	79	15	2.20
Hop	Hop	55	86	13	1.99
Hop	Hop	55	101	7	2.90
Hop	Hop	79	101	4	4.12
Hop	Hop	86	101	12	3.54
Hop	Hop	96	73	26	3.22
Hop	Hop	96	101	5	1.53
Hop	Hop	101	185	15	4.43
Hop	Hop	101	74	10	3.97
Hop	Hop	101	73	9	3.80
Hop	Hop	101	509	5	1.89
Hop	Hop	101	123	3	1.41
Hop	Hop	101	101	12	1.13
Hop	Hop	123	101	348	21.64
Hop	Hop	123	115	8	2.05
Hop	Hop	123	73	4	2.53
Hop	Hop	132	101	17	4.47
Hop	Hop	132	115	17	2.01
Hop	Hop	132	230	12	3.37
Hop	Hop	146	115	12	2.24
Hop	Hop	146	185	5	2.91
Hop	Hop	192	101	6	1.27
Hop	Hop	229	101	8	3.07
Hop	Hop	229	233	3	2.45
Hop	Hop	230	101	22	5.13
Hop	Hop	230	348	16	2.93
Hop	Hop	230	73	13	1.73
Hop	Hop	230	123	9	2.93
Hop	Hop	230	252	8	2.25
Hop	Hop	230	324	8	1.57
Hop	Hop	230	86	6	1.68
Hop	Hop	230	553	5	1.71
Hop	Hop	230	260	3	1.13
Hop	Hop	233	101	10	5.23
Hop	Hop	250	273	6	9.78
Hop	Hop	252	324	22	3.33
Hop	Hop	260	262	10	2.78
Hop	Hop	260	324	7	3.31
Hop	Hop	269	250	9	1.45
Hop	Hop	273	250	5	4.65
Hop	Hop	275	307	4	1.85
Hop	Hop	295	269	53	10.85
Hop	Hop	295	262	5	1.88
Hop	Hop	307	300	6	5.09
Hop	Hop	324	361	5	6.36
Hop	Hop	335	361	15	9.34
Hop	Hop	335	360	14	8.26
Hop	Hop	335	262	8	2.12
Hop	Hop	335	261	5	1.56
Hop	Hop	340	370	23	5.20
Hop	Hop	340	415	3	1.38
Hop	Hop	348	101	3	1.46
Hop	Hop	367	415	11	3.19
Hop	Hop	367	360	10	2.40
Hop	Hop	370	360	8	6.16
Hop	Hop	370	415	7	3.54
Hop	Hop	387	418	29	6.81
Hop	Hop	387	452	12	1.79
Hop	Hop	404	389	13	1.98
Hop	Hop	411	370	28	8.46
Hop	Hop	429	465	9	3.22
Hop	Hop	429	457	8	3.96
Hop	Hop	438	457	14	4.27
Hop	Hop	452	418	12	2.94
Hop	Hop	452	429	10	3.30
Hop	Hop	452	387	10	1.75
Hop	Hop	465	509	14	3.35
Hop	Hop	469	457	51	6.11
Hop	Hop	476	457	132	22.61
Hop	Hop	485	509	5	1.69
Hop	Hop	509	73	3	2.42
Hop	Hop	536	553	27	2.48
Hop	Hop	536	509	25	2.71
Hop	Hop	546	101	4	2.22
Hop	Hop	553	509	10	3.14
Hop	Hop	553	73	3	2.25
Hop	Hop	556	457	6	4.23
Hop	Hop	556	509	6	2.14
Hop	Hsp70	36	582	7	1.75
Hop	Hsp70	36	1	4	3.81
Hop	Hsp70	36	366	4	1.64
Hop	Hsp70	55	1	6	3.21
Hop	Hsp70	73	518	11	18.57
Hop	Hsp70	86	1	5	2.99
Hop	Hsp70	101	580	13	2.66
Hop	Hsp70	101	582	11	2.82
Hop	Hsp70	101	518	7	1.24
Hop	Hsp70	101	211	6	3.10
Hop	Hsp70	123	1	11	2.62
Hop	Hsp70	123	278	4	1.88
Hop	Hsp70	132	582	5	2.54
Hop	Hsp70	230	211	40	6.56
Hop	Hsp70	230	366	27	1.44
Hop	Hsp70	230	545	17	2.49
Hop	Hsp70	230	1	9	4.69
Hop	Hsp70	230	521	9	2.21
Hop	Hsp70	230	582	4	1.87
Hop	Hsp70	233	589	5	1.53
Hop	Hsp70	340	340	22	2.65
Hop	Hsp70	348	340	31	2.44
Hop	Hsp70	360	346	4	2.71
Hop	Hsp70	404	98	10	3.05
Hop	Hsp70	509	211	13	4.44
Hop	Hsp70	509	528	5	1.33
Hop	Hsp70	536	1	4	3.97
Hop	Hsp70	536	545	4	2.41
Hop	Hsp70	553	582	6	2.46
Hop	Hsp70	553	211	5	4.37
Hop	Hsp90	101	630	9	2.45
Hop	Hsp90	101	596	6	5.83
Hop	Hsp90	101	425	6	2.83
Hop	Hsp90	101	309	3	1.63
Hop	Hsp90	230	504	29	3.99
Hop	Hsp90	230	500	12	1.97
Hop	Hsp90	230	554	10	2.59
Hop	Hsp90	230	574	3	3.15
Hop	Hsp90	230	600	3	1.52
Hop	Hsp90	233	574	4	1.29
Hop	Hsp90	324	500	3	2.02
Hop	Hsp90	360	500	11	6.15

## Appendix

Hop	Hsp90	457	596	52	10.27	Hop	Tau	509	259	7	1.93
Hop	Hsp90	457	630	6	2.38	Hop	Tau	509	347	5	1.66
Hop	Hsp90	465	370	13	6.60	Hop	Tau	509	383	4	2.45
Hop	Hsp90	465	222	4	1.48	Hop	Tau	536	274	26	1.60
Hop	Hsp90	469	596	4	1.31	Hop	Tau	536	311	21	3.49
Hop	Hsp90	476	596	8	1.48	Hop	Tau	536	331	15	3.14
Hop	Hsp90	476	646	7	1.76	Hop	Tau	536	281	13	3.75
Hop	Hsp90	509	630	16	1.62	Hop	Tau	536	353	12	3.34
Hop	Hsp90	509	372	11	6.95	Hop	Tau	536	280	9	1.24
Hop	Hsp90	509	425	10	1.11	Hop	Tau	536	369	7	2.82
Hop	Hsp90	509	600	7	2.05	Hop	Tau	536	225	3	2.30
Hop	Hsp90	509	373	4	1.71	Hop	Tau	546	267	6	1.40
Hop	Hsp90	536	458	28	2.43	Hop	Tau	546	225	4	2.93
Hop	Hsp90	536	370	16	3.18	Hop	Tau	553	240	6	8.30
Hop	Hsp90	536	647	13	5.65	Hop	Tau	553	259	3	2.84
Hop	Hsp90	536	630	7	2.35	Hop	Tau	553	383	3	1.34
Hop	Hsp90	536	425	6	1.48	Hsp70	Hop	1	101	17	4.86
Hop	Hsp90	536	646	4	2.12	Hsp70	Hop	1	73	8	2.12
Hop	Hsp90	536	422	4	1.24	Hsp70	Hop	1	509	8	1.86
Hop	Hsp90	536	561	3	4.88	Hsp70	Hop	1	553	4	1.50
Hop	Hsp90	536	600	3	1.64	Hsp70	Hop	340	370	3	1.72
Hop	Hsp90	546	600	37	2.65	Hsp70	Hop	382	230	17	4.22
Hop	Hsp90	546	591	23	2.18	Hsp70	Hop	382	36	4	6.06
Hop	Hsp90	546	458	10	2.57	Hsp70	Hop	382	101	4	3.32
Hop	Hsp90	546	646	5	3.51	Hsp70	Hop	436	230	12	3.77
Hop	Hsp90	546	596	5	1.91	Hsp70	Hop	436	132	10	6.23
Hop	Hsp90	546	370	4	2.82	Hsp70	Hop	436	185	7	2.90
Hop	Hsp90	553	600	6	2.91	Hsp70	Hop	436	73	5	3.79
Hop	Hsp90	553	425	4	3.02	Hsp70	Hop	436	86	5	2.53
Hop	Hsp90	553	596	4	1.73	Hsp70	Hop	436	91	5	1.21
Hop	p23	36	1	4	3.25	Hsp70	Hop	436	101	4	2.65
Hop	p23	230	1	7	4.37	Hsp70	Hop	545	509	8	1.35
Hop	p23	348	1	19	1.91	Hsp70	Hop	582	73	13	3.56
Hop	Tau	36	174	4	1.36	Hsp70	Hop	618	101	12	6.09
Hop	Tau	73	225	7	5.31	Hsp70	Hop	618	73	11	2.26
Hop	Tau	73	383	4	4.71	Hsp70	Hop	618	230	8	2.83
Hop	Tau	101	281	14	4.42	Hsp70	Hop	618	132	5	3.43
Hop	Tau	101	240	13	3.47	Hsp70	Hop	618	86	5	3.06
Hop	Tau	101	174	12	3.49	Hsp70	Hop	618	36	4	3.40
Hop	Tau	101	225	11	4.92	Hsp70	Hop	618	185	4	2.07
Hop	Tau	101	259	8	3.18	Hsp70	Hop	618	509	3	1.28
Hop	Tau	101	234	8	2.93	Hsp70	Hop	649	73	10	7.92
Hop	Tau	101	343	7	1.88	Hsp70	Hop	649	101	6	2.42
Hop	Tau	101	347	4	2.95	Hsp70	Hop	649	132	4	1.42
Hop	Tau	101	383	4	2.06	Hsp70	Hsp70	1	366	21	6.94
Hop	Tau	101	280	4	1.84	Hsp70	Hsp70	1	129	13	3.64
Hop	Tau	101	370	3	2.36	Hsp70	Hsp70	1	533	13	2.93
Hop	Tau	132	321	6	1.24	Hsp70	Hsp70	1	528	9	3.89
Hop	Tau	185	370	3	1.49	Hsp70	Hsp70	1	545	8	2.63
Hop	Tau	230	267	18	1.97	Hsp70	Hsp70	1	521	8	2.05
Hop	Tau	230	240	9	1.33	Hsp70	Hsp70	1	582	7	2.50
Hop	Tau	230	370	7	2.01	Hsp70	Hsp70	1	547	7	1.46
Hop	Tau	230	274	7	1.36	Hsp70	Hsp70	1	518	6	2.08
Hop	Tau	230	259	6	2.67	Hsp70	Hsp70	1	211	5	3.75
Hop	Tau	230	174	6	1.95	Hsp70	Hsp70	1	472	5	2.34
Hop	Tau	230	281	6	1.51	Hsp70	Hsp70	1	98	3	3.86
Hop	Tau	230	385	5	2.25	Hsp70	Hsp70	24	1	50	5.94
Hop	Tau	230	234	4	1.24	Hsp70	Hsp70	24	533	5	2.90
Hop	Tau	230	180	3	1.36	Hsp70	Hsp70	24	528	5	1.16
Hop	Tau	415	225	17	6.20	Hsp70	Hsp70	46	1	11	2.31
Hop	Tau	415	240	3	8.84	Hsp70	Hsp70	77	278	6	3.21
Hop	Tau	457	240	8	6.37	Hsp70	Hsp70	109	278	36	2.18
Hop	Tau	457	225	4	2.65	Hsp70	Hsp70	121	98	19	3.53
Hop	Tau	465	281	4	1.98	Hsp70	Hsp70	123	1	19	2.58
Hop	Tau	476	174	3	1.36	Hsp70	Hsp70	133	1	13	4.25
Hop	Tau	509	280	14	3.20	Hsp70	Hsp70	147	1	12	2.48
Hop	Tau	509	343	13	1.73	Hsp70	Hsp70	180	1	25	4.56
Hop	Tau	509	234	9	1.22	Hsp70	Hsp70	267	272	51	6.39
Hop	Tau	509	240	8	3.71	Hsp70	Hsp70	267	278	5	3.66
Hop	Tau	509	225	8	3.64	Hsp70	Hsp70	366	518	3	1.51

## Appendix

Hsp70	Hsp70	382	369	192	17.34	Hsp70	Tau	366	225	8	3.69
Hsp70	Hsp70	382	1	11	7.52	Hsp70	Tau	366	383	5	3.56
Hsp70	Hsp70	382	545	8	1.98	Hsp70	Tau	382	225	3	1.85
Hsp70	Hsp70	382	528	7	1.67	Hsp70	Tau	436	370	19	4.52
Hsp70	Hsp70	382	533	6	1.69	Hsp70	Tau	436	369	17	4.10
Hsp70	Hsp70	382	366	4	1.45	Hsp70	Tau	436	234	14	4.91
Hsp70	Hsp70	382	521	3	1.38	Hsp70	Tau	436	331	13	4.13
Hsp70	Hsp70	436	547	48	8.22	Hsp70	Tau	436	281	12	5.44
Hsp70	Hsp70	436	1	22	7.26	Hsp70	Tau	436	274	12	2.83
Hsp70	Hsp70	436	533	11	2.53	Hsp70	Tau	436	353	11	3.13
Hsp70	Hsp70	444	521	19	11.20	Hsp70	Tau	436	385	9	6.78
Hsp70	Hsp70	444	1	7	1.91	Hsp70	Tau	436	267	9	3.77
Hsp70	Hsp70	472	211	8	5.18	Hsp70	Tau	436	259	8	4.02
Hsp70	Hsp70	518	211	3	6.98	Hsp70	Tau	436	298	7	3.78
Hsp70	Hsp70	521	582	15	2.01	Hsp70	Tau	436	321	7	3.04
Hsp70	Hsp70	521	211	8	3.31	Hsp70	Tau	436	383	7	2.75
Hsp70	Hsp70	528	211	6	5.13	Hsp70	Tau	436	254	7	2.10
Hsp70	Hsp70	528	533	5	1.84	Hsp70	Tau	436	395	4	5.78
Hsp70	Hsp70	533	211	8	2.45	Hsp70	Tau	436	343	4	1.92
Hsp70	Hsp70	545	1	18	3.31	Hsp70	Tau	436	225	4	1.66
Hsp70	Hsp70	545	211	6	1.55	Hsp70	Tau	436	180	3	2.49
Hsp70	Hsp70	560	472	14	2.52	Hsp70	Tau	472	225	10	2.47
Hsp70	Hsp70	571	588	13	1.96	Hsp70	Tau	472	281	9	1.67
Hsp70	Hsp70	571	589	9	2.27	Hsp70	Tau	472	370	6	2.19
Hsp70	Hsp70	571	1	6	3.61	Hsp70	Tau	472	240	3	4.08
Hsp70	Hsp70	580	588	17	6.39	Hsp70	Tau	472	234	3	2.36
Hsp70	Hsp70	580	589	3	5.29	Hsp70	Tau	518	225	4	3.92
Hsp70	Hsp70	610	618	5	1.25	Hsp70	Tau	545	225	9	3.64
Hsp70	Hsp70	618	1	10	7.98	Hsp70	Tau	545	274	8	1.17
Hsp70	Hsp70	618	610	4	11.95	Hsp70	Tau	545	234	5	2.85
Hsp70	Hsp90	1	425	15	2.05	Hsp70	Tau	545	267	5	1.13
Hsp70	Hsp90	1	422	13	4.24	Hsp70	Tau	545	385	4	2.56
Hsp70	Hsp90	1	76	12	2.11	Hsp70	Tau	545	240	4	1.61
Hsp70	Hsp90	1	309	9	2.72	Hsp70	Tau	545	370	4	1.43
Hsp70	Hsp90	1	92	7	3.40	Hsp70	Tau	545	174	3	1.97
Hsp70	Hsp90	1	370	3	3.99	Hsp70	Tau	545	369	3	1.50
Hsp70	Hsp90	1	203	3	2.00	Hsp70	Tau	560	225	13	3.16
Hsp70	Hsp90	98	309	46	6.72	Hsp70	Tau	560	274	6	1.39
Hsp70	Hsp90	121	309	28	3.30	Hsp70	Tau	560	281	3	2.02
Hsp70	Hsp90	180	76	71	11.06	Hsp70	Tau	571	225	7	4.40
Hsp70	Hsp90	180	309	19	1.55	Hsp70	Tau	571	281	3	3.58
Hsp70	Hsp90	180	92	6	1.72	Hsp70	Tau	571	267	3	1.82
Hsp70	Hsp90	292	675	3	3.01	Hsp70	Tau	571	274	3	1.26
Hsp70	Hsp90	436	422	6	5.65	Hsp70	Tau	571	370	3	1.19
Hsp70	Hsp90	533	425	11	5.50	Hsp70	Tau	582	347	3	2.28
Hsp70	Hsp90	545	425	8	1.60	Hsp70	Tau	618	281	10	1.66
Hsp70	Hsp90	618	265	6	1.72	Hsp70	Tau	618	353	8	1.75
Hsp70	Hsp90	618	600	3	2.09	Hsp70	Tau	618	369	7	3.65
Hsp70	Hsp90	618	596	3	1.47	Hsp70	Tau	618	395	6	3.55
Hsp70	p23	1	1	11	3.08	Hsp70	Tau	618	174	6	1.84
Hsp70	p23	109	1	12	2.88	Hsp70	Tau	618	298	5	3.02
Hsp70	p23	109	101	4	3.55	Hsp70	Tau	618	163	3	1.86
Hsp70	p23	267	1	5	1.59	Hsp70	Tau	649	321	4	1.44
Hsp70	p23	436	1	3	6.17	Hsp90	Hop	130	101	3	2.75
Hsp70	p23	545	1	3	1.68	Hsp90	Hop	227	509	6	2.65
Hsp70	p23	618	1	3	2.54	Hsp90	Hop	227	465	4	1.51
Hsp70	p23	618	41	3	1.37	Hsp90	Hop	265	79	4	1.44
Hsp70	Tau	1	267	20	1.87	Hsp90	Hop	286	429	3	1.76
Hsp70	Tau	1	225	16	2.83	Hsp90	Hop	329	457	16	5.86
Hsp70	Tau	1	385	13	2.89	Hsp90	Hop	329	465	5	2.87
Hsp70	Tau	1	281	11	4.45	Hsp90	Hop	329	469	5	1.24
Hsp70	Tau	1	174	9	2.22	Hsp90	Hop	329	509	3	2.24
Hsp70	Tau	1	240	8	1.80	Hsp90	Hop	370	509	76	5.68
Hsp70	Tau	1	259	7	2.34	Hsp90	Hop	370	553	18	4.25
Hsp70	Tau	1	274	7	1.37	Hsp90	Hop	370	101	7	5.66
Hsp70	Tau	1	163	6	2.35	Hsp90	Hop	422	509	13	1.46
Hsp70	Tau	1	370	5	1.70	Hsp90	Hop	422	101	8	3.41
Hsp70	Tau	1	375	5	1.25	Hsp90	Hop	422	553	4	2.69
Hsp70	Tau	1	234	4	3.62	Hsp90	Hop	422	73	4	1.29
Hsp70	Tau	278	240	4	2.73	Hsp90	Hop	451	411	8	3.82

## Appendix

Hsp90	Hop	451	457	7	3.87	Hsp90	Hsp90	561	504	68	19.09
Hsp90	Hop	451	370	6	3.81	Hsp90	Hsp90	561	597	3	2.06
Hsp90	Hop	458	509	19	2.26	Hsp90	Hsp90	561	647	3	2.92
Hsp90	Hop	458	553	7	2.45	Hsp90	Hsp90	573	504	19	6.34
Hsp90	Hop	514	360	13	1.51	Hsp90	Hsp90	573	580	7	1.93
Hsp90	Hop	514	367	9	1.86	Hsp90	Hsp90	574	582	8	1.24
Hsp90	Hop	549	536	27	13.36	Hsp90	Hsp90	574	580	8	3.02
Hsp90	Hop	549	546	11	2.08	Hsp90	Hsp90	582	575	7	3.95
Hsp90	Hop	549	553	9	2.25	Hsp90	Hsp90	588	600	9	1.33
Hsp90	Hop	549	509	9	1.12	Hsp90	Hsp90	591	580	17	5.72
Hsp90	Hop	549	101	4	4.45	Hsp90	Hsp90	591	600	3	1.16
Hsp90	Hop	561	536	122	21.14	Hsp90	Hsp90	597	580	15	2.66
Hsp90	Hop	561	546	16	3.84	Hsp90	Hsp90	597	630	5	1.97
Hsp90	Hop	561	509	6	2.45	Hsp90	Hsp90	600	580	67	7.65
Hsp90	Hop	600	553	9	2.92	Hsp90	Hsp90	600	591	9	1.68
Hsp90	Hop	600	509	9	1.31	Hsp90	Hsp90	600	630	5	1.80
Hsp90	Hop	600	101	8	2.51	Hsp90	Hsp90	646	600	24	6.76
Hsp90	Hop	630	73	3	2.88	Hsp90	Hsp90	646	591	15	2.13
Hsp90	Hop	646	457	18	6.87	Hsp90	Hsp90	647	630	33	2.50
Hsp90	Hop	646	553	11	2.56	Hsp90	Hsp90	647	596	16	2.69
Hsp90	Hop	646	101	9	3.86	Hsp90	Hsp90	647	422	4	1.78
Hsp90	Hop	646	509	9	2.53	Hsp90	Hsp90	675	596	22	1.96
Hsp90	Hop	647	476	16	3.32	Hsp90	Hsp90	675	588	3	1.45
Hsp90	Hop	647	546	12	3.79	Hsp90	Hsp90	708	672	198	8.52
Hsp90	Hop	647	509	12	2.10	Hsp90	Hsp90	708	669	8	3.97
Hsp90	Hop	647	553	6	2.66	Hsp90	p23	76	1	8	1.95
Hsp90	Hop	647	101	4	3.17	Hsp90	p23	130	1	3	1.99
Hsp90	Hop	647	469	4	1.60	Hsp90	p23	257	1	60	4.46
Hsp90	Hsp70	76	1	23	3.36	Hsp90	p23	675	1	5	4.61
Hsp90	Hsp70	130	1	15	3.76	Hsp90	p23	708	1	7	2.26
Hsp90	Hsp70	130	278	12	1.30	Hsp90	Tau	76	225	4	2.33
Hsp90	Hsp70	307	98	36	4.93	Hsp90	Tau	76	281	3	2.46
Hsp90	Hsp70	307	121	9	1.98	Hsp90	Tau	76	259	3	1.82
Hsp90	Hsp70	422	211	11	3.90	Hsp90	Tau	203	240	14	5.85
Hsp90	Hsp70	422	533	8	1.73	Hsp90	Tau	203	234	10	1.47
Hsp90	Hsp70	422	528	5	2.46	Hsp90	Tau	222	225	5	2.28
Hsp90	Hsp70	425	211	29	5.05	Hsp90	Tau	370	281	6	2.71
Hsp90	Hsp70	425	518	6	3.74	Hsp90	Tau	458	281	8	1.66
Hsp90	Hsp90	76	370	22	1.83	Hsp90	Tau	458	240	5	1.65
Hsp90	Hsp90	76	87	6	2.59	Hsp90	Tau	549	298	5	2.26
Hsp90	Hsp90	95	203	21	4.98	Hsp90	Tau	549	353	4	2.63
Hsp90	Hsp90	130	76	126	7.38	Hsp90	Tau	549	281	4	2.60
Hsp90	Hsp90	130	370	20	2.42	Hsp90	Tau	664	234	10	3.41
Hsp90	Hsp90	227	377	15	2.67	Hsp90	Tau	664	225	9	3.74
Hsp90	Hsp90	227	370	10	4.34	Hsp90	Tau	664	174	5	1.89
Hsp90	Hsp90	242	222	10	2.27	Hsp90	Tau	664	240	4	5.94
Hsp90	Hsp90	257	265	13	5.21	Hsp90	Tau	675	267	7	1.98
Hsp90	Hsp90	260	646	3	1.97	Hsp90	Tau	675	163	7	1.95
Hsp90	Hsp90	272	289	5	5.01	Hsp90	Tau	675	234	6	3.70
Hsp90	Hsp90	286	265	23	1.81	Hsp90	Tau	675	174	6	1.93
Hsp90	Hsp90	298	203	14	1.54	Hsp90	Tau	675	240	5	1.39
Hsp90	Hsp90	307	222	9	1.70	Hsp90	Tau	675	353	4	5.90
Hsp90	Hsp90	307	377	6	1.96	Hsp90	Tau	675	180	4	4.15
Hsp90	Hsp90	329	227	7	3.24	Hsp90	Tau	675	190	3	2.72
Hsp90	Hsp90	370	370	16	1.81	Hsp90	Tau	675	369	3	2.40
Hsp90	Hsp90	370	458	15	2.02	Hsp90	Tau	708	234	11	2.87
Hsp90	Hsp90	370	377	14	5.65	Hsp90	Tau	708	174	10	1.48
Hsp90	Hsp90	370	630	8	1.51	Hsp90	Tau	708	225	10	1.45
Hsp90	Hsp90	370	370	16	1.66	Hsp90	Tau	708	267	7	6.54
Hsp90	Hsp90	377	222	5	2.68	Hsp90	Tau	708	254	6	1.25
Hsp90	Hsp90	425	429	6	2.98	Hsp90	Tau	708	369	5	2.04
Hsp90	Hsp90	458	370	39	3.68	Hsp90	Tau	708	298	3	2.63
Hsp90	Hsp90	458	630	8	1.92	Hsp90	Tau	708	180	3	1.55
Hsp90	Hsp90	504	573	49	11.92	Hsp90	Tau	708	385	3	1.17
Hsp90	Hsp90	504	554	24	2.10	Hsp90	Tau	708	150	3	1.14
Hsp90	Hsp90	514	451	9	1.92	p23	Hop	1	101	11	4.57
Hsp90	Hsp90	514	458	7	1.29	p23	Hop	1	509	10	3.49
Hsp90	Hsp90	514	446	5	1.83	p23	Hop	1	73	8	1.37
Hsp90	Hsp90	549	561	47	13.15	p23	Hop	1	457	7	2.91
Hsp90	Hsp90	549	630	12	1.11	p23	Hop	1	415	4	2.47

## Appendix

p23	Hop	1	553	3	3.26	Tau	Hop	281	509	22	3.29
p23	Hop	101	101	14	3.49	Tau	Hop	281	73	6	6.16
p23	Hop	101	73	7	1.89	Tau	Hop	281	457	5	1.60
p23	Hsp70	1	366	16	3.78	Tau	Hop	290	509	19	3.64
p23	Hsp70	1	278	7	3.05	Tau	Hop	290	101	5	2.78
p23	Hsp70	1	129	3	1.39	Tau	Hop	298	536	16	5.91
p23	Hsp70	101	278	5	2.39	Tau	Hop	298	101	16	4.28
p23	Hsp90	1	203	7	2.05	Tau	Hop	298	509	14	2.28
p23	Hsp90	1	309	5	2.55	Tau	Hop	298	546	8	3.47
p23	Hsp90	1	458	3	2.04	Tau	Hop	298	73	6	1.54
p23	Hsp90	101	309	13	1.79	Tau	Hop	298	233	5	1.69
p23	Hsp90	101	458	9	1.69	Tau	Hop	298	553	4	1.92
p23	p23	41	1	5	2.43	Tau	Hop	298	457	3	4.23
p23	p23	54	1	43	2.95	Tau	Hop	311	101	15	3.60
p23	p23	101	1	12	2.20	Tau	Hop	311	509	8	1.30
p23	Tau	1	225	20	4.17	Tau	Hop	311	546	6	2.39
p23	Tau	1	174	13	4.06	Tau	Hop	311	73	6	1.53
p23	Tau	1	132	13	3.35	Tau	Hop	311	457	4	2.42
p23	Tau	1	150	12	2.07	Tau	Hop	321	509	23	3.10
p23	Tau	1	281	10	3.60	Tau	Hop	321	101	18	4.25
p23	Tau	1	234	10	3.49	Tau	Hop	321	536	16	2.31
p23	Tau	1	240	7	3.26	Tau	Hop	321	73	14	1.69
p23	Tau	1	259	7	1.75	Tau	Hop	321	546	11	2.78
p23	Tau	1	143	6	1.56	Tau	Hop	321	230	8	2.60
p23	Tau	54	180	4	1.50	Tau	Hop	321	457	8	1.92
p23	Tau	54	174	4	1.34	Tau	Hop	321	185	8	1.41
p23	Tau	54	225	4	1.14	Tau	Hop	321	348	5	1.86
p23	Tau	54	163	3	1.68	Tau	Hop	321	123	4	2.40
p23	Tau	101	163	10	3.01	Tau	Hop	321	553	4	1.62
p23	Tau	101	225	10	2.38	Tau	Hop	321	485	3	1.95
p23	Tau	101	174	10	2.08	Tau	Hop	331	509	22	1.23
p23	Tau	101	267	10	1.71	Tau	Hop	331	101	12	3.03
p23	Tau	101	150	8	1.88	Tau	Hop	331	457	8	1.92
p23	Tau	101	281	7	4.37	Tau	Hop	331	553	6	1.48
p23	Tau	101	259	6	2.33	Tau	Hop	331	546	4	2.37
p23	Tau	101	180	6	2.01	Tau	Hop	331	123	4	1.66
p23	Tau	101	234	5	2.92	Tau	Hop	331	348	3	1.24
p23	Tau	101	240	5	1.30	Tau	Hop	353	101	15	3.09
p23	Tau	101	347	4	1.36	Tau	Hop	353	509	10	1.70
p23	Tau	101	385	4	1.31	Tau	Hop	353	546	5	2.40
p23	Tau	101	254	4	1.18	Tau	Hop	353	476	3	2.09
p23	Tau	101	370	3	2.17	Tau	Hop	369	101	14	3.33
p23	Tau	101	143	3	1.53	Tau	Hop	369	509	10	3.06
Tau	Hop	87	101	6	2.29	Tau	Hop	369	73	7	2.71
Tau	Hop	87	261	3	3.61	Tau	Hop	370	415	4	9.81
Tau	Hop	163	415	5	2.80	Tau	Hop	370	73	3	4.49
Tau	Hop	163	101	5	1.44	Tau	Hop	375	509	6	1.62
Tau	Hop	163	457	3	1.31	Tau	Hop	375	73	5	2.72
Tau	Hop	174	457	5	2.67	Tau	Hop	385	101	10	3.17
Tau	Hop	174	415	5	1.46	Tau	Hop	385	509	10	2.10
Tau	Hop	180	101	4	1.65	Tau	Hop	385	73	6	1.53
Tau	Hop	180	457	3	1.74	Tau	Hop	385	457	5	3.33
Tau	Hop	190	101	5	2.27	Tau	Hop	385	415	3	1.82
Tau	Hop	234	457	8	2.34	Tau	Hop	395	509	12	2.73
Tau	Hop	234	73	6	1.41	Tau	Hop	395	101	9	4.12
Tau	Hop	234	415	3	1.12	Tau	Hop	395	73	5	2.07
Tau	Hop	240	415	5	15.16	Tau	Hop	395	230	3	3.03
Tau	Hop	240	273	4	2.39	Tau	Hop	438	101	9	5.32
Tau	Hop	254	101	10	2.86	Tau	Hop	438	509	8	2.42
Tau	Hop	254	73	6	2.25	Tau	Hop	438	536	5	4.05
Tau	Hop	254	509	4	2.32	Tau	Hop	438	55	4	3.43
Tau	Hop	254	553	4	1.60	Tau	Hop	438	36	3	4.34
Tau	Hop	254	457	3	1.33	Tau	Hop	438	387	3	2.39
Tau	Hop	259	73	6	2.47	Tau	Hop	438	73	3	1.76
Tau	Hop	259	457	3	1.68	Tau	Hsp70	24	366	7	1.43
Tau	Hop	267	509	12	1.91	Tau	Hsp70	87	109	4	5.91
Tau	Hop	267	73	10	2.24	Tau	Hsp70	87	366	4	5.12
Tau	Hop	267	101	10	2.01	Tau	Hsp70	87	1	4	2.36
Tau	Hop	267	457	7	1.13	Tau	Hsp70	150	366	4	1.64
Tau	Hop	280	73	4	3.78	Tau	Hsp70	163	366	11	3.61



## Appendix

Tau	Hsp70	174	278	7	3.85	Tau	p23	331	1	9	1.57
Tau	Hsp70	180	1	8	1.97	Tau	p23	340	1	4	2.19
Tau	Hsp70	240	518	9	7.57	Tau	p23	353	1	6	1.66
Tau	Hsp70	240	366	4	2.04	Tau	p23	353	101	5	2.37
Tau	Hsp70	240	211	3	12.12	Tau	p23	369	1	12	1.76
Tau	Hsp70	254	1	6	3.84	Tau	p23	385	1	19	3.09
Tau	Hsp70	267	582	6	1.78	Tau	p23	395	1	9	2.86
Tau	Hsp70	280	518	3	1.79	Tau	p23	438	1	9	3.35
Tau	Hsp70	281	366	4	3.42	Tau	p23	438	101	5	2.47
Tau	Hsp70	294	518	3	7.67	Tau	Tau	24	163	27	2.18
Tau	Hsp70	298	472	7	2.81	Tau	Tau	24	174	24	2.86
Tau	Hsp70	298	528	3	1.68	Tau	Tau	24	225	22	2.48
Tau	Hsp70	311	1	5	2.08	Tau	Tau	24	331	21	3.16
Tau	Hsp70	311	366	3	1.73	Tau	Tau	24	267	17	1.42
Tau	Hsp70	311	533	3	1.11	Tau	Tau	24	240	15	1.68
Tau	Hsp70	317	1	4	1.26	Tau	Tau	24	234	13	1.85
Tau	Hsp70	321	582	22	1.99	Tau	Tau	24	180	12	1.49
Tau	Hsp70	321	1	13	3.43	Tau	Tau	24	385	11	3.16
Tau	Hsp70	321	545	5	2.03	Tau	Tau	24	190	11	1.12
Tau	Hsp70	321	580	3	2.24	Tau	Tau	24	150	10	2.18
Tau	Hsp70	331	1	12	2.12	Tau	Tau	24	281	9	3.25
Tau	Hsp70	331	545	4	1.84	Tau	Tau	24	132	9	1.88
Tau	Hsp70	353	582	7	2.05	Tau	Tau	24	143	9	1.60
Tau	Hsp70	353	1	5	3.84	Tau	Tau	24	259	8	1.96
Tau	Hsp70	369	366	10	2.35	Tau	Tau	24	369	6	3.21
Tau	Hsp70	369	1	9	1.73	Tau	Tau	24	370	6	2.21
Tau	Hsp70	369	582	7	2.09	Tau	Tau	24	311	6	1.90
Tau	Hsp70	370	211	5	8.70	Tau	Tau	24	254	6	1.65
Tau	Hsp70	370	366	4	4.80	Tau	Tau	24	395	3	4.74
Tau	Hsp70	385	366	10	1.49	Tau	Tau	44	163	14	1.86
Tau	Hsp70	385	582	8	1.97	Tau	Tau	44	180	13	3.03
Tau	Hsp70	385	472	5	1.98	Tau	Tau	44	321	12	2.42
Tau	Hsp70	395	366	8	1.85	Tau	Tau	44	267	12	1.19
Tau	Hsp70	438	1	10	4.87	Tau	Tau	44	150	11	1.14
Tau	Hsp70	438	109	7	3.89	Tau	Tau	44	234	5	1.25
Tau	Hsp70	438	366	7	1.91	Tau	Tau	67	150	9	1.23
Tau	Hsp70	438	267	4	3.69	Tau	Tau	67	234	8	1.33
Tau	Hsp70	438	618	3	6.12	Tau	Tau	67	321	6	4.42
Tau	Hsp90	163	664	9	3.22	Tau	Tau	67	24	6	2.96
Tau	Hsp90	174	203	7	2.02	Tau	Tau	67	298	5	2.61
Tau	Hsp90	254	458	7	1.49	Tau	Tau	67	190	5	1.29
Tau	Hsp90	290	458	5	1.65	Tau	Tau	67	353	4	3.22
Tau	Hsp90	298	458	11	2.02	Tau	Tau	67	369	4	2.53
Tau	Hsp90	298	370	4	1.69	Tau	Tau	67	385	4	1.50
Tau	Hsp90	311	203	18	3.50	Tau	Tau	67	438	3	2.23
Tau	Hsp90	321	458	9	2.64	Tau	Tau	87	150	30	8.29
Tau	Hsp90	321	422	5	1.35	Tau	Tau	87	174	27	9.48
Tau	Hsp90	321	561	4	2.31	Tau	Tau	87	163	26	8.93
Tau	Hsp90	331	458	12	1.47	Tau	Tau	87	225	22	9.85
Tau	Hsp90	353	458	12	1.37	Tau	Tau	87	143	16	3.62
Tau	Hsp90	353	422	5	1.24	Tau	Tau	87	180	15	10.24
Tau	Hsp90	353	370	3	1.31	Tau	Tau	87	311	13	9.48
Tau	Hsp90	369	458	4	2.66	Tau	Tau	87	132	13	5.83
Tau	Hsp90	370	672	4	1.32	Tau	Tau	87	385	12	11.88
Tau	Hsp90	438	458	8	2.04	Tau	Tau	87	240	12	3.88
Tau	Hsp90	438	425	6	1.48	Tau	Tau	87	281	11	6.09
Tau	Hsp90	438	370	5	2.03	Tau	Tau	87	234	11	4.72
Tau	Hsp90	438	422	4	1.42	Tau	Tau	87	370	11	2.25
Tau	p23	24	1	9	3.93	Tau	Tau	87	259	10	7.74
Tau	p23	67	1	5	2.03	Tau	Tau	87	254	10	7.71
Tau	p23	87	1	14	4.20	Tau	Tau	87	274	9	8.64
Tau	p23	87	101	5	2.47	Tau	Tau	87	267	9	8.55
Tau	p23	163	1	13	2.56	Tau	Tau	87	130	9	6.23
Tau	p23	180	1	15	1.26	Tau	Tau	87	140	9	4.04
Tau	p23	190	1	12	2.89	Tau	Tau	87	190	8	6.74
Tau	p23	224	1	4	1.39	Tau	Tau	87	369	7	8.27
Tau	p23	254	1	10	3.01	Tau	Tau	87	353	7	4.07
Tau	p23	267	1	14	1.21	Tau	Tau	87	375	6	7.70
Tau	p23	298	1	14	3.84	Tau	Tau	87	298	5	9.47
Tau	p23	321	1	13	2.30	Tau	Tau	87	343	5	5.35

## Appendix

Tau	Tau	87	148	5	3.75	Tau	Tau	234	225	26	7.39
Tau	Tau	87	290	5	3.09	Tau	Tau	234	150	13	6.05
Tau	Tau	87	224	4	7.30	Tau	Tau	234	143	5	2.83
Tau	Tau	87	24	4	4.63	Tau	Tau	234	130	4	3.26
Tau	Tau	87	395	4	3.91	Tau	Tau	234	383	3	3.86
Tau	Tau	87	331	4	3.45	Tau	Tau	234	370	3	1.68
Tau	Tau	87	383	4	1.26	Tau	Tau	234	240	3	1.50
Tau	Tau	87	321	3	2.88	Tau	Tau	240	225	10	12.87
Tau	Tau	130	143	30	18.13	Tau	Tau	240	148	7	10.20
Tau	Tau	130	148	17	10.04	Tau	Tau	240	370	6	11.08
Tau	Tau	130	225	8	7.23	Tau	Tau	240	383	4	18.25
Tau	Tau	132	143	60	10.94	Tau	Tau	240	130	3	12.00
Tau	Tau	132	150	33	11.13	Tau	Tau	240	347	3	5.42
Tau	Tau	132	148	30	6.45	Tau	Tau	240	150	3	4.14
Tau	Tau	132	174	29	2.66	Tau	Tau	254	267	17	1.49
Tau	Tau	132	240	7	8.13	Tau	Tau	254	225	16	3.45
Tau	Tau	132	234	6	2.97	Tau	Tau	254	259	16	1.90
Tau	Tau	140	150	39	7.51	Tau	Tau	254	281	12	2.44
Tau	Tau	140	130	23	8.85	Tau	Tau	254	240	9	1.51
Tau	Tau	140	148	22	9.12	Tau	Tau	254	174	5	1.31
Tau	Tau	140	143	20	8.56	Tau	Tau	254	234	5	1.19
Tau	Tau	141	130	15	8.47	Tau	Tau	254	130	3	1.19
Tau	Tau	141	150	13	3.45	Tau	Tau	259	225	19	3.64
Tau	Tau	141	148	12	8.84	Tau	Tau	259	240	12	3.89
Tau	Tau	148	225	6	2.93	Tau	Tau	259	234	9	2.82
Tau	Tau	150	143	33	9.73	Tau	Tau	259	174	8	2.47
Tau	Tau	150	130	19	7.61	Tau	Tau	259	280	8	1.87
Tau	Tau	150	225	6	3.23	Tau	Tau	267	281	29	2.03
Tau	Tau	163	174	61	8.21	Tau	Tau	267	225	13	2.59
Tau	Tau	163	150	22	10.03	Tau	Tau	267	385	11	1.38
Tau	Tau	163	132	22	2.95	Tau	Tau	267	240	9	3.12
Tau	Tau	163	143	18	3.45	Tau	Tau	267	234	9	1.90
Tau	Tau	163	130	15	3.74	Tau	Tau	267	370	7	2.14
Tau	Tau	163	190	13	1.99	Tau	Tau	267	130	3	1.53
Tau	Tau	163	140	13	1.97	Tau	Tau	274	225	14	3.82
Tau	Tau	163	234	11	2.41	Tau	Tau	274	385	9	1.31
Tau	Tau	163	370	7	3.48	Tau	Tau	274	259	9	1.29
Tau	Tau	163	225	5	1.82	Tau	Tau	274	281	7	1.24
Tau	Tau	163	383	5	1.79	Tau	Tau	274	150	3	1.80
Tau	Tau	163	240	5	1.46	Tau	Tau	280	240	10	6.91
Tau	Tau	163	141	5	1.18	Tau	Tau	280	225	5	6.62
Tau	Tau	163	148	4	2.74	Tau	Tau	281	240	10	5.87
Tau	Tau	163	281	3	2.59	Tau	Tau	281	259	10	3.38
Tau	Tau	174	150	23	3.68	Tau	Tau	281	294	6	2.06
Tau	Tau	174	225	20	4.87	Tau	Tau	281	225	5	3.93
Tau	Tau	174	240	16	8.85	Tau	Tau	281	174	5	2.08
Tau	Tau	174	143	15	2.89	Tau	Tau	281	234	4	2.04
Tau	Tau	174	130	8	4.57	Tau	Tau	281	150	3	1.17
Tau	Tau	174	140	7	5.44	Tau	Tau	290	259	4	1.69
Tau	Tau	174	234	6	1.75	Tau	Tau	294	280	7	1.69
Tau	Tau	174	148	5	1.74	Tau	Tau	298	281	44	4.56
Tau	Tau	174	370	3	1.96	Tau	Tau	298	290	24	1.89
Tau	Tau	180	163	31	1.27	Tau	Tau	298	321	22	9.69
Tau	Tau	180	150	15	1.46	Tau	Tau	298	267	17	1.67
Tau	Tau	180	225	13	2.22	Tau	Tau	298	331	16	2.36
Tau	Tau	180	385	7	1.81	Tau	Tau	298	274	12	1.49
Tau	Tau	180	132	7	1.44	Tau	Tau	298	385	11	2.93
Tau	Tau	180	130	5	1.72	Tau	Tau	298	353	10	3.94
Tau	Tau	180	281	5	1.51	Tau	Tau	298	395	9	4.05
Tau	Tau	180	140	4	1.53	Tau	Tau	298	259	8	2.41
Tau	Tau	180	143	4	1.16	Tau	Tau	298	163	8	1.87
Tau	Tau	190	174	21	2.29	Tau	Tau	298	24	7	4.34
Tau	Tau	190	225	14	5.39	Tau	Tau	298	225	7	1.77
Tau	Tau	190	240	10	2.74	Tau	Tau	298	240	6	1.64
Tau	Tau	190	132	9	1.76	Tau	Tau	298	347	6	1.22
Tau	Tau	190	143	8	4.35	Tau	Tau	298	369	5	1.79
Tau	Tau	190	150	7	2.99	Tau	Tau	298	311	5	1.22
Tau	Tau	190	148	5	1.57	Tau	Tau	298	174	4	1.93
Tau	Tau	190	259	3	1.16	Tau	Tau	298	180	4	1.40
Tau	Tau	225	143	6	5.06	Tau	Tau	298	234	3	1.24

## Appendix

Tau	Tau	311	281	17	2.75
Tau	Tau	311	290	17	1.73
Tau	Tau	311	331	13	1.85
Tau	Tau	311	370	9	2.30
Tau	Tau	311	343	9	1.63
Tau	Tau	311	375	8	2.03
Tau	Tau	311	267	8	1.94
Tau	Tau	311	259	8	1.85
Tau	Tau	311	347	8	1.54
Tau	Tau	311	294	7	1.27
Tau	Tau	311	240	5	1.42
Tau	Tau	311	385	4	1.37
Tau	Tau	317	353	9	1.63
Tau	Tau	321	343	24	1.81
Tau	Tau	321	24	22	3.39
Tau	Tau	321	353	21	2.19
Tau	Tau	321	395	18	3.86
Tau	Tau	321	385	18	2.57
Tau	Tau	321	290	17	1.49
Tau	Tau	321	281	16	2.71
Tau	Tau	321	267	14	1.89
Tau	Tau	321	369	13	1.21
Tau	Tau	321	311	11	3.45
Tau	Tau	321	225	11	1.45
Tau	Tau	321	234	10	1.27
Tau	Tau	321	163	10	1.25
Tau	Tau	321	180	8	1.46
Tau	Tau	321	375	5	1.21
Tau	Tau	331	290	21	1.17
Tau	Tau	331	385	14	1.86
Tau	Tau	331	343	12	2.09
Tau	Tau	331	274	9	1.56
Tau	Tau	331	375	9	1.17
Tau	Tau	331	369	7	2.62
Tau	Tau	331	225	5	2.41
Tau	Tau	331	163	3	1.28
Tau	Tau	340	353	21	1.48
Tau	Tau	340	385	8	2.20
Tau	Tau	340	395	6	2.93
Tau	Tau	340	370	6	1.73
Tau	Tau	340	369	5	3.06
Tau	Tau	340	267	3	1.18
Tau	Tau	343	370	8	5.00
Tau	Tau	343	240	4	2.61
Tau	Tau	347	370	16	12.33
Tau	Tau	347	383	3	3.84
Tau	Tau	353	375	28	1.71
Tau	Tau	353	385	26	3.09
Tau	Tau	353	311	21	2.79
Tau	Tau	353	370	20	2.35
Tau	Tau	353	331	18	1.81
Tau	Tau	353	174	14	1.77
Tau	Tau	353	225	8	2.19
Tau	Tau	353	281	8	1.94
Tau	Tau	353	254	8	1.50
Tau	Tau	353	259	6	1.61
Tau	Tau	353	180	5	2.75
Tau	Tau	353	274	5	1.19
Tau	Tau	353	163	5	1.16
Tau	Tau	369	383	29	2.53
Tau	Tau	369	385	25	6.78
Tau	Tau	369	343	23	2.03
Tau	Tau	369	347	14	1.84
Tau	Tau	369	240	9	1.66
Tau	Tau	369	174	8	2.05
Tau	Tau	369	225	6	1.56
Tau	Tau	369	254	4	2.09
Tau	Tau	369	163	4	1.39
Tau	Tau	369	259	3	1.58
Tau	Tau	370	383	31	20.05
Tau	Tau	375	383	21	3.56
Tau	Tau	375	347	4	2.73
Tau	Tau	383	369	5	5.19
Tau	Tau	385	375	39	2.30
Tau	Tau	385	370	29	5.76
Tau	Tau	385	240	8	2.96
Tau	Tau	385	174	7	1.13
Tau	Tau	385	225	5	1.57
Tau	Tau	385	347	4	1.41
Tau	Tau	385	234	4	1.31
Tau	Tau	395	375	30	2.59
Tau	Tau	395	369	24	3.46
Tau	Tau	395	353	18	4.30
Tau	Tau	395	370	18	3.06
Tau	Tau	395	383	18	1.70
Tau	Tau	395	331	12	4.05
Tau	Tau	395	267	10	1.70
Tau	Tau	395	311	7	2.94
Tau	Tau	395	163	6	2.42
Tau	Tau	395	234	5	3.08
Tau	Tau	395	225	5	2.53
Tau	Tau	395	254	5	1.19
Tau	Tau	395	174	4	2.72
Tau	Tau	395	190	4	1.93
Tau	Tau	395	180	3	2.79
Tau	Tau	395	240	3	1.40
Tau	Tau	438	375	19	2.80
Tau	Tau	438	395	15	5.55
Tau	Tau	438	225	14	4.71
Tau	Tau	438	385	14	2.61
Tau	Tau	438	353	13	2.61
Tau	Tau	438	370	12	2.53
Tau	Tau	438	369	12	2.28
Tau	Tau	438	174	12	2.14
Tau	Tau	438	254	11	3.45
Tau	Tau	438	281	10	3.44
Tau	Tau	438	234	9	2.45
Tau	Tau	438	267	9	2.22
Tau	Tau	438	298	8	4.40
Tau	Tau	438	274	8	1.82
Tau	Tau	438	321	7	4.10
Tau	Tau	438	311	7	2.57
Tau	Tau	438	343	7	2.12
Tau	Tau	438	150	7	1.73
Tau	Tau	438	383	7	1.35
Tau	Tau	438	259	6	3.06
Tau	Tau	438	180	6	2.58
Tau	Tau	438	163	5	3.47
Tau	Tau	438	290	5	2.65
Tau	Tau	438	347	5	1.30
Tau	Tau	438	240	4	1.98
Tau	Tau	438	190	4	1.59

## Appendix

**Table A 4 Selected intra- and intermolecular cross-links within the Hsp70:Hop:Hsp90:Tau:p23 complex cross-linked with 1-ethyl-3-(3-dimethylaminopropyl) carbodiimid (EDC).**

Threshold: minimum of 3 hits and 5% of the maximum score ( $\geq 1.5225$ ).

Protein1	Protein2	Pos1	Pos2	Hits	Score
Hop	Hop	31	133	3	3.60
Hop	Hop	31	559	5	3.45
Hop	Hop	31	479	3	2.76
Hop	Hop	31	310	5	1.58
Hop	Hop	36	133	3	2.22
Hop	Hop	44	74	9	2.69
Hop	Hop	45	74	3	2.28
Hop	Hop	55	442	5	3.74
Hop	Hop	73	161	4	6.20
Hop	Hop	91	133	6	3.81
Hop	Hop	96	479	3	2.17
Hop	Hop	96	381	6	1.78
Hop	Hop	115	139	18	2.02
Hop	Hop	119	115	24	11.25
Hop	Hop	123	133	7	2.04
Hop	Hop	133	360	7	5.61
Hop	Hop	133	73	8	4.24
Hop	Hop	133	185	23	2.74
Hop	Hop	133	418	4	1.88
Hop	Hop	139	115	31	11.49
Hop	Hop	146	133	13	4.49
Hop	Hop	146	139	15	4.34
Hop	Hop	146	479	4	2.90
Hop	Hop	146	559	4	2.65
Hop	Hop	146	381	4	2.30
Hop	Hop	146	106	7	2.17
Hop	Hop	159	133	7	1.62
Hop	Hop	177	73	8	19.33
Hop	Hop	185	112	6	4.14
Hop	Hop	192	133	6	2.67
Hop	Hop	192	177	7	1.95
Hop	Hop	209	348	3	3.15
Hop	Hop	209	96	10	2.47
Hop	Hop	214	96	3	3.48
Hop	Hop	215	546	3	6.31
Hop	Hop	215	96	3	2.13
Hop	Hop	216	348	5	4.93
Hop	Hop	216	185	7	4.87
Hop	Hop	216	31	5	4.53
Hop	Hop	216	96	9	3.50
Hop	Hop	216	324	4	2.50
Hop	Hop	217	96	6	5.38
Hop	Hop	217	348	6	3.89
Hop	Hop	217	185	7	1.94
Hop	Hop	218	348	8	6.09
Hop	Hop	218	324	4	3.71
Hop	Hop	230	177	10	4.18
Hop	Hop	230	133	17	4.16
Hop	Hop	230	253	6	1.97
Hop	Hop	233	133	10	3.79
Hop	Hop	233	253	14	3.25
Hop	Hop	233	251	13	3.15
Hop	Hop	235	252	20	3.72
Hop	Hop	235	185	3	1.98
Hop	Hop	235	73	14	1.79
Hop	Hop	243	246	3	3.70
Hop	Hop	269	177	3	3.12
Hop	Hop	276	233	7	3.51
Hop	Hop	294	262	5	2.67
Hop	Hop	340	177	12	4.95
Hop	Hop	340	133	8	3.77
Hop	Hop	348	177	9	4.13
Hop	Hop	348	381	15	3.23
Hop	Hop	348	133	6	2.38
Hop	Hop	348	386	3	2.10
Hop	Hop	370	366	10	11.90
Hop	Hop	370	177	3	1.75
Hop	Hop	381	418	3	2.51
Hop	Hop	381	370	5	2.11
Hop	Hop	381	340	8	2.09
Hop	Hop	381	73	7	1.67
Hop	Hop	385	389	9	2.80
Hop	Hop	385	340	6	2.00
Hop	Hop	404	177	5	1.57
Hop	Hop	441	457	5	1.53
Hop	Hop	442	340	5	3.01
Hop	Hop	442	415	23	2.94
Hop	Hop	442	146	3	2.84
Hop	Hop	452	486	5	2.49
Hop	Hop	452	559	4	2.21
Hop	Hop	457	559	3	3.38
Hop	Hop	465	559	14	5.13
Hop	Hop	465	503	18	4.22
Hop	Hop	465	507	17	3.32
Hop	Hop	465	532	4	2.55
Hop	Hop	465	506	13	2.47
Hop	Hop	469	559	14	2.77
Hop	Hop	476	177	3	3.06
Hop	Hop	509	177	8	5.27
Hop	Hop	509	133	11	4.99
Hop	Hop	509	472	7	2.82
Hop	Hop	509	489	9	2.63
Hop	Hop	509	532	8	2.25
Hop	Hop	509	479	9	2.15
Hop	Hop	509	432	3	2.02
Hop	Hop	515	553	7	2.47
Hop	Hop	515	556	3	1.98
Hop	Hop	517	556	7	2.36
Hop	Hop	517	553	9	1.85
Hop	Hop	524	553	27	2.37
Hop	Hop	536	559	8	3.10
Hop	Hop	536	133	8	2.69
Hop	Hop	536	177	7	2.34
Hop	Hop	536	479	17	2.09
Hop	Hop	536	503	5	1.82
Hop	Hop	543	553	66	3.83
Hop	Hop	543	509	5	1.94
Hop	Hop	546	479	27	17.69
Hop	Hop	546	133	4	5.25
Hop	Hop	546	432	8	2.85
Hop	Hop	546	177	6	1.96
Hop	Hop	553	479	13	3.93
Hop	Hop	553	177	5	3.48
Hop	Hop	553	537	3	2.03
Hop	Hop	556	479	15	3.31
Hop	Hop	556	472	3	2.31
Hop	Hop	559	509	12	3.74
Hop	Hsp70	31	662	4	4.65
Hop	Hsp70	96	660	9	2.39
Hop	Hsp70	133	211	3	3.09
Hop	Hsp70	133	582	3	1.89
Hop	Hsp70	146	549	4	4.42
Hop	Hsp70	177	211	6	7.09
Hop	Hsp70	216	1	6	6.12
Hop	Hsp70	217	1	5	5.30
Hop	Hsp70	218	1	7	4.12
Hop	Hsp70	235	1	14	2.36
Hop	Hsp70	348	339	33	19.14
Hop	Hsp70	348	336	48	9.02
Hop	Hsp70	381	472	4	1.89

## Appendix

Hop	Hsp70	553	576	4	2.53	Hop	Tau	133	370	3	2.22
Hop	Hsp90	31	210	5	5.54	Hop	Tau	133	280	8	1.76
Hop	Hsp90	31	317	3	3.31	Hop	Tau	177	347	4	8.23
Hop	Hsp90	91	210	5	2.61	Hop	Tau	177	225	5	5.58
Hop	Hsp90	96	210	3	2.31	Hop	Tau	216	353	3	6.08
Hop	Hsp90	123	210	4	2.51	Hop	Tau	216	321	5	4.56
Hop	Hsp90	132	317	3	2.96	Hop	Tau	216	369	4	4.35
Hop	Hsp90	133	596	6	9.22	Hop	Tau	216	267	5	3.64
Hop	Hsp90	133	425	4	8.73	Hop	Tau	216	331	4	2.85
Hop	Hsp90	133	309	10	5.67	Hop	Tau	216	274	4	2.14
Hop	Hsp90	133	630	8	5.36	Hop	Tau	217	321	5	3.87
Hop	Hsp90	133	600	4	3.10	Hop	Tau	240	370	4	2.57
Hop	Hsp90	146	347	10	3.63	Hop	Tau	381	150	4	3.93
Hop	Hsp90	146	351	3	3.58	Hop	Tau	381	259	6	2.96
Hop	Hsp90	146	512	7	2.88	Hop	Tau	381	225	4	2.95
Hop	Hsp90	146	408	3	1.57	Hop	Tau	381	281	7	2.40
Hop	Hsp90	146	368	3	1.57	Hop	Tau	381	347	5	2.05
Hop	Hsp90	177	425	4	6.40	Hop	Tau	381	385	4	2.04
Hop	Hsp90	216	600	5	3.10	Hop	Tau	381	174	7	2.02
Hop	Hsp90	217	600	5	1.77	Hop	Tau	381	240	4	1.78
Hop	Hsp90	231	504	5	1.84	Hop	Tau	381	274	4	1.74
Hop	Hsp90	348	318	3	1.92	Hop	Tau	385	174	3	2.02
Hop	Hsp90	348	317	4	1.76	Hop	Tau	387	73	5	3.79
Hop	Hsp90	381	425	4	2.14	Hop	Tau	442	385	6	2.18
Hop	Hsp90	404	322	10	1.76	Hop	Tau	442	274	4	1.77
Hop	Hsp90	442	630	4	2.17	Hop	Tau	442	375	3	1.70
Hop	Hsp90	465	368	12	3.27	Hop	Tau	479	240	9	9.70
Hop	Hsp90	469	636	5	1.65	Hop	Tau	479	347	3	7.73
Hop	Hsp90	472	596	10	8.52	Hop	Tau	479	383	6	6.98
Hop	Hsp90	479	596	19	11.68	Hop	Tau	479	370	7	6.39
Hop	Hsp90	479	630	17	8.82	Hop	Tau	479	225	6	2.97
Hop	Hsp90	509	416	12	4.82	Hop	Tau	479	280	4	1.98
Hop	Hsp90	509	368	12	3.43	Hsp70	Hop	1	133	8	4.04
Hop	Hsp90	536	210	8	3.22	Hsp70	Hop	1	177	6	3.67
Hop	Hsp90	536	565	3	2.44	Hsp70	Hop	1	381	4	2.85
Hop	Hsp90	536	416	3	1.92	Hsp70	Hop	580	133	7	3.67
Hop	Hsp90	536	368	3	1.64	Hsp70	Hop	618	133	3	1.85
Hop	Hsp90	536	512	12	1.57	Hsp70	Hop	618	177	3	1.61
Hop	Hsp90	543	596	6	2.99	Hsp70	Hop	649	133	4	1.85
Hop	Hsp90	543	630	9	2.85	Hsp70	Hop	659	73	8	15.71
Hop	Hsp90	543	425	5	2.22	Hsp70	Hop	660	324	5	6.01
Hop	Hsp90	543	600	4	1.88	Hsp70	Hop	660	73	7	2.34
Hop	Hsp90	546	565	4	2.55	Hsp70	Hop	662	418	6	6.85
Hop	Hsp90	553	416	5	3.88	Hsp70	Hop	662	73	3	5.29
Hop	Hsp90	553	368	7	2.44	Hsp70	Hop	662	101	4	4.57
Hop	Hsp90	559	596	4	2.64	Hsp70	Hop	662	509	7	4.44
Hop	Hsp90	559	630	14	1.67	Hsp70	Hsp70	1	18	66	23.56
Hop	p23	25	1	4	2.42	Hsp70	Hsp70	1	662	28	7.90
Hop	p23	29	1	8	4.78	Hsp70	Hsp70	1	181	13	5.85
Hop	p23	31	117	4	2.10	Hsp70	Hsp70	1	67	10	5.16
Hop	p23	31	120	4	2.04	Hsp70	Hsp70	1	69	19	4.95
Hop	p23	45	1	6	2.26	Hsp70	Hsp70	1	576	9	4.14
Hop	p23	52	1	3	2.91	Hsp70	Hsp70	1	577	12	4.07
Hop	p23	209	1	9	3.01	Hsp70	Hsp70	1	659	5	3.87
Hop	p23	215	1	4	5.31	Hsp70	Hsp70	1	481	7	3.85
Hop	p23	216	1	22	8.30	Hsp70	Hsp70	1	660	8	3.85
Hop	p23	217	1	15	6.23	Hsp70	Hsp70	1	53	6	3.71
Hop	p23	218	1	9	3.31	Hsp70	Hsp70	1	544	5	3.43
Hop	p23	235	1	20	2.70	Hsp70	Hsp70	1	549	24	3.00
Hop	p23	238	1	46	3.69	Hsp70	Hsp70	1	612	4	2.21
Hop	p23	239	1	10	1.70	Hsp70	Hsp70	1	527	8	1.92
Hop	p23	276	1	4	3.05	Hsp70	Hsp70	18	518	6	5.98
Hop	p23	348	120	4	1.63	Hsp70	Hsp70	18	533	6	2.08
Hop	p23	381	1	13	2.89	Hsp70	Hsp70	24	404	8	12.62
Hop	p23	385	1	6	4.33	Hsp70	Hsp70	67	129	14	3.24
Hop	p23	442	1	7	4.05	Hsp70	Hsp70	120	98	24	5.18
Hop	p23	442	101	6	1.92	Hsp70	Hsp70	133	662	7	4.32
Hop	p23	536	87	3	2.07	Hsp70	Hsp70	150	1	6	1.71
Hop	Tau	133	240	9	9.02	Hsp70	Hsp70	153	1	3	2.74
Hop	Tau	133	383	4	5.28	Hsp70	Hsp70	173	1	8	7.00

## Appendix

Hsp70	Hsp70	180	662	5	3.24	Hsp70	p23	404	1	4	3.70
Hsp70	Hsp70	207	1	4	3.93	Hsp70	p23	416	1	8	3.94
Hsp70	Hsp70	246	340	15	3.14	Hsp70	Tau	1	402	4	1.93
Hsp70	Hsp70	310	272	19	2.19	Hsp70	Tau	313	225	5	1.96
Hsp70	Hsp70	313	1	6	1.75	Hsp70	Tau	313	353	4	1.72
Hsp70	Hsp70	349	339	7	2.51	Hsp70	Tau	339	240	3	3.36
Hsp70	Hsp70	366	373	27	2.33	Hsp70	Tau	416	353	5	5.67
Hsp70	Hsp70	382	662	3	2.74	Hsp70	Tau	416	274	6	2.76
Hsp70	Hsp70	404	1	29	6.82	Hsp70	Tau	416	267	6	2.40
Hsp70	Hsp70	404	528	7	2.53	Hsp70	Tau	416	369	4	2.34
Hsp70	Hsp70	407	1	16	10.36	Hsp70	Tau	416	225	7	1.85
Hsp70	Hsp70	411	1	23	7.34	Hsp70	Tau	416	370	5	1.58
Hsp70	Hsp70	411	533	17	2.49	Hsp70	Tau	549	225	6	7.82
Hsp70	Hsp70	411	528	12	1.81	Hsp70	Tau	549	280	4	6.74
Hsp70	Hsp70	416	1	30	6.35	Hsp70	Tau	549	370	7	5.01
Hsp70	Hsp70	416	528	38	3.53	Hsp70	Tau	576	240	4	8.47
Hsp70	Hsp70	444	18	4	1.70	Hsp70	Tau	577	383	6	3.51
Hsp70	Hsp70	465	528	5	1.91	Hsp70	Tau	577	370	5	2.45
Hsp70	Hsp70	527	211	3	6.82	Hsp70	Tau	594	358	4	1.66
Hsp70	Hsp70	528	18	6	2.32	Hsp70	Tau	659	370	4	3.29
Hsp70	Hsp70	544	211	4	6.02	Hsp70	Tau	659	385	3	2.03
Hsp70	Hsp70	545	18	7	1.68	Hsp70	Tau	660	281	5	2.94
Hsp70	Hsp70	547	544	13	13.41	Hsp70	Tau	662	294	4	7.00
Hsp70	Hsp70	549	211	4	6.18	Hsp70	Tau	662	281	16	6.78
Hsp70	Hsp70	560	662	4	4.50	Hsp70	Tau	662	370	15	6.52
Hsp70	Hsp70	571	662	4	2.28	Hsp70	Tau	662	225	8	5.69
Hsp70	Hsp70	575	588	9	1.81	Hsp70	Tau	662	240	7	5.43
Hsp70	Hsp70	576	588	9	14.78	Hsp70	Tau	662	385	7	4.56
Hsp70	Hsp70	576	589	8	2.69	Hsp70	Tau	662	383	7	3.87
Hsp70	Hsp70	577	588	38	29.72	Hsp70	Tau	662	259	11	3.81
Hsp70	Hsp70	577	589	10	5.13	Hsp70	Tau	662	234	11	3.48
Hsp70	Hsp70	580	662	12	3.12	Hsp70	Tau	662	174	11	2.92
Hsp70	Hsp70	582	662	13	3.39	Hsp70	Tau	662	375	9	2.76
Hsp70	Hsp70	582	577	5	2.57	Hsp70	Tau	662	280	8	2.67
Hsp70	Hsp70	603	1	4	1.67	Hsp70	Tau	662	130	3	2.12
Hsp70	Hsp70	609	1	11	5.28	Hsp90	Hop	76	543	3	2.54
Hsp70	Hsp70	618	660	3	1.53	Hsp90	Hop	92	133	3	1.67
Hsp70	Hsp70	619	594	4	8.28	Hsp90	Hop	274	418	3	2.01
Hsp70	Hsp70	660	580	3	3.16	Hsp90	Hop	307	398	6	1.67
Hsp70	Hsp70	662	211	4	5.78	Hsp90	Hop	317	146	4	3.99
Hsp70	Hsp70	662	588	4	5.28	Hsp90	Hop	317	509	4	3.45
Hsp70	Hsp70	662	369	10	4.56	Hsp90	Hop	317	96	9	2.71
Hsp70	Hsp70	662	518	11	4.43	Hsp90	Hop	318	348	8	2.28
Hsp70	Hsp70	662	580	12	3.77	Hsp90	Hop	318	185	3	1.77
Hsp70	Hsp70	662	278	7	3.13	Hsp90	Hop	318	91	3	1.67
Hsp70	Hsp70	662	582	15	2.95	Hsp90	Hop	318	96	13	1.63
Hsp70	Hsp70	662	366	17	2.48	Hsp90	Hop	322	469	3	2.13
Hsp70	Hsp90	1	210	21	6.74	Hsp90	Hop	322	404	10	1.88
Hsp70	Hsp90	1	416	12	4.75	Hsp90	Hop	347	73	5	3.48
Hsp70	Hsp90	1	351	15	4.14	Hsp90	Hop	347	101	6	3.33
Hsp70	Hsp90	1	72	15	3.17	Hsp90	Hop	368	509	18	3.72
Hsp70	Hsp90	1	408	10	3.14	Hsp90	Hop	370	177	8	5.13
Hsp70	Hsp90	1	407	10	2.83	Hsp90	Hop	370	559	14	4.69
Hsp70	Hsp90	1	104	4	2.04	Hsp90	Hop	370	532	15	4.19
Hsp70	Hsp90	1	347	3	1.62	Hsp90	Hop	370	506	34	3.50
Hsp70	Hsp90	173	309	30	2.58	Hsp90	Hop	370	537	3	3.19
Hsp70	Hsp90	180	317	3	2.43	Hsp90	Hop	370	503	7	3.02
Hsp70	Hsp90	234	433	6	3.25	Hsp90	Hop	370	543	15	2.63
Hsp70	Hsp90	407	422	5	2.10	Hsp90	Hop	370	133	6	2.24
Hsp70	Hsp90	411	422	13	1.81	Hsp90	Hop	370	507	8	2.21
Hsp70	Hsp90	416	422	28	2.35	Hsp90	Hop	391	546	3	1.74
Hsp70	Hsp90	533	416	5	1.86	Hsp90	Hop	395	509	18	3.42
Hsp70	Hsp90	544	425	4	1.96	Hsp90	Hop	416	73	5	12.67
Hsp70	Hsp90	662	458	4	1.78	Hsp90	Hop	422	177	8	3.22
Hsp70	p23	1	29	6	5.93	Hsp90	Hop	422	559	3	1.93
Hsp70	p23	67	1	8	3.86	Hsp90	Hop	422	133	7	1.81
Hsp70	p23	246	1	5	3.02	Hsp90	Hop	434	515	3	2.15
Hsp70	p23	304	1	5	1.53	Hsp90	Hop	458	177	3	2.31
Hsp70	p23	306	1	4	1.60	Hsp90	Hop	458	506	18	2.27
Hsp70	p23	313	1	13	1.99	Hsp90	Hop	458	503	4	1.93

## Appendix

Hsp90	Hop	487	123	5	2.59	Hsp90	Hsp90	303	222	41	1.87
Hsp90	Hop	487	367	15	1.78	Hsp90	Hsp90	304	309	12	7.47
Hsp90	Hop	488	367	12	2.07	Hsp90	Hsp90	317	630	6	3.77
Hsp90	Hop	494	360	15	2.80	Hsp90	Hsp90	318	298	5	2.74
Hsp90	Hop	512	509	15	6.63	Hsp90	Hsp90	322	298	5	3.91
Hsp90	Hop	512	185	7	5.65	Hsp90	Hsp90	337	630	4	1.80
Hsp90	Hop	512	553	15	4.46	Hsp90	Hsp90	351	630	3	2.58
Hsp90	Hop	561	543	10	1.96	Hsp90	Hsp90	368	630	7	2.29
Hsp90	Hop	561	177	4	1.60	Hsp90	Hsp90	391	425	52	2.74
Hsp90	Hop	597	177	15	20.77	Hsp90	Hsp90	395	370	42	3.33
Hsp90	Hop	597	133	9	5.45	Hsp90	Hsp90	407	92	7	1.79
Hsp90	Hop	597	537	4	4.16	Hsp90	Hsp90	422	512	9	2.56
Hsp90	Hop	597	543	5	2.18	Hsp90	Hsp90	458	368	14	3.76
Hsp90	Hop	600	177	13	5.52	Hsp90	Hsp90	466	630	29	2.16
Hsp90	Hop	630	472	9	6.24	Hsp90	Hsp90	504	565	32	6.43
Hsp90	Hop	630	503	5	2.53	Hsp90	Hsp90	504	562	17	2.80
Hsp90	Hop	630	161	3	2.32	Hsp90	Hsp90	504	571	3	2.31
Hsp90	Hop	630	177	10	1.77	Hsp90	Hsp90	504	570	9	2.28
Hsp90	Hop	630	506	7	1.76	Hsp90	Hsp90	512	630	45	8.69
Hsp90	Hop	636	509	8	3.42	Hsp90	Hsp90	514	487	14	4.91
Hsp90	Hop	646	472	24	5.12	Hsp90	Hsp90	515	597	8	5.79
Hsp90	Hop	646	479	33	3.87	Hsp90	Hsp90	515	630	11	3.05
Hsp90	Hop	646	543	15	3.20	Hsp90	Hsp90	515	600	3	2.10
Hsp90	Hop	646	133	7	2.70	Hsp90	Hsp90	538	458	9	1.82
Hsp90	Hop	647	537	5	2.97	Hsp90	Hsp90	542	630	8	1.54
Hsp90	Hop	729	96	4	1.81	Hsp90	Hsp90	549	466	12	1.69
Hsp90	Hop	730	260	17	1.83	Hsp90	Hsp90	561	542	4	3.53
Hsp90	Hop	730	261	11	1.80	Hsp90	Hsp90	562	597	51	24.10
Hsp90	Hop	730	262	7	1.78	Hsp90	Hsp90	562	600	9	3.50
Hsp90	Hop	735	360	9	6.91	Hsp90	Hsp90	562	630	7	3.31
Hsp90	Hop	738	360	9	9.27	Hsp90	Hsp90	565	597	8	2.66
Hsp90	Hop	738	262	29	4.13	Hsp90	Hsp90	565	504	12	1.53
Hsp90	Hop	739	262	13	4.24	Hsp90	Hsp90	569	575	4	2.12
Hsp90	Hsp70	95	181	4	2.90	Hsp90	Hsp90	570	500	29	4.78
Hsp90	Hsp70	175	1	6	3.91	Hsp90	Hsp90	570	574	5	4.75
Hsp90	Hsp70	176	1	8	3.17	Hsp90	Hsp90	571	500	13	2.25
Hsp90	Hsp70	279	1	7	3.65	Hsp90	Hsp90	572	575	8	2.87
Hsp90	Hsp70	280	1	3	2.53	Hsp90	Hsp90	572	574	14	2.06
Hsp90	Hsp70	317	1	4	4.51	Hsp90	Hsp90	575	654	13	1.79
Hsp90	Hsp70	317	98	9	3.26	Hsp90	Hsp90	580	584	21	9.67
Hsp90	Hsp70	317	267	3	2.25	Hsp90	Hsp90	582	666	7	2.23
Hsp90	Hsp70	318	1	14	4.80	Hsp90	Hsp90	626	647	7	4.64
Hsp90	Hsp70	422	542	5	3.16	Hsp90	Hsp90	626	561	3	3.02
Hsp90	Hsp70	554	549	3	2.05	Hsp90	Hsp90	626	600	7	2.92
Hsp90	Hsp90	72	370	22	3.61	Hsp90	Hsp90	626	458	3	2.44
Hsp90	Hsp90	76	416	4	4.04	Hsp90	Hsp90	636	630	4	2.90
Hsp90	Hsp90	76	80	10	2.79	Hsp90	Hsp90	636	458	6	1.89
Hsp90	Hsp90	80	76	10	4.05	Hsp90	Hsp90	647	636	8	3.54
Hsp90	Hsp90	104	309	9	4.62	Hsp90	Hsp90	654	575	48	2.35
Hsp90	Hsp90	130	416	6	4.97	Hsp90	Hsp90	659	582	16	3.20
Hsp90	Hsp90	130	368	6	3.05	Hsp90	Hsp90	659	575	7	1.71
Hsp90	Hsp90	130	72	6	2.14	Hsp90	Hsp90	676	669	17	1.73
Hsp90	Hsp90	203	196	88	15.37	Hsp90	Hsp90	694	630	8	1.82
Hsp90	Hsp90	203	193	27	6.91	Hsp90	Hsp90	729	514	4	5.98
Hsp90	Hsp90	218	222	16	4.21	Hsp90	Hsp90	729	500	17	4.61
Hsp90	Hsp90	227	322	10	3.05	Hsp90	Hsp90	730	422	3	5.04
Hsp90	Hsp90	241	298	104	15.95	Hsp90	Hsp90	730	514	5	4.09
Hsp90	Hsp90	241	296	9	3.36	Hsp90	Hsp90	730	500	4	1.96
Hsp90	Hsp90	241	222	6	2.29	Hsp90	p23	175	1	4	2.67
Hsp90	Hsp90	242	301	78	17.47	Hsp90	p23	176	1	12	3.57
Hsp90	Hsp90	242	317	3	2.05	Hsp90	p23	259	1	3	2.39
Hsp90	Hsp90	242	214	5	1.72	Hsp90	p23	261	1	6	2.22
Hsp90	Hsp90	257	261	102	19.41	Hsp90	p23	262	1	5	1.55
Hsp90	Hsp90	257	262	5	2.00	Hsp90	p23	274	1	10	5.84
Hsp90	Hsp90	257	263	13	1.71	Hsp90	p23	275	1	5	4.34
Hsp90	Hsp90	259	265	8	3.84	Hsp90	p23	279	1	33	4.57
Hsp90	Hsp90	260	255	7	5.59	Hsp90	p23	280	1	8	4.72
Hsp90	Hsp90	260	256	38	3.47	Hsp90	p23	281	1	5	3.45
Hsp90	Hsp90	301	309	3	3.77	Hsp90	p23	317	1	25	16.74
Hsp90	Hsp90	303	309	9	5.43	Hsp90	p23	317	101	7	3.16

## Appendix

Hsp90	p23	318	1	20	16.89	p23	Hop	1	253	6	3.28
Hsp90	p23	318	101	4	1.68	p23	Hop	1	479	10	3.19
Hsp90	p23	322	1	9	4.28	p23	Hop	1	432	3	2.67
Hsp90	p23	395	1	4	2.27	p23	Hop	1	341	7	2.21
Hsp90	p23	408	1	7	2.75	p23	Hop	32	73	3	7.12
Hsp90	p23	444	1	20	2.44	p23	Hop	71	133	4	2.11
Hsp90	p23	494	1	4	3.69	p23	Hop	87	360	7	2.80
Hsp90	p23	562	1	3	2.31	p23	Hop	101	133	10	3.02
Hsp90	p23	565	1	4	2.18	p23	Hop	101	381	5	2.86
Hsp90	p23	570	1	3	1.81	p23	Hop	101	543	4	2.64
Hsp90	p23	647	32	4	2.84	p23	Hop	101	25	4	2.27
Hsp90	p23	717	1	3	2.50	p23	Hop	101	177	5	2.20
Hsp90	p23	735	1	3	3.45	p23	Hop	101	386	4	1.99
Hsp90	p23	738	1	8	4.49	p23	Hop	101	29	4	1.89
Hsp90	Tau	104	281	8	4.60	p23	Hop	108	509	6	2.42
Hsp90	Tau	104	370	5	3.57	p23	Hop	120	348	10	2.68
Hsp90	Tau	104	174	4	3.16	p23	Hsp70	1	662	11	4.98
Hsp90	Tau	104	259	5	2.88	p23	Hsp70	1	577	7	4.89
Hsp90	Tau	104	343	3	1.55	p23	Hsp70	1	660	7	4.27
Hsp90	Tau	104	347	3	1.53	p23	Hsp70	1	336	8	2.63
Hsp90	Tau	176	174	3	2.13	p23	Hsp70	85	611	17	5.77
Hsp90	Tau	176	254	3	1.94	p23	Hsp70	101	662	3	3.30
Hsp90	Tau	176	267	7	1.84	p23	Hsp70	101	339	5	2.64
Hsp90	Tau	176	234	3	1.67	p23	Hsp70	114	1	7	4.46
Hsp90	Tau	176	240	5	1.66	p23	Hsp70	121	1	3	2.13
Hsp90	Tau	210	281	3	4.24	p23	Hsp90	1	210	16	5.62
Hsp90	Tau	210	370	5	3.74	p23	Hsp90	1	515	5	5.62
Hsp90	Tau	210	259	5	3.43	p23	Hsp90	1	416	3	5.27
Hsp90	Tau	210	174	6	3.26	p23	Hsp90	1	104	17	4.22
Hsp90	Tau	210	234	10	1.82	p23	Hsp90	1	72	8	4.10
Hsp90	Tau	214	234	4	1.70	p23	Hsp90	1	214	7	3.87
Hsp90	Tau	217	240	4	7.61	p23	Hsp90	1	347	13	3.66
Hsp90	Tau	217	225	5	6.95	p23	Hsp90	1	570	4	3.50
Hsp90	Tau	217	259	5	3.20	p23	Hsp90	1	196	13	3.12
Hsp90	Tau	274	274	5	1.80	p23	Hsp90	1	512	5	3.03
Hsp90	Tau	275	267	4	1.56	p23	Hsp90	1	351	24	2.98
Hsp90	Tau	279	383	3	1.97	p23	Hsp90	1	476	6	2.05
Hsp90	Tau	279	240	5	1.95	p23	Hsp90	1	303	4	1.87
Hsp90	Tau	279	225	5	1.55	p23	Hsp90	71	318	6	1.77
Hsp90	Tau	317	225	7	4.25	p23	Hsp90	101	210	3	3.94
Hsp90	Tau	317	259	3	3.06	p23	Hsp90	101	347	9	3.70
Hsp90	Tau	317	132	4	2.97	p23	Hsp90	101	407	10	2.64
Hsp90	Tau	317	150	3	2.82	p23	Hsp90	101	416	6	2.26
Hsp90	Tau	317	234	6	2.74	p23	Hsp90	101	408	7	1.64
Hsp90	Tau	317	383	5	2.45	p23	Hsp90	114	425	14	4.90
Hsp90	Tau	317	174	3	2.42	p23	Hsp90	117	425	49	9.51
Hsp90	Tau	318	281	5	4.80	p23	Hsp90	117	433	5	1.79
Hsp90	Tau	318	259	3	3.77	p23	Hsp90	118	425	7	1.95
Hsp90	Tau	318	240	5	3.61	p23	Hsp90	120	425	20	7.25
Hsp90	Tau	318	225	5	3.60	p23	Hsp90	120	422	7	2.08
Hsp90	Tau	318	163	5	2.81	p23	p23	1	32	44	30.55
Hsp90	Tau	318	174	6	2.65	p23	p23	1	87	22	4.81
Hsp90	Tau	318	254	4	2.51	p23	p23	1	38	20	4.18
Hsp90	Tau	318	383	3	1.96	p23	p23	1	108	4	2.40
Hsp90	Tau	318	148	3	1.59	p23	p23	28	1	59	5.13
Hsp90	Tau	351	281	4	4.16	p23	p23	29	1	114	9.00
Hsp90	Tau	351	370	4	3.99	p23	p23	39	87	50	9.56
Hsp90	Tau	351	259	6	3.44	p23	p23	41	87	7	2.12
Hsp90	Tau	351	234	3	2.22	p23	p23	51	1	23	4.95
Hsp90	Tau	351	375	4	2.12	p23	p23	58	41	47	22.52
Hsp90	Tau	351	174	4	1.76	p23	p23	60	41	43	5.33
Hsp90	Tau	512	225	3	2.30	p23	p23	60	1	29	2.44
Hsp90	Tau	708	430	12	2.92	p23	p23	60	39	5	1.66
Hsp90	Tau	708	421	6	2.76	p23	p23	69	1	10	2.85
Hsp90	Tau	735	298	3	2.19	p23	p23	71	118	12	2.00
p23	Hop	1	133	20	6.86	p23	p23	71	120	14	1.91
p23	Hop	1	310	9	4.00	p23	p23	71	116	6	1.60
p23	Hop	1	177	10	3.95	p23	p23	71	32	4	1.55
p23	Hop	1	543	12	3.52	p23	p23	85	38	3	6.40
p23	Hop	1	559	5	3.45	p23	p23	85	32	9	3.85



## Appendix

p23	p23	101	87	16	4.31	p23	Tau	121	267	5	2.43
p23	p23	101	32	6	2.10	p23	Tau	121	174	5	2.29
p23	p23	114	1	30	6.49	Tau	Hop	57	348	3	2.19
p23	p23	116	1	74	8.23	Tau	Hop	57	96	6	1.57
p23	p23	117	1	47	7.86	Tau	Hop	74	348	11	1.97
p23	p23	118	1	46	8.32	Tau	Hop	81	348	4	1.52
p23	p23	120	1	59	3.44	Tau	Hop	174	177	3	3.10
p23	p23	121	1	65	4.55	Tau	Hop	174	479	4	2.20
p23	p23	122	1	7	3.26	Tau	Hop	180	381	3	2.58
p23	p23	127	1	5	3.21	Tau	Hop	180	177	3	1.69
p23	p23	156	1	4	5.31	Tau	Hop	240	177	4	6.27
p23	p23	160	1	4	2.67	Tau	Hop	254	177	15	4.40
p23	Tau	1	402	6	4.30	Tau	Hop	254	133	9	4.15
p23	Tau	1	187	7	3.98	Tau	Hop	254	381	8	2.85
p23	Tau	1	252	8	3.57	Tau	Hop	254	442	3	2.44
p23	Tau	1	283	10	3.52	Tau	Hop	254	479	6	1.92
p23	Tau	1	391	7	2.51	Tau	Hop	259	133	7	2.67
p23	Tau	29	225	6	5.32	Tau	Hop	259	177	6	2.37
p23	Tau	29	150	5	3.49	Tau	Hop	267	177	4	3.80
p23	Tau	29	281	4	3.22	Tau	Hop	267	133	9	2.80
p23	Tau	29	375	7	3.11	Tau	Hop	267	442	5	2.34
p23	Tau	29	259	5	2.96	Tau	Hop	267	479	6	1.90
p23	Tau	29	234	11	2.91	Tau	Hop	274	479	7	1.82
p23	Tau	29	174	4	2.89	Tau	Hop	274	133	6	1.70
p23	Tau	29	132	4	2.73	Tau	Hop	281	177	6	3.06
p23	Tau	29	370	4	2.37	Tau	Hop	281	133	5	2.97
p23	Tau	29	240	17	2.26	Tau	Hop	281	479	6	2.54
p23	Tau	29	383	4	1.58	Tau	Hop	290	133	5	3.61
p23	Tau	32	225	10	12.15	Tau	Hop	298	133	6	3.14
p23	Tau	32	280	9	10.66	Tau	Hop	298	177	5	2.21
p23	Tau	32	240	6	9.16	Tau	Hop	298	559	3	1.81
p23	Tau	32	347	6	6.64	Tau	Hop	298	543	3	1.63
p23	Tau	32	370	4	4.51	Tau	Hop	298	479	5	1.58
p23	Tau	38	225	4	6.16	Tau	Hop	311	133	4	3.43
p23	Tau	69	281	3	2.02	Tau	Hop	311	177	10	3.15
p23	Tau	87	240	7	12.64	Tau	Hop	311	479	4	2.31
p23	Tau	87	225	4	6.42	Tau	Hop	311	381	7	1.94
p23	Tau	87	259	9	3.34	Tau	Hop	311	532	9	1.57
p23	Tau	87	383	4	1.95	Tau	Hop	311	161	11	1.53
p23	Tau	87	174	4	1.77	Tau	Hop	317	133	4	2.58
p23	Tau	114	280	5	5.21	Tau	Hop	317	177	5	1.94
p23	Tau	114	281	4	3.64	Tau	Hop	321	133	5	2.96
p23	Tau	114	163	5	3.60	Tau	Hop	321	235	3	1.92
p23	Tau	114	375	5	2.20	Tau	Hop	331	133	6	2.38
p23	Tau	114	174	4	2.10	Tau	Hop	343	479	7	3.59
p23	Tau	114	259	4	1.88	Tau	Hop	353	133	9	4.49
p23	Tau	114	274	5	1.84	Tau	Hop	353	385	3	2.25
p23	Tau	116	174	3	3.09	Tau	Hop	353	177	5	1.68
p23	Tau	116	267	5	2.34	Tau	Hop	369	133	4	2.58
p23	Tau	116	290	4	2.03	Tau	Hop	369	479	4	2.10
p23	Tau	116	254	4	2.01	Tau	Hop	375	479	4	2.88
p23	Tau	116	281	3	1.63	Tau	Hop	385	133	6	3.08
p23	Tau	117	254	4	4.40	Tau	Hop	385	479	4	1.67
p23	Tau	117	385	4	3.48	Tau	Hop	395	177	5	3.62
p23	Tau	117	370	3	3.13	Tau	Hop	395	133	4	3.32
p23	Tau	117	290	3	2.77	Tau	Hop	395	29	5	2.91
p23	Tau	117	267	6	2.71	Tau	Hop	395	381	8	1.74
p23	Tau	117	225	5	2.01	Tau	Hop	421	96	7	5.19
p23	Tau	117	274	3	1.67	Tau	Hop	421	546	3	3.62
p23	Tau	118	281	3	2.73	Tau	Hop	421	348	4	3.16
p23	Tau	118	370	3	2.36	Tau	Hop	421	509	17	2.70
p23	Tau	118	267	9	2.27	Tau	Hop	421	73	4	2.29
p23	Tau	120	225	6	4.08	Tau	Hop	421	387	6	2.14
p23	Tau	120	240	7	3.54	Tau	Hop	421	146	4	1.69
p23	Tau	120	281	5	2.97	Tau	Hop	430	31	3	6.19
p23	Tau	120	370	6	2.70	Tau	Hop	430	348	14	6.15
p23	Tau	120	174	3	2.37	Tau	Hop	430	509	10	3.21
p23	Tau	120	267	10	1.90	Tau	Hop	430	96	5	1.59
p23	Tau	120	290	3	1.81	Tau	Hop	431	536	4	5.08
p23	Tau	120	274	5	1.65	Tau	Hop	431	96	5	3.45

## Appendix

Tau	Hop	431	146	3	3.24
Tau	Hop	431	509	11	3.09
Tau	Hop	431	348	4	2.09
Tau	Hop	431	418	3	1.67
Tau	Hsp70	7	1	4	3.99
Tau	Hsp70	36	1	7	3.65
Tau	Hsp70	45	1	5	2.76
Tau	Hsp70	57	1	20	3.34
Tau	Hsp70	57	278	5	2.19
Tau	Hsp70	58	1	4	3.47
Tau	Hsp70	73	1	7	3.55
Tau	Hsp70	74	1	7	2.99
Tau	Hsp70	81	1	5	2.13
Tau	Hsp70	96	1	7	3.24
Tau	Hsp70	104	1	4	2.71
Tau	Hsp70	105	1	3	2.47
Tau	Hsp70	163	662	12	2.25
Tau	Hsp70	180	662	4	3.18
Tau	Hsp70	234	549	4	2.72
Tau	Hsp70	240	549	5	6.68
Tau	Hsp70	254	662	12	3.42
Tau	Hsp70	254	549	4	2.04
Tau	Hsp70	259	577	5	2.85
Tau	Hsp70	267	662	8	3.06
Tau	Hsp70	267	69	3	2.42
Tau	Hsp70	267	549	9	1.71
Tau	Hsp70	274	662	5	2.20
Tau	Hsp70	274	549	12	1.61
Tau	Hsp70	281	662	5	2.79
Tau	Hsp70	290	662	4	4.44
Tau	Hsp70	290	660	3	2.94
Tau	Hsp70	298	662	18	3.23
Tau	Hsp70	298	481	6	1.74
Tau	Hsp70	311	549	7	2.99
Tau	Hsp70	311	662	22	2.94
Tau	Hsp70	311	481	4	2.81
Tau	Hsp70	321	662	14	2.86
Tau	Hsp70	321	659	4	2.33
Tau	Hsp70	321	549	6	1.55
Tau	Hsp70	331	662	9	2.28
Tau	Hsp70	353	662	9	3.84
Tau	Hsp70	353	549	3	2.50
Tau	Hsp70	353	67	4	1.88
Tau	Hsp70	369	662	11	3.30
Tau	Hsp70	369	549	7	2.81
Tau	Hsp70	385	549	3	1.65
Tau	Hsp70	395	662	8	4.82
Tau	Hsp70	395	549	5	1.97
Tau	Hsp70	421	109	4	7.43
Tau	Hsp70	421	1	11	6.82
Tau	Hsp70	430	1	9	9.33
Tau	Hsp70	430	267	3	5.10
Tau	Hsp70	431	1	6	3.03
Tau	Hsp70	431	278	3	2.54
Tau	Hsp90	45	209	3	2.67
Tau	Hsp90	104	422	4	1.86
Tau	Hsp90	163	210	6	3.01
Tau	Hsp90	180	214	3	1.69
Tau	Hsp90	254	210	3	3.65
Tau	Hsp90	254	104	5	2.68
Tau	Hsp90	254	347	3	2.65
Tau	Hsp90	259	196	3	1.93
Tau	Hsp90	267	210	5	2.77
Tau	Hsp90	267	104	3	1.61
Tau	Hsp90	274	210	7	2.84
Tau	Hsp90	281	196	3	1.94
Tau	Hsp90	298	176	3	5.73
Tau	Hsp90	298	318	10	3.64
Tau	Hsp90	298	210	4	1.68
Tau	Hsp90	311	210	3	2.71
Tau	Hsp90	311	318	4	2.57
Tau	Hsp90	321	318	5	3.50
Tau	Hsp90	321	275	3	3.02
Tau	Hsp90	321	210	6	1.77
Tau	Hsp90	331	210	6	1.92
Tau	Hsp90	353	318	6	2.59
Tau	Hsp90	353	347	4	1.75
Tau	Hsp90	353	217	4	1.67
Tau	Hsp90	369	318	7	3.24
Tau	Hsp90	369	104	5	2.03
Tau	Hsp90	369	317	4	1.55
Tau	Hsp90	385	210	4	3.80
Tau	Hsp90	395	317	4	3.54
Tau	Hsp90	430	458	3	4.45
Tau	Hsp90	430	425	4	3.82
Tau	Hsp90	430	370	5	2.82
Tau	Hsp90	431	425	4	5.14
Tau	Hsp90	431	458	6	3.47
Tau	Hsp90	431	422	3	1.97
Tau	p23	7	1	29	4.56
Tau	p23	9	1	6	3.20
Tau	p23	25	1	5	2.40
Tau	p23	34	1	21	2.79
Tau	p23	36	1	45	3.50
Tau	p23	38	1	16	3.26
Tau	p23	45	1	15	6.82
Tau	p23	53	1	12	4.73
Tau	p23	53	71	4	1.78
Tau	p23	53	101	6	1.57
Tau	p23	54	1	7	2.33
Tau	p23	57	1	63	10.48
Tau	p23	57	101	5	1.59
Tau	p23	58	1	22	6.41
Tau	p23	62	1	5	2.06
Tau	p23	73	1	12	3.20
Tau	p23	74	1	35	3.21
Tau	p23	74	101	6	2.26
Tau	p23	81	1	12	4.32
Tau	p23	81	101	3	2.07
Tau	p23	82	1	5	3.91
Tau	p23	82	101	6	1.86
Tau	p23	96	1	26	5.24
Tau	p23	104	1	24	7.33
Tau	p23	104	101	5	1.72
Tau	p23	110	1	11	2.08
Tau	p23	163	29	3	3.31
Tau	p23	163	32	7	2.14
Tau	p23	174	32	7	3.86
Tau	p23	180	116	3	1.86
Tau	p23	180	114	3	1.85
Tau	p23	254	32	8	3.38
Tau	p23	254	87	10	2.61
Tau	p23	259	32	5	2.67
Tau	p23	267	87	9	3.93
Tau	p23	267	28	16	1.79
Tau	p23	274	87	13	1.78
Tau	p23	281	87	9	3.73
Tau	p23	281	32	5	3.24
Tau	p23	298	114	6	4.48
Tau	p23	298	117	3	2.68
Tau	p23	298	120	7	1.85
Tau	p23	298	32	7	1.61
Tau	p23	311	114	8	3.59
Tau	p23	311	87	8	3.34
Tau	p23	311	32	10	3.16
Tau	p23	314	1	4	1.66
Tau	p23	317	87	5	2.39
Tau	p23	317	32	5	2.29
Tau	p23	321	114	5	3.13
Tau	p23	321	120	12	2.78

## Appendix

Tau	p23	321	87	10	2.05	Tau	Tau	34	267	17	1.55
Tau	p23	331	117	4	2.75	Tau	Tau	34	225	8	1.54
Tau	p23	331	120	12	1.77	Tau	Tau	36	331	9	3.74
Tau	p23	338	1	3	2.92	Tau	Tau	36	180	24	2.94
Tau	p23	343	32	4	3.18	Tau	Tau	36	225	12	2.60
Tau	p23	353	117	6	3.64	Tau	Tau	36	150	16	2.52
Tau	p23	353	116	3	3.39	Tau	Tau	36	353	5	2.52
Tau	p23	353	114	4	3.21	Tau	Tau	36	281	12	2.51
Tau	p23	353	87	4	2.74	Tau	Tau	36	143	12	2.51
Tau	p23	353	32	9	1.84	Tau	Tau	36	174	23	2.37
Tau	p23	358	1	6	2.57	Tau	Tau	36	132	10	1.95
Tau	p23	369	117	6	3.64	Tau	Tau	36	290	14	1.86
Tau	p23	369	28	5	2.46	Tau	Tau	36	163	21	1.76
Tau	p23	370	32	4	3.76	Tau	Tau	36	311	6	1.71
Tau	p23	418	1	10	2.96	Tau	Tau	36	385	9	1.70
Tau	p23	421	1	13	3.80	Tau	Tau	36	370	18	1.69
Tau	p23	421	101	4	2.20	Tau	Tau	36	224	15	1.67
Tau	p23	430	1	23	7.04	Tau	Tau	36	259	6	1.66
Tau	p23	430	101	5	5.87	Tau	Tau	38	225	12	3.46
Tau	p23	431	1	33	6.80	Tau	Tau	38	150	11	2.95
Tau	Tau	7	150	17	4.24	Tau	Tau	38	132	7	2.69
Tau	Tau	7	132	5	4.17	Tau	Tau	38	163	3	2.64
Tau	Tau	7	174	9	3.85	Tau	Tau	38	254	3	2.05
Tau	Tau	7	385	4	3.80	Tau	Tau	38	385	5	2.03
Tau	Tau	7	163	17	3.45	Tau	Tau	38	143	8	1.84
Tau	Tau	7	281	8	3.33	Tau	Tau	38	343	6	1.83
Tau	Tau	7	225	11	3.22	Tau	Tau	38	234	13	1.69
Tau	Tau	7	240	9	3.02	Tau	Tau	38	370	4	1.54
Tau	Tau	7	234	12	2.85	Tau	Tau	40	225	7	3.35
Tau	Tau	7	180	12	2.68	Tau	Tau	40	150	7	1.64
Tau	Tau	7	259	9	2.46	Tau	Tau	40	259	5	1.60
Tau	Tau	7	130	4	2.45	Tau	Tau	44	74	3	1.84
Tau	Tau	7	294	3	2.21	Tau	Tau	45	174	9	6.79
Tau	Tau	7	370	10	2.14	Tau	Tau	45	225	12	6.19
Tau	Tau	7	143	4	2.04	Tau	Tau	45	259	3	5.46
Tau	Tau	7	254	3	2.01	Tau	Tau	45	234	9	4.49
Tau	Tau	7	274	10	1.98	Tau	Tau	45	267	9	4.06
Tau	Tau	7	280	5	1.97	Tau	Tau	45	163	14	4.02
Tau	Tau	7	311	3	1.59	Tau	Tau	45	150	13	3.43
Tau	Tau	7	375	10	1.56	Tau	Tau	45	180	4	3.33
Tau	Tau	7	190	4	1.55	Tau	Tau	45	274	6	3.11
Tau	Tau	9	174	7	4.62	Tau	Tau	45	321	6	2.85
Tau	Tau	9	281	14	4.08	Tau	Tau	45	24	12	2.33
Tau	Tau	9	132	3	3.30	Tau	Tau	45	383	7	2.19
Tau	Tau	9	225	6	3.29	Tau	Tau	45	140	4	1.93
Tau	Tau	9	150	3	3.15	Tau	Tau	45	132	3	1.67
Tau	Tau	9	259	5	2.99	Tau	Tau	45	311	14	1.66
Tau	Tau	9	234	9	2.90	Tau	Tau	53	150	12	16.51
Tau	Tau	9	254	6	2.84	Tau	Tau	53	163	21	14.38
Tau	Tau	9	180	8	2.66	Tau	Tau	53	240	10	11.43
Tau	Tau	9	369	10	2.62	Tau	Tau	53	174	23	9.25
Tau	Tau	9	190	7	2.35	Tau	Tau	53	180	32	6.76
Tau	Tau	9	163	9	2.27	Tau	Tau	53	370	7	6.37
Tau	Tau	9	143	3	1.58	Tau	Tau	53	259	13	5.73
Tau	Tau	12	150	3	3.84	Tau	Tau	53	140	5	5.69
Tau	Tau	12	225	8	3.60	Tau	Tau	53	311	11	4.63
Tau	Tau	12	240	4	2.14	Tau	Tau	53	321	24	4.49
Tau	Tau	12	163	3	1.73	Tau	Tau	53	190	10	4.07
Tau	Tau	24	82	3	5.02	Tau	Tau	53	294	6	3.83
Tau	Tau	24	9	59	3.79	Tau	Tau	53	24	49	3.38
Tau	Tau	24	7	13	3.70	Tau	Tau	53	281	18	3.38
Tau	Tau	24	74	7	3.12	Tau	Tau	53	353	26	3.36
Tau	Tau	24	73	15	2.86	Tau	Tau	53	274	43	3.18
Tau	Tau	24	81	3	2.45	Tau	Tau	53	395	11	3.07
Tau	Tau	24	40	4	1.69	Tau	Tau	53	143	5	2.70
Tau	Tau	25	174	4	1.53	Tau	Tau	53	369	18	2.58
Tau	Tau	34	163	11	1.94	Tau	Tau	53	290	13	2.57
Tau	Tau	34	369	6	1.84	Tau	Tau	53	267	25	2.56
Tau	Tau	34	150	5	1.78	Tau	Tau	53	254	12	2.37
Tau	Tau	34	174	21	1.65	Tau	Tau	53	234	13	2.29

## Appendix

Tau	Tau	53	375	11	1.88	Tau	Tau	62	267	5	2.59
Tau	Tau	53	132	10	1.88	Tau	Tau	62	130	5	2.03
Tau	Tau	53	225	11	1.60	Tau	Tau	62	347	3	1.97
Tau	Tau	54	280	6	9.36	Tau	Tau	62	383	12	1.67
Tau	Tau	54	234	5	6.36	Tau	Tau	67	36	4	1.58
Tau	Tau	54	267	5	5.16	Tau	Tau	73	163	7	18.11
Tau	Tau	54	150	25	5.09	Tau	Tau	73	150	35	15.78
Tau	Tau	54	369	4	4.32	Tau	Tau	73	174	19	11.78
Tau	Tau	54	130	14	2.72	Tau	Tau	73	225	13	4.03
Tau	Tau	54	163	7	2.63	Tau	Tau	73	132	35	3.90
Tau	Tau	54	24	8	2.43	Tau	Tau	73	259	14	3.26
Tau	Tau	54	180	3	2.37	Tau	Tau	73	281	15	2.79
Tau	Tau	54	281	6	2.27	Tau	Tau	73	234	26	2.74
Tau	Tau	54	375	6	2.23	Tau	Tau	73	130	39	2.62
Tau	Tau	54	254	3	1.89	Tau	Tau	73	343	18	2.49
Tau	Tau	54	190	10	1.73	Tau	Tau	73	141	13	2.20
Tau	Tau	54	140	6	1.57	Tau	Tau	73	143	25	2.12
Tau	Tau	57	225	30	24.44	Tau	Tau	73	240	24	1.92
Tau	Tau	57	150	39	21.95	Tau	Tau	73	369	5	1.87
Tau	Tau	57	281	9	16.84	Tau	Tau	73	370	12	1.85
Tau	Tau	57	163	19	11.30	Tau	Tau	73	267	10	1.81
Tau	Tau	57	143	18	10.87	Tau	Tau	73	190	9	1.80
Tau	Tau	57	280	12	10.34	Tau	Tau	73	254	4	1.78
Tau	Tau	57	267	30	9.07	Tau	Tau	73	375	18	1.54
Tau	Tau	57	259	12	8.76	Tau	Tau	73	274	11	1.53
Tau	Tau	57	234	33	8.66	Tau	Tau	74	150	11	23.50
Tau	Tau	57	174	31	8.09	Tau	Tau	74	163	29	16.92
Tau	Tau	57	370	17	6.69	Tau	Tau	74	174	30	14.08
Tau	Tau	57	148	27	5.99	Tau	Tau	74	254	28	5.29
Tau	Tau	57	130	33	5.42	Tau	Tau	74	369	14	4.98
Tau	Tau	57	180	7	4.71	Tau	Tau	74	240	10	4.52
Tau	Tau	57	383	6	4.25	Tau	Tau	74	132	50	3.76
Tau	Tau	57	132	19	4.23	Tau	Tau	74	148	3	3.50
Tau	Tau	57	321	13	3.45	Tau	Tau	74	225	22	3.49
Tau	Tau	57	375	20	3.27	Tau	Tau	74	290	14	3.45
Tau	Tau	57	385	17	3.24	Tau	Tau	74	281	9	3.44
Tau	Tau	57	343	10	3.13	Tau	Tau	74	311	15	3.24
Tau	Tau	57	24	7	2.77	Tau	Tau	74	140	11	2.89
Tau	Tau	57	290	9	2.71	Tau	Tau	74	143	6	2.44
Tau	Tau	57	140	15	2.68	Tau	Tau	74	385	12	2.32
Tau	Tau	57	141	6	2.65	Tau	Tau	74	259	6	2.18
Tau	Tau	57	340	5	2.58	Tau	Tau	74	331	8	2.06
Tau	Tau	57	190	4	2.31	Tau	Tau	74	375	20	2.04
Tau	Tau	57	331	20	2.19	Tau	Tau	74	141	14	2.01
Tau	Tau	57	353	6	2.11	Tau	Tau	74	130	14	1.97
Tau	Tau	57	224	9	1.81	Tau	Tau	74	383	7	1.86
Tau	Tau	57	240	11	1.79	Tau	Tau	74	343	3	1.85
Tau	Tau	57	257	4	1.68	Tau	Tau	74	234	6	1.82
Tau	Tau	57	311	6	1.66	Tau	Tau	74	274	21	1.79
Tau	Tau	57	274	24	1.64	Tau	Tau	74	190	15	1.75
Tau	Tau	58	259	10	20.17	Tau	Tau	74	280	8	1.66
Tau	Tau	58	234	7	11.18	Tau	Tau	74	180	29	1.66
Tau	Tau	58	225	8	10.26	Tau	Tau	81	150	7	4.40
Tau	Tau	58	148	4	7.77	Tau	Tau	81	281	10	4.27
Tau	Tau	58	163	8	5.51	Tau	Tau	81	259	4	3.73
Tau	Tau	58	140	18	5.30	Tau	Tau	81	225	7	3.51
Tau	Tau	58	150	8	2.93	Tau	Tau	81	132	15	3.15
Tau	Tau	58	132	8	2.84	Tau	Tau	81	148	8	3.15
Tau	Tau	58	375	6	2.75	Tau	Tau	81	385	6	2.99
Tau	Tau	58	281	7	2.46	Tau	Tau	81	311	7	2.82
Tau	Tau	58	331	3	2.40	Tau	Tau	81	140	3	2.62
Tau	Tau	58	267	4	2.30	Tau	Tau	81	383	10	2.17
Tau	Tau	58	383	9	2.00	Tau	Tau	81	180	9	2.05
Tau	Tau	58	347	4	1.90	Tau	Tau	81	143	9	1.90
Tau	Tau	58	240	4	1.84	Tau	Tau	81	369	5	1.80
Tau	Tau	58	141	3	1.64	Tau	Tau	81	331	5	1.77
Tau	Tau	58	294	5	1.55	Tau	Tau	81	141	3	1.70
Tau	Tau	62	240	11	5.62	Tau	Tau	81	294	3	1.61
Tau	Tau	62	132	7	3.05	Tau	Tau	81	375	3	1.59
Tau	Tau	62	259	5	3.03	Tau	Tau	81	163	6	1.55

## Appendix

Tau	Tau	82	150	15	23.21	Tau	Tau	105	190	8	4.86
Tau	Tau	82	163	6	10.48	Tau	Tau	105	140	8	4.66
Tau	Tau	82	143	14	8.78	Tau	Tau	105	163	6	3.82
Tau	Tau	82	225	11	4.23	Tau	Tau	105	240	3	3.77
Tau	Tau	82	281	9	3.66	Tau	Tau	105	143	3	3.75
Tau	Tau	82	259	9	3.10	Tau	Tau	105	225	9	2.44
Tau	Tau	82	174	17	2.92	Tau	Tau	105	259	4	2.31
Tau	Tau	82	290	5	2.88	Tau	Tau	105	343	3	2.29
Tau	Tau	82	132	19	2.81	Tau	Tau	105	132	12	2.10
Tau	Tau	82	343	9	2.78	Tau	Tau	105	290	4	2.08
Tau	Tau	82	375	8	2.62	Tau	Tau	105	281	4	1.82
Tau	Tau	82	234	9	2.59	Tau	Tau	110	174	13	11.85
Tau	Tau	82	347	10	2.33	Tau	Tau	110	132	28	5.86
Tau	Tau	82	240	10	2.13	Tau	Tau	110	143	62	5.59
Tau	Tau	82	267	7	2.09	Tau	Tau	110	234	9	5.46
Tau	Tau	82	370	6	2.07	Tau	Tau	110	163	8	5.10
Tau	Tau	82	383	9	1.92	Tau	Tau	110	150	16	4.59
Tau	Tau	82	274	9	1.77	Tau	Tau	110	225	15	4.46
Tau	Tau	82	280	10	1.59	Tau	Tau	110	130	32	4.14
Tau	Tau	96	163	13	8.88	Tau	Tau	110	281	3	3.96
Tau	Tau	96	385	6	6.29	Tau	Tau	110	141	22	3.76
Tau	Tau	96	180	8	5.54	Tau	Tau	110	259	5	3.51
Tau	Tau	96	130	12	3.64	Tau	Tau	110	383	7	3.44
Tau	Tau	96	353	5	2.59	Tau	Tau	110	180	4	3.31
Tau	Tau	96	321	3	2.50	Tau	Tau	110	140	25	3.27
Tau	Tau	96	311	7	2.46	Tau	Tau	110	254	6	3.15
Tau	Tau	96	369	3	2.03	Tau	Tau	110	148	20	2.68
Tau	Tau	96	141	5	1.98	Tau	Tau	110	240	5	1.67
Tau	Tau	96	259	4	1.89	Tau	Tau	110	375	4	1.61
Tau	Tau	96	383	15	1.78	Tau	Tau	115	132	20	6.38
Tau	Tau	96	174	4	1.54	Tau	Tau	115	140	10	6.26
Tau	Tau	99	143	5	14.95	Tau	Tau	115	240	9	4.71
Tau	Tau	99	130	8	8.84	Tau	Tau	115	163	7	3.59
Tau	Tau	99	132	9	8.24	Tau	Tau	115	370	4	2.39
Tau	Tau	99	180	17	4.93	Tau	Tau	115	143	9	1.94
Tau	Tau	104	150	33	18.66	Tau	Tau	116	163	5	5.02
Tau	Tau	104	143	30	16.56	Tau	Tau	133	150	9	4.93
Tau	Tau	104	132	54	7.49	Tau	Tau	139	150	27	11.26
Tau	Tau	104	148	13	7.15	Tau	Tau	163	57	20	2.87
Tau	Tau	104	163	36	7.01	Tau	Tau	163	187	5	2.43
Tau	Tau	104	234	20	6.01	Tau	Tau	163	53	6	2.32
Tau	Tau	104	281	28	5.95	Tau	Tau	174	187	15	2.80
Tau	Tau	104	130	55	5.60	Tau	Tau	187	225	7	5.27
Tau	Tau	104	259	11	5.58	Tau	Tau	187	240	9	2.28
Tau	Tau	104	385	7	5.51	Tau	Tau	187	150	4	1.56
Tau	Tau	104	290	17	5.26	Tau	Tau	252	259	19	3.99
Tau	Tau	104	254	22	5.14	Tau	Tau	252	225	7	2.61
Tau	Tau	104	321	7	5.10	Tau	Tau	252	234	7	2.41
Tau	Tau	104	140	54	5.04	Tau	Tau	252	240	4	1.88
Tau	Tau	104	383	43	5.02	Tau	Tau	254	283	9	2.02
Tau	Tau	104	298	5	5.01	Tau	Tau	259	283	5	3.08
Tau	Tau	104	225	11	4.50	Tau	Tau	264	240	16	11.17
Tau	Tau	104	174	32	4.49	Tau	Tau	264	280	7	3.10
Tau	Tau	104	353	14	3.74	Tau	Tau	267	252	10	2.55
Tau	Tau	104	438	3	3.69	Tau	Tau	267	283	6	1.92
Tau	Tau	104	369	10	3.46	Tau	Tau	267	402	4	1.67
Tau	Tau	104	141	23	3.28	Tau	Tau	274	402	7	1.73
Tau	Tau	104	375	18	3.03	Tau	Tau	274	283	18	1.71
Tau	Tau	104	240	28	2.95	Tau	Tau	281	264	9	3.89
Tau	Tau	104	180	4	2.70	Tau	Tau	298	74	16	5.55
Tau	Tau	104	347	11	2.64	Tau	Tau	298	57	14	5.38
Tau	Tau	104	224	18	2.52	Tau	Tau	298	53	17	5.24
Tau	Tau	104	24	6	2.26	Tau	Tau	298	36	6	4.77
Tau	Tau	104	267	19	2.21	Tau	Tau	298	9	9	4.66
Tau	Tau	104	274	13	1.72	Tau	Tau	298	34	4	3.80
Tau	Tau	105	150	13	15.05	Tau	Tau	298	73	10	3.74
Tau	Tau	105	174	10	12.91	Tau	Tau	298	283	12	2.74
Tau	Tau	105	130	19	7.60	Tau	Tau	311	7	6	3.52
Tau	Tau	105	234	16	4.97	Tau	Tau	311	402	4	2.61
Tau	Tau	105	254	9	4.90	Tau	Tau	311	283	10	2.59

## Appendix

Tau	Tau	311	358	6	2.51	Tau	Tau	421	383	17	3.97
Tau	Tau	311	9	7	1.92	Tau	Tau	421	281	6	3.89
Tau	Tau	311	264	4	1.76	Tau	Tau	421	340	3	3.11
Tau	Tau	311	391	6	1.73	Tau	Tau	421	370	24	3.05
Tau	Tau	317	9	4	1.57	Tau	Tau	421	331	8	2.82
Tau	Tau	317	74	15	1.53	Tau	Tau	421	375	18	2.78
Tau	Tau	321	34	14	4.06	Tau	Tau	421	224	6	2.76
Tau	Tau	321	9	3	3.83	Tau	Tau	421	132	3	2.26
Tau	Tau	321	358	3	3.14	Tau	Tau	421	347	13	2.24
Tau	Tau	321	74	22	3.09	Tau	Tau	421	280	7	2.13
Tau	Tau	321	81	9	2.69	Tau	Tau	421	240	8	1.85
Tau	Tau	321	36	15	2.45	Tau	Tau	421	274	14	1.54
Tau	Tau	338	343	16	2.05	Tau	Tau	430	150	8	9.01
Tau	Tau	338	347	7	1.88	Tau	Tau	430	385	31	8.91
Tau	Tau	340	73	4	2.88	Tau	Tau	430	225	8	8.85
Tau	Tau	353	74	17	6.63	Tau	Tau	430	353	34	8.55
Tau	Tau	353	82	6	4.48	Tau	Tau	430	395	33	7.95
Tau	Tau	353	73	7	3.09	Tau	Tau	430	369	26	7.70
Tau	Tau	353	402	8	2.77	Tau	Tau	430	375	26	7.61
Tau	Tau	353	9	4	2.50	Tau	Tau	430	281	9	7.29
Tau	Tau	353	7	4	2.38	Tau	Tau	430	259	14	7.12
Tau	Tau	353	81	6	1.88	Tau	Tau	430	234	7	6.97
Tau	Tau	353	338	4	1.60	Tau	Tau	430	343	18	6.88
Tau	Tau	358	370	21	7.20	Tau	Tau	430	331	9	6.81
Tau	Tau	358	343	13	2.92	Tau	Tau	430	321	6	6.78
Tau	Tau	358	375	8	2.33	Tau	Tau	430	298	7	6.68
Tau	Tau	358	385	5	2.26	Tau	Tau	430	267	11	6.28
Tau	Tau	358	347	11	1.81	Tau	Tau	430	370	24	5.94
Tau	Tau	369	391	10	2.46	Tau	Tau	430	174	4	5.80
Tau	Tau	369	402	11	2.18	Tau	Tau	430	254	13	4.82
Tau	Tau	369	387	4	1.86	Tau	Tau	430	180	10	4.59
Tau	Tau	370	53	3	2.40	Tau	Tau	430	132	3	4.33
Tau	Tau	375	391	10	2.08	Tau	Tau	430	224	6	4.30
Tau	Tau	385	402	10	4.97	Tau	Tau	430	383	23	4.18
Tau	Tau	387	375	9	3.34	Tau	Tau	430	280	12	3.44
Tau	Tau	391	383	13	11.35	Tau	Tau	430	240	7	2.66
Tau	Tau	391	375	20	3.28	Tau	Tau	430	290	4	2.25
Tau	Tau	391	370	12	2.60	Tau	Tau	430	163	3	2.12
Tau	Tau	391	343	7	1.85	Tau	Tau	430	311	7	2.10
Tau	Tau	395	81	7	5.81	Tau	Tau	430	190	6	2.09
Tau	Tau	395	74	9	4.44	Tau	Tau	430	274	13	1.96
Tau	Tau	395	358	3	2.31	Tau	Tau	430	143	4	1.66
Tau	Tau	402	383	6	12.44	Tau	Tau	431	298	3	9.75
Tau	Tau	402	240	4	4.73	Tau	Tau	431	225	8	9.44
Tau	Tau	402	343	5	4.71	Tau	Tau	431	385	31	9.10
Tau	Tau	402	281	3	4.30	Tau	Tau	431	290	7	8.63
Tau	Tau	402	375	19	4.00	Tau	Tau	431	150	8	8.33
Tau	Tau	402	370	8	2.95	Tau	Tau	431	375	42	8.20
Tau	Tau	402	259	3	1.90	Tau	Tau	431	163	11	7.60
Tau	Tau	418	267	3	4.42	Tau	Tau	431	395	16	6.51
Tau	Tau	418	375	5	2.39	Tau	Tau	431	259	7	6.36
Tau	Tau	421	395	67	8.04	Tau	Tau	431	370	31	6.35
Tau	Tau	421	298	13	7.90	Tau	Tau	431	281	7	6.32
Tau	Tau	421	353	30	7.13	Tau	Tau	431	343	17	6.24
Tau	Tau	421	343	11	6.81	Tau	Tau	431	174	9	6.17
Tau	Tau	421	163	6	6.63	Tau	Tau	431	353	15	5.95
Tau	Tau	421	385	22	6.06	Tau	Tau	431	347	7	5.76
Tau	Tau	421	259	11	5.76	Tau	Tau	431	224	12	5.39
Tau	Tau	421	150	7	5.68	Tau	Tau	431	267	14	5.22
Tau	Tau	421	180	5	5.67	Tau	Tau	431	383	20	5.17
Tau	Tau	421	190	7	4.99	Tau	Tau	431	180	8	4.51
Tau	Tau	421	321	9	4.90	Tau	Tau	431	331	5	4.42
Tau	Tau	421	290	4	4.82	Tau	Tau	431	254	4	4.32
Tau	Tau	421	225	10	4.81	Tau	Tau	431	369	9	3.70
Tau	Tau	421	267	7	4.65	Tau	Tau	431	240	8	3.35
Tau	Tau	421	234	15	4.63	Tau	Tau	431	132	5	3.04
Tau	Tau	421	254	16	4.21	Tau	Tau	431	280	6	2.88
Tau	Tau	421	369	24	4.15	Tau	Tau	431	190	3	2.80
Tau	Tau	421	174	11	4.14	Tau	Tau	431	234	5	2.45
Tau	Tau	421	311	12	4.02	Tau	Tau	431	143	10	2.30

## Appendix

Tau	Tau	431	130	5	2.02	Tau	Tau	431	274	7	1.56
Tau	Tau	431	294	3	1.83	Tau	Tau	438	402	5	4.27